UNIVERSIDAD AUTÓNOMA DE MADRID

DEPARTAMENTO DE BIOLOGÍA MOLECULAR

WOX9 CONTROL BY THE DELLAs MEDIATES SALT TOLERANCE AND ROOT HAIR DIFFERENTIATION IN ARABIDOPSIS

TESIS DOCTORAL

Pilar Lasierra Resa

Madrid, 2016

DEPARTAMENTO DE BIOLOGÍA MOLECULAR

FACULTAD DE CIENCIAS

UNIVERSIDAD AUTÓNOMA DE MADRID

WOX9 CONTROL BY THE DELLAs MEDIATES SALT TOLERANCE AND ROOT HAIR DIFFERENTIATION IN ARABIDOPSIS

Pilar Lasierra Resa

Licenciada en ciencias biológicas

Directora: Salomé Prat Monguió

Centro Nacional de Biotecnología

Madrid

Acknowledgements

En primer lugar, agradecer a Salomé por aceptarme en el laboratorio y guiarme a lo largo de toda la tesis.

A todos los servicios del CNB, en especial a confocal, fotografía, genómica, histología e invernadero.

A Olena Poretska por ayudarme con los experimentos de SAM.

A todo el departamento de GMP, y un poquito más al 314.

Los que me conocen saben que soy de pocas palabras; así que seré breve.

A mis padres, que siempre me han dejado tomar mis propias decisiones y al mismo tiempo me han apoyado en todas ellas. Gracias por estar allí guiándome y animándome cuando más lo he necesitado. En estos años algún llorico y alguna crisis ha habido, y la solución siempre pasaba por llamar a casa.

A toda mi familia, por el apoyo y todos los buenos momentos juntos. En especial a mi hermana la pequeña, que me ha tenido que sufrir los últimos meses y los días que llegaba tarde a casa me tenía la cenica preparada, ¡gracias!

Empezar en el CNB surgió después de tomar una decisión difícil pero sin duda acertada. Mis ánimos por entonces no estaban muy altos así que quiero agradecer a todas las personas que entonces formábais parte de mi vida y que estuvisteis cerca de mí.

No hace mucho mi madre me dijo que yo siempre he sido más de “picotear” que de tener un solo grupo de amigos. Y echando la vista atrás me doy cuenta de que sí, que en estos años he conocido mucha gente: en el Colegio Mayor, en la universidad, compartiendo piso, en el CBGP, en el CNB y finalmente “en Madrid”, que engloba a todos los que conoces por “amigos de amigos” y acaban siendo amigos de verdad. La gente viene y va, y aunque a día de hoy queden unos pocos, todos han sido importantes en alguna etapa de mi vida y me han aportado algo.

Así que gracias a todos los que seguís ahí y me habéis estado animando estos últimos años y sobre todo estos últimos meses, que sé que he estado un poco más pesadita de lo normal. Tanto los que habéis pasado por esto y lo entendíais como los que pertenecéis a otras áreas, os habéis interesado, me habéis aguantado y apoyado en todo momento. Gracias, de igual manera, por todos esos momentos de ocio que hemos compartido y que nada tenían que ver con ciencia. Quiero pensar que todos los que sois importantes para mí lo sabéis, así que no voy a dar nombres (así seguro que no me dejo ninguno). Sólo voy a resaltar a una choni que he tenido detrás todo el verano, y que por cercanía ha tenido que oir mis lamentos durante muchas horas hasta el último día.

Lo dicho, ¡muchas gracias a todos!

Esta tesis doctoral ha sido realizada en el departamento de genética molecular de plantas del Centro Nacional de Biotecnología y ha sido financiada mediante el programa de becas predoctorales La Caixa-CNB de la fundación Obra Social La Caixa.

Summary

Gibberellins (GA) play a pivotal role in the control of plant growth. Its signaling is suppressed by the DELLA repressors, a group of GRAS-type regulators that block GA-regulated gene expression and which are stabilized in the absence of GAs. DELLAs suppress growth by direct interaction with the DNA-recognition domain of Phytochrome Interacting Factors (PIFs) and Brassinazole Resistant 1 and 2 (BZR1/2) to inhibit their interaction with DNA (Bernardo-García et al. 2014; de Lucas et al. 2008). This sequestration mechanism has been described for many of the DELLA interactors, but some evidences show that DELLAs also activate transcription by some factors through binding to non DNA-recognition domain.

Besides suppressing growth, DELLAs play an important role in conferring tolerance to abiotic stresses (Achard et al. 2006; reviewed in Colebrook et al. 2014), although the implicated mechanisms are little understood. To look into this, our lab screened a collection of β-estradiol inducible transgenic lines in the presence of NaCl and GAs. Out of over 500 transcription factors (TF), we identified 32 whose over-expression confers tolerance to salt stress, even in the presence of GAs. We show in this work that 60% of these factors physically interact with the DELLAs, and that in most cases the interaction requires a different domain from the LHRI motif, involved in PIFs interaction. This indicates that DELLAs control growth and abiotic stress responses by different mechanisms, and that this responses could be uncoupled.

We selected the WOX9 homeodomain for further characterization, as over-expression of this factor confers strong tolerance to salt, and members of this gene family had not been previously associated to salt stress. WOX9 strongly interacts with all Arabidopsis DELLAs (RGA, GAI, RGL1-3), and the WUS-box and a conserved EAR motif in the protein are both sufficient for this interaction. WOX9 binds the co-repressor TOPLESS (TPL) through this EAR motif, and binding of DELLAs competes for WOX9-TPL interaction, suggesting that WOX9 is a transcriptional repressor and DELLAs de-repress its downstream targets.

WOX9 is expressed in the shoot (SAM) and root meristems. Consistent with this expression pattern, the *wox9*/*stip-2* mutant has a smaller SAM and shorter root meristem. This mutant has also shorter roots, a reduced number of lateral roots and shorter root hairs.

WOX9 over-expression leads to a hypersensitive response both to abscisic acid (ABA) and cytokinins (CK), while these plants are insensitive to GAs. Although levels of CKs and GAs are indeed lower, ABA content is normal, hence suggesting an important role of WOX9 in the cross-talk regulation of cytokinin and gibberellin homeostasis.

WOX9 induction correlates with down-regulation of several genes, and this repression is reversed by paclobutrazol-mediated stabilization of the DELLA proteins, in agreement with the proposed model that WOX9 is a repressor and accumulation of DELLAs de-represses its target genes.

Presentación

Las giberelinas (GA) juegan un papel crucial en el control del crecimiento vegetal. Su señalización está suprimida por los represores DELLA, un grupo de reguladores tipo GRAS que bloquean la expresión de genes dependientes de GAs y que se estabilizan en ausencia de GAs. Las DELLAs paran crecimiento a través de la interacción directa con el dominio de reconocimiento de ADN de los *Phytochrome Interacting Factors* (PIFs) y *Brassinazole Resistant 1/2* (BZR1/2) para bloquear su interacción con el ADN (Bernardo-García et al. 2014; de Lucas et al. 2008). Este mecanismo de secuestro se ha descrito para otros muchos interactores de las DELLAs, pero hay evidencias de que las DELLAs también activan la transcripción a través de otros factores, interaccionando con otros dominios diferentes.

Además de parar el crecimiento, las DELLAs tienen un papel importante en conferir tolerancia a estreses abióticos (Achard et al. 2006; revisado en Colebrook et al. 2014), aunque los mecanismos implicados están poco descritos. Para profundizar en esto, nuestro laboratorio hizo un escrutinio de líneas transgénicas inducibles por β-estradiol en presencia de NaCl y GAs. De más de 500 factores de transcripción (TF), identificamos 32 cuya sobre-expresión confiere tolerancia a estrés salino, incluso en presencia de GAs. En este trabajo mostramos que el 60% de estos factores interacciona físicamente con las DELLAs, y en la mayoría de los casos lo hace a través de un dominio diferente al LHRI, implicado en la interacción con los PIFs, lo que indica que las DELLAs controlan crecimiento y respuestas a estrés abiótico por mecanismos diferentes, que podrían ser desacoplados.

Seleccionamos al *homedomain* WOX9 para una mayor caracterización, debido a que la sobre-expresión de este factor confiere una fuerte tolerancia a sal, y ningún miembro de la familia había sido previamente relacionado con estrés salino. WOX9 interacciona de manera fuerte con todas las DELLAs de Arabidopsis (RGA, GAI, RGL1-3), y la caja WUS y el motivo EAR son suficientes para la interacción. WOX9 también interacciona con TOPLESS (TPL) por el motivo EAR, y las DELLAs y TPL compiten por la interacción con WOX9, lo que sugiere que WOX9 es un represor transcripcional y las DELLAs des-reprimen sus genes diana.

WOX9 se expresa en los meristemos apical (SAM) y de raíz. Acorde con este patrón de expresión, el mutante *wox9*/*stip-2* tiene un SAM más pequeño y un meristemo de raíz más corto. Este mutante también tiene raíces más cortas, un número reducido de raíces laterales y pelos radiculares más cortos.

La sobre-expresión de *WOX9* lleva a una hipersensibilidad al ácido abscísico (ABA) y citokininas (CK), mientras que estas plantas son insensibles a GAs. Aunque los niveles de CKs y GAs son, de hecho, menores, el contenido en ABA es normal, lo que apunta a un posible papel de WOX9 en la regulación cruzada de la homeostasis de citokininas y giberelinas.

La inducción de *WOX9* se corelaciona con la represión de varios genes, y esta represión es revertida por la estabilización de las DELLAs por paclobutrazol, en concordancia con el modelo propuesto de que WOX9 interacciona con TPL para reprimir la transcripción, y que una acumulación de las DELLAs des-reprime a los genes regulador por WOX9.

Index

Index

ABBREVIATIONS **21**

INTRODUCTION **29**

1. Gibberellins 29
    1.1. Gibberellin biosynthesis and catabolism 29
    1.2. Regulation of gibberellin levels 32
    1.3. Gibberellin signaling 33
2. The DELLA proteins: central repressors of the gibberellin signaling pathway 34
    2.1. DELLAs bind and inactivate a wide range of transcription regulators 34
    2.2. DELLAs as transcriptional activators 35
    2.3. DELLAs crosstalk with other hormone pathways 37
    2.4. DELLA-PIF interaction suppresses hypocotyl growth 38
    2.5. Role of DELLAs in stress 40
        2.5.1. Biotic stress 40
        2.5.2. Abiotic stress 41
3. WUSCHEL-related Homeobox 9 (WOX9) 42
    3.1. The WOX homeodomain family 42
    3.2. WOX9 regulates cytokinin signaling 43
    3.3. WOX proteins are transcriptional repressors 45
4. The plant meristems 45
    4.1. The shoot apical meristem 45
    4.2. The root apical meristem 46
        4.2.1. Root patterning 46
        4.2.2. Effects of salt on root growth 48
        4.2.3. The root hairs 48

OBJECTIVES **53**

MATERIALS AND METHODS **57**

1. Plant material 57
2. Growing conditions 57
3. Cloning 57
4. Floral-dip transformation of Arabidopsis 58
5. Transformation of bacteria 58
    5.1. *Agrobacterium tumefaciens* transformation 58
    5.2. *Escherichia coli* transformation 59
6. Screening of TRANSPLANTA lines 59
7. Salt tolerance assays 59
8. Seed germination assays 60
9. Root length measurements 60
10. Hormone measurements 60
11. Cytokinin response studies 61

12. Gibberellin response studies 61
13. Shoot apical meristem size 61
14. Root meristem size and root hairs formation 62
15. Protein expression studies 62
16. Protein interaction studies 63
16.1. Yeast-Two-Hybrid (Y2H) 63
16.2. Co-immunoprecipitation studies 63
16.3. Bimolecular fluorescence complementation assays 64
17. GUS staining 64
18. Histological sections 65
19. Gene expression analysis 65
19.1 Quantitative real-time PCR 65
19.2. Microarray experiments 66
20. Statistical and bioinformatics analysis 67
RESULTS 77
1. 66% of the candidates interact with DELLA proteins 77
2. Different protein regions mediate interaction with the selected transcription factors 79
3. Selection of WUSCHEL-related Homeobox 9 (WOX9) as the final candidate 81
4. Not all WOX homologues interact with the DELLA proteins 81
5. WOX9 confers tolerance to salt stress 83
6. WOX9 interacts with RGA *in planta* 84
7. RGA binds the C-terminal region of WOX9 85
8. WOX9 interacts with TOPLESS and RGA competes for the interaction 88
9. *WOX9* is expressed in the SAM and root meristems and in floral carpels 89
10. The *stip-2* mutant has a smaller shoot apical meristem and shorter root meristem than Col-0 92
11. Misexpression of *WOX9* leads to root growth defects 95
12. Over-expression of *WOX9* enhances ABA sensitivity in seeds 97
13. *WOX9* over-expression causes a decrease in gibberellin and cytokinin levels 97
14. *WOX9* over-expression leads to an enhanced cytokinin sensitivity and reduced response to gibberellins 100
15. WOX9 controls root hair formation 102
16. WOX9 gene regulated expression 103
DISCUSSION 115
CONCLUSIONS 125
CONCLUSIONES 129
BIBLIOGRAPHY 133
ANNEX 1: SUPPLEMENTAL DATA 147

Abbreviations

2,4-D: 2,4-Dichloro-phenoxyacetic Acid

ABA: Abscisic Acid

ABI3: ABA-Insensitive 3

ABI5: ABA-Insensitive 5

AHK: Histidine Kinases

ALC: Alcatraz

AP: Apetala

ARF: Auxin Response Factor

ARR: Arabidopsis Response Regulator

BAK1: BRI1-Associated Kinase 1

BBX24: B-Box Domain Protein 24

BES1/BZR2: BR-Insensitive-EMS-Suppressor 1

BiFC: Bimolecular Fluorescence Complementation

BIN2: Brassinosteroid Insensitive 2

BKI1: BRI1 Kinase Inhibitor 1

BOI: Botrytis Susceptible1 Interactor

BP: Base Pair

BR: Brassinoesteroid

BRG: BOI-Related Gene

BRI1: Brassinosteroid Insensitive 1

BSL: BSU1-Like

BSU1: BRI1 Suppressor 1

BZR1: Brassinazole-Resistant 1

CDK: Cyclin Dependent Kinase

CDS: Coding Sequence

ChIP: Chromatine Immunoprecipitation

ChIP-seq: ChIP followed by sequencing

Abbreviations

CK: Cytokinin

CLV: Clavata

COI1: Coronative Insensitive 1

CoIP: Coimmunoprecipitation

Col-0: Columbia

CPC: Caprice

CPP: *ent*-Copalyl Diphosphate

CRF: Cytokinin Response Factor

CYC: Cyclin

DDF1: Dwarf and Delayed Flowering 1

DHZ: Dihydrozeatin

EAR: ERF- Associated Amphiphilic Repression

EGL3: Enhancer of Glabra 3

EIN3: Ethylene Insensitive 3

ER: Endoplasmic Reticulum

ERF: Ethylene Response Factor

ET: Ethylene

FC: Fold Change

FLC: Flowering Locus C

GA: Gibberellin

GA_3: Gibberellic Acid

GA2ox: GA 2-Oxidases

GA3ox: GA 3-Oxidases

GA20ox: GA 20-Oxidases

GAF1: GAI-Associated Factor 1

GAI: Gibberellic Acid Insensitive

GGPP: *trans*-Geranyl Geranyl Diphosphate

GID1: Gibberellin Insensitive Dwarf 1

GL: Glabra

GM: Growth Medium

GO: Gene Ontology

GW: Gateway Cassette

HD: Homeodomain

IAA: Auxin Indole Acetic

IDD: Indeterminate Domain

iP: Isopentenyladenine

JA: Jasmonic Acid

JAZ: JA ZIM-domain

KAO: *ent*-Kaurenoic Acid Oxidase

KO: *ent*-Kaurene Oxidase

LD: Long Day

LHRI/II: Leucine Heptad Repeat I/II

LR: Lateral Root

MBP: Maltose Binding Protein

MEP pathway: 2-C-methyl-D-erythritol-4-phosphate pathway

ML1: Meristem Layer 1

MS: Murashige and Skoog medium

MVA pathway: Mevalonate pathway

MW: Molecular Weight

OD: Optical Density

ORF: Open Reading Frame

PAC: Paclobutrazol

PDF2: Protodermal Factor 2

PHY: Phytochrome

Abbreviations

PI: Propidium Iodide

PIF: Phytochrome Interacting Factor

PP2C: Protein Phosphatase Type 2C

PR: Primary Root

PYL: PYR1-Like

PYR: Pyrabactin Resistance 1

QC: Quiescent Center

qRT-PCR: quantitative Real-Time PCR

RAM: Root Apical Meristem

RAP2.3: Related to AP2 3

RCAR: Regulatory Components of ABA Receptor

RGA: Repressor of *ga1-3*

RGL1; 2; 3: RGA-like 1; 2; 3

RLCK: Receptor-Like Cytoplasmic Kinase

ROS: Reactive Oxygen Species

RPM: Revolutions Per Minute

RT: Room Temperature

SA: Salicylic Acid

SAM: Shoot Apical Meristem

SCF: SKP1-Cullin-F-box Complex

SCL: Scrambled

SCL3: Scarecrow Like 3

SCR: Scarecrow

SD: Short Day

SDS-PAGE: Sodium Dodecyl Sulfate Polyacrylamide Gel Electrophoresis

SEM: Scanning Electron Microscope

SHR: Short-Root

SIM: Selected Ion Monitoring

SL: Strigolactones

SLR: Slender Rice 1

SLY: Sleepy

SNE: Sneezy

SnRK: SNF1-Related Protein Kinase

SOD: Zn/Cu Superoxide Dismutases

SOM: Somnus

SPL9: Squamosa Promoter Binding Protein–Like 9

SPT: Spatula

STM: Shootmeristem-Less

SWI/SNF: Switch/Sucrose Nonfermenting

SWI3C: SWI/SNF-type Chromatin Remodeling Complex (CRC) 3

TCP: Teosinte Branched1/Cycloidea/Proliferating Cell Factor

TF: Transcription Factor

TPL: Topless

TPR: TPL-related

TRY: Triptychon

TTG: Transparent Testa Glabra

tZ: *trans*-zeatin

WB: Western Blot

WER: Werewolf

WT: Wild Type

WOX: WUSCHEL-Related Homeobox

WUS: Wuschel

Y2H: Yeast-Two-Hybrid

YFP: Yellow Fluorescent Protein

Introduction

As sessile organisms, plants have to cope with multiple adverse conditions they face in the course of their life. As such, it is not surprising that they evolved complex regulatory mechanisms to sense and adapt to many biotic and abiotic stresses. Plant development, from seed germination to senescence, is determined by the interaction of both internal (hormones levels, circadian rhythm, etc.) and external signals (photoperiod, temperature, etc.). Correct integration of these signals is pivotal for plant survival in a natural environment, in which climatic conditions can largely vary with the year seasons.

Environmental stress has a strong impact in agriculture, because it can seriously compromise crop's productivity. 20% of the global cultivated area is affected by salinity, one of the most devastating abiotic stresses worldwide. In arid and semi-arid climates, soils are often salinized and irrigation aggravates the problem. First, salinity leads to osmotic stress, which is sensed by the plant as nutrient deficiency and drought stress. A second problem of salinity is ion toxicity, as K^+ is replaced by Na^+ in biochemical reactions; in addition, Na^+ and Cl^- provoke notable changes in protein conformation which may result in their inactivation (Shrivastava & Kumar 2015).

The first response of the plant to salinity and osmotic stresses is growth restraint, which in turn affects yield and productivity. Secondly, to increase their tolerance, plants activate a signal transduction cascade involving "the stress hormone" abscisic acid (ABA), which ends in a variety of adaptive changes that prevent plant death.

1. GIBBERELLINS

Gibberellins (GA) are a large family of diterpenoid hormones, out of which only a small number corresponds to bioactive molecules as positive growth regulators, while the rest are inactive precursors or catabolic products. These hormones have been shown in Arabidopsis to play important functions throughout the whole life cycle of the plant, by promoting seed germination, stem elongation, leaf expansion, and flower development, in addition to being implicated in the control of several transition processes, such as shoot apical meristem (SAM) differentiation, juvenile to adult phase transition, or transition from vegetative to reproductive growth (Schwechheimer 2012).

1.1 GIBBERELLIN BIOSYNTHESIS AND CATABOLISM

First steps of GA biosynthesis occur in plastids and end in the production of *ent*-kaurene from *trans*-geranyl geranyl diphosphate (GGPP) via the ent-copalyl diphosphate (CPP) intermediate. GGPP is mostly produced by the plastidic 2-C-methyl-D-erythritol-4-phosphate (MEP) pathway, although the cytosolic mevalonate (MVA) pathway also has a minor contribution (reviewed in Vranová et al. 2013). In Arabidopsis, the enzymes catalyzing these two biosynthetic steps

are encoded by single genes. Mutations in either of them (*ga1* and *ga2*) lead to drastic GA-deficiency symptoms, such as severe dwarfism, failure in seed germination, delayed flowering and male sterility (Koornneef & van der Veen 1980).

The second main step occurs in the endoplasmic reticulum (ER) and involves membrane-associated cytochrome P450 mono-oxygenases. These include *ent*-kaurene oxidase (KO; CYP701A), whose mutation also causes severe GA-deficiency symptoms (Koornneef & van der Veen 1980) and *ent*-kaurenoic acid oxidase (KAO; CYP88A), which is encoded by two largely redundant genes, so that GA-deficiency symptoms are only observed upon mutation of both genes (Regnault et al. 2014). These enzymes convert *ent*-kaurene to GA_{12}, which can then be oxidized in the C-13 to produce the GA_{53} intermediate (13-hydroxylation pathway).

The third phase takes place in the cytosol and starts with GA_{12} and GA_{53}, which are subsequently oxidized by dioxygenase enzymes to GA_4 and GA_1, respectively. In a first step, C-20 is sequentially oxidized to be lost as CO_2 by GA 20-oxidases (GA20ox), whose activity was shown in Arabidopsis to be limiting for bioactive GA production and be encoded by five partially redundant genes (Rieu, Ruiz-Rivero et al. 2008). GA 3-oxidases (GA3ox) catalyze the last reaction to bioactive GA production, involving the 3β-hydroxilation of GA_9 and GA_{20} to produce GA_4 and GA_1, respectively. Four Arabidopsis genes code for GA3ox, of which GA3ox1 and GA3ox2 are involved in vegetative development, whereas all four are expressed in reproductive tissues (Hu et al. 2008; Mitchum et al. 2006) (Figure 1).

GAs are synthesized in young leaves, from which they move to the SAM (Eriksson et al. 2006). In the root, the meristem and elongation zones are the major places of GA biosynthesis (Dugardeyn et al. 2008). Based on the expression pattern of *GA20ox* and *GA3ox* it was concluded that GAs are in general directly produced in the cells where they exert their action (Kaneko et al. 2003). However, GAs have been later found to move in the plant, being recently described that GA_{12} is the major mobile GA, which is transported from root to shoot through the xylem, and from source to sink tissues through the phloem (Regnault et al. 2015; Regnault et al. 2016).

GA signaling down-regulates the expression of three out of five *GA20ox* and the expression of *GA3ox1* (Chiang et al. 1995; Mitchum et al. 2006; Phillips et al. 1995; Rieu, Ruiz-Rivero, et al. 2008), but does not influence earlier steps of the pathway. These hormones also up-regulate the expression of the inactivating enzymes *GA 2-oxidases* (*GA2ox*), and down-regulate the gibberellin receptor (*Gibberellin Insensitive Dwarf 1*; *GID*) genes (Griffiths et al. 2006; Thomas et al. 1999), which indicates that signaling by these hormones is under strong feedback regulation.

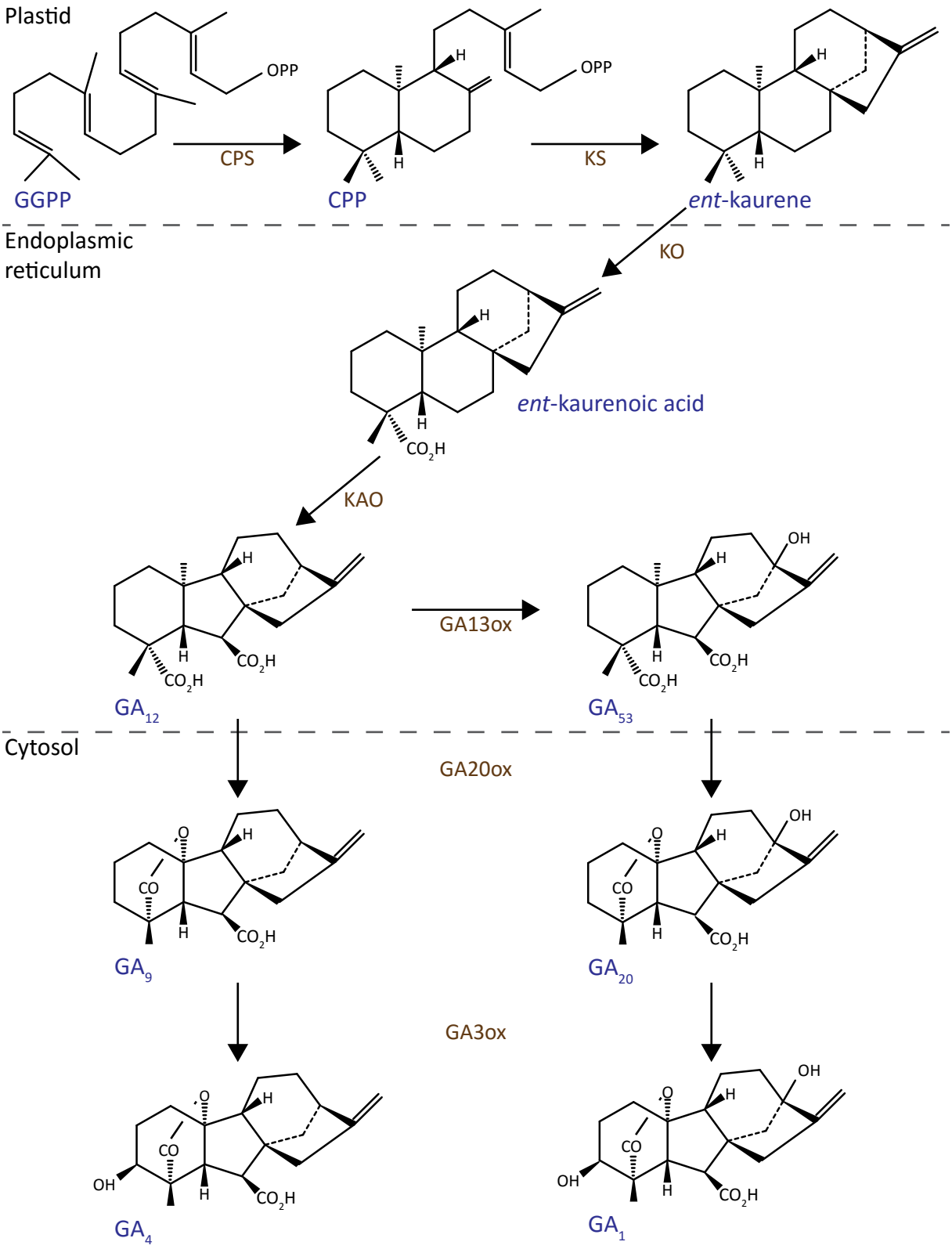

Figure 1. Gibberellin biosynthesis. In plastids, *trans*-geranyl geranyl diphosphate (GGPP) is converted into *ent*-kaurene via the *ent*-copalyl diphosphate (CPP) intermediate and involving the CPP synthase (CPS) and *ent*-kaurene synthase (KS). In the endoplasmic reticulum, *ent*-kaurene is converted via the *ent*-kaurenoic acid into the intermediate GA_{12}, which is oxidized to GA_{53}. Enzymes involved in these steps are *ent*-kaurene oxidase (KO), *ent*-kaurenoic acid oxidase (KAO) and GA 13-oxidases (GA13ox). In the cytosol, GA_{12} and GA_{53} are oxidized by GA 20-oxidases (GA20ox) and GA 3-oxidases (GA3ox) to produced GA_4 and GA_1, respectively (Adapted from Hedden 2016).

Although GA13-/12α oxidases have been recently discussed to reduce GA activity, so far the described inactivating enzymes are: GA2ox, GA-methyltransferases and GA16,17-oxidases. GA2ox convert either bioactive or intermediate GAs into inactive forms by 2β-hydroxylation. There are seven described genes in Arabidopsis (Thomas et al. 1999) and a quintuple mutant shows a GA-overdose phenotype (Rieu, Eriksson, et al. 2008). The GAMT1 and GAMT2 methyltransferases catalyze methylation of the C-6 carboxy group of GAs, by using S-adenosyl-L-methyonine as a methyl donor. Over-expression of these enzymes leads to a GA-deficiency phenotype (Varbanova et al. 2007; Xing et al. 2007). The 16α, 17-epoxidation of non-hydroxylated GAs is catalyzed by CYP714 enzymes, encoded in Arabidopsis by two members, whose over-expression also causes a GA-deficiency phenotype (Nomura et al. 2013; Yingying Zhang et al. 2011). Conjugation of GAs with sugars might also be an inactivation process, although it could also be important for transport or subcellular compartmentalization of these hormones (Schneider & Schliemann 1994).

1.2. REGULATION OF GIBBERELLIN LEVELS

GA levels depend in every moment on the relative expression of the biosynthetic and catabolic enzymes, which is regulated by several different mechanisms. One of these mechanisms is by hormonal crosstalk, with auxin signaling shown to promote GA synthesis (Frigerio et al. 2006). In addition, ABA has an antagonistic effect to GAs, and down-regulates the GA biosynthetic genes, while up-regulates the inactivating enzymes, leading to decreased levels of GAs (Seo et al. 2006). On the other hand, GAs also repress ABA synthesis (Oh et al. 2007). Ethylene (ET) inhibits GA synthesis (Achard et al. 2007; Foo et al. 2006) and GAs in turn exert a negative regulation on ethylene (De Grauwe et al. 2008). Also, brassinosteroids (BR) were shown to induce rice GA biosynthesis (Tong et al. 2014), while in Arabidopsis, BR-insensitive mutants are also insensitive to GAs (Bai et al. 2012; Gallego-Bartolomé et al. 2012). Cytokinins (CK) were reported to activate the expression of *GA2ox* in SAM, suggesting that these hormones inhibit bioactive GA levels, although determination of hormone levels is needed to confirm this negative function (Jasinski et al. 2005).

Light regulates several developmental processes by inducing changes in hormonal levels. In seeds, light promotes ABA degradation and GA synthesis, inducing a shift in the relative levels of these hormones that is required for germination (Ogawa et al. 2003; Seo et al. 2006). After germination, seedling de-etiolation requires degradation of GAs, which is mediated by light (Symons et al. 2008; Zhao et al. 2007). Likewise, induction of GA synthesis in response to long day (LD) photoperiods plays a relevant role in flowering transition (reviewed in Mutasa-Göttgens & Hedden 2009).

During seed maturation, cold treatments induce GA inactivation (Kendall et al. 2011), which leads to increased seed dormancy, while low temperatures right after imbibition

(stratification) activate the expression of *GA20ox* and *GA3ox*, and repress that of *GA2ox*, promoting GA accumulation and thus germination (Yamauchi et al. 2004; Yamauchi et al. 2007). Similarly, in young seedlings, high temperatures activate biosynthetic while repress GA catabolic gene expression, hence promoting hypocotyl growth (Stavang et al. 2005).

Moreover, GA levels decrease in response to abiotic stresses, and the role of this regulation in the activation of stress-related pathways will be discussed below (reviewed in Colebrook et al. 2014).

1.3 GIBBERELLIN SIGNALING

GAs are sensed by the GID1 receptor, a soluble protein that shares similitude with bacterial α/β- hydrolases and is distributed in the nucleus and cytosol. In Arabidopsis, this receptor is encoded by three genes: *GID1a*, *GID1b* and *GID1c*, whose products show the greatest affinity for GA_4 (Nakajima et al. 2006). While single mutations do not produce any visible phenotype, double and triple mutants cause strong dwarfism, indicating a functional redundancy of these genes (Griffiths et al. 2006; Iuchi et al. 2007; Willige et al. 2007). Bioactive GAs bind the N-terminal domain of GID1 and promote a conformational change of the protein such that allows its interaction with the so-called DELLA motif, at the N-terminus of the DELLA proteins, which act as central repressors of the pathway (Murase et al. 2008).

GID1-DELLAs interaction induces a conformational change in the DELLA proteins and allows their recognition by the E3 ubiquitin ligases SCF^{SLY1} or SCF^{SNE} (SKP1-CULLIN-F-box complex with F-box SLEEPY1 or SNEEZY), which ubiquitinate these repressors and mark them for degradation by the 26S proteasome (McGinnis et al. 2003; Strader et al. 2004). Mutation in the F-box SLY1 leads to a GA-insensitive phenotype (McGinnis et al. 2003) in opposite to SNE mutations (Ariizumi & Steber 2011), hence indicating that the role of SNE is minor. Besides triggering DELLAs degradation, GID1-DELLA interaction is sufficient to inactivate these repressors (Ariizumi et al. 2008), which explains the relatively mild phenotype of *sly* mutants.

DELLAs belong to the plant specific GRAS family, whose members share a conserved C-terminus comprised by related Leucine Heptad Repeat I (LHRI), VHIID, LHRII, PFYRE and SAW motifs. The DELLA repressors differ from the rest of GRAS proteins in their N-terminal domain which contains the DELLA and TVHYNP motifs, shown to mediate interaction with GID1. In Arabidopsis there are five DELLA genes: *REPRESSOR OF ga1-3* (*RGA*), *GA-INSENSITIVE* (*GAI*), *RGA-like 1* (*RGL1*), *RGL2* and *RGL3* (Cheng et al. 2004; Lee et al. 2002; Peng et al. 1997; Silverstone et al. 1998; Wen & Chang 2002). RGA and GAI interact preferentially with GID1b, while RGL1, RGL2 and RGL3 do it with GID1a (Suzuki et al. 2009).

2. THE DELLA PROTEINS: CENTRAL REPRESSORS OF THE GIBBERELLIN SIGNALING PATHWAY

These five genes have been shown to be partially redundant, although they were also independently associated to different developmental processes. RGA and GAI, for instance, control root and shoot elongation, leaf expansion, and flowering (Cao et al. 2006; Cheng et al. 2004; Dill & Sun 2001; Fu & Harberd 2003; King et al. 2001; Silverstone et al. 1997). RGL2 is involved in seed germination and flower development (Cheng et al. 2004; Lee et al. 2002; Tyler et al. 2004), while RGL3 plays a minor role in germination (Piskurewicz & Lopez-Molina 2009) and is up-regulated in response to biotic and abiotic stresses (Achard, Gong, et al. 2008; Colebrook et al. 2014; Wild et al. 2012).

In the nucleus, DELLAs suppress GA-regulated gene expression by interaction with a wide variety of transcription factors (TF) and other regulators. These repressors were initially shown to block transcriptional activity of their partners, by forming an inactive complex unable to bind DNA, which is known as the sequestration model. More recently, they were also found to contribute to up-regulated expression of the downstream targets of some interacting partners (co-activation model). Although the inactivation or sequestration mechanism mediates growth inhibitory effects of DELLAs accumulation, co-activation is emerging as a further relevant mechanism that mediates increased tolerance to abiotic stresses, and is also involved in the control of other developmental processes.

2.1 DELLAs BIND AND INACTIVATE A WIDE RANGE OF TRANSCRIPTION REGULATORS.

DELLAs interact with a wide variety of proteins to block their function and thus repress GA signaling. The first identified TFs controlled by DELLAs through a sequestration mechanism were PHYTOCHROME INTERACTING FACTORs 3 and 4 (PIF3 and PIF4), which belong to the bHLH family of TFs and were reported to promote hypocotyl elongation (de Lucas et al. 2008; Feng et al. 2008; detailed below). Besides PIFs, other TFs of the same clade also interact with the DELLAs, as is the case of ALCATRAZ (ALC) that regulates fruit patterning (Arnaud et al. 2010) or SPATULA (SPT), involved in cotyledon expansion (Josse et al. 2011). Despite belonging to a different clade, MYC2, GLABRA 3 (GL3) AND ENHANCER OF GLABRA 3 (EGL3) are other bHLH found to interact with the DELLA proteins to control volatile production in flowers (MYC2; Hong et al. 2012) and trichome development (GL3, EGL3), a developmental process controlled by the DELLAs also through interaction with the MYB factor GLABRA 1 (GL1) (Qi et al. 2014). Many other proteins have been described as interactors of DELLAs, such as SQUAMOSA PROMOTER BINDING PROTEIN-LIKE 9 (SPL9) that controls flowering (Yu et al. 2012); MERISTEM LAYER 1 (ML1) and PROTODERMAL FACTOR 2 (PDF2) to regulate seed germination (Rombolá-Caldentey et al. 2014); BRASSINAZOLE-RESISTANT 1 (BZR1)/BRI1-EMS-SUPPRESSOR 1 (BES1/BZR2) to

repress hypocotyl elongation (Bai et al. 2012; Gallego-Bartolomé et al. 2012; Li et al. 2012); PICKLE, which plays an important role in hypocotyl growth (Zhang et al. 2014); ETHYLENE INSENSITIVE 3 (EIN3) and RELATED TO AP2 3 (RAP2.3) involved in apical hook development (An et al. 2012; Marín-de la Rosa et al. 2014); SCARECROW LIKE 3 (SCL3), shown to play an important role in seed germination and in root and shoot elongation (Z.-L. Zhang et al. 2011); FLOWERING LOCUS C (FLC) that controls flowering (M. Li et al. 2016); TEOSINTE BRANCHED1/ CYCLOIDEA/PROLIFERATING CELL FACTORs (TCP) which regulate seed germination and shoot meristem activity (Davière et al. 2014; Resentini et al. 2015); Jasmonic Acid (JA) ZIM-domain 1 (JAZ1) which controls JA signaling (Hou et al. 2010; Wild et al. 2012); and the regulator B-BOX DOMAIN PROTEIN 24 (BBX24), which releases PIF4 from DELLAs to the activation of shade avoidance responses (Crocco et al. 2015) (Figure 2A).

2.2 DELLAs AS TRANSCRIPTIONAL ACTIVATORS

Besides being involved in inactivation of several TFs, DELLAs have been shown to actively modulate transcription. As they do not have a DNA-binding motif, this regulation must be mediated through the interaction with different TFs, which provide DNA recognition ability to the complex. Microarray studies revealed that the DELLA-dependent transcriptome is involved in seed germination and flower development (Cao et al. 2006), in seedlings regulated gene expression (Zentella et al. 2007), and in the response to salt stress (Achard, Renou, et al. 2008). Although different studies contributed to the identification of a specific set of DELLA regulated genes, overlapping between these datasets is very low, but still shows that DELLAs repress expression of genes related with cell wall reorganization, activate ABA and ethylene–regulated responses and reduce reactive oxygen species (ROS) accumulation. Zentella et al. (2007) also confirmed that eight of these genes are direct targets of RGA. Among them, XERICO has been described by having a role in drought responses activating ABA biosynthesis (Ko et al. 2006), meaning that DELLAs enhance ABA synthesis through the activation of *XERICO* expression. In large scale analysis, putative DELLA-direct targets were as well identified by chromatin immunoprecipitation followed by sequencing (ChIP-seq), which revealed that these represors activate transcription through the interaction with TFs of 12 different families (bZIP, DOF, GARP-ARR, GARP-G2, HD-ZIP, HD-WUS, IDD, MADs, MYB, MYC, WRKY, YABBY). One example of such co-activation function is the interaction of DELLAs with the ARABIDOPSIS RESPONSE REGULATOR 1 (ARR1), which plays an important role in root meristem maintenance and in skotomorphogenesis (Marín-de la Rosa et al. 2015). Additional processes regulated by a co-activation mechanism are the response to high temperature in seeds, where DELLAs interact with ABA-insensitive 3 (ABI3) and 5 (ABI5) to activate the expression of *SOMNUS* (*SOM*) and inhibit germination (Lim et al. 2013), and in floral transition, where DELLAs interact with SQUAMOSA PROMOTER BINDING PROTEIN–LIKE 9 (SPL9) to activate *APETALA 1* (*AP1*) expression (Yamaguchi et al. 2014). Last, DELLAs interact with the INDETERMINATE DOMAIN

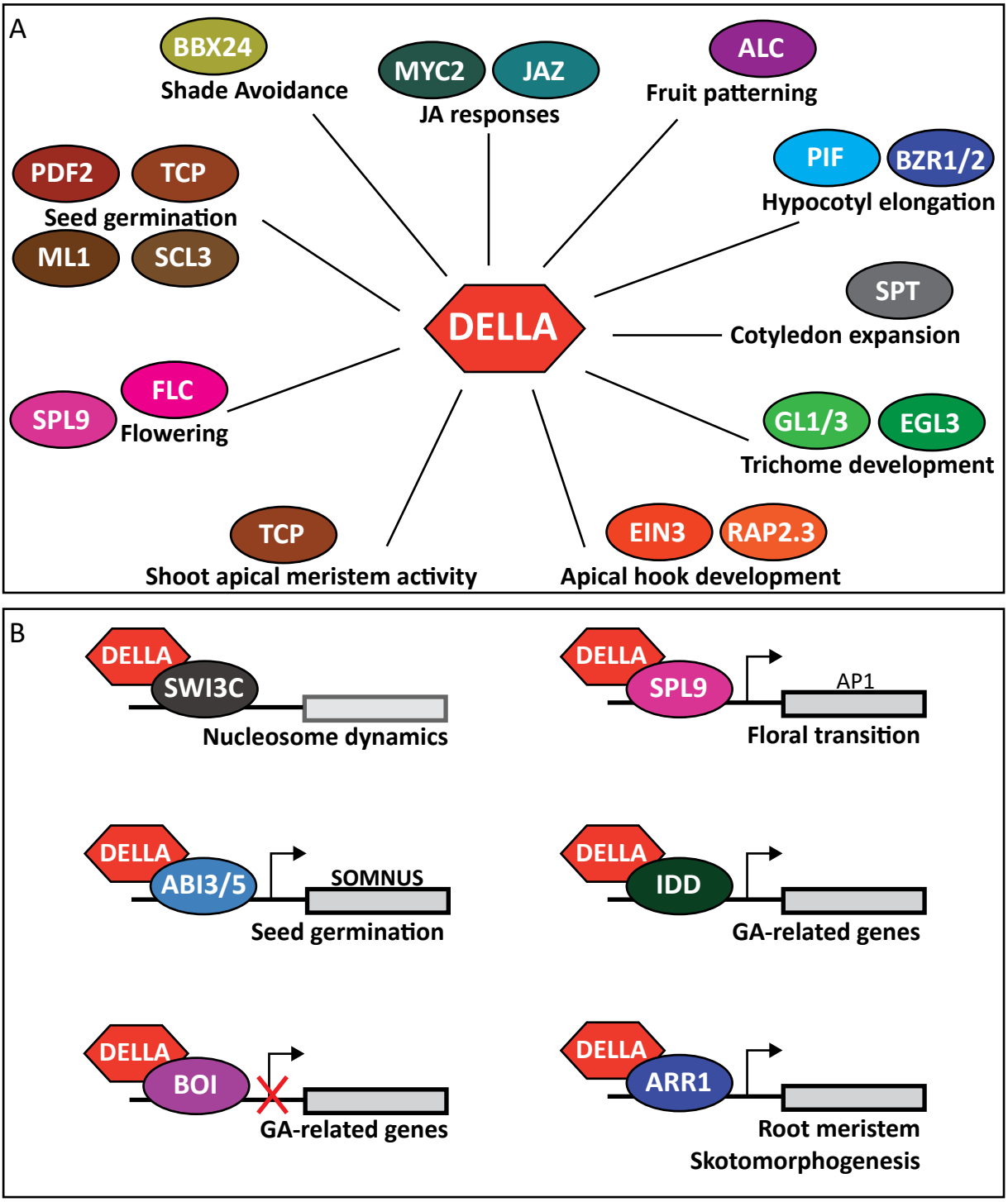

Figure 2. DELLAs mechanism of action (A) DELLAs interact with a wide range of transcriptional regulators to inhibit their action and thus control several processes such as jasmonic acid (JA) responses (MYC2, JAZ), fruit patterning (ALC), hypocotyl elongation (PIF, BZR1/2), cotyledon expansion (SPT), trichome development (GL1/3, EGL3), apical hook development (EIN3, RAP2.3), shoot apical meristem activity (TCP), flowering (FLC, SPL9), seed germination (PDF2, SCL3, ML1, TCP), shade avoidance (BBX24). (B) Reported interactors through which DELLAs directly modulate transcription to control nucleosome dynamics (SWI3C), seed germination (ABI3/5), gibberellin (GA)-related genes (BOI, IDD), floral transition (SPL9), root meristem and skotomorphogenesis (ARR1). DELLAs general mechanism is activation of transcription, but in the case of SWI3C, which is a chromatin remodelator, and BOI, which represses transcription in collaboration with DELLAs.

(IDD) factors to activate GA biosynthesis-related genes as shown for GAI-ASSOCIATED FACTOR 1 (GAF1; Fukazawa et al. 2014) and IDD3, 4, 5, 9, 10 (Yoshida et al. 2014) (Figure 2B).

Although this model of DELLAs action mostly explains activated gene expression by the DELLAs, these repressors were also shown to interact with BOTRYTIS SUSCEPTIBLE1 INTERACTOR (BOI), BOI-RELATED GENE1 (BRG1), BRG2, and BRG3 to bind as a complex with these factors the promoters of GA-related genes and repress their expression (Park et al. 2013). Moreover, DELLAs also regulate transcription by controlling nucleosome dynamics through the interaction with Switch (SWI)/Sucrose Nonfermenting (SNF)-type chromatin remodeling complex (CRC) 3 (SWI3C; Sarnowska et al. 2013) (Figure 2B).

Thus, DELLAs seem to interact with different DNA-binding proteins to activate transcription. This activation ability has been proven in SLENDER RICE 1 (SLR1) to rely on conserved motifs located at the N-terminus of the protein (i.e. the DELLA and TVHYNP motifs) (Hirano et al. 2012; Ogawa et al. 2000). Furthermore, it has been established that RGA binds to the regulatory DNA regions (2500bp up- or 500bp downstream of the gene) of at least 421 genes (Marín-de la Rosa et al. 2015).

Interaction with the DELLA repressors, regardless if it results in inhibition or activation of transcription, occurs through the conserved GRAS domain, except for JAZ1, in which the N-terminal region has some role (Hou et al. 2010). The LHRI motif is also important in many reported interactions, e.g. PIF4, BZR1, MYC2, JAZ1, EIN3 (An et al. 2012; Gallego-Bartolomé et al. 2012; Hong et al. 2012; Hou et al. 2010) as the SAW and/or PFYRE domains are for the interaction with BZR1, MYC2, and EIN3 (An et al. 2012; Gallego-Bartolomé et al. 2012; Hong et al. 2012).

2.3 DELLAs CROSSTALK WITH OTHER HORMONE PATHWAYS

Auxin promotes the synthesis of GAs and this seems to mediate the crosstalk between the auxin and GA pathways. Several GA responsive genes are also regulated by auxin, but auxins do not seem to have a direct effect on DELLA stability (Chapman et al. 2012). Ethylene is reported to facilitate DELLA accumulation by decreasing GA levels (Achard et al. 2007; De Grauwe et al. 2008; Vandenbussche et al. 2007). ABA protects DELLA degradation by GAs, although this effect was only observed for a tagged RGA, and not the endogenous protein (Zentella et al. 2007).

DELLAs physically interact with many regulators of other hormone pathways. DELLA crosstalk with BR signaling occurs by the interaction with BZR1/BZR2 (Bai et al. 2012; Gallego-Bartolomé et al. 2012; Li et al. 2012), which mediates hypocotyl elongation and will be discussed in the following section. DELLAs bind EIN3 and RAP2.3 (An et al. 2012; Marín-de la Rosa et al.

2014), which are positive regulators of ethylene signaling, and impair their interaction with DNA, thus repressing the ethylene pathway. They also bind the JAZ proteins, which act as repressors of the jasmonic acid (JA) pathway (Hou et al. 2010; Wild et al. 2012), and modulate in this way defence response to necrotrophic pathogens (detailed below). In seeds, DELLAs were shown to interact with the TFs ABI3 and ABI5 to activate the transcription of *SOMNUS*, and thus positively regulate ABA signaling (Lim et al. 2013).

2.4 DELLA-PIF INTERACTION SUPPRESSES HYPOCOTYL GROWTH (Figure 3)

PIF4 plays a central role in the control of hypocotyl growth. Nuclear levels of this factor are regulated by phytochromes (PHYB) that signal PIF4 phosphorylation and its degradation by the 26S proteasome(Chen & Chory 2011). In the dark, PIF4 accumulates and binds to conserved G-box (CACGTG) or E-box (CANNTG) elements in the promoters of its target genes, which are mostly involved in cell wall loosening and auxin biosynthesis and signaling, to activate their expression (Hornitschek et al. 2012; Oh et al. 2012; Pfeiffer et al. 2014; Zhang et al. 2013).

Accumulation of DELLAs inhibits growth by interfering with PIF4 activity. When GA levels are low, DELLAs accumulate in the nucleus and interact with the PIFs bHLH domain, blocking these factors. After GA synthesis, DELLAs are degraded and PIFs are released, and they can bind and activate their target genes (de Lucas et al. 2008; Feng et al. 2008). Besides this sequestration mechanism, it has been recently reported that DELLAs also promote degradation of PIFs through the 26S proteasome (K. Li et al. 2016).

Brassinosteroids act coordinately with GAs to regulate hypocotyl growth. One point of convergence of these two pathways are the DELLAs, as they have been shown to interact with the BZR1/BZR2 factors and sequester them into an inactive form, in a similar way as reported for PIFs (Bai et al. 2012; Gallego-Bartolomé et al. 2012; Li et al. 2012). BZR1/BZR2 activity is essential for BR-regulated gene expression. In the absence of BRs, the GSK3-like kinase BRASSINOSTEROID INSENSITIVE 2 (BIN2) phosphorylates these TFs, targeting them for degradation, which leads to suppressed growth (He et al. 2002; Yin et al. 2002). Our group published that besides BZR1/BZR2, BIN2 also phosphorylates PIFs, which are then degraded by the 26S proteasome (Bernardo-García et al. 2014). BRs are sensed by BRASSINOSTEROID INSENSITIVE 1 (BRI1), a leucine-rich repeat receptor kinase (LRR-RK) that localizes in the plasma membrane. Upon BRs recognition, BRI1 interacts with its co-receptor BRI1-ASSOCIATED KINASE 1(BAK1) and phosphorylates BRI1 KINASE INHIBITOR 1 (BKI1), which interacts with the kinase domain of BRI1, and prevents its interaction with BAK1. Phosphorylation of BKI1 promotes its dissociation from the plasma membrane and enables BRI1 and BAK1 interaction, which then phosphorylate each other. This activates a phosphorylation cascade that involves the receptor-like cytoplasmic kinase (RLCK) protein family and terminates in the phosphorylation of BRI1 SUPPRESSOR 1/BSU1-LIKE (BSU1/BSL) (Belkhadir & Jaillais 2015). This phosphatase acts as a

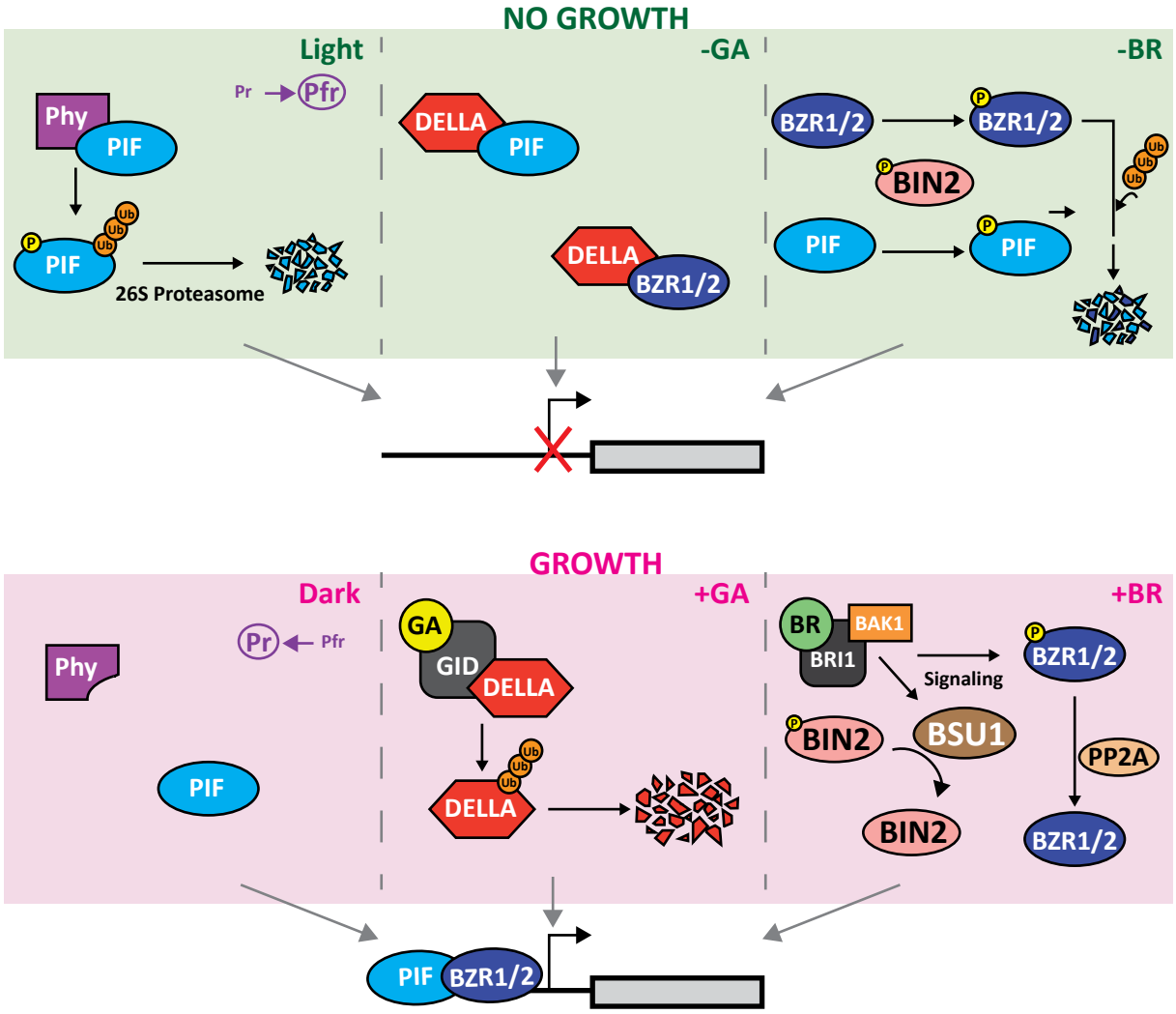

Figure 3. Function of PIF4 in integrating light, brassinoesteroid (BR), and gibberellin (GA) signals. In the light, PhyB is in its active form and translocated into the nucleus, where it interacts with PIF4, triggering PIF4 ubiquitination and degradation by 26S proteosome. In the dark, PhyB is in its inactive cytosolic form, PIF4 accumulates and binds to the promoters of its target genes. In the absence of GAs, DELLAs accumulate. These repressors interact with PIF4 and block its DNA binding ability. In the presence of GAs, DELLAs are destabilized and PIF4 is free to regulate its downstream targets. BRs are required for PIF4 regulated expression. Without BRs, the negative regulator BIN2 kinase is active and phosphorylates PIF4, destabilizing this factor. In the presence of BRs, BIN2 is inactivated and PIF4 accumulates. Besides, the nuclear accumulation of the BZR1/2 factors, regulated by DELLAs and BRs, contributes to PIF4 regulated gene expression through formation of a co-activator complex with PIF4.

positive regulator of BR signaling by dephosphorylating BIN2 at Tyr200 and inactivating this kinase, which means that BZR1/BZR2 and PIFs are then stabilized, so they bind the promoters of their target genes to mediate BR-regulated gene expression (Kim et al. 2009).

PIF4 and BZR1/BZR2 have been shown to bind as a transcriptional co-activation complex the promoters of their target genes. Actually, there is a strong overlap between GA and BR activated gene expression, and is now fully accepted that DELLA-PIFs-BES1/BZR1 interaction has a major role in the control of cell elongation growth (Oh et al. 2012).

2.5 ROLE OF DELLAs IN STRESS

2.5.1 BIOTIC STRESS

JA mediates defense against necrotrophic pathogens. JAZ proteins act as negative regulators of the JA pathway by blocking transcriptional activity of the MYC2 factors, responsible for activating JA-regulated gene expression (Chini et al. 2007). The E3-ligase CORONATIVE INSENSITIVE 1 (COI1) functions as JA receptor, and in response to JA it interacts with the JAZs and marks these repressors for degradation by the 26S proteasome. JAZs degradation releases MYC2 from inhibition by these repressors, so that MYC2 can bind DNA and activate JA-responsive genes. DELLAs and JAZs interaction controls the balance between JA-mediated biotic responses and growth. In normal conditions, JAZs repress JA signaling by interacting with MYC2, but also promote growth by interacting with DELLAs, which allows free PIF4 and BZR1/BZR2 nuclear accumulation and activation of genes with a role in cell elongation. On the other hand, after a pathogenic attack, JA accumulates and triggers JAZs degradation. In the absence of JAZs, MYC2 can activate JA responses, but at the same time DELLAs accumulate free in the nucleus, thus sequestering PIF4 and the BES1/BZR1 factors, which leads to growth inhibition (reviewed in Hou et al. 2013; Figure 4).

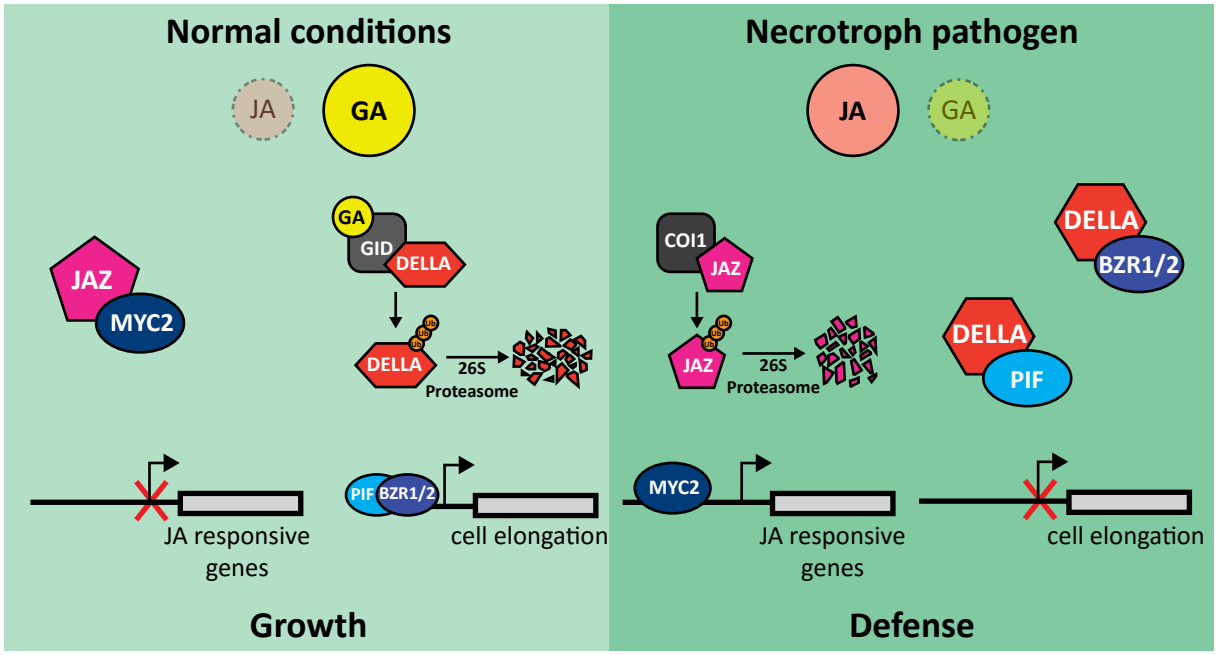

Figure 4. Equilibrium between growth and defense to pathogens. In normal conditions, when gibberellins (GA) are accumulated, DELLAs are degraded, and PIFs and BZR1/2 can bind their target gene promoters. Besides, JAZ can bind MYC2 and block its function. The coordination of these two leads to growth. When a necrotroph pathogen attacks, jasmonic acid (JA) is accumulated. This triggers the degradation of JAZs, so MYC2 can activate the transcription of its target genes. At the same time, GA levels decrease, so DELLAs accumulate and block PIFs and BZR1/2. In this situation growth genes are not expressed and JA-responsive ones are, allowing the plant to defense itself at the expense of growth.

2.5.2. ABIOTIC STRESS

In response to osmotic stresses ABA accumulates. This "stress" hormone binds the PYRABACTIN RESISTANCE 1 (PYR1)/ PYR1-LIKE (PYL)/ REGULATORY COMPONENTS OF ABA RECEPTOR (RCAR) receptors, and induces a conformational change in these proteins that allows their interaction with the protein phosphatases type 2C (PP2C), which act as main repressors of the pathway. This interaction allows activation of the PP2C-suppressed SNF1-related protein kinases (SnRK) that then phosphorylate themselves and other downstream regulators, activating the ABA signaling pathway. In the absence of ABA, PP2Cs dephosphorylate and inactivate SnRKs, blocking the signaling cascade (Umezawa et al. 2010). In addition to its role in stress, ABA controls acquisition of desiccation tolerance during seed maturation and maintenance of seed dormancy, while the antagonistic function of GAs is essential for seed germination (Sah et al. 2016). In response to stress, GA levels decrease and this reduction has a relevant role in stress adaptation as indicated by the finding that GA-deficient mutants are more tolerant to osmotic stress, while mutants with higher GA levels display a hypersensitive response (Achard et al. 2006; Colebrook et al. 2014). The inhibitor of GA synthesis paclobutrazol (PAC) increases tolerance to salt and osmotic stresses in different species, such as wheat or groundnut (Hajihashemi et al. 2007; Sankar et al. 2007). As inhibitor of GAs, PAC treatment induces the accumulation of DELLAs, hence pointing to a function of these repressors as positive regulators of abiotic stress responses.

In response to high salinity, DWARF AND DELAYED FLOWERING 1 (DDF1) has been shown to activate the expression of *GA2ox7*, which leads to a reduction in GA levels and thus to DELLA accumulation (Magome et al. 2008). DELLAs are also stabilized by sumoylation, with mutants lacking SUMO-peptidase activity being shown to be more tolerant to drought and salt stress (Conti et al. 2014). The quadruple DELLA (*qdella*) mutant (which lacks RGA, GAI, RGL1 and RGL2) is more sensitive to salt than the wt, while mutants that accumulate DELLAs, such as *gai* (insensitive to GA) and *ga1-3* (GA deficient) are more tolerant. Accumulation of DELLAs upon salt stress is also mediated by ethylene, whose signaling pathway ends in the stabilization of ETHYLENE INSENSITIVE 3 (EIN3), which enhances DELLAs function (Achard et al. 2006). In response to osmotic stress, ETHYLENE RESPONSE FACTOR 6 (ERF6) activates the expression of *GA2ox6* (Dubois et al. 2013) and reduces bioactive GA levels. This leads to DELLA accumulation and to an arrest of growth. These repressors have been shown to control mitotic exit in favor of endoreduplication in leaves (Claeys et al. 2012), in addition to promoting survival by decreasing ROS production through the up-regulation of Zn/Cu superoxide dismutases and catalases, which delay cell death (Achard, Renou, et al. 2008). As mentioned above, DELLAs also activate the expression of XERICO, which induces ABA accumulation (Ko et al. 2006). Last, the levels of cytokinins (CK), antagonistic to ABA, decrease in response to stress (Nishiyama et al. 2011) (Figure 5).

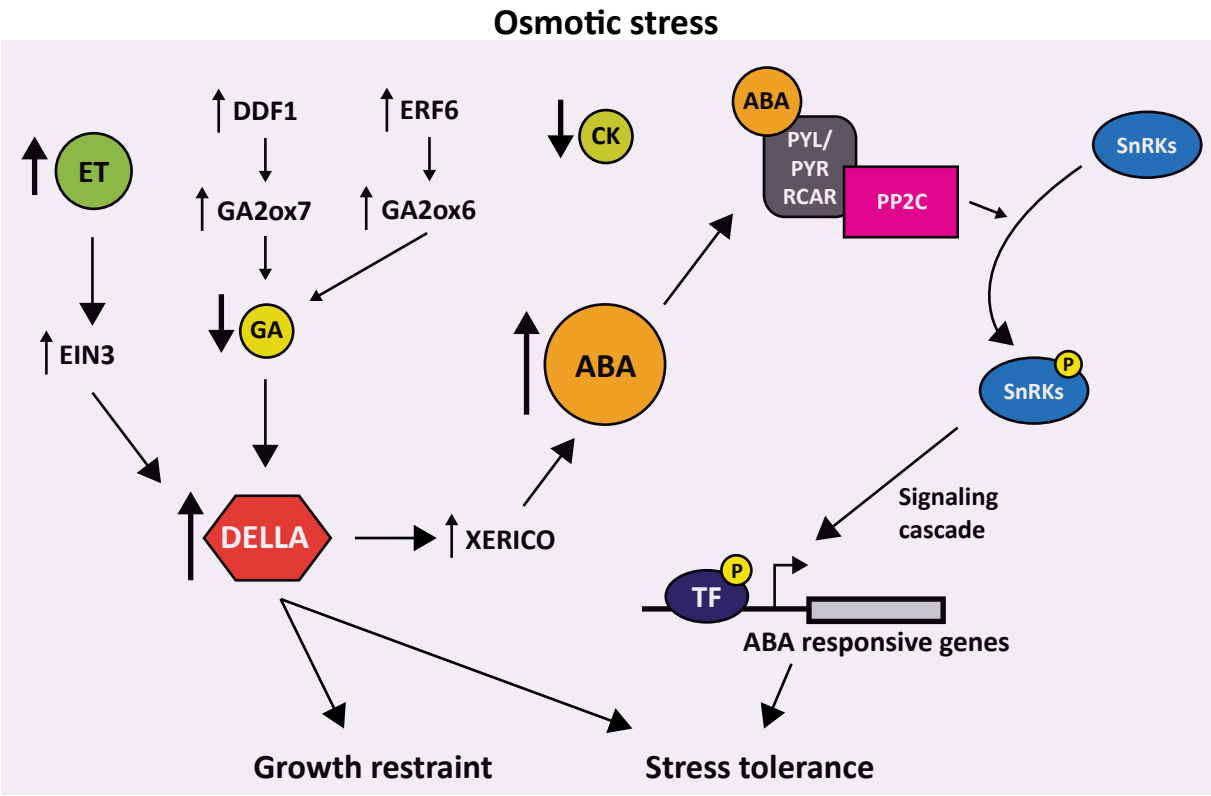

Figure 5. GA-related response to osmotic stress. Different hormone signaling pathways play a role in response to osmotic stress. DDF1 and ERF6 accumulate and activate the degrading GA-enzymes GA2 oxidases 7 and 6, respectively, which turns into a decrease in gibberellin (GA) levels, promoting DELLA accumulation. Ethylene (ET) levels increase, which activates its signaling pathway, involving EIN3, which promotes DELLAs accumulation. Cytokinin (CK) levels decrease and ABA synthesis is rapidly induced in response to osmotic stress. DELLAs contribute to ABA accumulation through XERICO. ABA binds to the receptor PYL/PYR/RCAR, which can then bind the PP2C phosphatases. The kinases SnRKs are then released and can autophosphorylate and phosphorylate other transcription factors (TF) to activate ABA-responsive genes, which promote stress tolerance acquisition, also mediated by DELLAs. So far, the best described role of DELLAs in response to stress is arresting growth.

3. WUSCHEL-related HOMEOBOX 9 (WOX9)

3.1 THE WOX HOMEODOMAIN FAMILY

Homeobox transcription factors are characterized by having a conserved 60 amino acids DNA-binding domain, called the homeodomain (HD), which is comprised by three α-helices, the second and third of these helices forming a helix-turn-helix structure. Compared to animals, plant HDs frequently have insertions among the helices. Based on their conserved domains, plant homeobox factors can be classified into different classes: HD-ZIP I-IV, PLINC Zinc Finger, TALE (KNOX and BEL), WOX, DDT, PHD, LD and SAWADEE. In Arabidopsis there have been identified 110 homeobox genes, 14 of which belong to the WOX class. Members of WOX class include in their HDs extra amino acids between the first and second (1-2) or second and third (4-5) helices, respectively (Mukherjee et al. 2009).

The WUSCHEL (WUS)-related homeobox (WOX) family can be sub-divided in three clades: the WUS or modern clade (WUS, WOX1-7), which is only present in higher flowering plants; the intermediate clade (WOX8, 9, 11 and 12), present in vascular plants; and the ancient clade (WOX10, 13 and 14), which is common to all plant kingdom. WOX proteins are characterized by having a larger HD (66 amino acids in the case of WUS, 65 in WOX), in addition to a conserved WUS-box, and one or several ETHYLENE RESPONSE FACTOR (ERF)-associated amphiphilic repression (EAR) motifs or EAR-like motifs (two EAR-like motifs and three L-X-L repeats in WOX9). Besides, the WOX9-clade has a conserved C-terminal domain (Haecker et al. 2004; van der Graaff et al. 2009).

In general, expression of WOX family members is associated with meristems. WUS is pivotal to the maintenance of floral and shoot apical meristems by promoting stem cell fate (Laux et al. 1996; Mayer et al. 1998). All members of the modern clade except WOX4 can replace WUS in this function, the canonical WUS-box and acidic domain being shown to be required for stem cell maintenance and gynoecium development, respectively (Dolzblasz et al. 2016). *WOX5* is expressed in the root quiescent center (QC) and its function in root meristem maintenance is interchangeable with WUS (Sarkar et al. 2007). WOX1 also controls SAM development, by regulating polyamine homeostasis (Yanxia Zhang et al. 2011) and WOX9 promotes cell division both in the SAM (in part by WUS activation via a sucrose-dependent pathway) and root meristem (Wu et al. 2005).

Leaving aside the SAM and root apical meristem (RAM), every developing organ requires a meristematic activity for cell division and its *de novo* formation and WOXs have been implicated in several of these processes. During embryogenesis, WOX9 is essential for cell division and WOX8 acts redundantly with WOX9. Besides, WOX2 is critical to shoot patterning, while WOX1, 3, 5 and 8 play minor and redundant roles (Breuninger et al. 2008; Lie et al. 2012; Wu et al. 2007). In roots, WOX7 inhibits lateral root (LR) initiation by repressing expression of cell cycle genes (Kong et al. 2016), whereas WOX11 and WOX12 are both important for *de novo* root organogenesis (Liu et al. 2014). WOX4 is a cambium regulator in the hypocotyl (Hirakawa et al. 2010) and stem (Suer et al. 2011) and controls redundantly with WOX14 vascular cell division (Etchells et al. 2013). WOX2 and WOX8 control cotyledon boundaries formation (Lie et al. 2012) and WOX1 and WOX3 regulate lateral development in leaves (Nakata et al. 2012) and flowers (Costanzo et al. 2014). WOX6 controls ovule development (Park et al. 2005) and last, WOX13 regulates fruit development by promoting formation of the replum (Romera-Branchat et al. 2013) (Table 1).

3.2 WOX9 REGULATES CYTOKININ SIGNALING

Regarding WOX9, this factor has been reported to act downstream of CK signaling, by activating the expression of type-A ARRs, and CYTOKININ RESPONSE FACTORS (CRF) (Skylar et

al. 2010). In addition, the *WOX9 stip-1* mutant was shown to be hypersensitive to CKs in de-etiolation experiments in the dark (Skylar & Wu 2010), which suggests different roles of the WOX9 factor in light and dark. WOX9 promotes cell division by activating *CYCB1;1* and *CDKB1;1* expression during the G2 to M transition, and this regulation is dependent on sugar signals (Skylar et al. 2011).

Indeed, CKs are adenine derivatives that control growth by promoting cell division. During CK biosynthesis, the isoprenoid side chain of isopentenyladenine (iP) is hydroxylated in the *trans*-terminal position to produce the most abundant CK in Arabidopsis, *trans*-zeatin (tZ), which is then reduced to produce dihydrozeatin (DHZ). CKs are reversibly inactivated by conjugation to glucose or irreversibly inactivated by oxidation (Kieber & Schaller 2014). In response to osmotic stress, CK levels were shown to decrease and lines with reduced CK levels, such as the *ipt1357* mutant (with a loss-of-function in biosynthetic genes) or *35S::CKX* over-expressers (expressing any of the CK oxidase catabolic enzymes) to be more tolerant to salt and drought (Nishiyama et al. 2011), hence pointing to a negative role of CKs in abiotic stress responses. Conversely, the CK receptor ARABIDOPSIS HISTIDINE KINASE 1 (AHK1) was reported to be a positive regulator of osmotic responses, in contrast to AHK2, 3, and 4 that would not play any role (Tran et al. 2007). More recently, a role for AHK2 in positive regulation of responses to salt has also been reported (Kumar & Verslues 2015), which shows that the role of CKs in salt stress is not yet clear. It is quite possible that CK feed-back regulation mediates increased tolerance to salt stress, but this role remains to be established.

Table 1. Reported functions of WOX **family members**

Member	Function
WUS	shoot apical meristem (SAM)
WOX1	SAM; embryogenesis; lateral development
WOX2	embryogenesis; cotyledon boundary
WOX3	embryogenesis; lateral development
WOX4	cambium
WOX5	embryogenesis; root meristem
WOX6	ovule development
WOX7	lateral root formation
WOX8	embryogenesis; cotyledon boundary
WOX9	SAM; embryogenesis
WOX10	-
WOX11	root organogenesis
WOX12	root organogenesis
WOX13	fruit development
WOX14	cambium

3.3 WOX PROTEINS ARE TRANSCRIPTIONAL REPRESSORS

WUS and other members of the gene family have been described as repressors of transcription (van der Graaff et al. 2009). In the case of WUS, the WUS-box is essential for this repression activity, and the EAR-like motif is also important (Ikeda et al. 2009; Kieffer et al. 2006). Because the co-repressor TOPLESS (TPL) was shown to interact with transcriptional repressors through their conserved EAR domains (Szemenyei et al. 2008), repressor activity of members of the WOX family could be mediated by TPL. As a matter of fact, TPL and TPL-related 4 (TPR4) were initially identified as WUS interactors (Kieffer et al. 2006). However, although all WOX family members have EAR or EAR-like motifs, the only WOX factors shown to interact with TPL to the date are WOX2 and WOX4 (Arabidopsis Interactome Mapping Consortium 2011; Causier et al. 2012).

Also, despite WUS is accepted to be a repressor, it activates the expression of *CLAVATA3* (*CLV3*) in the SAM (Yadav et al. 2011), and *AGAMOUS* (*AG*) in floral meristems (Lohmann et al. 2001). The mechanism responsible for this switch from repressor to activator function has not been elucidated but it is possible that interaction with an additional partner competes for TPL binding, as described for DELLAs and IDDs. The IDD zinc finger factors function as activators when they interact with DELLAs, but as repressors when they interact with TPR4 (in the case of GAF1; Fukazawa et al. 2014) or SCL3 (for IDD3, 4, 5, 9, 10; Yoshida et al. 2014).

4. THE PLANT MERISTEMS

4.1 THE SHOOT APICAL MERISTEM

All above-ground organs derive from SAM cells. Maintenance of these stem cells is regulated by WUS, which is expressed in the central zone and CLAVATA (CLV), which is expressed in the meristem, while SHOOTMERISTEM-LESS (STM) represses their differentiation. STM activates CK biosynthesis, with WUS and WOX9 shown to control cell division in the SAM by modulating CK signaling. Lines with reduced levels of CKs have smaller SAM and form less leaves than the wt (Werner et al. 2003), supporting the need of CKs for normal SAM function. STM also down-regulates GA levels, by activating *GA2ox* in the base of the SAM (Jasinski et al. 2005). However, although GA levels are low in the central zone, DELLAs do not seem to play any essential role in the SAM. Auxins, together with GAs and BRs, are important to establish the boundary between the meristem and the new forming organs and for the control of lateral organ initiation. Auxins induce the synthesis of ethylene, which might work as a feedback loop to limit auxin signaling (Barton 2010; Veit 2009).

In response to salt stress, cell division stops due to a repression of cyclins (CYC) and cyclin dependent kinases (CDK). In the SAM, expression of *CYCB1;1* and *CYCA2;1* decreases, which

correlates with a reduction in the number and size of the new formed leaves, which also show a smaller number of epidermal cells. This, together with the fact that the hypocotyl and petioles stop elongating, make plants grown in salt much smaller than those grown in normal conditions (Burssens et al. 2000).

4.2 THE ROOT APICAL MERISTEM

As for the SAM, all under-ground tissues derive from the apical root meristem. Auxins were shown to promote cell proliferation in the proximal part of the RAM, while CKs promote cell differentiation in the transition/elongation zones. However, a high auxin:CK ratio is needed in the QC to maintain stem cell activity (Kieber & Schaller 2014).

CKs inhibit lateral root formation, while auxins are crucial to LR initiation, although high concentrations inhibit their growth (Schaller et al. 2015). Lines accumulating lower levels of CKs have longer primary roots (PR), which correlates with a larger meristem and more adventitious roots, and is not necessarily associated with more LRs (Werner et al. 2003).

Although auxins and cytokinins are the main hormones controlling root meristem function, cell cycle progression of QC stem cells is also controlled by BRs (González-García et al. 2011) and GAs (Achard et al. 2009); and auxins promote GA signaling (Fu and Harberd 2003).

4.2.1 ROOT PATTERNING

In a transversal section, Arabidopis roots show several concentric cell layers: epidermis, cortex, endodermis, pericycle and vascular tissue, which includes the phloem, xylem and procambium. The pericycle and vascular tissues form the so-called stele. The epidermis is comprised by two main cell types: the trichoblasts, which are in contact with two adjacent cortical cells and differentiate into root hairs; and the atrichoblasts, which are in contact with only one cortical cell, and stay hairless (Scheres et al. 2002; Figure 6B).

Longitudinally, the root cap is at the tip of the root, where cell renewal rate is very high, and is comprised by the central columella and the peripheral lateral root cap (Kumpf & Nowack 2015). As the rest of root cells, the root cap derives from the QC, a group of slowly dividing cells that give rise outward to the root cap and inward to the different root cell layers. The root meristem initiates at the QC, and in this zone cells divide instead of elongating. The further the cells are from the QC, the lower the division:elongation rate of these cells is, which leads to a transition zone, and then to the elongation/differentiation zone, where cells have stopped dividing and are just expanding (Scheres et al. 2002; Figure 6A and 6C).

Lateral roots develop post-embrionically and derive from the primary root pericycle which is comprised by phloem pole and xylem pole cells. These later ones are specified as LR founder

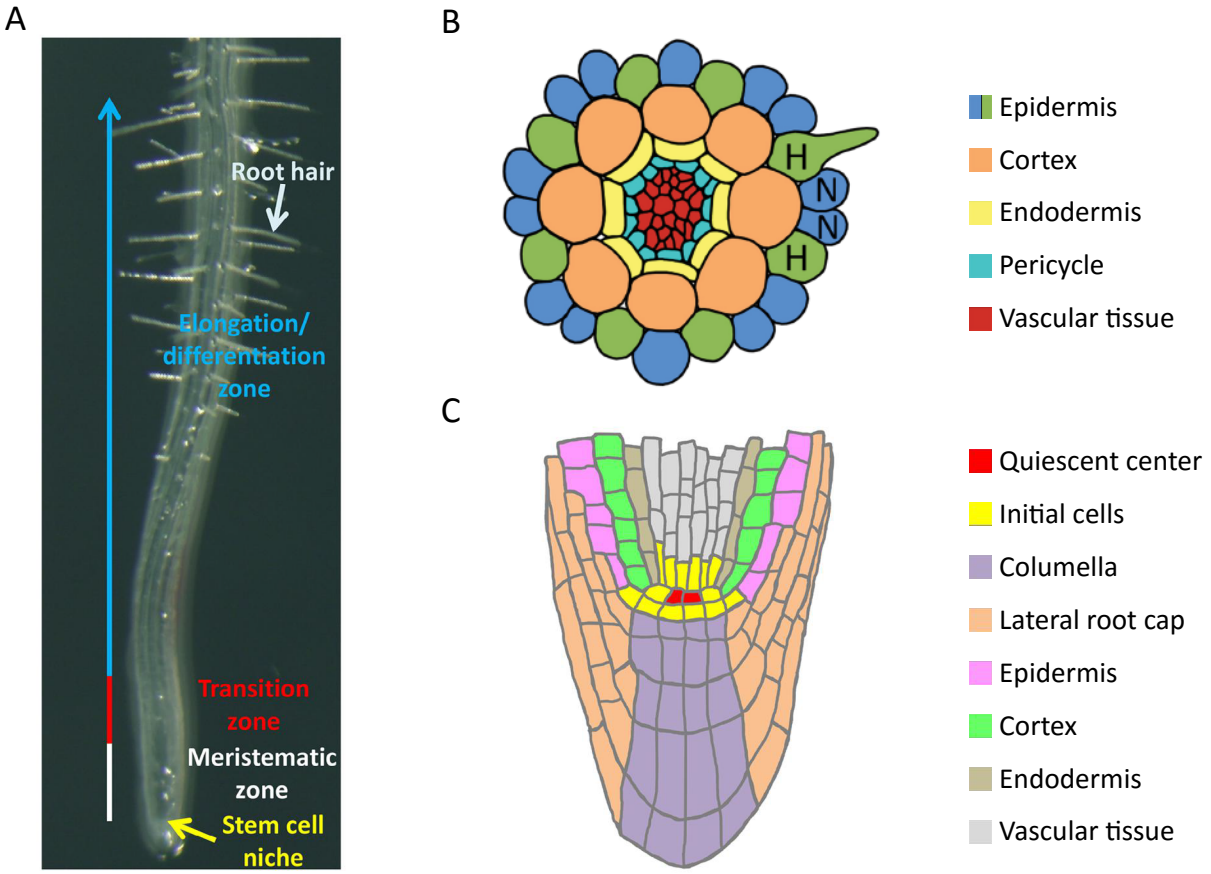

Figure 6. Arabidopsis root patterning (A) Longitudinally, root is divided in the stem cell niche at the tip, from where all cells come from; followed by the meristematic zone, where cells divide; the transition zone; and the elongation/differentiation zone, where cells divide and root hairs are produced. (B) Transversal representation of root cell layers showing the epidermis, composed by root hair (H) and non-hair (N) cells, cortex, endodermis, pericycle and vascular tissue. (C) Longitudinal representation of the root tip cell layers showing the epidermis, cortex, endodermis and vascular tissue but also the lateral root cap, columella, quiescent center and initial cells. (Adapted from Balcerowicz et al. 2015; Takatsuka et al. 2015)

cells in the so-called oscillation zone, from where lateral roots are initiated in response to auxin signaling. Signals produced at the founder cells are perceived by the endodermis, which plays an essential role in modulating founder cell growth and entrance into mitosis (Vermeer & Geldner 2015). Endodermal cells are surrounded by the Casparian strip, which is a rigid hydrophobic lignin-rich structure. To allow penetration of the LR primordium, endodermal cells lose volume until fusion of the opposing plasma membranes, and the Casparian strip is locally degraded, while cortical and epidermal cells do not seem at this stage to undergo any visible changes. Later on, the pectin cell wall of cortical and epidermal cells is degraded, and these cells are pushed apart by the new emerging root (Vilches-Barro & Maizel 2014).

GAs promote root growth and exert this effect mainly in the endodermis (Ubeda-Tomás et al. 2008). Studies using fluorescent GA derivatives showed that GAs indeed accumulate in endodermal cells of the root elongation zone (Shani et al. 2013). The GRAS *SCL3* factor is

specifically expressed in the endodermis (Zentella et al. 2007) and this expression is mediated by SCARECROW (SCR) and SHORT-ROOT (SHR), in addition to its own autoregulation (Cui et al. 2007). Direct SCL3 interaction with the DELLAs antagonizes DELLAs repressor function, and has been shown to play a critical role in promoting GA-regulated gene expression in the root endodermal cell layer (Z.-L. Zhang et al. 2011).

4.2.2 EFFECTS OF SALT ON ROOT GROWTH

Salt inhibits primary root growth, and both emergence and growth of lateral roots. This inhibition is mediated by ABA, and involves DELLA stabilization (Duan et al. 2013). In the presence of salt, expression of cell cycle regulators such as *CYCB1;1* and *CYCA2;1* is reduced, leading to a decrease in root meristem size, length of primary and lateral roots, and number of LRs (Burssens et al. 2000; West et al. 2004). Besides the stop of growth, roots were shown to bend and run away from salt, a process which is controlled by a re-localization of auxins (Galvan-Ampudia et al. 2013).

Reduced auxin levels in response to salt stress were recently reported to be mediated by an increase in nitric oxide (NO; Liu et al. 2015), and JA signaling has also been shown to play a role in root growth inhibition in response to salt and osmotic stress (Valenzuela et al. 2016). Regarding LRs, less and more elongated lateral roots appears to be the ideal root architecture to cope with high salinity, but additional studies are required to establish how root architecture affects response to salt (Julkowska & Testerink 2015).

4.2.3 THE ROOT HAIRS

In Arabidopsis, epidermal root cell patterning is specified during embryogenesis, such that the root epidermis shows 8 trichoblasts cell layers, separated by 10 to 14 atrichoblast layers. WEREWOLF (WER), TRANSPART TESTA GLABRA (TTG), GLABRA 2 (GL2), GL3, AND ENHANCER OF GLR (EGL3) were shown to be the main regulators that signal atrichoblasts specification, while CAPRICE (CPC), TRIPTYCHON (TRY) and ENHANCER OF TRY AND CPC1 are responsible for trichoblast fate specification. SCRAMBLED (SCM) is important for patterning of these two different type of cells (Grierson et al. 2014). Root hair differentiation showed to display a great plasticity, as post-embryonic cell specification is found to rapidly change in response to different stimuli.

Root hairs elongate rapidly without losing cell wall integrity, and this growth process has been shown to implicate a highly coordinated action of calcium signaling, cytoskeleton dynamics, vesicle trafficking, pH regulation and ROS production. Constant changes in pH and ROS in the apoplast control calcium concentration within the cell, which in turn promotes ROS production and an increase in pH. In order to support rapid growth, new materials for

membrane and cell wall building are delivered by endomembrane vesicles to the root hair tip. Actin cytoskeleton plays an important role in endocellular trafficking, while microtubules are required for maintenance of cell polarity and directed growth. Last, cellulose synthases and extensins are crucial for cell wall formation and stability (Mendrinna & Persson 2015).

Major hormones involved in root hair formation appear to be ethylene, auxins, BRs and strigolactones (SL) (Grierson et al. 2014). Moreover, DELLAs repress root hair growth, as indicated by the observation that *ga1-3* mutants display shorter root hairs, while those of the *ga1-3 quadruple-DELLA* mutant are longer than the wt ones. Such repressive effects were shown to rely on DELLAs mediated control of ROS levels (Achard, Renou, et al. 2008).

Root hairs confer an advantage for nutrient uptake, as increased root hair length and number contributes to dramatically increase of the root surface area. In fact, roots respond to nutrients deficiency by increasing their hair density and length. The best studied examples for triggering this response are phosphorous and iron starvation, although a shortage in manganese and zinc also activates root hair differentiation (Grierson et al. 2014).

On the contrary, root hair density and length decrease in response to salt. Under salt stress conditions, epidermal cells become larger and the pattern of cell specification is altered. The number of trichoblasts does not change, but fewer of them differentiate into root hairs, while the number of atrichoblast cells decrease. Salt stress was shown to induce *GL2* expression in the trichoblasts, thus switching their fate into non-hair cells. Therefore, although trichoblasts maintain their position, they are unable to form root hairs. Conversely, in response to nutrient deficiency, *GL2* expression is repressed in atrichoblasts and leads to root hair differentiation in wrong positions, which results in the formation of extra root hairs (Wang & Li 2008; Wang et al. 2008). Altogether, these findings indicate that root hair formation is a developmental process that is subjected to strong environmental control. However, the exact molecular mechanism controlling activated *GL2* expression in trichoblast/atrichoblast cells is still poorly understood.

Objectives

DELLAs interact with a wide variety of TFs and other non-TF proteins to regulate different developmental processes. Depending on the partner, interaction with the DELLAs leads to an inhibition of the TF activity (sequestration model) or to a shift in activity, from repression to activation function (co-activator model). This second mechanism would lead to activated gene expression in response to DELLAs accumulation, and in fact recent ChIP-seq studies showed that DELLAs sit on the promoters of several genes (Marín-de la Rosa et al. 2015). Moreover, cumulative evidence indicates that, in addition to growth inhibition, DELLAs play a pivotal role in activation of a yet poorly characterized pathway that confers increased tolerance to salt stress. Given that a few examples exist in the literature, it was reasonable to assume that DELLAs fulfill this stress-related function by physically interacting with some unknown TFs, and that a complex formation with these factors contributes to the activation of their gene targets. To gain insight into these unknown regulators we screened a collection of Arabidopsis lines that over-express different families of TFs under the control of a β-estradiol inducible promoter (TRANSPLANTA collection; Coego et al. 2014). The screening was performed in the presence of β-estradiol plus 175mM NaCl plus 25µM GA_3, to search for regulators that confer increased tolerance to salt independently of GA levels. Such screening conducted to the identification of more than 30 regulators. Also, since DELLAs restrain growth by binding the bHLH domain of PIFs, we hypothesized that DELLAs might bind a region outside the DNA-recoginition domain of these new identified regulators through a different domain from the LHRI repeat, involved in PIFs interaction. If this premise were confirmed, it would open the possibility of uncoupling the growth restraint and stress-tolerance activity of these repressors, by selecting allelic mutations that impair interaction with PIFs, but do not affect binding to these novel regulators. Generating transgenic lines expressing these allelic variants is foreseen to lead to increased environmental stress tolerance, without a trade-off in growth and productivity. Therefore, the main objectives for this work are:

1. Testing whether the TFs identified in the screening correspond to DELLA partners.

2. Mapping the interaction domain in the DELLA proteins.

3. Characterizing the mechanism of action of one of the identified regulators.

As lines expressing the homeodomain *WOX9* showed a strong salt tolerance phenotype and this family of TFs had not been associated to a stress-related function, we selected this gene for further characterization, and decided to address the following specific objectives:

3.1. Mapping the DELLA binding domain in the WOX9 protein.

3.2. Analyzing the salt tolerance phenotype of *wox9* and over-expression lines.

3.3. Determining the hormone sensitivity and hormone levels in these plants.

3.4. Identifying WOX9 downstream regulated targets.

Materials and Methods

1. PLANT MATERIAL

All mutants and transgenic lines are in the Columbia (Col-0) background. *stip-D* and *stip-2* mutants were obtained from the NASC (The European Arabidopsis Stock Centre). *pWOX9::GUS* was described in Wu et al. (2005) and was directly obtained from these authors.

pMDC7-GFP/GUS and *pMDC7-WOX9* (induced by estradiol) were obtained from the TRANSPLANTA consortium. New *pMDC7-WOX9* lines, exhibiting higher expression levels, were selected from the T_0 generation provided by the TRANSPLANTA consortium.

35S::HA-WOX9 was obtained by cloning the *WOX9* coding sequence (CDS) into pPZP15 vector, which was generated by the introduction of the "gateway cassette" (GW) of pGWB15 (Nakagawa et al. 2007) into the StuI-HindIII sites of the pPZPXomegaL+ vector (Steve Kay lab). The construct was introduced into *Arabidopsis thaliana* (L.) Heynh ecotype Col-0 by floral-dip transformation (Clough & Bent 1998).

2. GROWING CONDITIONS

For *in vitro* conditions studies, seeds were surface sterilized by 15min incubation in 70% (v/v) ethanol 0.1% (v/v) Tween-20, followed by 2x 2min washes in 100% ethanol, and let dry in the sterile bench. Seeds were plated on 0.5x Murashige and Skoog medium (MS; Duchefa) supplemented with 0.25% (w/v) sucrose (from now on, growth medium [GM]) and 0.6% (w/v) or 1% (w/v) agar, depending if plants were grown horizontally or vertically, respectively. Seeds were stratified for three days in darkness at 4°C and transferred to light in short day (8h light; 16h dark) (SD) or LD (16h light; 8h dark) conditions at 22°C, depending on the experiment.

For studies with adult plants, seedlings were grown for one week in LD conditions as described above and then transferred to pots with soil:vermiculite (3:1). Plants were grown in controlled growth chambers at 22°C, in SD or LD conditions depending on the experiment.

Specific conditions for each experiment are specified in the different sections.

3. CLONING

PCRs were performed with primers ordered from Sigma-Aldrich (listed in Table 2). PCR reactions were set with 0.3µM primers, 3.5U Expand High Fidelity Taq polymerase (Roche) and 0.3mM each dNTP (dATP, dTTP, dGTP, dCTP) in a 50µl final volume. Annealing temperature and extension time were decided according to the melting temperature of the primers and the length of the amplicon (1min/kb), respectively.

The Gateway Cloning System (Invitrogen) was used for cloning of the genes. In general, PCR amplified fragments were first inserted into pENTR™/D-TOPO® vector and then mobilized by incubation with the LR clonase mix (Invitrogen) into different destination vectors. All pMDC7 (Curtis & Grossniklaus 2003) constructs were obtained from the TRANSPLANTA consortium. A BP clonase reaction was performed to transfer the corresponding Open Reading Frames (ORF) into pDONR201 (Invitrogen), followed by a LR reaction, to clone them into different pDEST vectors. In specific cases when the Gateway system did not work out, traditional cloning with restriction enzymes was used. The pGEM®-T Easy plasmid (Promega) was used as intermediate vector. All constructs were analysed by sequencing (STABvida). Constructs used in this work are listed in Table 3.

4. FLORAL-DIP TRANSFORMATION OF ARABIDOPSIS

For Arabidopsis transformation, 500ml culture of *Agrobacterium tumefaciens* (*A.tumefaciens*) harboring the construct was grown overnight at 28°C until an optical density at a wavelength of 600nm (OD_{600}) of 0.6-0.8 was reached. The culture was then pelleted by centrifugation at 20°C and 6000 revolutions per minute (rpm) for 15min. Pellet was resuspended in 200ml MS with 5% (w/v) sucrose and 40µl Silwet L-77 (Lehle Seeds). The flowers of the plant were immersed in the suspension for 10min. Plants were then covered with a plastic bag and kept in the dark overnight. The next day, the bag was removed and the plants were kept growing in LD conditions until they produced seeds.

Seeds (T_0) transformed with constructs in the pPZP15 vector were plated on 0.5x MS supplemented with 1% (w/v) sucrose (GM-S), including 250µg/ml claforan and 150µg/ml gentamycin. Selection of homozygous lines in subsequent generations was done on GM-S plates with gentamycin.

Selection of *pMDC7-WOX9* homozygous lines was done on GM-S with 15µg/ml hygromicin.

Selection of *stip-D* and *stip-2* was done on GM-S with 5µg/ml phosphinothricin.

5. TRANSFORMATION OF BACTERIA

5.1. *Agrobacterium tumefaciens* TRANSFORMATION

DNA was incubated with 500µl competent cells for 5min on ice, 5min in liquid nitrogen and 5min at 37°C. 1ml YEB (5g/l beef extract; 1g/l yeast extract; 5g/l peptone; 5g/ sucrose; 2mM $MgSO_4$; pH 7.2) was then added and cells were recovered by incubation at 28°C for 2h before being plated on selective media.

The strain used was GV3101 (Holsters et al. 1980). For growing on solid or in liquid media, YEB was supplemented with 100µg/ml rifampicin plus antibiotics for selection of each construct. The concentrations used are: 100µg/ml streptomycin, 300µg/ml spectinomycin, and 25µg/ml kanamycin. Liquid cultures were grown at 28°C and 200-250rpm shaking.

5.2. *Escherichia coli* TRANSFORMATION

DNA was incubated with 100µl competent cells for 20min on ice, followed by 1min 40s heat-shock at 42°C, and 5min incubation on ice. 250µl LB (10g/l tryptone; 5g/l yeast extract; 10g/l NaCl; pH 7.5) was then added and cells were recovered by incubation at 37°C for 1h before being plated on selective media.

Strain used was DH5α (Woodcock et al. 1989) for all constructs, except for the empty vectors with the GW *ccdB* gene cassette, which were grown in the DB3.1 strain (Bernard & Couturier 1992).

Antibiotic selection depended on the vectors. The concentrations used were: 100 µg/ml carbenicillin; 50µg/ml streptomycin; 12.5µg/ml spectinomycin; 25µg/ml kanamycin. Liquid cultures were grown at 37°C with 200-250 rpm shaking.

6. SCREENING OF TRANSPLANTA LINES

The TRANSPLANTA lines (Coego et al. 2014) express more than 500 independent TFs from Arabidopsis under the control of a β-estradiol inducible promoter. This collection was screened for regulators able to confer increased tolerance to salt in the presence of 25µM GA_3. The screening was performed in LD conditions. Seeds were germinated on plates for two days and then transferred to 96-well plates containing 200µl liquid GM, 10µM β-estradiol (Sigma-Aldrich), 175mM NaCl, ± 25µM GA_3 (Sigma-Aldrich). Eight seedlings were tested per well.

Plates were incubated with gentle shaking until differences among independent lines were observed. Sensitive genotypes showed cotyledon bleaching, while in tolerant lines cotyledons remained green in most of the plants. Lines showing green cotyledons independently of the presence of GA_3 were selected for further analyses. Assays were repeated twice with similar results.

7. SALT TOLERANCE ASSAYS

Seeds were surface sterilized as described and grown on GM in LD conditions for 4 days. Seedlings were then transferred to vertical plates containing GM supplemented with 150mM NaCl ± 25µM GA_3. To avoid contact of the cotyledons with the media, a strip of Parafilm M® film (pre-treated with 100% ethanol for 15min) was placed in between. After six days of treatment

pictures of the plates were taken and survival rates were scored. Assays were repeated twice with similar results.

8. SEED GERMINATION ASSAYS

For seed germination assays, seeds were surface sterilized as described before and plated on GM containing 0, 1 or 2µM ABA (Sigma-Aldrich). 50 seeds of each genotype were plated on four independent plates for each treatment. After three days of stratification at 4°C in the dark, plates were transferred to LD conditions and daily scored for seedling germination rates (emergence of the radicle), and expansion and greening of the cotyledons, for a total interval of 10 days. Assays were repeated twice with similar results.

9. ROOT LENGTH MEASUREMENTS

Sensitivity to ABA and salt treatments was also determined by measuring the root lengths of the different genotypes. Seeds were surface sterilized and plated on GM as described. After three days of stratification at 4°C in the dark, plates were incubated in LD, and 3-day-old seedlings were then transferred to vertical GM plates (mock), or plates supplemented with 10µM ABA or 100mM NaCl. Seedlings were grown for 7 days in LD conditions, and pictures of the plates were taken for primary root length and lateral root formation measurements. PR length was determined with Fiji software (Schindelin et al. 2012). Likewise, number of LR was counted for each of genotype. Assays were repeated twice with similar results.

10. HORMONE MEASUREMENTS

Endogenous hormone levels in *35S::HA-WOX9* and Col-0 genotypes were measured at the Hormone Detection Service of the *Instituto de Biología Molecular y Celular de Plantas* (IBMCP UPV-CSIC) in Valencia. Plants were grown in SD conditions for four weeks, and whole rosettes harvested for hormone determination. Fresh rosette leaves were frozen in liquid nitrogen, grinded, and 100-200mg material was sent on dry ice to the IBMCP for analysis. Three biological replicates were analyzed for each genotype.

Material was extracted in 80% (v/v) methanol-1% (v/v) acetic acid containing the internal standards, by shaking for 1 hour at 4°C. Extracts were kept overnight at -20°C, clarified by centrifugation, and dried in a vacuum evaporator, to be dissolved in 1% (v/v) acetic acid and cleaned through an Oasis HLB (reverse phase) column as described in Seo et al (2011).

For GAs, IAA, ABA, SA and JA quantification, the dried eluates were dissolved in 5% (v/v) acetonitrile-1% (v/v) acetic acid, and were separated by reverse phase UHPLC chromatography (2.6µm Accucore RP-MS column, 50mm length x 2.1 mm i.d.; ThermoFisher Scientific), using a

5 to 50% (v/v) acetonitrile- 0.05% (v/v) acetic acid gradient, at a flow rate of 400 µl/min over 14min.

For CKs, the extracts were additionally passed through an Oasis MCX (cationic exchange) column and eluted with 60% (v/v) methanol-5% (v/v) NH_4OH to obtain the basic fraction containing cytokinins. The final eluate was dried, dissolved in 5% (v/v) acetonitrile-1% (v/v) acetic acid and CKs were separated with a 5 to 50% (v/v) acetonitrile gradient over 7min.

Quantification was performed by targeted Selected Ion Monitoring (SIM), using a Q-Exactive Mass Spectrometer (Orbitrap detector; Thermo Fisher Scientific). Hormone levels were measured using the embedded calibration curves and the Xcalibur 2.2 SP1 build 48 and TraceFinder programs. Internal standards for quantification were the deuterium-labelled hormones, except for JA, for which the dhJA compound was used.

11. CYTOKININ RESPONSE STUDIES

Sensitivity to cytokinin of Col-0, *35S::HA-WOX9* and *stip-2* genotypes was tested *in vitro*, by incubation of the hypocotyls on calli induction media. Hypocotyls from 10-day-old seedlings were excised and transferred to GM supplemented with 100ng/ml 2,4-dichloro-phenoxyacetic acid (2,4-D; Duchefa) and 0, 25, 200 or 1000 ng/ml kinetin (Duchefa). Pictures were taken after culture for 20 days in SD condition. As a control of the experiment, double mutant *cre1-3 ahk3-4* seedlings, with an insensitive response to CKs (Franco-Zorrilla et al. 2002, 2005), were obtained from Dr. Javier Paz-Ares' lab and included in the assay. Assays were repeated twice with similar results.

12. GIBBERELLIN RESPONSE STUDIES

For GA response studies, seeds were surface sterilized, plated on GM and stratified as described. After one day in SD conditions, they were transferred to vertical plates containing GM or GM plus 25µM GA_3 (Sigma-Aldrich) and kept in SD conditions for five additional days. Pictures were then taken and hypocotyls lengths were measured with Fiji software (Schindelin et al. 2012). Assays were repeated twice with similar results.

13. SHOOT APICAL MERISTEM SIZE

Scanning electron micrographs were used for the analyses of SAM phenotypes. Studies were performed at the Technical University of Munich (TUM). 7-day-old seedlings grown on GM were fixed in FAA (5% [v/v] formaldehyde; 5% [v/v] acetic acid; 50% [v/v] ethanol) for 3 days at 4°C. Samples were then dehydrated with increasing ethanol concentrations and subsequently dried, by means of a critical point dryer (Leica EM CPD300). Seedlings were placed on double-sided Tissue-Tek tape (Sakura Finetek) and a stereomicroscope (Olympus SZX10)

was used for taking the leaves apart, so that the SAM would become visible. Samples were then mounted onto the specimen stub and pictures were then taken using a table scanning electron microscope (SEM; Hitachi TM3000). Assays were repeated twice with similar results.

14. ROOT MERISTEM SIZE AND ROOT HAIR FORMATION

To test differential sensitivity of Col-0, *35S::HA-WOX9*, *stip-D* and *stip-2* seedlings to ABA, salt or GA application, seeds were plated on GM as described. After 3 days culture in LD conditions, seedlings were transferred to vertical plates containing GM (mock), or GM supplemented with 10µM ABA, 50mM NaCl or 25µM GA_3. Instead of agar, 1% (w/v) Phytagel was used in the root hair formation studies.

After culture in LD conditions for three additional days, pictures of the plates were taken. Seedlings were then stained with propidium iodide (PI; 10µg/ml) and root tips photographed with a Leica TCS SP5 confocal microscope, using the excitation Beam Splitter FW (DD 488/561) and an objective HCX PL APO CS 20x0.70 DRY. Emission band width was set to 580-630nm. Length of the meristems was measured with the Fiji software (Schindelin et al. 2012). Assays were repeated twice with similar results.

15. PROTEIN EXPRESSION STUDIES

Western blot (WB) analyses were performed to detect protein expression levels. Total protein extracts from Arabidopsis seedlings were obtained by homogenization in 2 volumes extraction buffer (150mM Tris-HCl pH 7; 150mM NaCl; 0.5% [v/v] Igepal® CA-630; 0.05% [w/v] sodium deoxycholate; Protease Inhibitors: 1mM PMSF; 10µg/ml Aprotinin; 12µg/ml Leupeptin; 6.8 µg/ml Pepstatin; 17.5 µg/ml E-64; 10 µg/ml MG-132). Extracts were clarified by centrifugation at 14.000rpm for 10 min at 4°C, and protein concentration was quantified using the Bradford assay (Bio-Rad Protein Assay). An equal volume of TMx2 (0.125M Tris-HCl pH 7.4; 20% [v/v] glycerol; 4% [w/v] SDS; 0.04 [w/v] bromophenol blue) with 10% (v/v) β-mercaptoethanol was added to the samples and 30µg used for sodium dodecyl sulfate polyacrylamide gel electrophoresis (SDS-PAGE).

According to the molecular weight (MW) of the proteins, 8% or 10% polyacrylamide (Bio-Rad) gels were used for separation, by running the gels at 150W for 2h. Proteins were then transferred to a 0.2µm nitrocellulose membrane (Amersham) at 20V for 1h, using a semi-dry transfer system (48mM Tris-HCl pH 9; 39mM Glycine; 20% [v/v] methanol; 0.025% [w/v] SDS). Membranes were blocked for 1h at room temperature (RT) with 10% (w/v) powdered milk in TBS buffer (50mM Tris-HCl pH 7.4; 150mM NaCl) with 0.1% (v/v) Tween-20 (TBS-T). After one quick wash with TBS-T, incubation with the primary antibody was done overnight at 4°C. The following day, membranes were washed 3 times for 5min with TBS-T, and incubated with the

secondary antibody for 1h 30min. Membranes were washed 3 times for 5min with TBS-T and 3 times with TBS, before incubation for 2min with the SuperSignal™ West Pico Chemiluminescent Substrate (Thermo Fisher Scientific). Then, they were exposed on an autoradiography film (Agfa) and developed using a Konica SRX-101A machine. Times of incubation with the substrate and exposition varied depending on the intensity of the signal. Primary antibodies: anti-MBP (1:10000; Abcam; anti-Rabbit); anti-GFP-HRP (1:1000; Milteny); anti-HA-HRP (1:1000; Roche); anti-RGA (1:1000; from Dr. Claus Schwechheimer´s lab; anti-Rabbit); anti-RPT5 (1:10000; Enzo Life Sciences; anti-Rabbit). Secondary antibodies: anti-Rabbit-HRP (1:10000; GE Healthcare).

16. PROTEIN INTERACTION STUDIES

Direct protein-protein interactions were assessed by three different methods: Yeast-Two-Hybrid (Y2H); Bimolecular Fluorescence Complementation (BiFC) , and co-immunoprecipitation (coIP) assays. BiFC and coIP studies were done expressing the proteins in *Nicotiana benthamiana* (*N.benthamiana*) leaves.

16.1. YEAST-TWO-HYBRID (Y2H)

Yeast transformation and interaction assays were performed as described in Yeast Protocols Handbook (Clontech). Incubation temperature for yeast cells was always 28°C. The yeast Y187 and AH109 strains were used for transformation (small-scale LiAc procedure) with the pGADT7 and pGBKT7 constructs, and plated on selective media lacking leucine (SD-L) or tryptophan (SD-W), respectively. For convenience, we used modified vectors harboring the GW casette in NdeI-BamHI restriction sites, obtained from Dr. Roberto Solano´s lab. After three days, colonies of both strains, bearing the desired constructs were pairwise incubated overnight in 500µl YPDA (20g/l peptone; 10g/l yeast extract; 2% [w/v] glucose; 0.003 [w/v] adenine; pH 5.8) for mating. The following day, 50µl of the mating culture was plated on SD-LW plates and incubated for two days. Diploid colonies were then grown overnight in 200µl SD-LW liquid media and 3µl of 1; 1:10; and 1:100 dilutions of the cultures dropped on SD-LW (growth control), SD-LW and histidine (H), SD-LWH+ 0.5mM 3-amino-triazol (3-AT) and SD-LWH and adenine (A) plates, to assay for interaction. Pictures were taken after 4 days. Cultures in liquid media were incubated at 28°C with 200-250rpm shaking and solid media was prepared with 2% (w/v) agar.

16.2. CO-IMMUNOPRECIPITATION STUDIES

The proteins to be tested, fused to a specific tag, were transiently expressed in *N.benthamiana* leaves, by infiltration with the *A.tumefaciens* cells harboring the corresponding constructs. In all experiments, pBIN-P19 was included as a suppressor of gene silencing. For agroinfiltration, bacterial cultures were grown overnight at 28°C in 12.5ml YEB medium plus

antibiotics. After 20min centrifugation at 4000rpm at RT, cells were suspended in 2ml 10mM MES pH 5.8, 10mM $MgSO_4$, 150µM acetosyringone and let in dark with gently shaking for 3 hours. Absorbance at a wavelength of 600nm was measured and cultures were diluted at a final optical density of 0.5 (OD_{600}=0.5). Combinations of the cultures were then prepared and infiltrated in the abaxial side of the leaves with the help of a 1ml syringe.

After three days, leaves were collected, grinded in liquid nitrogen with the help of a mortar, and distributed in 500µl aliquots in 1.5ml tubes. Proteins were extracted with the double volume of extraction buffer (150mM Tris-HCl pH 7; 150mM NaCl; 0.5% [v/v] Igepal® CA-630; 0.05% [w/v] sodium deoxycholate; 10mM β-mercaptoethanol; Protease Inhibitors: 1mM PMSF; 10µg/ml Aprotinin; 12µg/ml Leupeptin; 6.8 µg/ml Pepstatin; 17.5 µg/ml E-64; 10 µg/ml MG-132.) and clarified twice by centrifugation for 10min at 14000rpm and 4°C. Protein extracts were then incubated at 4°C for two hours with 2.4µg of anti-MBP antibody, followed by 30min with 50µl (30mg/ml) Dynabeads® Protein G (Invitrogen). As a control of the experiment, 75µl of the protein extract were taken before addition of the antibody (Input), and 75µl after binding to the beads (Unbound). Beads were washed three times with the extraction buffer, and the help of a magnet (Invitrogen), and proteins were eluted from the magnetic beads in 60µl TMX2 with 10% (v/v) β-mercaptoethanol. Different proteins in these samples were analyzed by western blot.

16.3. BIMOLECULAR FLUORESCESCENCE COMPLEMENTATION ASSAYS

The ORFs corresponding to the proteins of interest in the pDONR/ pENTR™/D-TOPO® vectors were mobilized by LR clonase recombination into the YFN43 and YFC43 vectors (Belda-Palazo et al. 2012), to express N-terminal fused versions of these proteins to the N-terminus or C-terminus of the Yellow Fluorescent Protein (YFP), respectively. Transient expression of these constructs in *N.benthamiana* leaves was performed as previously described. Three days after agroinfiltration, pictures of the leaves were taken with the aid of a confocal microscope (Leica TCS SP5), using the excitation Beam Splitter FW (TD 488/561/633) and an objective HCX PL APO CS 20x0.70 DRY. An emission band width from 510-550nm was used for YFP detection and 660-750nm for detection of auto-fluorescence of the chlorophyll.

17. GUS STAINING

To study tissue specific expression of the *WOX9* gene, we used the *pWOX9::GUS* line. GUS staining was performed as described by Jefferson et al. (1987). Before staining, seedlings were fixed for 30min in 90% (v/v) acetone and washed with water for 10min, on ice. Seedlings were then placed in the GUS staining solution (100mM Tris-HCl pH 7; 50mM NaCl; 2mM 5-bromo-4-chloro-3-indolyl-β-D-glucuronic acid [X-Gluc; Glycosynth], 5mM potassium ferricyanide, 5mM potassium ferrocyanide, 0.2% [v/v] Triton X-100) and vacuum was shortly applied to

let the solution get into the tissue. Incubation was driven at 37°C, for either 2h or overnight, depending on the experiment. For detection of differences in GUS levels among treatments, seedlings were incubated for 2 hours. For detection of GUS activity in the root, around the SAM, flowers and embryos, seedlings were incubated overnight . Plants were then dehydrated by 1 hour incubation with increasing concentrations of ethanol (30%-50%-70%-100% [v/v]) and kept in 100% ethanol until the chlorophyll was completely removed. Seedlings used for sectioning were fixed with 4% (v/v) glutaraldehyde for 4 days at 4°C, before being dehydrated, to avoid GUS staining diffusion.

Pictures of the stained seedlings were taken with a stereomicroscope (Leica M165 FC; camera: Leica DFC295), or a microscope (Leica DMR; camera: Olympus DP70), when a higher magnification was required. Assays were repeated twice with similar results.

18. HISTOLOGICAL SECTIONS

Histological sections of the seedlings were performed by the Histology Service of the *Centro Nacional de Biotecnología* (CNB), following the protocol described in Chevalier et al. (2014). Briefly, samples were pre-incubated in pre-infiltration solution (50% ethanol and 50% infiltration solution [v/v]), before being transferred to the infiltration solution of the Historesin Standard kit (Leica). Subsequent steps were done according to the manufacturer's instructions. For GUS staining visualization, seedlings were sliced into 7µm sections using a Leica microtome equipped with tungsten carbide blades. Sections were floated in a 50°C water bath, collected on a glass porta slide, and allowed to dry.

For morphological studies of non-stained roots, seedlings were fixed in 90% [v/v] acetone for 30min, followed by 4% [v/v] glutaraldehyde for 4 days, and dehydrated by incubation in increasing concentrations of ethanol, as before. Seedlings were then cut into 3µm sections and stained with 1% (w/v) cresyl violet before being mounted in Surgipath micromount medium (Leica).

Pictures of the sections were taken with an optical microscope (Leica DMR) attached to an Olympus DP70 camera.

19. GENE EXPRESSION ANALYSIS

For gene expression analysis, total RNA was extracted by homogenizing the frozen tissues in Z6-buffer (8M guanidinium-HCl; 20mM MES pH 7; 20mM EDTA; 50mM β-mercaptoethanol) and addition of an equal volume of phenol-chloroform. After 30min centrifugation at 14000rpm and 4°C, the aqueous phase containing the RNA was mixed with an equal volume of the binding buffer provided by the "High Pure RNA Extraction Kit" (Roche) and bound into

the kit purification columns. The rest of the extraction was done following the manufacturer´s protocol.

19.1. QUANTITATIVE REAL-TIME PCR (qRT-PCR)

2µg of RNA were used for cDNA synthesis, which was carried out with the "Transcription First Strand cDNA Synthesis Kit" from Roche. Random hexamers were used as primer and the manufacturer´s intructions were followed except for the following: 30µM random hexamer, 0.5mM each dNTP, 6U Reverse Transcriptase (instead fo 60µM, 1mM, and 10U, respectively).

The cDNA product was diluted 1:10 in water and qRT-PCR reactions were carried out with 4µl of the diluted samples, 0.2µM of each primer, and 5µl EvaGreen® dye (Biotium) in a 10 µl final volume. Amplification of *ACTIN8* was used as internal reference. Reactions were performed with the aid of Applied Biosystems Instruments (7500 and 7900HT) using the following conditions: 50°C 2min; 95°C 10min; (95°C 15s; 60°C 1min; 95°C 15s)x40. Relative expression was calculated with the –ΔΔCt Pfaffl method (Pfaffl 2001). Primers used for amplification are listed in table 2.

19.2. MICROARRAY EXPERIMENTS

Microarray hybridization was performed at the Genomics Service of the *Centro Nacional de Biotecnología* (CNB). RNA integrity of the samples provided was first checked with Bioanalyzer2100 (Agilent), before proceeding to their labeling.

Total RNA (500ng each) was amplified and labelled with Cyanine 3 (Cy3), by using the One-Color Low Input Quick Amp Labeling Kit (Agilent Technologies), following the manufacturer´s instructions. Briefly, total RNA was converted into double stranded cDNA using an oligo-dT-T7 primer and the AffinityScript Reverse Transcriptase. The cDNA was then used as template for *in vitro* transcription reaction with T7 RNA polymerase, in the presence of Cy3-CTP. Cy3-labelled cRNA was purified with RNeasy columns (Qiagen) and RNA yield and Cy3 incorporation measured with the aid of a Nanodrop spectrophotometer (Nanodrop Technologies).

Preparation of probes and hybridization was performed as described (One-Color Microarray-Based Gene Expression Analysis, Agilent Technologies). Briefly, for each hybridization 600ng of Cy3-labelled cRNA were added to 5µl of 10x Blocking Agent, 1µl of 25x Fragmentation Buffer in a 25µl reaction, and incubated at 60°C for 30min to fragment RNA. Reaction was stopped with 25µl 2xHybridization Buffer and samples were placed on ice, before they were quickly loaded onto the arrays. These were hybridized at 65°C for 17h and then washed at RT once for 1min in GE wash buffer 1 and once for 1min in GE Wash Buffer 2 at 37°C. Arrays were drained by centrifugation at 2000rpm for 2min, before Cy3 channel Images

were captured at a resolution of 2µm with an Agilent DNA Microarray Scanner, and spots quantified using the Agilent Feature Extraction Software.

Background correction and quantile normalization of the expression data were performed using LIMMA (Smyth 2004). Linear model methods were used for determining differentially expressed genes. Each probe was tested for changes in expression over three replicates, by using an empirical Bayes moderated t-statistic method (Smyth 2004). For false discovery rates, p-values were corrected by using the Benjamini and Hochberg method (Benjamini & Hochberg 1995). The expected false discovery rate (FDR) was controlled to be less than 5%.

20. STATISTICAL AND BIOINFORMATICS ANALYSIS

The GraphPad Prism version 6.04 for Windows (GraphPad Software, La Jolla California USA, www.graphpad.com) was used for statistical analysis. T-test or ANOVA tests were applied based on variables of the experiment and expected false discovery rates assessed to be less than 1% (**) or 5% (*) for statistical significance.

For phylogenetic analysis of the WOX family, amino acid sequence alignment of the homeodomains was first performed using Clustal Omega (Sievers et al. 2011). Construction of the phylogenetic tree was done with the MEGA 6 software (Tamura et al. 2013) using the neighbor-joining method and 1000 bootstraps.

Clustering of the differentially expressed genes was done with MeV (Saeed et al. 2003), using K-means/K-medians clustering (KMC) and Euclidean distance.

Gene ontology (GO) term enrichment within each cluster was analyzed with the GeneCodis tool (Carmona-Saez et al. 2007; Nogales-Cadenas et al. 2009; Tabas-Madrid et al. 2012). Comparisons among lists were done with the VENNY program (Oliveros 2007).

Figures were prepared using Adobe Ilustrator CS6.

Table 2. Primers used in this work

NAME	SEQUENCE	USE	REMARKS
ACT8L	GACTCAGATCATGTTTGAGACCTT	qRT-PCR of *ACT8* (*At*1g49240)	lab 314
ACT8R	GACTCAGATCATGTTTGAGACCTTT	qRT-PCR of *ACT8* (*At*1g49240)	lab 314
del1 AtRGAs	CACCCCGCCGCAGAATCAGATCG	Cloning of del1 truncated version of *RGA*	
del2 AtRGAs	CACCCCACCGGCGCCGGATAATTCTG	Cloning of del2 truncated version of *RGA*	
delWUSbox F	TCCGTCGACTGTCGGAGGGTTTGAAGG	Cloning of *WOX9*ΔWUSbox	
delWUSbox R	ACAGTCGACGGAAACATCCCCATCATTTGAC	Cloning of *WOX9*ΔWUSbox	
F1 AtRGAas	CTATTAAACTTCATGAAGATGATCAG	Cloning of F1 truncated version of *RGA*	
IK054	ATGTGATATCTAGATCCGAAAC	Genotyping of *stipD*; *stip2*	Wu et al. 2005
oXW55	GGGTAATATATTTGATAGAGTAC	Genotyping of *stipD*; *stip2*	Wu et al. 2005
oXW56	GGGATGAGTAATGTAGAAGC	Genotyping of *stipD*; *stip2*	Wu et al. 2005
qGA20ox1 F	GATCCATCCTCCACTTTAGA	qRT-PCR of *GA20ox1* (*At*4g25420)	Rieu et al. 2008
qGA20ox1 R	GTGTATTCATGAGCGTCTGA	qRT-PCR of *GA20ox1* (*At*4g25420)	Rieu et al. 2008
qRT-EXPA7 F	GCCCTACCAAACGAAAACGG	qRT-PCR of *EXPA7* (*At*1g12560)	
qRT-EXPA7 R	TAACATAAAGCCGGGCCACC	qRT-PCR of *EXPA7* (*At*1g12560)	
qRT-RHS2 F	TGGCGTCAACTGAGGAGGA	qRT-PCR of *RHS2* (*At*1g12950)	
qRT-RSH2 R	GAAGATGCTCTGCTTCCGACT	qRT-PCR of *RHS2* (*At*1g12950)	
qRT-WOX9 for2	CAAGCGGACGCACGAATAAG	qRT-PCR of *WOX9*	
qRT-WOX9 rev2	TCCCCAAATGCATCCCTCAC	qRT-PCR of *WOX9*	
Relig AtRGAs	CACCATGCTTGAGCTTAGACCGAGC	Cloning of Relig truncated version of *RGA*	
RGA-SAWR	GGTGGTAATGAGTGGACGAGTGT	Cloning of *RGA*ΔSAW	
RGA-YFP-F	CACCATGAAGAGAGATCATCAC	Cloning of F1*RGA*	lab 314
RGA-YFP-R	GTACGCCGCCGTCGAGAG	Cloning of del1; del1; Relig; ΔSAW-*RGA*	lab 314
WOX1 for	CACCATGTGGACGATGGGTTACAACGA	Cloning of *WOX1*	
WOX1 rev	TTAGTTCTTCAATGGCAGAAACTC	Cloning of *WOX1*	
WOX2 for	CACCATGGAAAACGAAGTAAACGCAGGA	Cloning of *WOX2*	
WOX2 rev	TTACAACCCATTACCATTACTATCGA	Cloning of *WOX2*	
WOX3 for	CACCATGAGTCCTGTGGCTTCAACGA	Cloning of *WOX3*	
WOX3 rev	TTAAAGTTTGGTACTGTCTTGTTTG	Cloning of *WOX3*	

Table 2. Primers used in this work (cont.)

NAME	SEQUENCE	USE	REMARKS
WOX4 for	CACCATGAAGGTTCATGAGTTTTCGAATG	Cloning of *WOX4*	
WOX4 rev	TCATCTCCCTTCAGGATGGAGA	Cloning of *WOX4*	
WOX5 for	CACCATGTCTTTCTCCGTGAAAGGTCGA	Cloning of *WOX5*	
WOX5 rev	TTAAAGAAAGCTTAATCGAAGATCTAATG	Cloning of *WOX5*	
WOX6 for	CACCATGGGCTACATCTCCAACAACAAC	Cloning of *WOX6*	
WOX6 rev	TCAGTTCTTCAGAGGCATGAACTC	Cloning of *WOX6*	
WOX7 fw (oMB235)	ggggacaagtttgtacaaaaaagcaggcttcATGTCGT CGAGAGGATTCAAC	Cloning of *WOX7*L	from Dr. R. Solano´s lab
WOX7L rv (oMB293)	ggggaccactttgtacaagaaagctgggtcTCATAGA AAGCTTAATCGGAGATC	Cloning of *WOX7*L	from Dr. R. Solano´s lab
WOX8 for	CACCATGTCCTCCTCAAACAAAAATTGG	Cloning of *WOX8*	
WOX8 rev	CTAAATAAGATAATAGATTGCGCCA	Cloning of *WOX8*	
WOX9 Ct for	CACCATGTTGCAACAGCCACAGACTCAG	Cloning of Ct*WOX9*	
WOX9 for	CACCATGGCTTCTTCGAATAGACAC	Cloning of Nt*WOX9*; mtEAR1; mtEAR2; delWUSbox -*WOX9*	
WOX9 M for-pGEMT	CCAAACCCCGAAAAAGCAAGAAC	Cloning of M*WOX9*	
WOX9 M rev-XhoI	CCCTCGAGCTAAGAAGCTATTTGATGATT AGTG	Cloning of M*WOX9*	
WOX9 mtEAR1 F	AATAACATCATGgcTCATgcTCCTCCCACTACT	Mutation of EAR1 of *WOX9*	
WOX9 mtEAR1 R	AGTAGTGGGAGGAgcATGAgcCATGATGT TATT	Mutation of EAR1 of *WOX9*	
WOX9 mtEAR2 F	GCGGACGCACGAgcAAGAGcTTTCgcCAAT GAAATGGAG	Mutation of EAR2 of *WOX9*	
WOX9 mtEAR2 R	CTCCATTTCATTGgcGAAAgCTCTTgcTCGT GCGTCCGC	Mutation of EAR2 of *WOX9*	
WOX9 Nt rev	GTTAGGTGGATTTGGAGGAGGAAG	Cloning of Nt*WOX9*	
WOX9 rev	CTAGATCAGATAGTACGAGGCT	Cloning of Ct*WOX9*; mtEAR1; mtEAR2; delWUSbox -*WOX9*	
WOX10 for	CACCATGGAGCAAGAGAGCCTAAACGGT	Cloning of *WOX10*	
WOX10 rev	TCAGTCTATAAACTTGTCCCTATTC	Cloning of *WOX10*	
WOX11 for	CACCATGGACCAAGAACAAACACCACA	Cloning of *WOX11*	
WOX11 rev	TCATGTCTGTCTTGGAACCAGGA	Cloning of *WOX11*	
WOX12 for	CACCATGAATCAAGAAGGTGCTTCACATAG	Cloning of *WOX12*	
WOX12 rev	TCATGTCTGTCTCGGTACCAGGA	Cloning of *WOX12*	
WOX13 for	CACCATGATGGAATGGGATAATCAGCTAC	Cloning of *WOX13*	
WOX13 rev	TCAGCCTGACATGCCATAATCTTC	Cloning of *WOX13*	
WOX14 for	CACCATGGTAAAAAAAAAAAAGGAAAA GGAG	Cloning of *WOX14*	
WOX14 rev	TTAAGTCTCCATAAATTTCCCTATAC	Cloning of *WOX14*	

Table 3. Constructs used in this work

VECTOR	INSERT	METHOD OF CLONING	REMARKS
pDONR201	*WOX9* CDS (*At*2g33880)	BP reaction from pMDC7-*WOX9*	
pDONR201	*IAA7* CDS (*At*3g23050)	BP reaction from pMDC7-*IAA7*	
pDONR201	*ERF6* CDS (*At*4g17490)	BP reaction from pMDC7-*ERF6*	
pDONR201	*ANAC87* CDS (*At*5g18270)	BP reaction from pMDC7-*ANAC87*	
pDONR201	*bHLH13* CDS (*At*3g18400)	BP reaction from pMDC7-*bHLH13*	
pDONR201	*HDG1* CDS (*At*3g61150)	BP reaction from pMDC7-*HDG1*	
pDONR201	*TINY* CDS (*At*5g25810)	BP reaction from pMDC7-*TINY*	
pDONR201	*RAP2.6* (*At*1g43160)	BP reaction from pMDC7-*RAP2.6*	
pDONR201	*ANT* (*At*4g37750)	BP reaction from pMDC7-*ANT*	
pDONR201	*MYB116* (*At*1g25340)	BP reaction from pMDC7-*MYB116*	
pDONR201	*STH* CDS (*At*2g31380)	BP reaction from PDMC7-*STH*	
pDONR201	*DREB2C* CDS (*At*3g40340)	BP reaction from pMDC7-*DREB2C*	
pDONR201	*MYB99* CDS (*At*5g62320)	BP reaction from pMDC7-*MYB99*	
pDONR201	*SEP2* CDS (*At*3g02310)	BP reaction from pMDC7-*SEP2*	
pDONR201	*MYB46* CDS (*At*5g12870)	BP reaction from pMDC7-*MYB46*	
pDONR201	*bZIP63* CDS (*At*5g28770)	BP reaction from pMDC7-*bZIP63*	
pDONR201	*TT2* CDS (*At*5g35550)	BP reaction from pMDC7-*TT2*	
pDONR201	*HB53* CDS (*At*5g66700)	BP reaction from pMDC7-*HB53*	
pDONR201	*HECATE1* CDS (*At*5g67060)	BP reaction from pMDC7-*HECATE1*	
pDONR201	*MYB38* CDS (*At*2g36890)	BP reaction from pMDC7-*MYB38*	
pDONR201	*ERF037* CDS (*At*1g77200)	BP reaction from pMDC7-*ERF037*	
pDONR201	*SUVH7* CDS (*At*1g17770)	BP reaction from pMDC7-*SUVH7*	
pDONR201	*NAC038* CDS (*At*2g24430)	BP reaction from pMDC7-*NAC038*	
pDONR201	*WOX7*L CDS (*At*5g05770)	BP reaction from PCR product (WOX7 fw+WOX7L rv)	
pENTR™/D-TOPO®	del1*RGA* (*At*2g01570)	PCR product (del1AtRGAs+RGAYFPR)	
pENTR™/D-TOPO®	del2*RGA* (*At*2g01570)	PCR product (del2AtRGAs+RGAYFPR)	
pENTR™/D-TOPO®	Relig*RGA* (*At*2g01570)	PCR product (ReligAtRGAs+RGAYFPR)	
pENTR™/D-TOPO®	F1*RGA* (*At*2g01570)	PCR product (RGAYFPF+F1AtRGAas)	
pENTR™/D-TOPO®	Nt*WOX9*	PCR product (WOX9for+WOX9Ntrev)	
pENTR™/D-TOPO®	Ct*WOX9*	PCR product (WOX9Ctfor+WOX9rev)	
pENTR™/D-TOPO®	EAR1*WOX9*	PCR product ([WOX9 for+WOX9mtEAR1R; WOX9mtEAR1F+WOX9rev]; WOX9for+WOX9rev)	
pENTR™/D-TOPO®	EAR2*WOX9*	PCR product ([WOX9 for+WOX9mtEAR2R; WOX9mtEAR2F+WOX9rev]; WOX9for+WOX9rev)	

Table 3. Constructs used in this work (cont.)

VECTOR	INSERT	METHOD OF CLONING	REMARKS
pENTR™/D-TOPO®	*WOX9*ΔWUSbox	PCR product ([WOX9for+delWUSboxR] + [delWUSboxF+WOX9 rev])	
pENTR™/D-TOPO®	*RGA*ΔSAW	PCR product (RGAYFPF+RGA-SAW R)	
pENTR™/D-TOPO®	*RGA*		lab 314
pENTR™/D-TOPO®	del1*RGA*ΔSAW	PCR product (del1AtRGAs + RGA-SAW R)	
pENTR™/D-TOPO®	*WOX1* CDS (*At*3g18010)	PCR product (WOX1for+WOX1rev)	
pENTR™/D-TOPO®	*WOX2* CDS (*At*5g59340)	PCR product (WOX2for+WOX2rev)	
pENTR™/D-TOPO®	*WOX3* CDS (*At*2g28610)	PCR product (WOX3for+WOX3rev)	
pENTR™/D-TOPO®	*WOX4* CDS (*At*1g46480)	PCR product (WOX4for+WOX4rev)	
pENTR™/D-TOPO®	*WOX5* CDS (*At*3g11260)	PCR product (WOX5for+WOX5rev)	
pENTR™/D-TOPO®	*WOX6* CDS (*At*2g01500)	PCR product (WOX6for+WOX6rev)	
pENTR™/D-TOPO®	*WOX8* CDS (*At*5g45980)	PCR product (WOX8for+WOX8rev)	
pENTR™/D-TOPO®	*WOX10* CDS (*At*1g20710)	PCR product (WOX10for+WOX10rev)	
pENTR™/D-TOPO®	*WOX11* CDS (*At*3g03660)	PCR product (WOX11for+WOX11rev)	
pENTR™/D-TOPO®	*WOX12* CDS (*At*5g17810)	PCR product (WOX12for+WOX12rev)	
pENTR™/D-TOPO®	*WOX13* CDS (*At*4g35550)	PCR product (WOX13for+WOX13rev)	
pENTR™/D-TOPO®	*WOX14* CDS (*At*1g20700)	PCR product (WOX14for+WOX14rev)	
pGEM®-T Easy	M*WOX9*	PCR product (WOX9Mfor+WOX9Mrev-XhoI) cloned in PstI/XhoI	
pGADT7gw	*WOX9*	LR reaction from pDONR201-*WOX9*	
pGADT7gw	*IAA7*	LR reaction from pDONR201-*IAA7*	
pGADT7gw	*ERF6*	LR reaction from pDONR201-*ERF6*	
pGADT7gw	*ANAC87*	LR reaction from pDONR201-*ANAC87*	
pGADT7gw	*bHLH13*	LR reaction from pDONR201-*bHLH13*	
pGADT7gw	*HDG1*	LR reaction from pDONR201-*HDG1*	
pGADT7gw	*TINY*	LR reaction from pDONR201-*TINY*	
pGADT7gw	*RAP2.6*	LR reaction from pDONR201-*RAP2.6*	
pGADT7gw	*ANT*	LR reaction from pDONR201-*ANT*	
pGADT7gw	*MYB116*	LR reaction from pDONR201-*MYB116*	
pGADT7gw	*STH*	LR reaction from pDONR201-*STH*	
pGADT7gw	*DREB2C*	LR reaction from pDONR201-*DREB2C*	
pGADT7gw	*MYB99*	LR reaction from pDONR201-*MYB99*	
pGADT7gw	*SEP2*	LR reaction from pDONR201-*SEP2*	
pGADT7gw	*MYB46*	LR reaction from pDONR201-*MYB46*	
pGADT7gw	*bZIP63*	LR reaction from pDONR201-*bZIP63*	
pGADT7gw	*TT2*	LR reaction from pDONR201-*TT2*	
pGADT7gw	*HB53*	LR reaction from pDONR201-*HB53*	

Table 3. Constructs used in this work (cont.)

VECTOR	INSERT	METHOD OF CLONING	REMARKS
pGADT7gw	*HECATE*	LR reaction from pDONR201-*HECATE1*	
pGADT7gw	*MYB38*	LR reaction from pDONR201-*MYB38*	
pGADT7gw	*ERF037*	LR reaction from pDONR201-*ERF037*	
pGADT7gw	*SUVH7*	LR reaction from pDONR201-*SUVH7*	
pGADT7gw	*NAC038*	LR reaction from pDONR201-*NAC038*	
pGADT7gw	*WOX7*L	BP reaction from PCR product (WOX7 fw+WOX7L rv)	
pGADT7gw	*WOX7*		from Dr. R. Solano´s lab
pGADT7gw	*WOX1*	LR reaction from pDONR201-*WOX1*	
pGADT7gw	*WOX2*	LR reaction from pDONR201-*WOX2*	
pGADT7gw	*WOX3*	LR reaction from pDONR201-*WOX3*	
pGADT7gw	*WOX4*	LR reaction from pDONR201-WOX4	
pGADT7gw	*WOX5*	LR reaction from pDONR201-*WOX5*	
pGADT7gw	*WOX6*	LR reaction from pDONR201-*WOX6*	
pGADT7gw	*WOX7*		from Dr. R. Solano´s lab
pGADT7gw	*WOX8*	LR reaction from pDONR201-*WOX8*	
pGADT7gw	*WOX9*	LR reaction from pDONR201-*WOX9*	
pGADT7gw	*WOX10*	LR reaction from pDONR201-*WOX10*	
pGADT7gw	*WOX11*	LR reaction from pDONR201-*WOX11*	
pGADT7gw	*WOX12*	LR reaction from pDONR201-*WOX12*	
pGADT7gw	*WOX13*	LR reaction from pDONR201-*WOX13*	
pGADT7gw	*WOX14*	LR reaction from pDONR201-*WOX14*	
pGADT7gw	*WUS* (*At*2g17950)		from Dr. R. Solano´s lab
pGADT7gw	Nt*WOX9*	LR reaction from pENTR™/D-TOPO®-Nt*WOX9*	
pGADT7gw	Ct*WOX9*	LR reaction from pENTR™/D-TOPO®-Ct*WOX9*	
pGADT7gw	EAR1WOX9	LR reaction from pENTR™/D-TOPO®-EAR1*WOX9*	
pGADT7gw	EAR2*WOX9*	LR reaction from pENTR™/D-TOPO®-EAR2*WOX9*	
pGADT7gw	*WOX9*ΔWUSbox	LR reaction from pENTR™/D-TOPO®-*WOX9*ΔWUSbox	
pGADT7	M*WOX9*	EcoRI/XhoI sites	
pGBKT7gw	M5*RGA*		de Lucas et al. 2008
pGBKT7gw	M5*GAI* (*At*1g14920)		de Lucas et al. 2008
pGBKT7gw	M5*RGL1* (*At*1g66350)		de Lucas et al. 2008

Table 3. Constructs used in this work (cont.)

VECTOR	INSERT	METHOD OF CLONING	REMARKS
pGBKT7gw	M5*RGL2* (*At*3g03450)		de Lucas et al. 2008
pGBKT7gw	M5*RGL3* (*At*5g17490)		de Lucas et al. 2008
pGBKT7gw	del1*RGA*	LR reaction from pENTR™/D-TOPO®-del1*RGA*	
pGBKT7gw	del2*RGA*	LR reaction from pENTR™/D-TOPO®-del2*RGA*	
pGBKT7gw	Relig*RGA*	LR reaction from pENTR™/D-TOPO®-Relig*RGA*	
pGBKT7gw	F1*RGA*	LR reaction from pENTR™/D-TOPO®-F1*RGA*	
pGBKT7gw	del1*RGA*ΔSAW	LR reaction from pENTR™/D-TOPO®-del1*RGA*ΔSAW	
pGBKT7gw	*RGA*ΔSAW	LR reaction from pENTR™/D-TOPO®-*RGA*ΔSAW	
pGBKT7gw	*RGA*	LR reaction from pENTR™/D-TOPO®-*RGA*	
YFC43	*WOX9*	LR reaction from pDONR201-*WOX9*	
YFN43	*RGA*		lab 314
YFN43	*TPL* (*At*1g15750)		lab 314
pMDC-MBP*	*WOX9*	LR reaction from pDONR201-*WOX9*	
pYL-YFP	*RGA*		lab 314
pK7TmGW43D	*TPL*		from Dr. R. Solano´s lab
pPZP-15	*WOX9*	LR reaction from pDONR201-*WOX9*	

*pMDC-MBP vector was obtained from Dr. P. Vera´s lab and was constructed cloning the XbaI/SalI digested fragment (including MBP) from pMGWA (Busso et al. 2005) into pMDC32 at BamHI/SalI sites.

Results

A screening of the TRANSPLANTA collection (Coego et al. 2014), expressing more than 500 TFs under control of an estradiol inducible promoter, had been carried out in the lab to search for regulators with a role in salt stress tolerance dependent on the DELLA repressors. Seedlings were independently grown in microtiter plates in GM supplemented with 175mM NaCl and ± 25 µM GA_3. Lines that grew into green seedlings in the presence of GA, suggesting a role of these TFs in reversing the negative stress signaling by this hormone, were selected for further characterization. Out of 1000 screened lines, 32 genes were identified as putative candidate genes.

1. 66% OF THE CANDIDATES INTERACT WITH DELLA PROTEINS

DELLAs are known to play a central role in suppressing GA-regulated gene expression, by physical interaction with several families of TFs. Specific functions of the Arabidopsis RGA, GAI, and RGL1-RGL3 DELLA proteins were also shown to depend on their different expression patterns, rather than on their ability to interact with different TFs. Studies using RGA, which is expressed in vegetative tissues, and RGL2, which controls seed germination, showed that both DELLAs bind the same PIFs, and that expression of *RGA* under the control of the *RGL2* promoter complements the *rgl2* mutation (Gallego-Bartolomé et al. 2010). Therefore, in a first approach we decided to test the interaction of the identified TFs in the screening with RGA and RGL2, the most distantly related DELLAs out of the five Arabidopsis gene copies. For the Y2H screening, we used the M5 deletion version of these proteins, as full-length copies were reported to result in auxotrophy autoactivation. The RGA N-terminal F1 deletion, including the GID1 interaction domain (DELLA domain), was also used as prey to cover all different regions of the RGA repressor.

Results from this secondary screening are shown in Figure 7. All construct combinations were able to grow normally on SD-LW (Figure S1), which shows that the expressed proteins do not have a toxic effect in yeast. One third of the analyzed proteins did not interact with RGA or RGL2, but immunodetection of the GAL4 fusion protein evidenced that in some instances negative interaction was caused by failure in expression of the proteins in the yeast cells. The rest of the proteins (66%) interact with RGA, RGL2 or both, indicated by growth of the cells expressing the GAL4BD-RGA/RGL2 and GAL4AD-TF fusion constructs on selective media lacking leucine, tryptophan and histidine (SD-LWH). Moreover, half of these TFs bind with similar affinities the RGA and RGL2 proteins (i.e. WOX9, IAA7, ERF6, TINY, ANT, MYB116, SEP2, bZIP63, TT2, HECATE1, ERF037, MYB38 and NAC038). For some of the proteins, an interaction was observed only with RGA (ANAC087, bHLH13, RAP2.6, DREB2C, SUVH7) or with RGL2 (MYB46). This behavior was unexpected, considering previous reports indicating that RGA and RGL2 share the same partner proteins (Gallego-Bartolomé et al. 2010). However, it is worth noting that in that original report interactions were limited to members of the basic-Helix-loop-Helix (bHLH) family, while here we analyzed TFs from several ones. Thus, although DELLAs

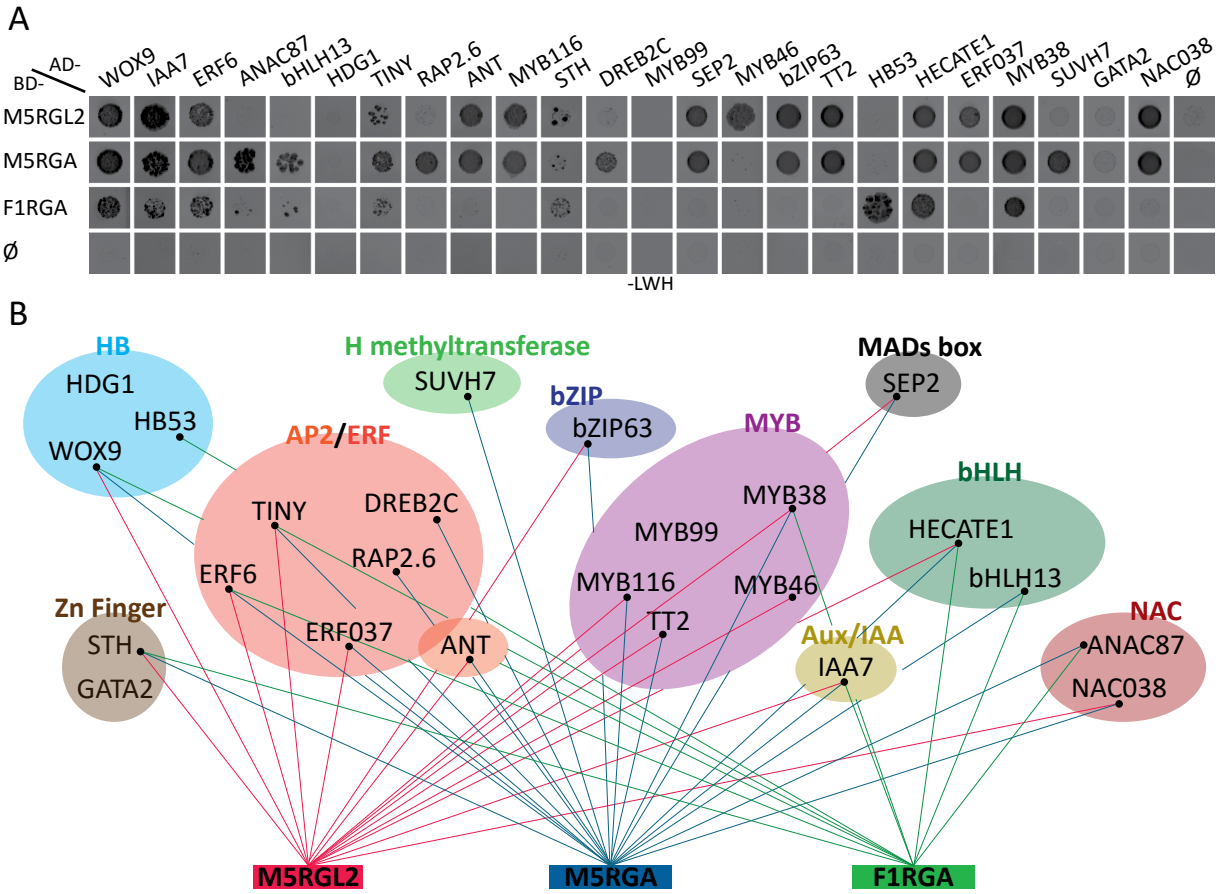

Figure 7. Yeast-Two-Hybrid screening (A) Interaction of the DELLA constructs (M5RGL2, M5RGA, F1RGA) and the different candidate proteins identified in the salt tolerance screening (WOX9, IAA7, ERF6, ANAC87, bHLH13, HDG1, TINY, RAP2.6, ANT, MYB116, STH, DREB2C, MYB99, SEP2, MYB46, bZIP63, TT2, HB53, HECATE1, ERF037, MYB38, SUVH7, GATA2, NAC038). AH109 and Y187 yeast strains were respectively transformed with pGBKT7 (BD) and pGADT7 (AD) fusion constructs and mating was performed with the different construct combinations as specified. A control of growth was performed by plating cells on minimal medium lacking leucine (L) and tryptophan (W) and is illustrated in supplemental figure S1. Protein interaction was analysed by growing cells on minimal medium lacking leucine (L), tryptophan (W) and histidine (H). (B) Schematic representation showing the families of transcription factor showing a positive interaction. Candidate genes belong to ten different gene families: homeodomain (HB), Zinc Finger, AP2/ERF, MYB, MADs box, bHLH, and Histone methyltransferase (H methyltransferase).

may indistinctly interact with members of the bHLH family, here we show that this cannot be generalized to the rest of TF families.

As for RGA-interactors, 6 transcriptional regulators (WOX9, IAA7, ERF6, TINY, HECATE1, MYB38) bound both the M5 and F1 constructs. An interaction with these fragments had also been observed for bHLH factors, suggesting that all these partners bind the first leucine heptad repeat (LHRI) region, present in both deletions (Figure 8A). On the other hand, in a greater number (12) of cases, the partner proteins (ANAC087, bHLH13, RAP2.6, ANT, MYB116, DREB2C, SEP2, bZIP63, TT2, ERF037, SUVH7, NAC038) did not interact with the F1 deletion. This means that the interaction domain of these factors likely maps to the non-overlapping

RGA C-terminal region. In addition, one of the partners (HB53) bound only the F1 deletion of RGA, implying that its interaction requires of the N-terminal region including the DELLA motif. Taken together, these results provided two essential lines of information: 1) that the identified TFs in the screening were strongly enriched in DELLA-interactors and 2) that interaction with the DELLAs involves in several cases a protein domain different from the LHRI region, shown to be involved in interaction with the PIFs.

2. DIFFERENT PROTEIN REGIONS MEDIATE INTERACTION WITH THE SELECTED TRANSCRIPTION FACTORS

From the whole list of interacting partners, those that showed a stronger binding affinity to the DELLAs were further studied. Since not every factor bound to RGA and RGL2, we analyzed the interaction with each of the Arabidopsis DELLA proteins, to further map the protein domain mediating this interaction. To this second aim, we used different truncated versions of RGA protein: one which lacks the C-terminal region, but still includes the LHRI motif (F1) and four subsequent N-terminal deletions of the protein missing the DELLA motif (M5), the DELLA plus the LHRI motif (del1), DELLA plus LHRI plus VHIID motifs (del2) or the whole N-terminal region including the leucine heptad repeat II (LHRII) motif (Relig) (Figure 8A).

As shown in Figure 8B, these transcriptional regulators were in most cases found to interact with the five DELLAs, in agreement with the notion that these repressors are highly redundant at the protein level. However, there were also some exceptions. For example, ERF037 interacts with all DELLAs, but this interaction seems to be weaker for RGL2 and GAI. The TT2 factor does not interact with GAI, while RAP2.6, DREB2C do not do it with RGL2. SUVH7, on the other hand, does not bind either RGL2 or GAI. From these findings we can conclude that RGA interacts with all TFs analyzed, RGL2 is not able to interact with three of these TFs, and GAI with one of them, which points to some functional differences among members of the DELLA family (Figure 8B).

Yeast interaction studies using truncated versions of the RGA protein, in addition, showed that interaction with three of these factors (ERF6, HECATE1, MYB38) involves the LHRI domain, shown to bind the bHLH factors. For nine of these factors (RAP2.6, MYB116, DREB2C, SEP2, bZIP63, TT2, ERF037, SUVH7, NAC038) interaction was only observed for the M5 deletion, but not for any of the other truncated proteins, meaning that although the LHRI domain plays a relevant role in interaction, there are additional motifs at the C-terminal region of the RGA protein which are essential but not sufficient for protein-protein interaction. On the other hand, WOX9 was found to interact with all constructs analyzed. This would indicate that this factor binds more than one motif in the RGA protein, and that each of these motifs is sufficient for the interaction (Figure 8B). Growth controls on SD–LW selection media are shown in Figure S2.

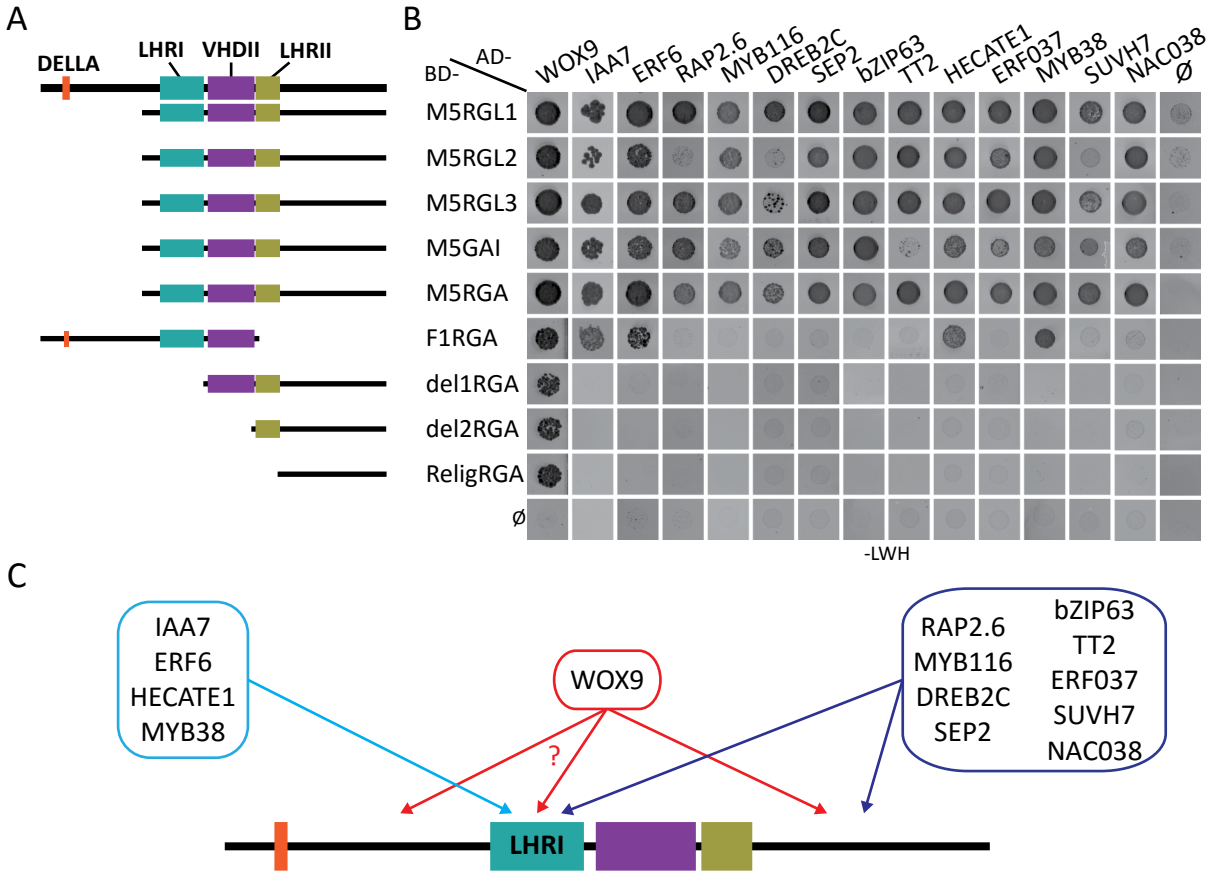

Figure 8. Yeast-Two-Hybrid mapping of the interaction domain of the best interactors (A) Scheme of the five Arabidopsis DELLAs M5 constructs (RGL1, RGL2, RGL3, GAI, RGA) and RGA deletions (F1, del1, del2, Relig) used for localization of the interaction domain. The DELLA (DELLA), first leucine heptad repeat (LHRI), VHDII and second leucine heptad repeat (LHRII) motifs are highlighted. (B) Interaction of the DELLA constructs and the different candidate genes. AH109 and Y187 yeast strains were transformed with pGBKT7 (BD) and pGADT7 (AD) fusion constructs of the DELLAs and candidate genes, respectively, and mating was performed with the different indicated combinations. To the control of growth, cells were plated on minimal medium lacking leucine (L) and tryptophan (W) (Figure S2). Protein interaction was analysed by plating cells on minimal medium lacking leucine (L), tryptophan (W) and histidine (H). (C) Schematic representation of the mapping domain results with RGA. IAA7, ERF6, HECATE1 and MYB38 interact with LHRI; WOX9 binds at least two motifs, which could not be determined; RAP2.6, MYB116, DREB2C, SEP2, bZIP63, TT2, ERF037, SUVH7 and NAC038 bind in addition to LHRI a second motif at the C-terminus of the RGA protein.

We can conclude from these studies that most of the salt stress-related factors identified in the screening bind RGA via an additional domain to the LHRI motif. This motif was shown to interact with the DNA-binding domain of PIF4, which leads to the inactivation of this factor (de Lucas et al. 2008), and to the growth inhibition response of DELLAs. Indeed, all but three of these factors bind the DELLAs through other regions different from the LHRI motif. Because these TFs were selected in the first place for conferring increased tolerance to salt stress, it is reasonable to assume that the interaction of these transcriptional regulators plays a role in DELLA-dependent activation of the abiotic stress pathway. Our findings show that DELLAs bind PIF4 and these stress-related factors via different domains, which indicates that identification

of allelic RGA mutations that impair interaction with PIF4 but not with these factors should be achievable. Expression of these RGA mutations in crop species will contribute to increase tolerance of these plants to environmental stresses without a growth penalty, by uncoupling abiotic stress and growth restraint function of these repressors.

3. SELECTION OF WUSCHEL-RELATED HOMEOBOX 9 (WOX9) AS THE FINAL CANDIDATE

Out of the different regulators identified, WOX9 inducible lines probed to be amongst those with a strongest salt tolerant phenotype. To the date, WUSCHEL-related homeobox factors had not been associated to abiotic stress responses, and therefore we considered that understanding the mechanism of action of this factor would be extremely relevant.

An additional reason for the selection of WOX9 was that this protein shows in Y2H assays a very strong binding affinity for the five DELLAs of Arabidopsis (Figure 7 and 8). For this particular factor, growth of yeast cells was observed on either SD-LWH or SD-LWHA (adenine) selective media (Figure 12C), hence indicating a higher binding affinity for the DELLAs than the other protein partners. Based on its salt tolerance and very strong interaction with the DELLA proteins, we selected WOX9 as our final candidate to further characterization.

4. NOT ALL WOX HOMOLOGUES INTERACT WITH THE DELLA PROTEINS

WOX9 belongs to a family of 14 members. Because over-expression of this protein leads to a salt tolerant phenotype we wondered if other WOX family members might also share a similar stress related function. As generating transgenic lines for all these genes was out of the scope of this work, we decided to test whether all family members interacted with the DELLA proteins, which would indicate that they share a similar mechanism of action. To this end, we amplified the ORFs for the fourteen members, including the two described variants of WOX7 (WOX7 and WOX7L) and that of WUSCHEL (WUS), the founder family member. These were then cloned into pGADT7 and tested for interaction with all five Arabidopsis DELLAs.

As previously seen, WOX9 strongly interacts with all five DELLA proteins. Its closest homolog, WOX8, also interacts strongly with RGL1, RGL2 and RGL3, weakly with RGA, and not with GAI. For the other two members of the intermediate clade, WOX11 can also interact weakly with the five DELLAs, while WOX12 do not bind any of these proteins (Figure 9A).

Concerning members of the ancient clade (WOX13, WOX10 and WOX14), we only observed a weak interaction of WOX14 with RGL1, whereas none of the other members were able to bind any of the DELLAs. Therefore, we can conclude that ancient clade members do not bind the DELLAs and have a diversified function (Figure 9A).

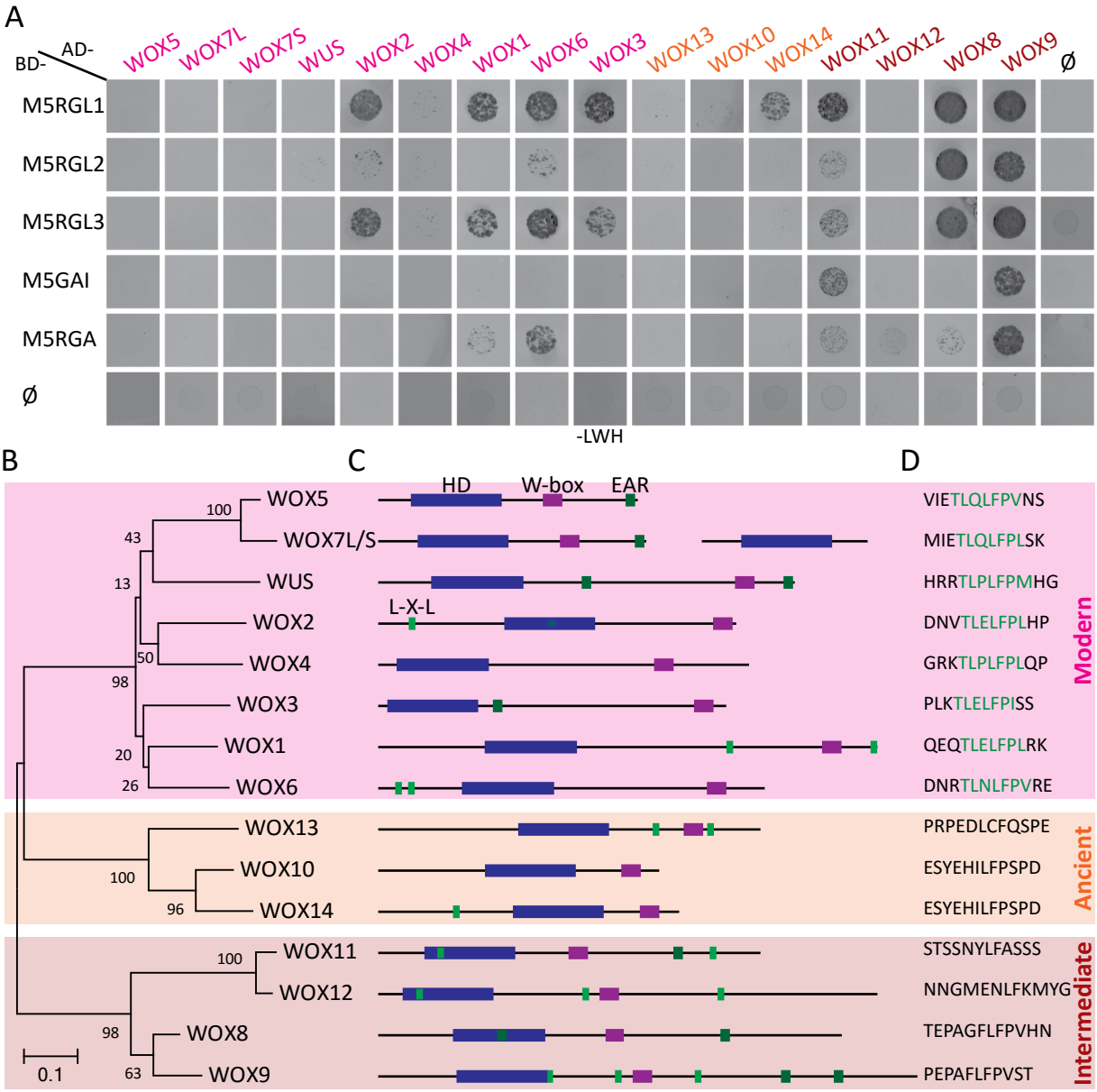

Figure 9. Yeast-Two-Hybrid interaction studies of DELLAs and the WOX family members (A) Interactions of the M5 DELLAs constructs (RGL1, RGL2, RGL3, GAI, RGA) and WOX family members (WOX1-WOX14, WUS). AH109 and Y187 yeast strains were transformed with the DELLA pGBKT7 (BD) and WOX pGADT7 (AD) constructs and mating was performed with the different construct combinations as indicated. A control of growth on minimal medium lacking leucine (L) and tryptophan (W) is shown in supplemental figure S3. Interaction of these proteins was analyzed on minimal medium lacking leucine (L), tryptophan (W) and histidine (H). (B) Phylogenetic tree of the WOX family. WOX proteins are grouped in three different clades: the modern (WUS, WOX1-7), the ancient (WOX10, WOX13-14) and the intermediate clade (WOX8-9, WOX11-12), statistically supported by bootstrap values. (C) Schematic representation of the WOX proteins showing the conserved homeodomain (blue), WUS-box (purple), EAR domains (dark green) and L-X-L repeats (light green). (D) Amino acid sequence of the conserved WUS-box in the different WOX members. Members of the modern clade contain an EAR domain (dark green) within the WUS-box.

For members of the modern clade, results were mixed. WUS and its closest homologues WOX5 and WOX7 did not bind the DELLA proteins, so did not WOX4. The rest of the family members (WOX2, WOX1, WOX6 and WOX3) bound specifically RGL1 and RGL3, while WOX6 also interacted with RGA. Moreover, a very weak interaction was observed for RGL2 and WOX2/WOX6, and for RGA and WOX1 (Figure 9A). Yeast cells transformed with the different constructs combinations grew normally on SD-LW (Figure S3).

These results demonstrate that not all WOX family members are partners of the DELLAs. Furthermore, there is a correlation between binding to the DELLAs and emergence of these proteins in evolution. In general, DELLAs were observed to bind members of the intermediate clade (except WOX12) and some members of the modern clade, hence indicating that this is a relatively recent molecular feature. WOX9 is by far the strongest interactor (Figure 9A), although we cannot exclude that other members of the intermediate clade have a redundant function in abiotic stress responses.

5. WOX9 CONFERS TOLERANCE TO SALT STRESS

To further characterize the stress-related function of WOX9, we ordered from the NASC two previously described mutants for this gene: *stip-D*, which corresponds to an activation-tagging line, and *stip-2*, which is a loss-of-function mutant. Both mutants are sterile in homozygosis, pointing to an important function of this factor at the floral reproductive stage or during embryogenesis. We also generated a tagged line that over-expresses WOX9 fused to the hemagglutinin tag (*35S::HA-WOX9*). This line has a slightly milder phenotype than the *stip-D* mutant but is still semi-sterile. Both *35S::HA-WOX9* and *stip-D* seedlings have epinastic cotyledons, and adult plants are characterized by having serrated leaves and displaying a branching phenotype, in addition to morphological defects in the flowers. On the contrary, loss-of-function *stip-2* mutant has hyponastic cotyledons, but adult plants do not show any phenotypic alterations compared to Col-0 (Wu, Dabi, & Weigel, 2005; Figure 10).

We next tested these lines for survival under salt stress conditions, by growing them on GM supplemented with 150 mM NaCl ± GA, as before. *35S::HA-WOX9* line is more tolerant to salt than Col-0 (100% vs. 80% survival), while *stip-2* is more sensitive to salt stress (survival was only 20%). Besides, although tolerance is reduced in the presence of GAs, the over-expression line is still clearly more tolerant than Col-0 while *stip-2* is more sensitive, being the survival rates 100%, 30% and 0%, respectively (Figure 11).

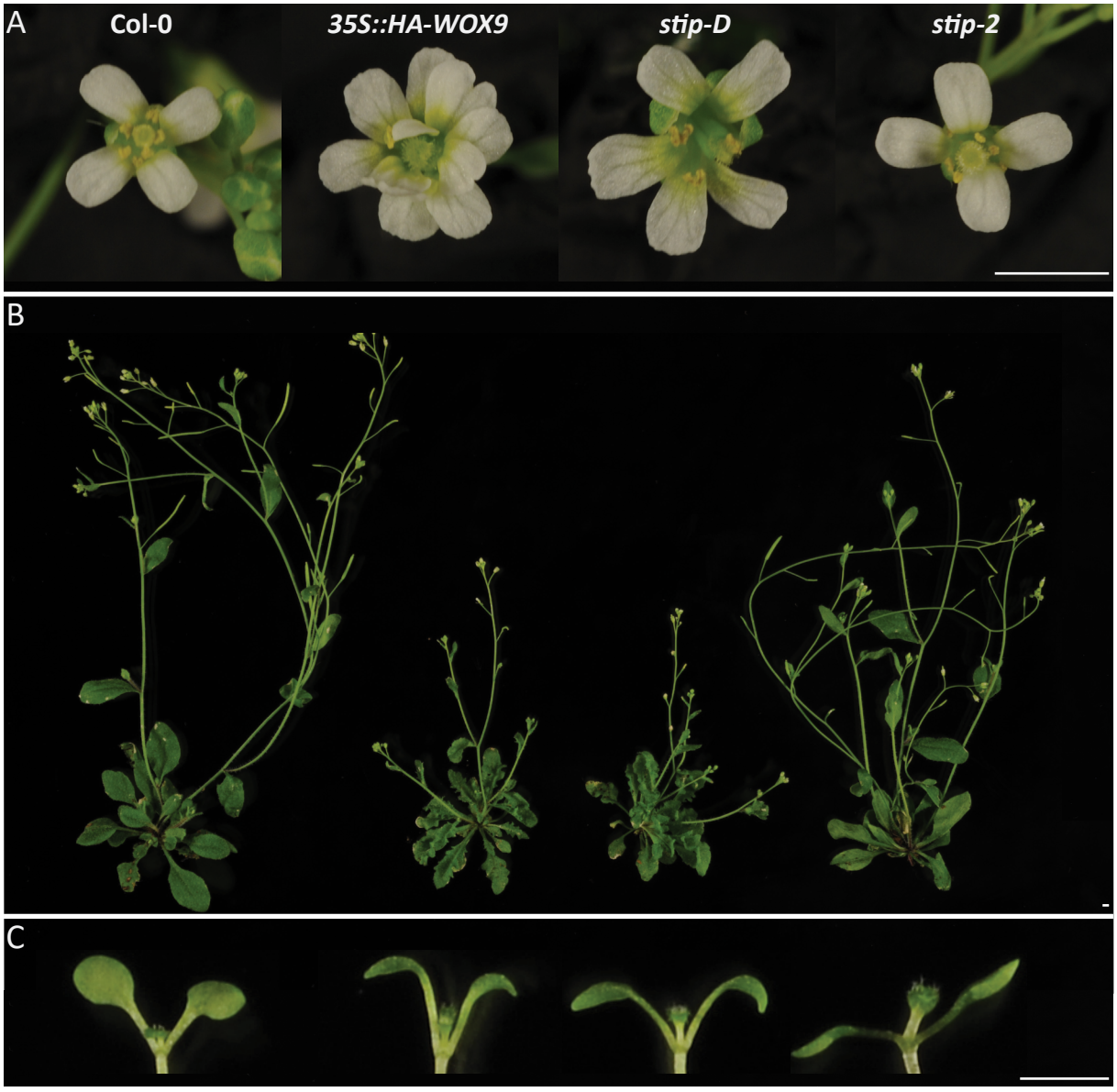

Figure 10. Phenotypes of Col-0 and WOX9 lines: *35S::HA-WOX9*, *stip-D* and *stip-2* (A) Flowers of the *35S::HA-WOX9* and *stip-D* over-expressor lines show extra petals. (B) Adult plants grown on long day conditions, showing the reduced apical dominance and wavy margin leaves of *35S::HA-WOX9* and *stip-D* over-expressors (C) Cotyledons of *35S::HA-WOX9* and *stip-D* are epinastic, while those of *stip-2* mutant seedlings are hiponastic. Scale bar=2mm.

6. WOX9 INTERACTS WITH RGA *IN PLANTA*

We then investigated that WOX9-RGA interaction occurs in the plant. To this aim, BiFC and coIP assays were performed with the proteins transiently expressed in *N.benthamiana* leaves. WOX9 and RGA were inserted downstream of N-terminal (YFN) and C-terminal (YFC) regions of the yellow fluorescence protein (YFP), in the gateway YFN43 and YFC43 vectors. Combinations of these fusion proteins, as well as the control empty vector were agroinfiltrated into *N.benthamiana* leaves, and three days after infiltration leaves were observed at the confocal microscope, for reconstituted YFP activity. A nuclear interaction was observed for

WOX9 fused to the C-terminal half of the YFP (YFC-WOX9) and RGA fused to the N-terminal YFP region (YFN-RGA). Expression of these tagged proteins with the complementary empty vectors did not produce any fluorescence, showing that nuclear YFP activity is due to WOX9 and RGA interaction, and reconstitution of the split YFP protein (Figure 12A).

To confirm the interaction of these proteins, we co-expressed in *N.benthamiana* leaves RGA-YFP and WOX9 fused to the maltose binding protein (MBP-WOX9), or the MBP protein used as a negative control. Total protein extracts were obtained three days after infiltration, and incubated with an anti-MBP antibody to immunoprecipitate the MBP-WOX9 (or MBP) proteins. After several washes, the immunoprecipitated fraction was eluted from the magnetic beads and analyzed by western blot for the presence of both MBP-WOX9 and RGA-YFP proteins. RGA-YFP was detected in the MBP-WOX9 but not in the MBP immunoprecipitated fraction, which means that RGA specifically interacts with WOX9 and is pulled-down together with the MBP-WOX9 protein (Figure 12B).

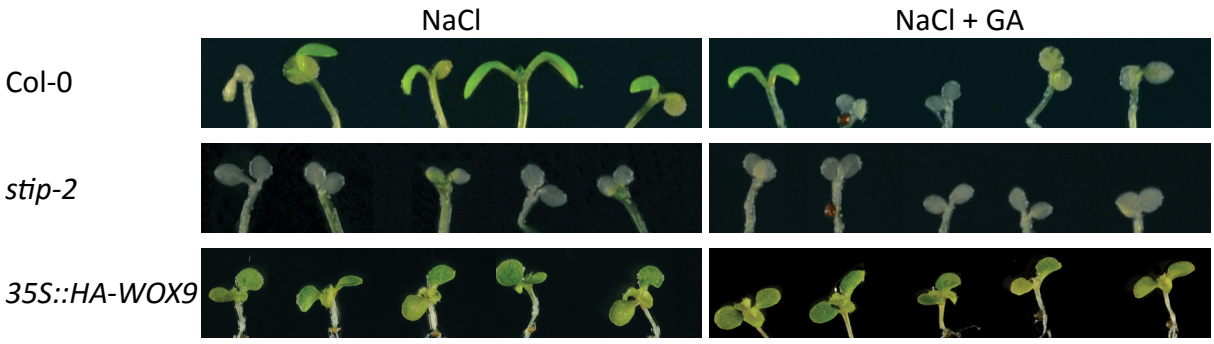

Figure 11. Salt tolerance phenotype of WOX9 lines. 4-day-old Col-0, *stip-2* and 35S::HA-WOX9 seedlings grown on GM were transferred to vertical plates containing GM plus 150mM NaCl (NaCl) +/- 25µM GA_3 (GA), and grown for 6 additional days. It is observed that *stip-2* seedlings are more sensitive to salt than Col-0, while *35S::HA-WOX9* is more tolerant, also in the presence of GAs.

7. RGA BINDS THE C-TERMINAL REGION OF WOX9

Y2H studies showed that WOX9 binds all deletions of the RGA protein, suggesting that more than one RGA protein domain is involved in WOX9 interaction. Indeed, interaction with the truncated RGA Relig protein indicates that one of the binding domains is located at the C-terminal end of the RGA protein and, therefore, we generated two additional constructs lacking the C-terminal SAW motif (del1-SAW and RGA-SAW in pGBKT7). Interaction studies with these new construct evidenced that binding to WOX9 is not impaired by deletion of the SAW motif (Figure 12C). This indicates that WOX9 interaction involves at least two RGA motifs, and that each of these motifs is sufficient for WOX9 binding.

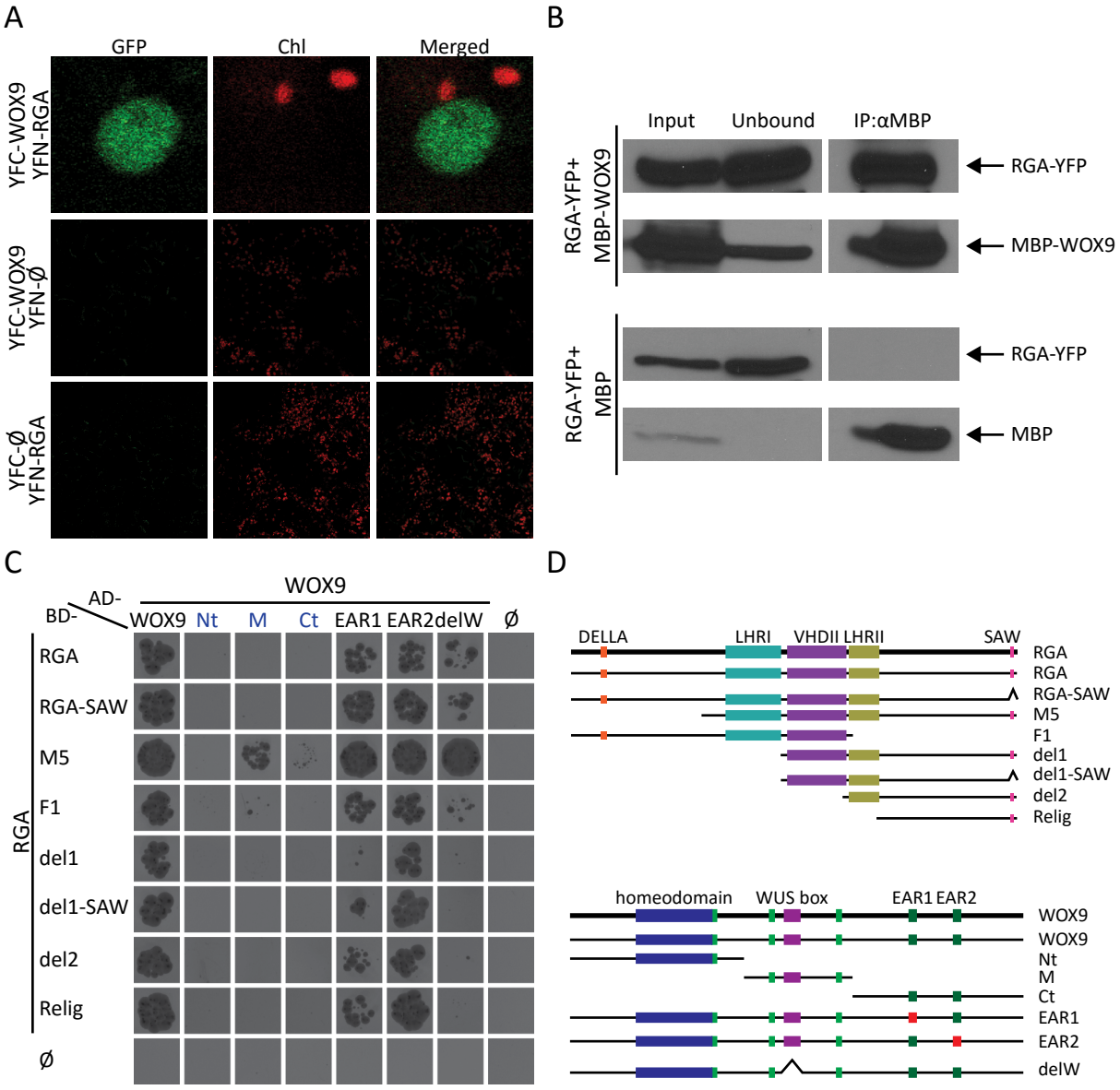

Figure 12. ***In vivo*** **interaction of the WOX9 and RGA proteins** (A) Bimolecular Fluorescence Complementation (BiFC) showing interaction of the WOX9 and RGA proteins. WOX9 fused to the C-terminus of the Yellow Fluorescent Protein (YFP) (YFC-WOX9) and RGA fused to the N-terminus of YFP (YFN-RGA) were transiently co-expressed in *Nicotiana benthamiana* leaves. As a negative control, the tagged proteins were also expressed with the complementary empty vector. (B) Co-immunoprecipitation (Co-IP) studies showing the interaction of RGA-YFP and WOX9 fused to the maltose binding protein (MBP-WOX9). Proteins were immuno-precipitated with an anti-MBP antibody and proteins detected by Western Blot using the anti-MBP and anti-GFP antibodies. RGA-YFP was co-expressed with the MBP protein as a negative control. (C) Yeast-Two-Hybrid (Y2H) assay with the truncated WOX9 (Nt, M, Ct, EAR1, EAR2, delW) and RGA proteins (RGA-SAW, M5, F1, del1, del1-SAW, del2, Relig) to map their interaction domains. AH109 and Y187 strains were transformed with the pGBKT7 (BD) and the pGADT7 (AD) constructs and mating was performed with the indicated combinations. Interaction was analyzed by growing cells on minimal medium lacking leucine (L), tryptophan (W), histidine (H) and adenine (A) except for the WOX9 Nt, M and Ct deletions, which were grown on minimal medium lacking leucine (L), tryptophan (W) and histidine (H). A control of growth on minimal medium lacking leucine (L) and tryptophan (W) is shown in supplemental figure S6. (D) Schematic representation of the RGA and WOX9 deletions used in Y2H. Light green boxes represent the leucine repeats (L-X-L). EAR1 (IMLHI) is mutated to IMAHA in the so-called EAR1 deletion, and EAR2 (IRVFI) to ARAFA (orange boxes) in the EAR2 deletion.

To further map the interaction domain in the WOX9 protein, WOX9 was fragmented into three regions: the N-terminus, containing the DNA-binding homeodomain motif (Nt); the central part, containing the WUS box (M); and the C-terminus, containing two conserved EAR motifs. Interaction studies with these fragments showed that, unlike most DELLA partners reported to the date, RGA-WOX9 interaction does not involve the WOX9 DNA-binding homeodomain (Figure 12C). The Nt-WOX9 deletion was in fact unable to interact with M5-RGA, in contrast to the M-WOX9 fragment, which displays a strong interaction. Likewise, the Ct-WOX9 deletion still interacted with M5-RGA, although the interaction was much weaker than for the M-WOX9 fragment. From these results we can conclude that the main RGA interacting domain in the WOX9 protein is the WUS-box, although the EAR motifs at the C-terminal of the protein may also contribute to interaction.

To further look into the function of these conserved boxes, we generated three additional constructs which consisted of the whole protein lacking the WUSbox (delW), the whole protein with the first EAR motif mutated (EAR1) or with mutations in the second EAR motif (EAR2). To delete the WUSbox, the N-terminal and C-terminal regions of WOX9 were amplified using the primers WOX9for+delWUSbox and delWUSboxF+WOX9rev, that introduced a SalI restriction in the deleted WUSbox region. PCR products were cut with SalI, ligated, and used as template for amplification of the full length WOX9 protein lacking the WUS-box, with the primers WOX9for and WOX9rev. Mutation of the EAR motifs was likewise done in two steps. First, PCRs were set with the primers WOX9mtEAR1/2F+WOX9rev and WOX9for+WOX9mtEAR1/2R to introduce the Leu/Ile to Ala mutations. The two generated fragments were then annealed, and full-length protein with the introduced mutations was amplified with primers WOX9for+WOX9rev, to be cloned into pENTRY-S/D-TOPO, and mobilized by LR recombination into pGADT7.

Interaction studies with the delW, EAR1 and EAR2 constructs confirmed that RGA-WOX9 interaction occurs via two independent regions in each of these proteins. The WUS-box deleted delW protein interacted with RGA, RGA-SAW, and M5-RGA, but showed a very weak interaction with F1-RGA. Deletion of the LHRI motif in del1RGA completely abolished delW-del1RGA interaction, indicating that LHRI is critical for the interaction with the WOX9 protein lacking the WUS-box. As for the WOX9 EAR motifs, mutation of EAR2 did not affect the interaction with any of the RGA constructs, indicating that EAR2 plays no role in the interaction. Conversely, mutation of EAR1 motif made interactions with del1-RGA, del1-SAW, del2 and Relig much weaker, indicating that this repressive motif contributes to enhance RGA-WOX9 interaction by binding to the LHRI domain (Figure 12C). We can thus conclude that both the LHRI domain and the C-terminal RGA end mediate WOX9 interaction, with LHRI displaying preferential binding affinity to the EAR1 motif, while the C-terminal end of RGA mediates interaction with the WOX9 WUS-box.

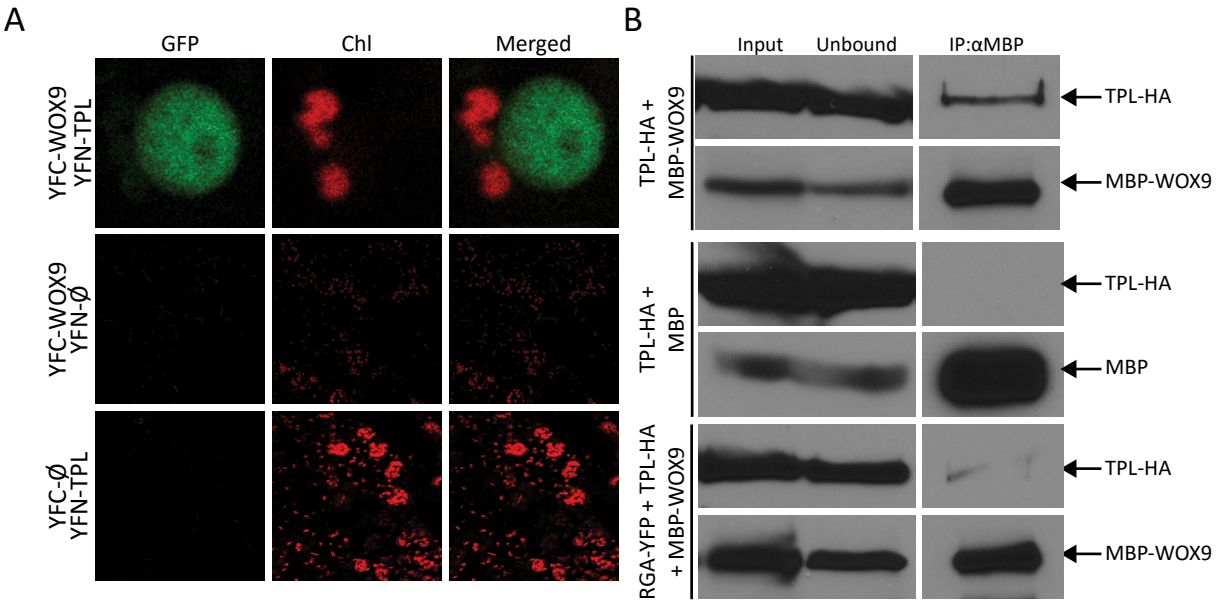

Figure13. WOX9 interacts with TOPLESS (TPL) and RGA competes for this interaction (A) Bimolecular Fluorescence Complementation (BiFC) assay showing the interaction of WOX9 fused to the C-terminus of the Yellow Fluorescent Protein (YFP) (YFC-WOX9) and TPL fused to the N-terminus of YFP (YFN-TPL). As a negative control, the tagged proteins were expressed with the complementary empty vectors. (B) Co-immunoprecipitation (coIP) assay showing an interaction of TPL-HA and WOX9 fused to the maltose binding protein (MBP-WOX9). Proteins were immunoprecipitated with an anti-MBP antibody and detected by western blot with the anti-MBP and anti-HA antibodies. TPL-HA was co-expressed with MBP as a negative control. TPL-WOX9 interaction is disrupted when RGA-YFP is co-expressed with TPL-HA and MBP-WOX9.

8. WOX9 INTERACTS WITH TOPLESS AND RGA COMPETES FOR THIS INTERACTION

The finding that WOX9 has two conserved EAR motifs and several L-X-L repeats, shown in other transcriptional regulators to be recognized by the co-repressor TOPLESS (Szemenyei et al. 2008), prompted us to test whether WOX9 was a TPL interactor. To this end, the *TPL* ORF was inserted into the YFN43 and YFC43 BiFC vectors, and combinations of the different WOX9 and TPL split YFP constructs, along with the empty vector controls, infiltrated into *N.benthamiana* leaves. Confocal microscopy detection of the reconstituted YFP protein showed that YFC-WOX9 interacts with YFN-TPL in the nucleus. Expression of these proteins with the complementary empty vectors did not produce any fluorescence, confirming a specific interaction (Figure 13A). We also performed coIP studies of total leaf extracts expressing the TPL protein fused to the Hemagglutinin tag (TPL-HA) and MBP-WOX9. After MBP-WOX9 immunoprecipitation with an anti-MBP antibody, we analyzed this fraction for the presence of both MBP-WOX9 and TPL-HA proteins, by western blot inmunodetection with anti-MBP and anti-HA antibodies. As a negative control, we co-expressed TPL-HA with the MBP protein. We detected TPL-HA in the MBP-WOX9 immunoprecipitated fraction, but not in the fraction retrieved by immunoprecipitation of MBP. This result confirmed that WOX9 and TPL interact

in vivo, as TPL-WOX9 complex formation pulls-down the TPL-HA protein during MBP-WOX9 immunoprecipitation (Figure 13B).

Notably, the finding that TPL interacts with WOX9 suggests that this factor is a transcriptional repressor. Moreover, we showed that the WOX9 EAR1 motif plays an important role in RGA interaction. The ability of WOX9 to interact with both the co-repressor TPL and the DELLA proteins fits with a working model where WOX9 represses gene expression and RGA de-represses WOX9 regulated genes by competing for TPL interaction. To test this hypothesis, we transiently co-expressed the TPL-HA and MBP-WOX9 proteins in *N.benthamiana* leaves, in the presence or absence of RGA-YFP. Immuno-precipitation studies, followed by WB detection of the TPL-HA and WOX9-MBP proteins, showed that the amount of TPL-HA pulled-down by WOX9-MBP was strongly reduced in the presence of RGA-YFP, even though WOX9-MBP protein levels were similar in these two fractions (Figure 13B). This means that RGA interferes with TPL for WOX9 interaction, in support of a mechanistic model whereby RGA de-represses WOX9 target gene expression, by competing for WOX9 and TPL interaction.

9. *WOX9* IS EXPRESSED IN THE SAM AND ROOT MERISTEMS AND IN FLORAL CARPELS.

To gain insight into WOX9 function, we analyzed its expression pattern by staining *pWOX9::GUS* transgenic lines. Staining of 4-day-old seedlings evidenced that *WOX9* is highly expressed in the root meristem and it forms a ring at the base of the SAM. This SAM pattern reminds that of genes specifically expressed in organ boundaries and in fact, staining of older seedlings showed that GUS activity was confined to the basis of new emerging leaves (Figure 15A). Histochemical sections of the SAM and root meristems showed that, in the shoot apex, GUS staining is located at both sides of the central meristem, marking the bases of the new forming leaves (Figure 14A). In the root meristem, staining was localized in the transition-elongation zone and was specific to trichoblasts, which are the cells that will differentiate into root hairs (Figure 14C). Remarkably, a root specific expression pattern is already seen in mature embryos (Figure 14B), suggesting a role of this factor during early root development.

Interestingly, GUS staining in adult plants was detected in the gynoecium of the flowers (Figure 14D), but not in the boundaries between floral organs. This suggests that the ring of stained cells aroung the SAM do not mark shoot organ boundary cells, but most likely correspond to cells that are in train of exiting the meristem to initiate a leaf differentiation program. Therefore, despite being expressed in the shoot and root meristems, WOX9 is not detected in undifferentiated stem cells, but in the meristematic transition zones, which points to an important role of this factor in the control of meristem cell differentiation.

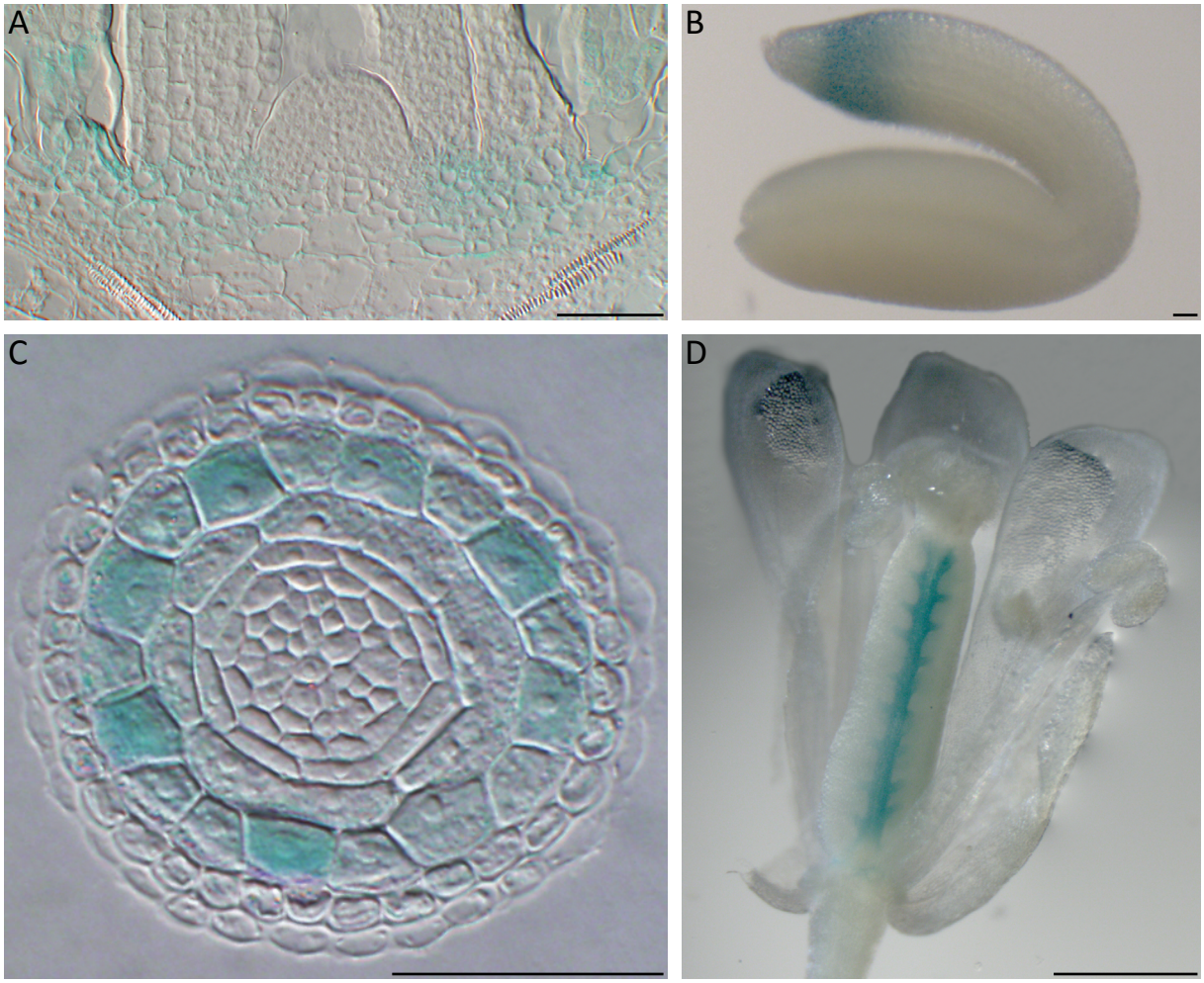

Figure 14. GUS staining of *pWOX9::GUS* seedlings. 4-day old seedlings (A, C) or adult plants (B, D) were fixed and over-night stained as described in materials and methods. (A) Longitudinal sections of the shoot apical meristem of 4-day-old-seedlings showing staining at the base of the meristem. Scale bar=50µM. (B) Mature embryo showing staining in embryonic radicle. Whole seeds were stained and the testa was removed right before taking the pictures. Scale bar=50µM. (C) Transversal section of the root apical meristem of 4-day-old seedlings, showing staining in trichoblasts. Scale bar=50µM. (D) Flower of an adult plant, showing staining in carpels. Scale bar=1mm.

As *WOX9* over-expression was found to confer increased tolerance to salt stress independently from GAs, we analyzed if its expression pattern changed in response to salt or GAs. ABA was also included in these studies, as salt is known to induce ABA synthesis, and it is reported that ABA and GA exert antagonistic roles during abiotic stress (Colebrook et al. 2014). To this end, 4-day-old seedlings were treated for six days with GM (mock), GM supplemented with 100 mM NaCl (NaCl), 10µM ABA (ABA), 25µM GA_3 (GA) or a combination of these treatments, before being subjected to GUS staining. A notable reduction in GUS activity was observed in response to NaCl application, and especially in response to ABA. Moreover, a similar reduction in GUS activity was observed in the SAM and the roots, indicating that salt and ABA indistinctly suppress *WOX9* expression in these two tissues. GA application, on the other hand, did not affect GUS levels and did not reverse the inhibitory effects of salt or

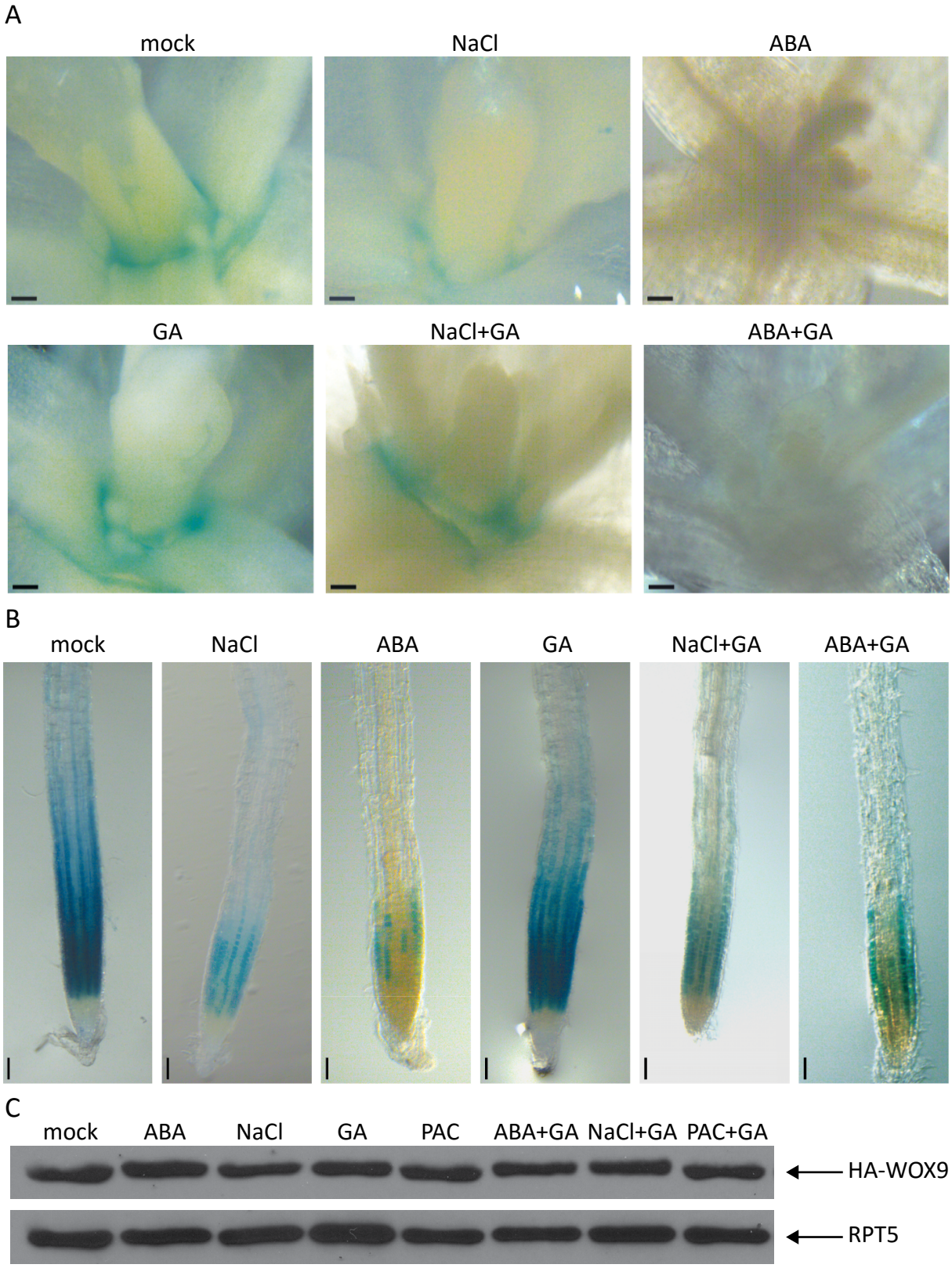

Figure 15. Changes in WOX9 expression in response to salt, GA, ABA and PAC treatments. 4-day-old seedlings were transferred to GM vertical plates (mock), with 10µM ABA (ABA), 100mM NaCl (NaCl), 25µM GA_3 (GA), 2µM PAC (PAC) or combinations of those and grown for six additional days before harvesting. (A,B) *pWOX9::GUS* seedlings stained for 2h at 37ºC for GUS detection at the base of the SAM (A) and root meristem (B). Scale bar=50µm. (C) Total proteins were extracted from *35S::HA-WOX9* seedlings and HA-WOX9 protein levels analysed by western blot. RPT5 was used as loading control.

ABA (Figure 15A and B). Thus, these results indicate that *WOX9* gene expression is negatively regulated by ABA, and that inhibition of this gene is not antagonistically regulated by GA.

Effects of salt and ABA on *WOX9* transcription prompted us to investigate whether these treatments also affected WOX9 protein stability. The *35S::HA-WOX9* line, constitutively expressing the HA-tagged protein, was used to these studies. 4-day-old seedlings were transferred for 6 days to GM (mock), 10µM ABA (ABA), 100mM NaCl (NaCl), 25µM GA_3 (GA), or 2µM paclobutrazol (PAC) and analyzed by WB for HA-WOX9 protein levels. WOX9 protein levels were in all cases similar, which indicates that salt and ABA inhibit *WOX9* expression at the transcriptional level, but do not affect stability of the protein (Figure 15C).

10. THE *stip-2* MUTANT HAS A SMALLER SHOOT APICAL MERISTEM AND SHORTER ROOT MERISTEM THAN Col-0

Because *WOX9* is actively expressed in the SAM and root meristems we assessed whether the *WOX9* over-expressor lines (*35S::HA-WOX9* and *stip-D*) and *stip-2* mutants displayed smaller or larger meristems than Col-0. For the SAM studies we used 7-day-old-seedlings, which were fixed with FAA, dehydrated and dried using a critical point dryer. Leaves were separated with the aid of a stereomicroscope and pictures taken of the apical meristem with a table scanning electron microscope. Comparison of these pictures showed that the SAM of *35S::HA-WOX9* seedlings was slightly larger than that of Col-0, but this difference was not statistically significant. Conversely, the meristem of *stip-D* mutants, expressing very high levels of the wild-type protein, was larger than the SAM of Col-0, while of the one of *stip-2* mutant was clearly smaller (Figure 16A and C).

To analyze the root meristem size, we used 6-day-old seedlings, which were stained with propidium iodide and observed at the confocal microscope. Size of this meristem was determined by measuring the distance from QC to the first elongated cells (length is longer than their diameter) in the epidermis or cortex. The size of the Col-0, *35S::HA-WOX9* and *stip-D* root apical meristems were similar, whereas a clearly shorter RAM was observed in *stip-2* seedlings (Figure 16B and C). Moreover, we noticed that *stip-2* roots were thinner than the ones of the other genotypes, so we decided to perform transversal sections of the roots to see if their cellular pattern was altered or they displayed smaller cells instead. *stip-2* roots did not lack any of the normal root cell layers, but we observed that the pattern of trichoblast and atrichoblast cells in the epidermis was somehow abnormal. While Col-0, *35S::HA-WOX9* and *stip-D* roots have in general two non-hair cells between hair cells, in the *stip-2* mutant there is only one non-hair cell intercalated between hair cells, which leads to the same number of trichobasts but a reduced number of epidermal cells. Besides, in *stip-D* we observed a slight contrary phenotype, as in some cases three atrichoblasts are between two trichoblasts (Figure 16D).

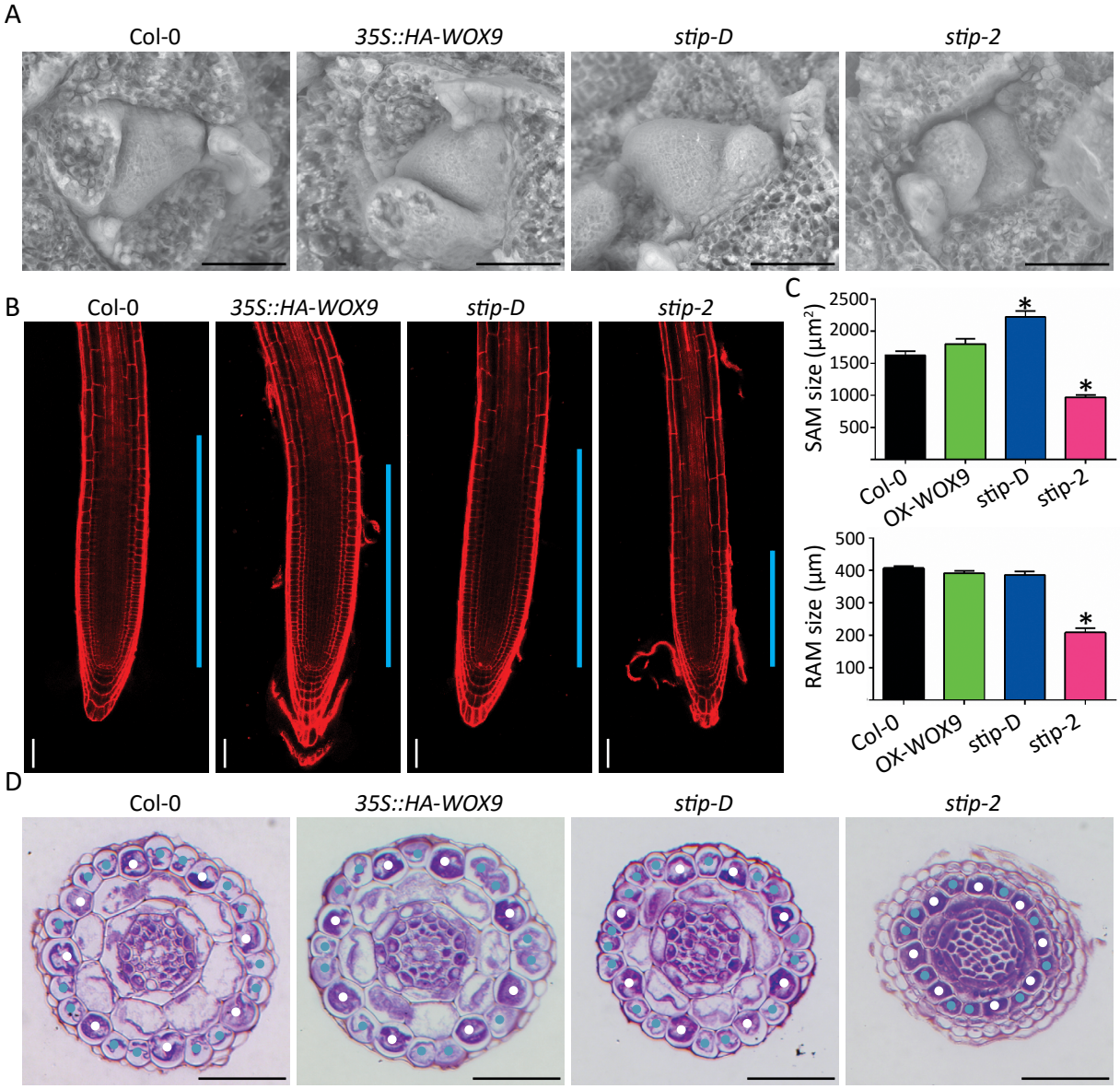

Figure 16. Meristem size of Col-0 and *WOX9* lines: *35S::HA-WOX9*, *stip-D* and *stip-2* (A) Scanning microscopy pictures of the shoot apical meristems (SAM). (B) Confocal microscopy pictures of propidium iodide (PI)-stained roots. Size of the root meristem is indicated by a blue line. (C) Histograms showing the SAM area and the RAM lengths. Means and their standard error (error bars) values are shown. n=10. (D) Transversal sections of the meristematic zone of the roots showing the number of trichoblasts (white circle) and atrichoblasts (blue circles). Scale bar=50µm

Altogether, specific *WOX9* expression in the SAM and root meristems, and reduced meristem sizes of the *stip-2* mutant, suggest an important function of this homeobox factor in preventing premature meristem cell differentiation. On the other hand, its trichoblast specific expression and reduced number of atrichoblast cells in the loss-of-function mutant, would suggest an additional role of WOX9 in root epidermal cell patterning.

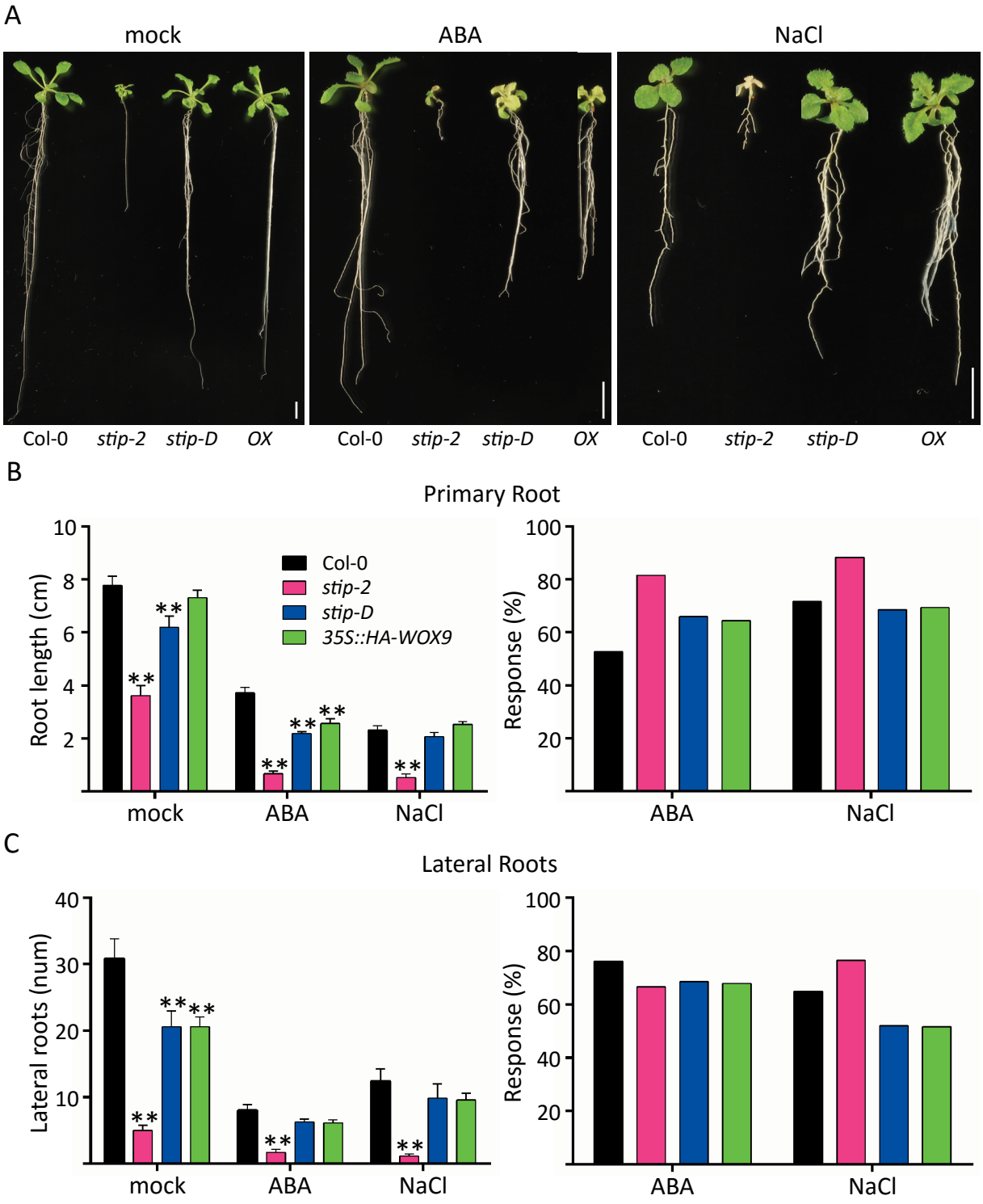

Figure 17. Root phenotypes of seedlings treated with ABA and NaCl. 3-day-old seedlings were transferred to vertical GM plates (mock), plus 10µM ABA (ABA) or 100mM NaCl (NaCl). Pictures were taken after 7 days of treatment and used to measure primary root length and the number of lateral roots. (A) Representative pictures of the plants in each of these treatments. Scale bar= 1cm. (B) Effect of these treatments on primary root length. (C) Effect of treatments on the number of lateral roots. Means and their standard error (error bars) values are shown. n=20.

11. MISEXPRESSION OF *WOX9* LEADS TO ROOT GROWTH DEFECTS

Because of its specific expression in the root transition zone we wondered if WOX9 would modulate root growth and architecture. To test this, all different genotypes were germinated on GM media, and 3-day-old seedlings were transferred to the same media (mock), or to GM media supplemented with 10µM ABA or 100mM NaCl. Pictures of the plants were taken at day 10, and used to measure primary root length (PR) and to count the number of lateral roots (LRs).

stip-2 seedlings were smaller than Col-0 and in mock conditions developed much shorter roots, in addition to producing less lateral roots. *stip-D* and *35S::HA-WOX9* seedlings have also shorter roots, although in this case differences were smaller than in *stip-2*. Indeed, differences were statistically significant for *stip-D* but not for *35S::HA-WOX9* seedlings. Moreover, both over-expression lines produced lateral roots, but the number of LRs was reduced compared to Col-0. These root phenotypes were far more drastic in the mutant, so we can affirm that WOX9 is required for normal root growth (Figure 17).

ABA caused growth inhibition of all four genotypes. Besides inhibition of root growth and a reduction in the number of LRs, ABA induced senescence of the leaves which were observed to turn yellow. In the presence of ABA, all three WOX9 genotypes were smaller than Col-0 and had shorter primary roots. When compared to mock, they displayed a hypersensitive root growth inhibition response, which was more evident in the *stip-2* mutant. However, when LR number was analyzed, *stip-D* and *35S::HA-WOX9* lines seemed to be less sensitive to ABA. Regarding the aerial part, *stip-2* completely stopped growing, while *stip-D* and *35S::HA-WOX9* were smaller and paler than the wild-type (Figure 17).

Salinity, on the other hand, reduced both shoot and root growth. All seedlings were smaller than in mock conditions and had shorter roots. *stip-D* and *35S::HA-WOX9* seedlings were more tolerant to salt and compared to mock conditions showed a smaller inhibition of root growth. However, their tolerant phenotype was especially evident when we counted their number of LRs, which were also longer than in Col-0. Growth of *stip-2* seedlings was in the end completely inhibited, and these plants did not survive on the salt media. These phenotypes confirmed that the over-expression lines are more tolerant to NaCl than Col-0, while *stip-2* is more sensitive, meaning that WOX9 plays a pivotal role in the adaptation response to salt stress (Figure 17).

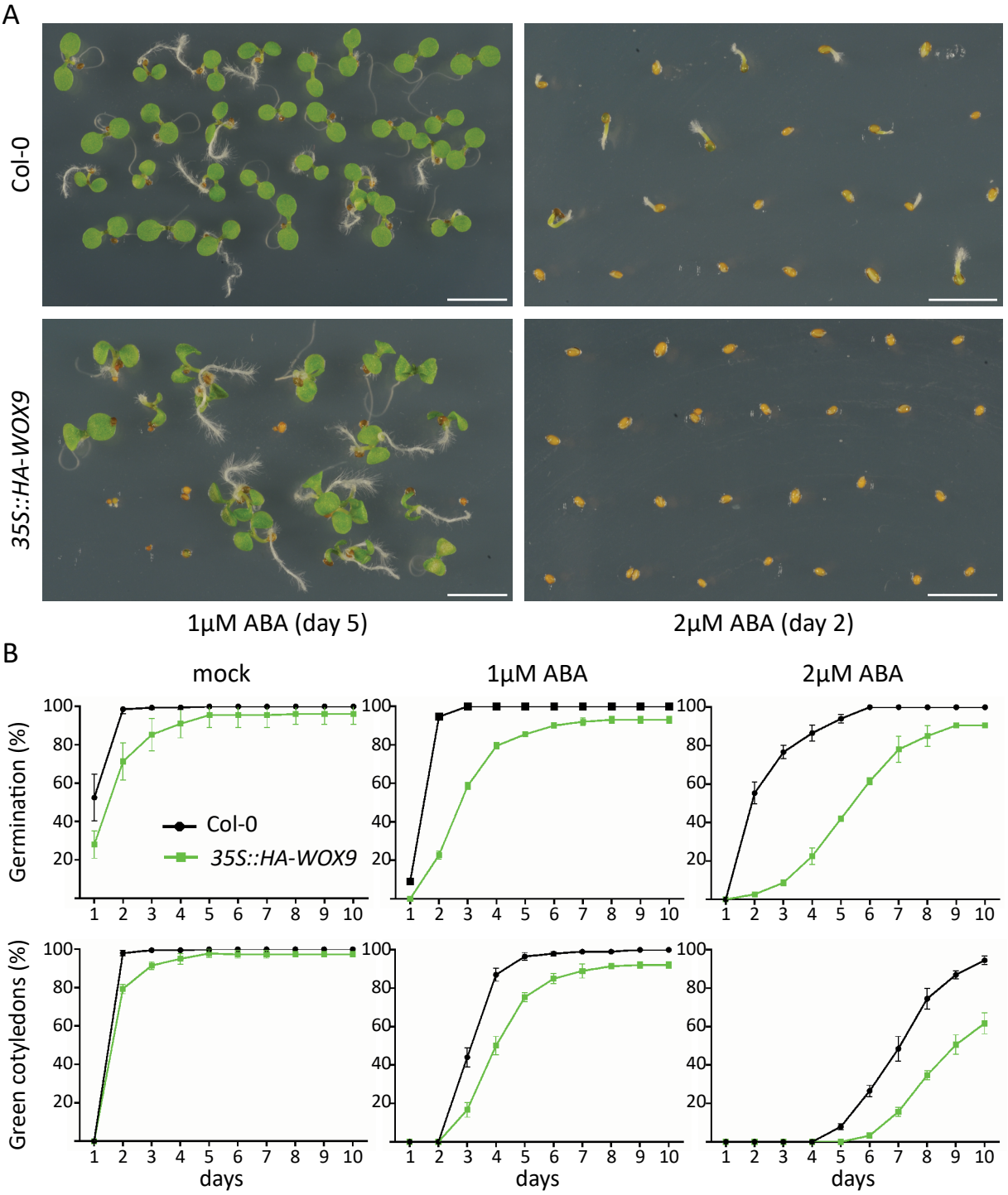

Figure 18. *35S::HA-WOX9* line is hypersensitive to ABA (A) Pictures of Col-0 and *35S::HA-WOX9* seeds germinated on 1µM ABA for 5 days and on 2µM ABA for 2 days, where it is observed a delay in germination and cotyledon opening and greening in the over-expressor line. (B) Graphs showing the germination and cotyledon greening rates. Seeds were plated on GM (mock), or GM supplemented with 1 or 2µM ABA and number of germinated seeds was scored every day for ten days. 4 replicates of 50 seeds were used for quantification of the germination response in these genotypes. Means and their standard errors (error bars) are shown. On ABA media, *35S::HA-WOX9* seeds showed a reduced rate of germination and greening of the emerging seedlings. Scale bar=5mm.

12. OVER-EXPRESSION OF *WOX9* ENHANCES ABA SENSITIVITY IN SEEDS

Previous root growth studies evidenced that WOX9 lines display an altered response to ABA, but this phenotype was somehow inconsistent when analyzing primary root growth or number of lateral roots. In fact, *stip-D* and *35S::HA-WOX9* lines display a reduced sensitivity to ABA for LR formation, but still a hypersensitive response for primary root growth. To better characterize the response to ABA in these plants, we performed germination and post-germinative growth assays, by growing Col-0 and *35S::HA-WOX9* seeds in GM or in the presence of ABA (1 and 2 µM).

In mock conditions, germination of *35S::HA-WOX9* seeds and seedling establishment was slower in comparison to Col-0 but these differences were only observed for day 1-3. At day 5, both genotypes have managed to develop green cotyledons at a 100% rate. ABA was observed to inhibit germination in a concentration dependent manner, and by comparing the timing of germination and cotyledon greening we can see that Col-0 reaches in 1µM ABA 100% germination rates at day 3 and in 2µM ABA at day 6. Delay in seed germination was found to be much stronger in *35S::HA-WOX9* lines and the higher the concentration of ABA, the bigger the differences are. In 1µM ABA, a 90% germination rate is reached at day 6, while in 2µM ABA it takes until day 9. This tendency is similar for opening of the cotyledons. It is important to note that, although ABA slows down germination, by day 10 Col-0 seeds had germinated and developed green cotyledons in all conditions tested, while for *35S::HA-WOX9* line, this was true in mock and 1µM ABA conditions, but not in 2µM ABA, where only 60% of the seedlings had opened the cotyledons (Figure 18B). Pictures of the seeds at day 2 in 2µM ABA are shown to exemplify the differences in germination rates (55% vs 3%) between these two genotypes. Pictures taken at day 5 in 1µM ABA are also shown for differences in the cotyledon opening rates (96% vs 75%) (Figure 18A). These results demonstrate that *35S::HA-WOX9* seeds are hypersensitive to ABA , hence suggesting a function of WOX9 in ABA signaling.

13. *WOX9* OVER-EXPRESSION CAUSES A DECREASE IN GIBBERELLIN AND CYTOKININ LEVELS

As the observed phenotypes linked WOX9 function to ABA and GA signaling, we decided to measure levels of these hormones in the *35S::HA-WOX9* line. To this aim, Col-0 and *35S::HA-WOX9* plants were grown in soil in SD controlled conditions for 4-weeks, and aerial rosettes collected from these plants. Triplicated samples were obtained for each of these genotypes and the frozen materials sent to the Hormone Analyses Service of the IBMCP in Valencia, for determination of ABA, JA, SA, IAA, GA, and CK levels.

Endogenous levels of ABA in these plants turned out to be identical to those of Col-0, which shows that the different response to this hormone is not caused by a defect in ABA

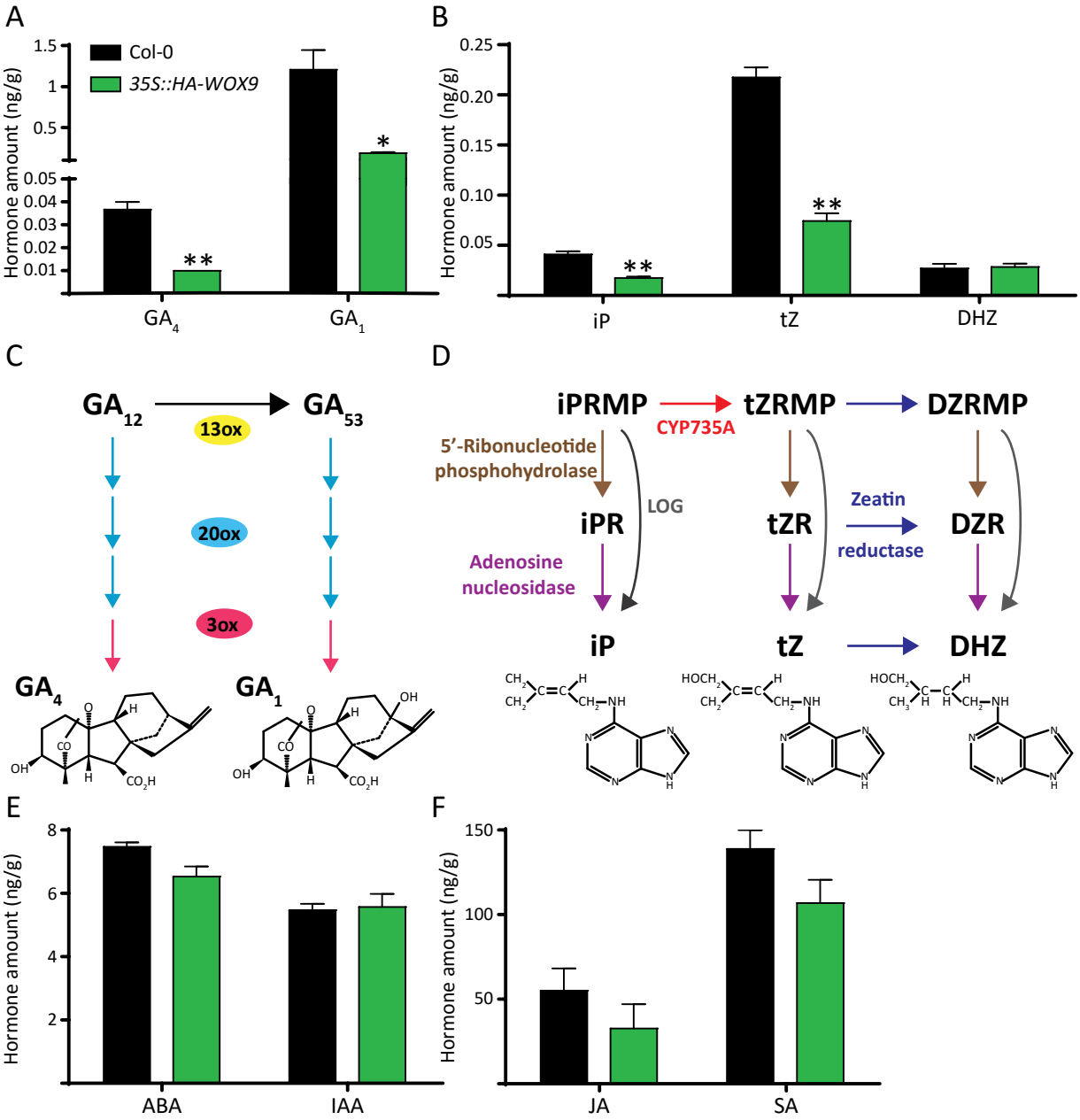

Figure 19. Hormones measurements. 4-week-old Col-0 and *35S::HA-WOX9* rosettes were collected, frozen in liquid nitrogen and sent to the IBMCP for hormone measurements. (A) Levels of bioactive gibberellins: GA_4 and GA_1. (B) Levels of the cytokinins: isopentenyladenine (iP), *trans*-Zeatin (tZ) and dihidrozeatin (DHZ). (C) Last steps of the GA biosynthesis pathway, involving the GA13-oxidase (13ox), GA20-oxidase (20ox) and GA3-oxidase (3ox) enzymes. (D) Last septs of iP, tZ and DHZ biosynthesis, involving CYP735A, 5'-Ribonucleotide phosphohydrolase, Adenosine nucleosidase, and Zeatin reductase enzymes. Cytokinins nucleoside 5'-monophosphate (iPRMP, tZRMP, DZRMP) are activated in a two-step reaction catalysed by 5'-Ribonucleotide phosphohydrolase and Adenosine nucleosidase or by a one-step reaction catalysed by LONELY GUY (LOG). (E) Levels of abscisic acid (ABA) and indole acetic acid (IAA). (F) Levels of jasmonic acid (JA) and salycilic acid (SA). Graphs show means and their standard error (error bars) values (n=3).

biosynthesis. Levels of JA, SA or IAA were also similar to Col-0, which confirmed that plants used for the analyses did not suffer from any abiotic or biotic stress (Figure 19E and F). However, notable differences in both GA and CK levels were observed in *35S::HA-WOX9* plants.

Levels of GA_4 and GA_1, the bioactive forms of GA, were actually strongly reduced in *35S::HA-WOX9* plants compared to Col-0, with these differences being statistically significant for both of them (Figure 19A).

As for CK, *35S::HA-WOX9* line showed a significant reduction in *trans*-zeatin (tZ) and isopentenyladenine (iP) levels, and those of dihydrozeatin (DHZ) were identical to Col-0 control (Figure 19B). Notably, these three CK forms predominantly originate from the methylerythritol 4-phosphate (MEP) pathway, isopentenyl nucleotides being converted into the corresponding tZ-nucleotides by cytochrome P450 monooxygenases (CYP735s). Both CK-nucleotides are then directly converted into the active iP and tZ free bases by LOG phosphoribohydrolases (Figure 19D). Quite remarkably, *stip-D* and *35S::HA-WOX9* leaves display wavy margins, a phenotype that has been associated to an altered balance between CKs and GAs (Blein et al. 2013).

Reduced levels of bioactive GAs in *35S::HA-WOX9* line prompted us to analyze whether these plants accumulated higher DELLA levels. To this aim, Col-0, *35S::HA-WOX9* and *stip-2* seeds were germinated on GM media, and 4-day-old seedlings transferred to GM (mock) or GM supplemented with 10µM ABA (ABA), 100mM NaCl (NaCl), or 2µM paclobutrazol (PAC), to be cultivated for 6 additional days. Total protein extracts were then obtained and analyzed by western blot, using an anti-RGA specific antibody (kindly provided by Dr. Claus Schwechheimer). In contrast to our expectations, *35S::HA-WOX9* seedlings accumulated similar RGA protein levels to Col-0, with increased levels of this repressor being instead detected in the *stip-2* loss-of-function mutant. ABA and PAC treatments induced a similar stabilization of RGA in both *35S::HA-WOX9* and Col-0 plants, further increased protein accumulation levels being also observed in *stip-2* mutants (Figure 20). Even though it is reported that RGA accumulates in response to salt (Achard et al. 2006), in our hands this response was very mild, but clearly stronger in *stip-2* lines as compared to *35S::HA-WOX9* and Col-0.

These results would indicate that WOX9 function is required for proper regulation of DELLAs protein stability and GA homeostasis, although additional studies would need to be performed to further understand why reduced GA levels as a result of WOX9 over-expression are not associated to RGA accumulation or growth inhibition. In this sense, it should be critical to determine the levels of GA and CKs in *stip-2* plants, as this might provide new hints on the mechanisms underlying this regulation.

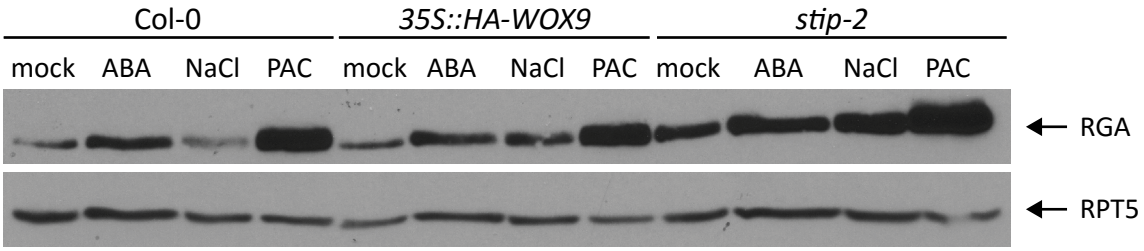

Figure 20. RGA accumulation levels in *WOX9* lines. 4-day-old Col-0, *35S::HA-WOX9* and *stip-2* seedlings were transferred to GM (mock), or GM supplemented with 10µM ABA (ABA), 100mM NaCl (NaCl), or 2µM PAC, and cultivated for 6 additional days. Total protein extracts were analysed for RGA protein levels by western blot by incubation with an anti-RGA antibody. RPT5 was used as loading control.

14. *WOX9* OVER-EXPRESSION LEADS TO AN ENHANCED CYTOKININ SENSITIVITY AND REDUCED RESPONSE TO GIBBERELLINS

The observation that *35S::HA-WOX9* plants accumulate reduced levels of *trans*-zeatin (tZ) and isopentenyladenine (iP) links function of this homeodomain factor with CK signaling. Indeed, it has been reported that CK signaling activates *WOX9* expression in meristematic tissues, WOX9 being shown to be involved in the activation of several CK signaling components (Skylar et al. 2010; Skylar & Wu 2010). CKs are also known to negatively regulate salt signaling, CK-deficient mutants being shown to exhibit a strong stress-tolerant phenotype (Kumar & Verslues 2015; Nishiyama et al. 2011; Tran et al. 2007). To analyze sensitivity of *WOX9* lines to CK, we excised the hypocotyls of 10-day-old Col-0, *stip-2*, and 3*5S::HA-WOX9* seedlings and cultivated them on media containing 100ng/ml 2,4-dichlorophenoxyacetic acid and increasing concentrations of kinetin (0, 25, 200 and 1000 ng/ml), to assess for callus formation. *cre1-3 ahk3-4* seedlings, with knock-out mutations in the CK receptor *CRE1* and *AHK3* genes, were also included in these assays as a control for CK insensitivity.

A dose-dependent response to increased CK concentrations could be observed in Col-0, with larger calli being generated with higher concentrations of kinetin, whereas *cre1-3 ahk3-4* mutants did not produce calli at any of the tested concentrations. *stip-2* mutants behaved as Col-0, but response to CK was enhanced in the *35S::HA-WOX9* explants. In fact, although no differences were observed at low concentrations of kinetin (0 and 25ng/ml), these hypocotyls developed larger calli that turned green at 200 and 100ng/ml kinetine, indicating an enhanced sensitivity of these lines to exogenous CKs (Figure 21).

ABA and GA exert antagonistic effects on gene expression, and we hypothesized that *35S::HA-WOX9* hypersensitivity to ABA might cause a reduced response to GA and impaired feed-back regulation of GA synthesis. Therefore, we investigated sensitivity to GA application

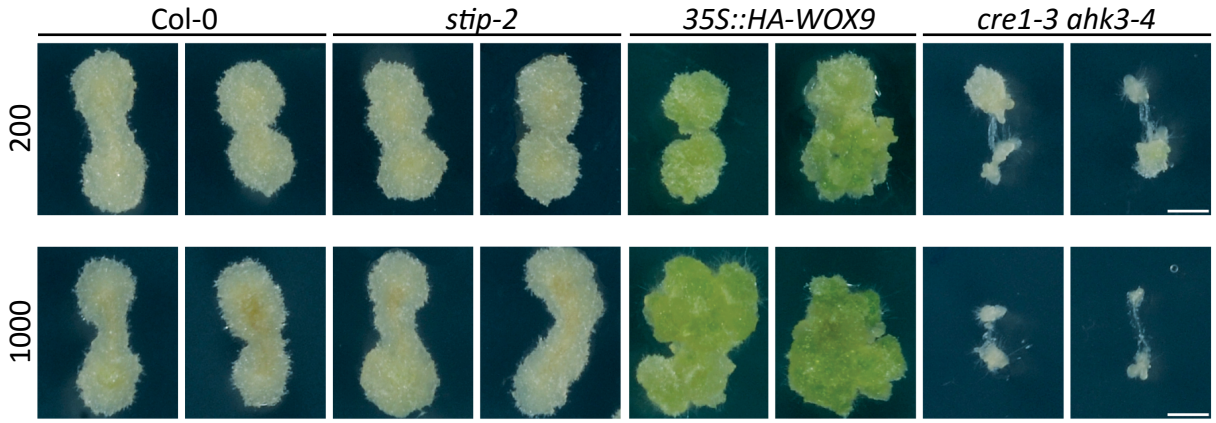

Figure 21. Cytokinin response of *WOX9* lines. Hypocotyls of 10-day-old Col-0, *stip-2*, *35S::HA-WOX9* seedlings were excised and placed on GM supplemented with 100ng/ml 2, 4- dichlorophenoxyacetic acid (2,4-D) and 200 or 1000 ng/ml kinetin, and calli induction was evaluated twenty days later. *cre1-3 ahk3-4* seedlings were used as positive controls. Scale bar=2mm.

of *35S::HA-WOX9* and *stip-2* seedlings, by measuring hypocotyl growth effects of this hormone. Seeds were germinated on GM and after 1 day they were transferred to vertical GM plates (mock) or supplemented with 25 µM GA_3. On GM media hypocotyl lengths of *35S::HA-WOX9* and *stip-2* seedlings were similar to those of Col-0 seedlings. However, in the presence of GA, the *stip-2* mutant showed taller hypocotyls, while in *35S::HA-WOX9* these were shorter than the Col-0 wild-type, hence demonstrating that loss-of-function of *WOX9* leads to a hypersensitive response to GA, whereas increased levels of this homeodomain factor result in reduced sensitivity to this hormone (Figure 22).

Altogether, these results point to a pivotal role of WOX9 in regulating the balance between GA and CK signaling, such that increased WOX9 levels lead to a hypersensitive response to CK

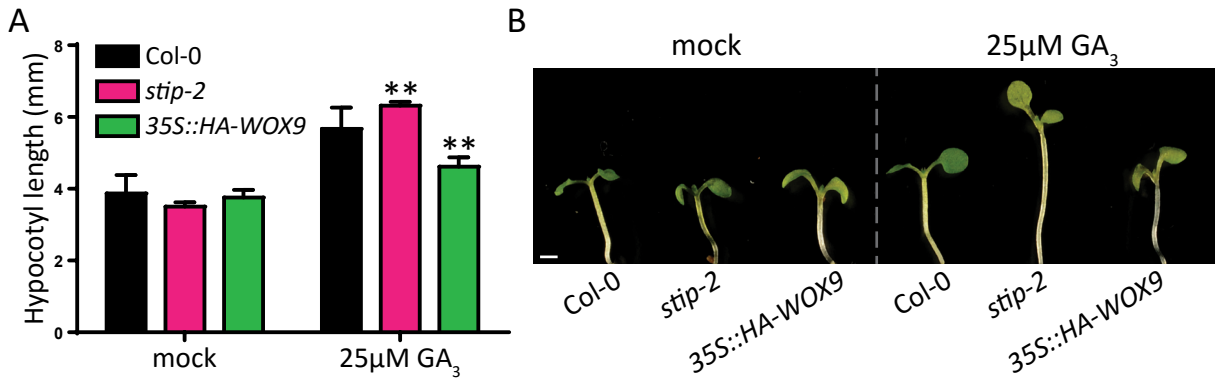

Figure 22. Sensitivity to gibberellins of *WOX9* lines (A) Measurement of the hypocotyl lengths of 6-day-old seedlings grown for five days on GM (mock) or GM supplemented with 25µM GA_3. Graphs show the means and their standard errors (error bars) values (n=20). (B) Representative pictures of the measurements. Scale bar=1mm

and reduced response to GA. This dual effect on CK and GA signaling likely affects homeostasis of these hormones, and leads to the reduced GA and CK levels seen in *35S::HA-WOX9* plants.

15. WOX9 CONTROLS ROOT HAIR FORMATION

Due to the specific expression of *WOX9* in the root trichoblasts we investigated whether *stip-2* or *35S::HA-WOX9* plants had any root hair formation defects. To this end, Col-0, *stip-2* and *35S::HA-WOX9* seedlings were germinated on GM and transferred after 3 days to vertical GM plates (mock) and GM plates supplemented with 10µM ABA, 50mM NaCl or 25µM GA_3. Seedlings were grown for 3 additional days in LD conditions, and pictures of the roots were taken to study root hair morphology, by selecting equally distant zones from the root tip.

stip-2 mutants showed in mock conditions shorter root hairs, while root hairs of *35S::HA-WOX9* seedlings were slightly longer than those of Col-0, although both phenotypes were mild. GA application did not affect root hair length, in contrast to the inhibitory effects of ABA and NaCl treatments. Inhibition was much stronger in *stip-2* mutants than in Col-0 and *35S::HA-*

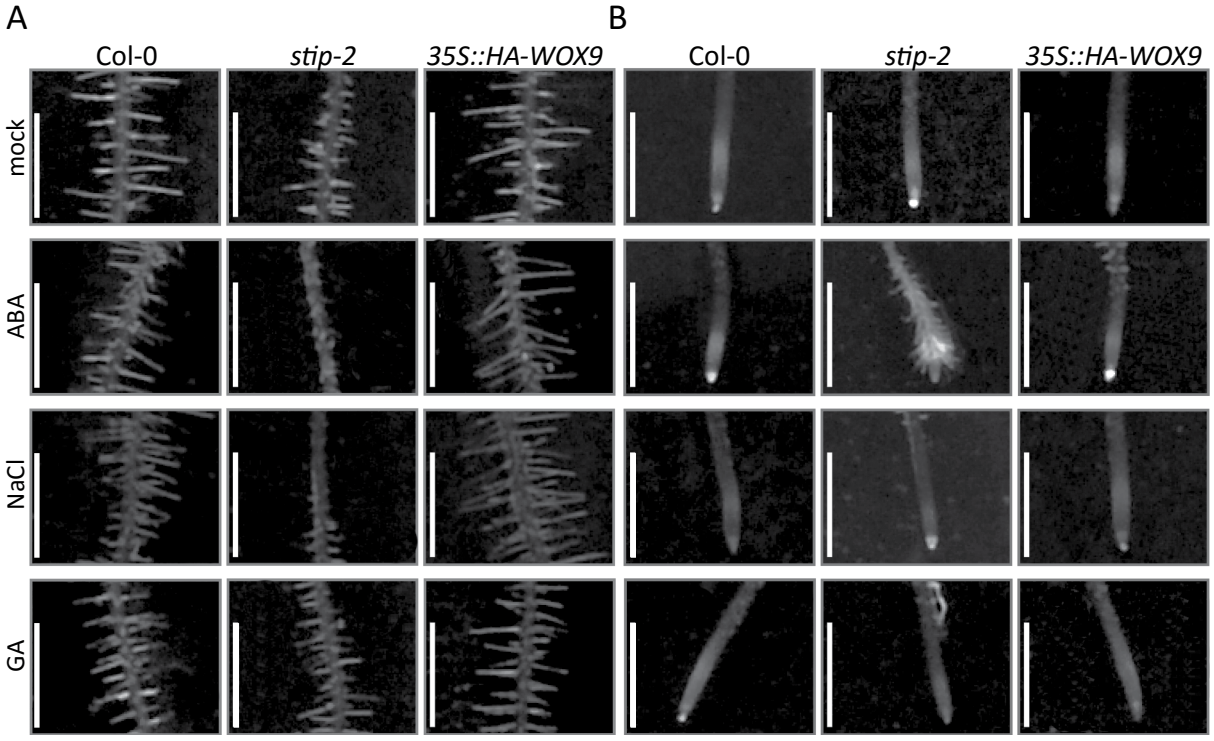

Figure 23. ***WOX9*** **lines show a root hair phenotype.** 3-day-old seedlings were transferred to vertical GM plates (mock) or GM supplemented with 10µM ABA (ABA), 100mM NaCl (NaCl) or 25µM GA_3 (GA), and pictures were taken after 3 days of treatment. Whole pictures of the roots are shown in Supplementary figure S5. (A) Detail of root hair lengths of Col-0, *stip-2* and *35S::HA-WOX9* roots. Pictures correspond to regions located at an equivalent distance from the root tip. (B) Root tip detail of Col-0, *stip-2* and *35S::HA-WOX9* seedlings subjected to the different treatments. Scale bar= 1mm.

WOX9 lines, such that roots of this mutant looked almost hairless on ABA or NaCl. Differences between Col-0 and *35S::HA-WOX9* roots were still minor, except for a smaller inhibitory effect of NaCl on *35S::HA-WOX9* root hair elongation (Figure 23A).

Besides the strong inhibition of root hair elongation, ABA provokes a striking effect on *stip-2* promoting differentiation of the cells immediately adjacent to the root tip into root hairs, although this zone includes the RAM and does not normally produce root hairs (Figure 23B).

Closer inspection of these roots with propidium iodide staining and confocal microscope, showed no major differences in the zone of root hair initiation between the three genotypes in mock, NaCl, or GA (Figure 24). At this magnification we observed that 50mM NaCl starts causing root cell damage, but this occurs at a similar extent in all three genotypes. Moreover, although GA seemed to promote earlier root hair differentiation, this response did not differ among genotypes. On the contrary, large phenotypic changes were observed in response to ABA treatment. ABA application indeed promoted *stip-2* mutants to develop root hairs very close to the tip, thus triggering premature differentiation of the trichoblasts. Furthermore, these cells were not elongated, as cells producing root hairs usually are.

Looking to a magnification of the meristem zone we observed that, upon ABA or NaCl treatments, *35S::HA-WOX9* roots had disorganized columella cells. However, this phenotype was mild and not observed in all roots. Again, major phenotypic differences were observed upon ABA application in the *stip-2* root meristem. This mutant has already a shorter meristem in mock conditions (Figure 16), but its root meristem size was strongly reduced after ABA application. Besides, cortex and epidermis cells fail to elongate after differentiation, and display a hexagonal shape (Figure 24B).

Therefore, its specific expression in trichoblast cells, together with the root hair phenotype of *stip-2* mutants, indicates that WOX9 plays a pivotal role in the control of root hair development by preventing premature differentiation of trichoblast cells triggered by ABA signaling.

16. WOX9 GENE REGULATED EXPRESSION

To gain insight into WOX9 downstream gene regulation, we carried out microarray hybridization studies using the WOX9 β-estradiol-inducible lines. Since this factor was identified by conferring tolerance to salt in the presence of GAs, and that it directly binds the DELLA proteins, we decided to perform gene expression studies under three different conditions: ± β-estradiol, which would inform about the WOX9 downstream targets; paclobutrazol (PAC) ± β-estradiol (WOX9 + DELLA), to test the effect of DELLAs accumulation on WOX9 gene

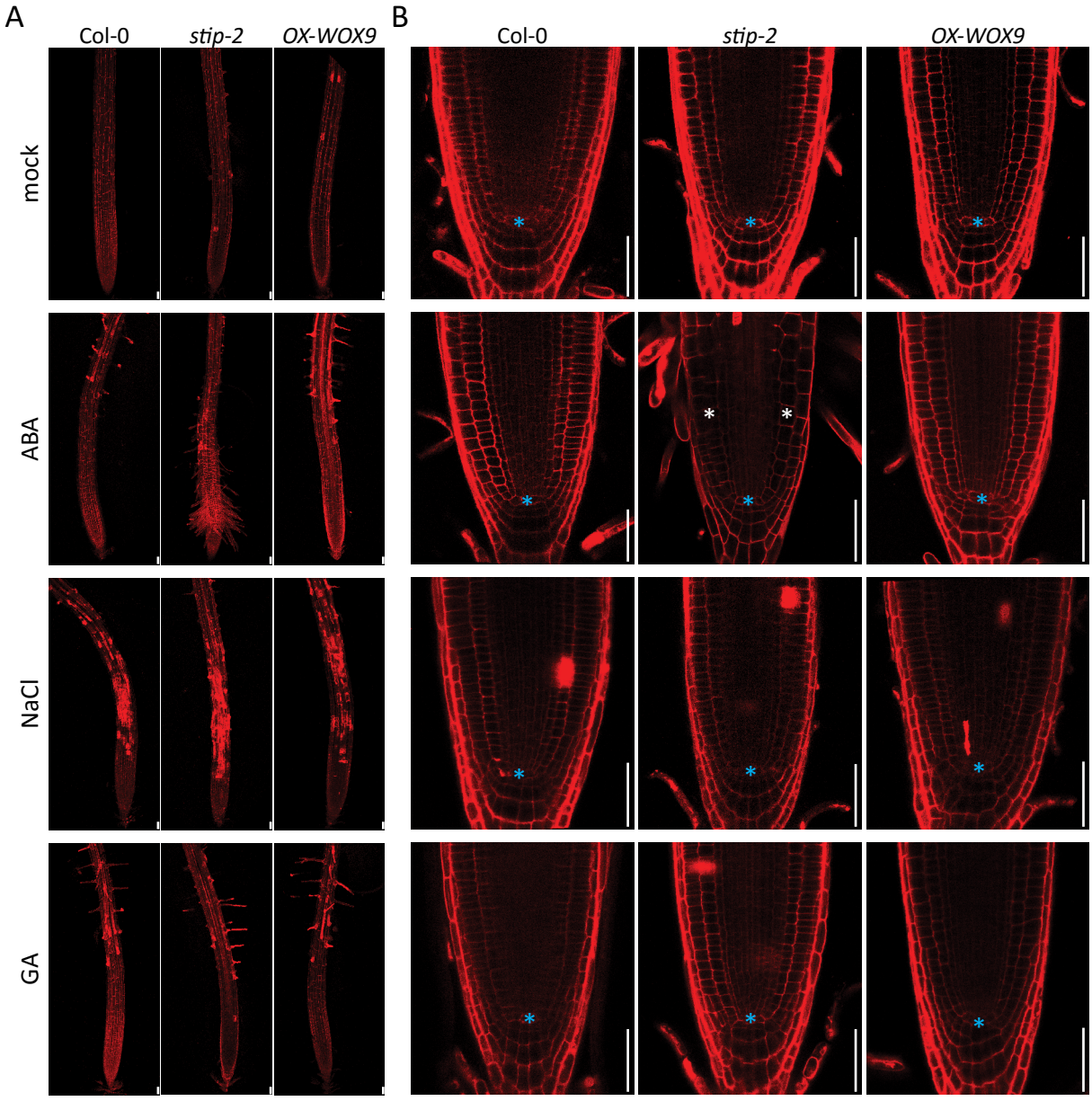

Figure 24. Root meristem differentiation and root hair formation. 3-day-old seedlings were transferred to vertical GM plates (mock), plus 10µM ABA (ABA), 100mM NaCl (NaCl) or 25µM GA3 (GA) and confocal microscopy pictures were taken after 3 days of treatment. (A) Pictures showing the initial formation of root hairs. (B) Higher magnification of the root tip, showing the quiescent center (QC; blue asterisk), columella and root meristem cells. End of the root meristem is indicated by white asterisks. At this magnification termination of the root meristem is only appreciated in *stip-2* roots treated with ABA. Differentiation of the meristem cells coincides with a massive formation of root hairs. Roots are stained with propidium iodide (10µg/ml). Scale bar=50µm.

expression; and GA+PAC ± β-estradiol (WOX9 –DELLA), which reproduce the conditions used in the screening and would inform about any potential role of DELLAs in modifying WOX9 target specificity.

For RNA extraction, seedlings were grown for 10 days on GM or 0,2µM PAC and then transferred to liquid media containing GM ± 10µM β-estradiol (mock-; mock+) or PAC ± 10µM

β-estradiol (PAC-; PAC+). For GA+PAC treatments seedlings were first transferred to PAC ± 10μM β-estradiol, and 10μM GA_3 was added 30 min before harvesting (PAC/GA-; PAC/GA+). Total incubation time in these media for β-estradiol induction was four hours. Microarray hybridization was performed by the Genomics Unit of the CNB.

Generated datasets were first selected for WOX9 regulated targets by comparing differential gene expression in mock- vs mock+ conditions. By applying a statistical cut of a fold change (FC) ≥ 2 and a p-value < 0.01 (Rank Products), we identified a total of 1634 differentially expressed genes. With this list of WOX9 targets we then queried the rest of hybridization conditions (PAC+, GA/PAC+, PAC-, GA/PAC-) and grouped them according to their differential expression pattern, applying K-means/K-medians clustering (KMC) and Euclidean distance using MeV program. Based on the trend of their expression profiles, we finally divided the genes into 5 clusters: 1-5, whose expression profiles are shown in Figure 25. Clusters 1 and 5 represent WOX9 activated genes, while clusters 2-4 include genes that are repressed by WOX9. The number of repressed genes is higher than the one of activated genes, which indicates that WOX9 mainly functions as a transcriptional repressor, consistent with the observed interaction with the co-repressor TOPLESS.

Notably, genes included in clusters 1 and 2 show opposite patterns of expression. Cluster 1 groups genes that are induced by WOX9 in mock conditions, but are no longer regulated by this factor in the presence of PAC or after a 30min GA treatment. On the other hand, cluster 2 groups genes that are repressed by WOX9 in mock conditions, but are no longer repressed after PAC or GA/PAC treatments. Interestingly, all these genes are either activated or repressed by PAC, which indicates that they are targets of the DELLAs. Although GA application should reverse this regulation, we see that GA reduces their fold change, but does not overcome PAC effects. It is thus likely that a 30min treatment with 10μM GA_3 was not sufficient for GA-regulated expression and longer incubation intervals should have been used. Thus, these clusters include DELLA-responsive genes that are also regulated by WOX9 in opposite ways (Figure 25).

Genes grouped in cluster 3 are repressed by WOX9 in mock conditions, but de-repressed by PAC. This effect is partially reversed by GA but not completely. Regarding PAC and GA/PAC treatments, these genes are negatively regulated by DELLAs, but its repression is lower than the one for genes in cluster 2. Moreover, for these genes, GA treatment partially compensated the negative effects of PAC, suggesting a faster response to DELLAs destabilization. Therefore, like cluster 2, this cluster includes GA/PAC-dependent genes regulated by WOX9 in opposite ways (Figure 25).

Clusters 4 and 5 include genes whose expression hardly change in response to GA or PAC treatments. However, they are WOX9-regulated genes (repressed in cluster 4 and activated in

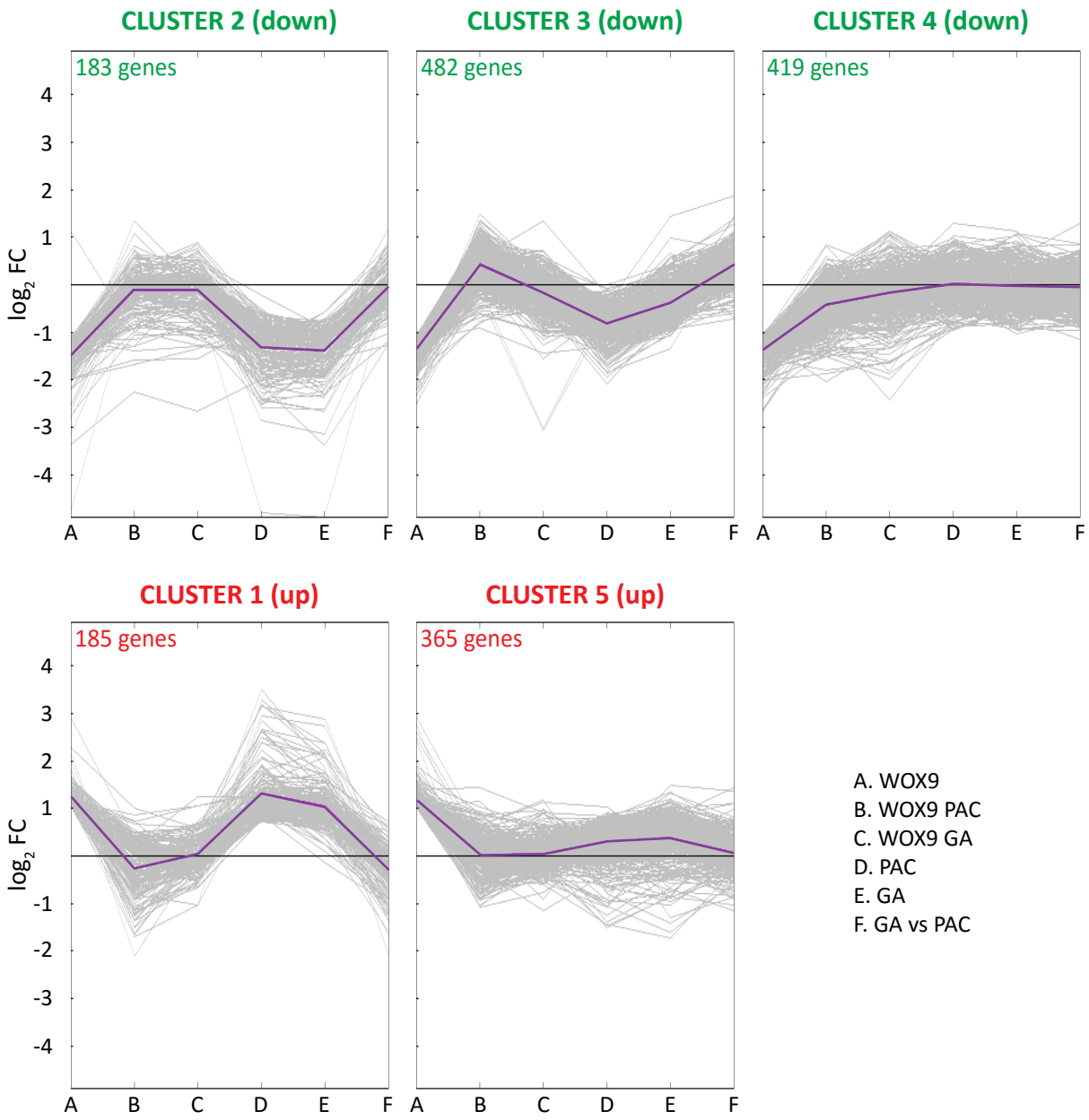

Figure 25. Clusterization of WOX9 regulated genes. Differentially expressed genes (-2≥FC≥2; p-value <0.01 [Rank Products]) in the WOX9 β-estradiol lines were clusterized according to their expression levels in seedlings treated with β-estradiol (WOX9; A), β-estradiol + paclobutrazol (WOX9 PAC; B), β-estradiol + gibberellin (WOX9 GA; C), paclobutrazol (PAC; D) and paclobutrazol + gibberellins, compared to mock (GA; E) or to PAC (GA vs PAC; F). WOX9 induction by β-estradiol led to identification of a higher number of repressed genes, indicating that WOX9 is a transcriptional repressor. Repressed genes grouped into three clusters (cluster 2, 3 and 4, whereas WOX9 activated genes grouped into two clusters (cluster 1 and 5). Graphs show the log2 FC of genes in each cluster. The purple line shows the expression trend of each cluster.

cluster 5) and this regulation is reversed by PAC treatment. In other words, these genes do not respond to GAs, but their regulation by WOX9 is reversed by an accumulation of the DELLAs (Figure 25).

To functionally characterize these clusters, we classified their genes based on a Gene Ontology (GO) Biological Process Enrichment, using the GeneCodis tool. GO terms enriched in cluster 1 are: defense response to fungus (10 genes), defense response to bacterium (7 genes), lipid transport (5 genes), response to chitin (5 genes), response to bacterium (4 genes) and nuclear-transcribed mRNA poly(A) tail shortening (2 genes), indicating that genes included in this cluster are involved in response to biotic stress (Figure 26).

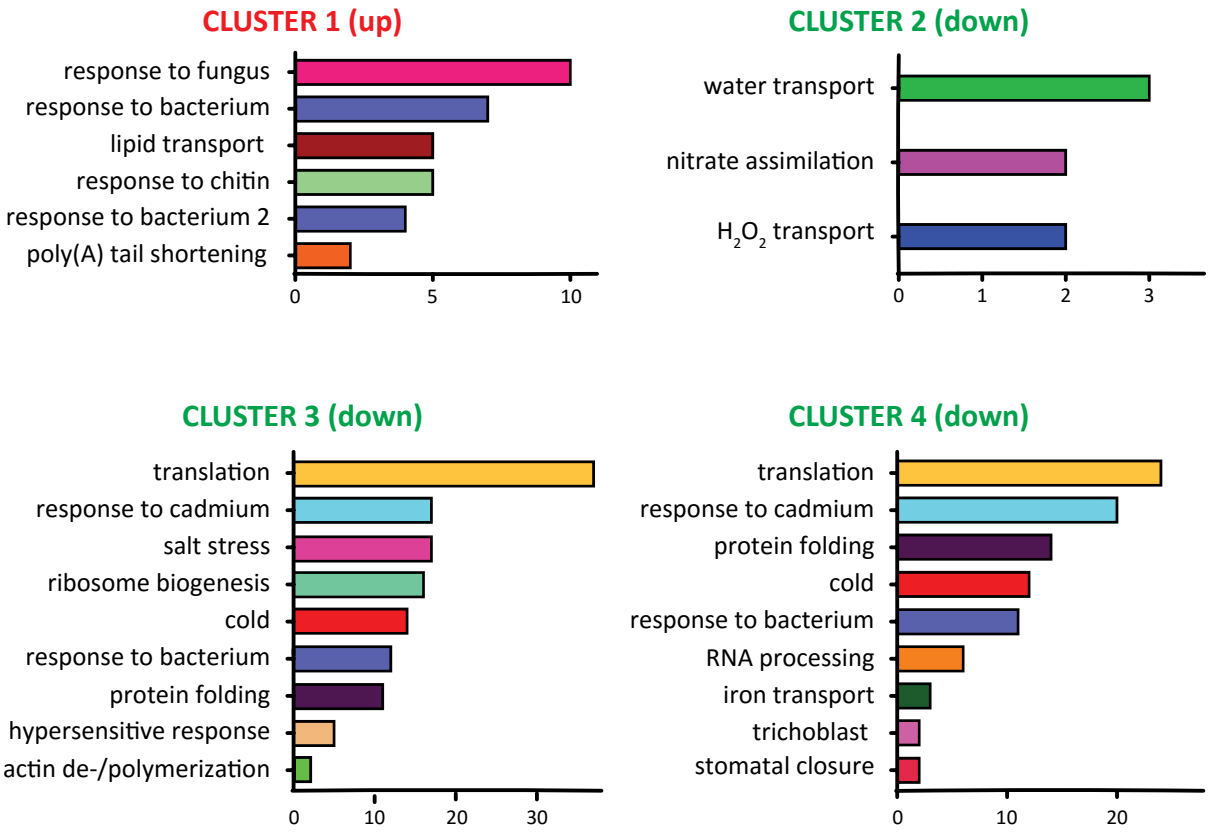

Figure 26. Gene Ontology (GO) Biological Process enrichment of genes grouped in each cluster. Cluster 1 is enriched in genes reported to have a role in defense response to fungus, defense response to bacterium, lipid transport, response to chitin, response to bacterium (bacterium2), and mRNA poly(A) tail shortening. Cluster 2 in genes with a role in water transport, nitrate assimilation, and hydrogen peroxide transmembrane transport. Cluster 3 in genes with a role in translation, response to cadmium ion, response to salt stress, ribosome biogenesis, response to cold (cold), defense response to bacterium, protein folding, plant-type hypersensitive response (hypersensitive response), and actin polymerization and depolymerization. Cluster 4 in translation, response to cadmium ion, protein folding, response to cold (cold), defense response to bacterium, RNA processing, iron ion transport (iron transport), trichoblast differentiation (trichoblast), and stomatal closure. p-values for GO term enrichment were lower than 0.01, and between 0.01-0.05 for “lipid transport”, “response to bacterium” and “response to chitin” in cluster 1; “hydrogen peroxidase transmembrane transport” and “nitrate assimilation” in cluster 2; “RNA processing”, “iron ion transport” and “stomatal closure” in cluster 4. The GeneCodis tool was used for the analysis.

Cluster 2 is enriched in three categories: water transport (3 genes), nitrate transport (2 genes) and hydrogen peroxide transmembrane transport (2 genes). Although number of genes included in each of these categories is small, out of 7 genes, 5 are transmembrane proteins, indicating that genes in this cluster are important for mobilization of molecules across membranes (Figure 26).

For cluster 3, the most enriched GO term is translation (37 genes). Out of these 37 genes, 14 are also classified as ribosome biogenesis (16 genes). Another enriched category is protein folding (11 genes), with the rest of enriched GO terms related to stress. These include both abiotic: response to cadmium ion (17 genes); response to salt stress (17 genes); and response to cold (14 genes), and biotic stress: defense response to bacterium (12 genes); plant-type hypersensitive response (5 genes). Actin polymerization and depolymerization is also enriched with 2 genes. Thus, within this cluster are genes involved in the protein translation machinery and in biotic and abiotic stress responses (Figure 26).

Cluster 4 shares some similarities with cluster 3, with the GO terms: translation (24 genes), response to cadmium ion (20 genes), protein folding (14 genes), response to cold (12 genes), and defense response to bacterium (11 genes), found to be enriched in both clusters. Besides, this cluster includes four extra groups: RNA processing (6 genes), iron ion transport (3 genes), trichoblasts differentiation (2 genes) and stomatal closure (2 genes), hence indicating that genes in this cluster are related to responses to stress (Figure 26).

No significant enrichment was observed for cluster 5, suggesting that genes included in this cluster may not be real WOX9 targets, but their differential expression derive from artefacts in the experimental set up. Actually, these genes are up-regulated in response to β-estradiol, but their fold-change is low.

Since *WOX9* is expressed in trichoblasts (Figure 14) and *stip-2* has a remarkable root hair phenotype (Figure 23), we next investigated to which extent our differential dataset overlapped with the published root hair specific transcriptomes. Four “root hair-specific” datasets (Brady et al. 2007; Bruex et al. 2012; Deal & Henikoff 2010; Lan et al. 2013) were used to these studies, called from now on as Brady, Bruex, Deal and Lan. As shown in Figure 27C, overlap among these datasets varied. The poorest overlap was observed for Lan´s and Bruex´s lists, where out of 1617 and 1582 genes, only 30% overlap. For Deal, almost 40% of the 945 genes appear in any of the other lists, and for Brady, 57% out of 505 genes were also identified elsewhere. Comparison of our WOX9-regulated dataset with these lists, showed an overlap of 97 genes with Deal, 223 with Lan, 37 with Brady and 118 with Bruex. The 37 genes that overlap with Brady were equally distributed among clusters, although a more significant enrichment is observed for cluster 4. Similar patterns were observed for the shared genes with the other root hair datasets, with a more significant enrichment observed for clusters 3 and 4, followed

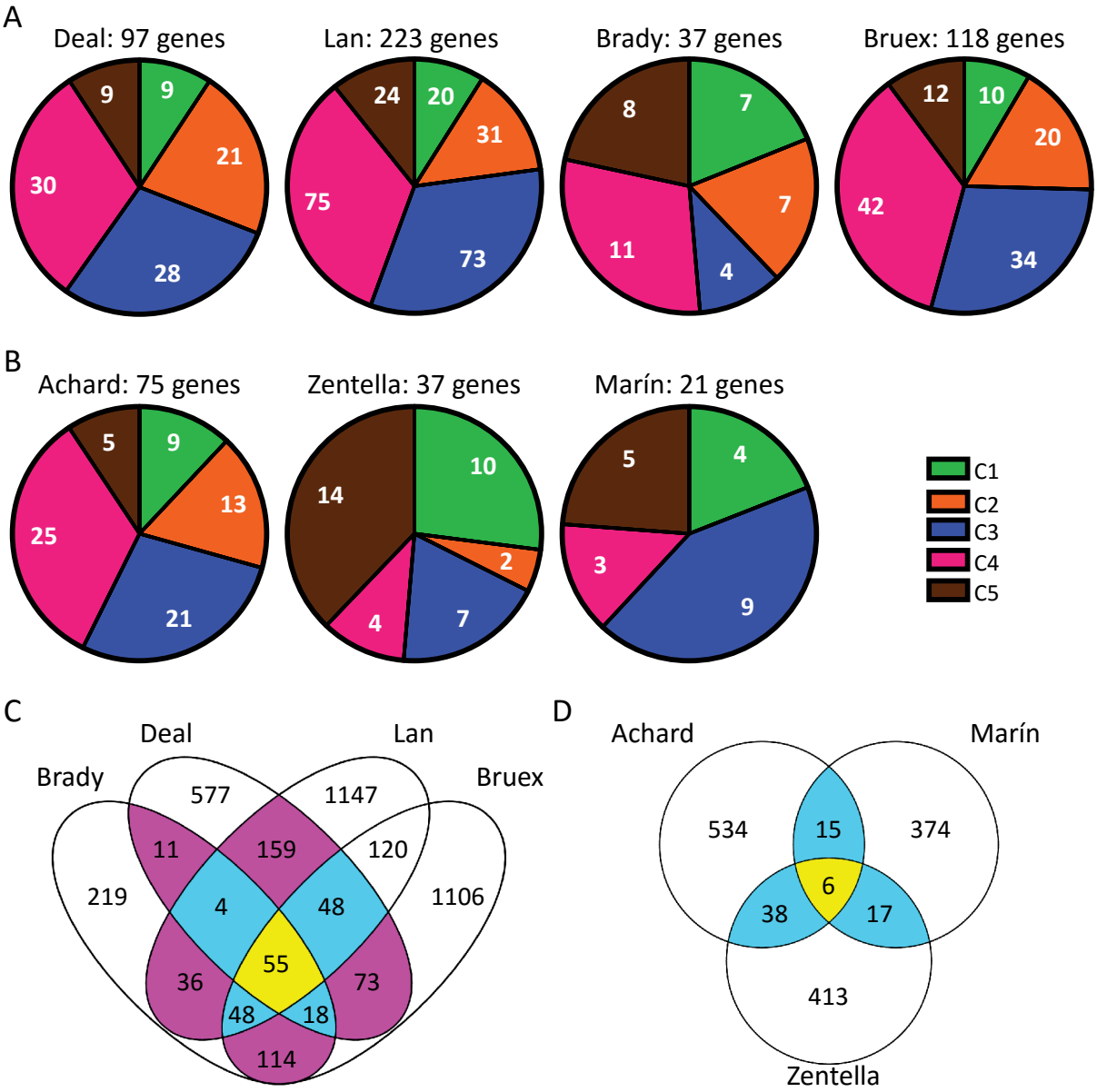

Figure 27. Comparison of WOX9 regulated genes with root hair and DELLA transcriptomes (A) Overlap of WOX9 regulated genes and root hair specific transcriptomes: Deal et al. 2010 (Deal); Lan et al. 2013 (Lan); Brady et al. 2007 (Brady); Bruex et al. 2012 (Bruex). Venn diagrams show the overlap with genes in each cluster. (B) Overlap of WOX9 regulated genes and DELLA targets identified by gene expression or ChIP-seq studies: Achard et al. 2008 (Achard); Zentella et al. 2007 (Zentella); Marín de la Rosa et al. 2015 (Marín). Venn diagrams show the overlap with each cluster. (C) Overlap of the root hair transcriptomes. (D) Overlap of DELLA targets among the gene expression and ChIP-seq studies.

by cluster 2 (Figure 27A). This indicates that the WOX9 factor directly regulates several root hair specific genes, and that most of these genes are negatively regulated by WOX9, consistent with a role of this homeodomain factor in preventing premature differentiation of trichoblasts.

Likewise, we tested whether our WOX9 regulated dataset was enriched in genes reported to be stress regulated in a DELLA-dependent manner, or that had been identified as direct targets of the DELLAs in dexamethasone-activation or RGA ChIP studies (Achard et al. 2008;

Marín-de la Rosa et al. 2015; Zentella et al. 2007), and which from now on are named as Achard, Marín and Zentella. As seen in figure Figure 27D there is not much overlap among the experiments, opposite to what occurred with the root hair specific data. This is not totally odd, if we take into account that experimental designs to generate these datasets were very different.

Nevertheless, by comparing our dataset with these studies, we observed that 75 of the WOX9 regulated genes overlap with the Achard dataset, with more than half of these genes belonging to cluster 3 (21) and cluster 4 (25). This would suggest that the most highly significant genes are in these two clusters. On the other hand, of the 37 genes that overlap with Zentella, most are grouped in clusters 1 and 5 (10 and 14 genes, respectively), and therefore correspond to WOX9 up-regulated genes. Hence, there is not a consistent correlation with the DELLA-regulated targets reported in this microarray experiment. The Marín dataset was generated by ChIP-seq studies with RGA, and therefore is the more reliable list for direct DELLA targets. Notably, 43% of the 21 common genes group in cluster 3, which includes also an important number of the root hair specific genes in the Deal, Lan and Bruex datasets. The rest of genes are distributed as follows: cluster 5 (5 genes), cluster 1 (4 genes) and cluster 4 (3 genes) (Figure 27B).

Altogether, these analyses revealed that genes grouped in all clusters may indeed correspond to WOX9 regulated genes, although more significant targets are those included in clusters 3 and 4, which correspond to WOX9 down-regulated genes. All differentially expressed genes, grouped in the described clusters 1 to 5, are listed in the supplemental tables S1 to S5, respectively. It is also highlighted whether these genes are DELLA-regulated or root hair-specific, and the original studies reporting this regulation.

Finally, to validate the microarray data, new RNA was isolated out of seedlings subjected to the same treatments. This RNA was used in qRT-PCR studies to confirm differential expression of some of the genes. More than 200-fold induction of the *WOX9* gene was observed after β-estradiol treatment in these samples. *GA20ox1* expression was also analyzed as a control for PAC application, and a 6-fold induction was detected for this gene. GA+PAC application resulted in similar levels of expression as in the mock seedlings, proving that the GA treatment was effective. Analysis of *RHS2* gene expression, a root hair specific gene that groups in cluster 2, showed that this gene is indeed repressed by WOX9. PAC treatment, on the other hand, suppressed the negative control by WOX9, while PAC+GA restored this repression, hence correlating with the gene expression data observed in the array. Similar results were also obtained for the root hair specific *EXPA7* gene, although in this case reversal of PAC effects by GA application was not as evident as for *RHS2*. It is also noteworthy that fold change in mRNA levels was also small, as seen in the array. This may indicate that although these genes are repressed in response to the WOX9 signaling pathway, they are not direct targets of WOX9.

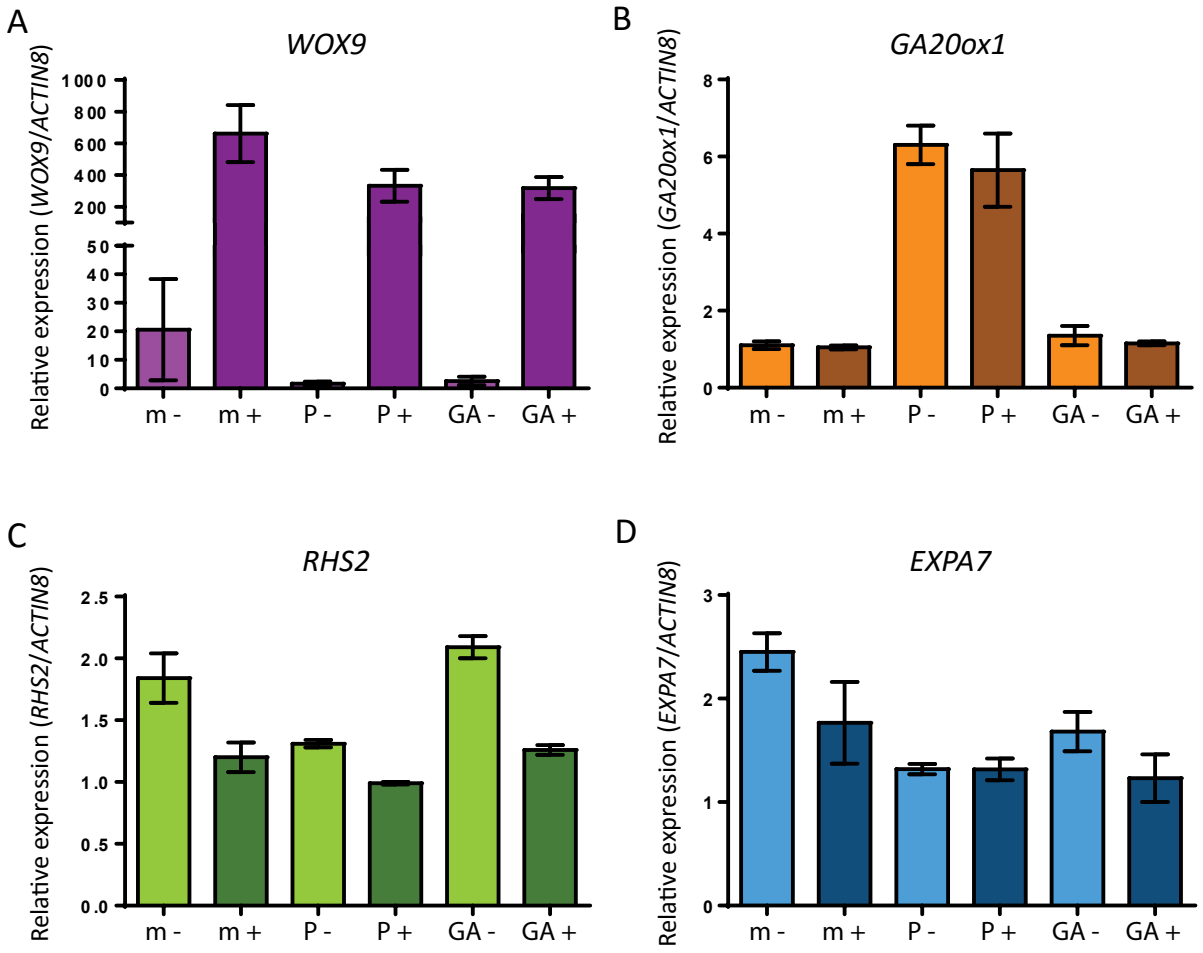

Figure 28. Validation of the genes identified in the array. 10-day-old β-WOX9 seedlings were treated with mock (m), paclobutrazol (P) and P+gibberellins (P+GA) and +/- β-estradiol (+/-) in the same way as for the microarray experiment, and extracted RNAs used for gene expression analysis by quantitative real-time PCR (A) Expression of *WOX9*, showing an effective β-estradiol induction. (B) *GA20ox1* expression used as a control for PAC and GA treatments. (C, D) Expression of WOX9-regulated genes: *RHS2* (C) and *EXPA7* (D). Relative expression levels were calculated with the Pfaffl method and compared to *ACTIN8* expression. Graphs show means and their standard errors (error bars) (n=2).

Alternatively, it is possible that WOX9 acts in concert with other transcriptional regulators, and expression of WOX9 alone is not sufficient for full regulation of these genes (Figure 28).

Altogether, these analysis confirm a role of WOX9 in suppressing expression of stress-related and root hair specific genes. Clusters 2, 3, and 4 were in fact enriched in genes related to abiotic tress and trichoblast differentiation. According to our working model, PAC-induced accumulation of the DELLA repressors contributed to de-repress these genes, which can be then considered as "DELLA-activated". This effect was further reversed by GA-induced destabilization of DELLAs, proving that this regulation is DELLA-specific. A pending question is understanding why fold change in levels of expression of these targets is so small. qRT-PCR analysis of *35S::HA-WOX9* lines and *stip-2* mutants grown in the presence of ABA will likely contribute to solve this question.

Discussion

In a screening aimed to identify TFs implicated in the DELLA-dependent stress pathway, the TRANSPLANTA collection of Arabidopsis lines were grown in microtiter plates, in liquid GM supplemented with salt and GAs ± β-estradiol (Marisa Rodriguez, personal communication). A total of 32 TFs were selected by their ability to confer increased tolerance to salt, also after application of GAs, which identified them as putative candidates for a role in the DELLA stress pathway.

The DELLA repressors act as master regulators of GA signaling and suppress GA-regulated gene expression through direct protein-protein interaction with different families of TFs. Therefore, we started this work by analyzing if the identified factors interacted with the DELLAs. In Y2H experiments we could prove that 21 of these stress-related factors directly bind the DELLAs, which showed that by including GAs in the selection media we strongly enriched for regulators with a DELLA-dependent function. These DELLA interactors belong to different families: the homeobox (WOX9, HB53, HDG1); AP2 (ANT)/ERF (ERF6, TINY, RAP2.6, DREB2C, ERF037); NAC (ANAC087; NAC038); bHLH (bHLH13, HECATE1); MYB (MYB116, MYB46, TT2, MYB38, MYB99); Zinc Finger (STH, GATA2); MADs-box (SEP2); bZIP (bZIP63); Aux/IAA (IAA7) and histone methyltransferase (SUVH7) families (Figure 7).

After the initial reports showing that DELLAs inhibit plant growth by sequestering the PIF factors, DELLAs were found to interact with many different families of proteins to regulate multiple biological processes (Davière & Achard 2016). Interaction with the DELLAs mostly blocks the function of these regulators, although additional evidences indicate that DELLAs may also function as co-activators of some factors. A positive role of the DELLAs in salt tolerance was reported ten years ago (Achard et al. 2006), but so far transcriptional regulators implicated in this response have not been identified. Except for WOX9 and STH, identified in a high throughput screening for GAI interactors (Marín-de la Rosa et al. 2014), the other 19 stress-related factors correspond to novel interactors. We can thus hypothesize that DELLAs play a relevant role in modulating the function of these TFs to promote plant survival under salt stress.

DELLAs are encoded in Arabidopsis by 5 gene copies (*RGA*, *GAI*, *RGL1*-*RGL3*) with partly redundant but also distinct functions. In studies using *RGA* and *RGL2* genes, it was shown that RGA is able to substitute RGL2 activity in the control of seed germination, when it is expressed under control of the *RGL2* promoter (Gallego-Bartolomé et al. 2010). These two DELLAs were also found to interact with the same bHLH partners, which led to conclude that their distinct functions in hypocotyl growth and seed germination rely on the expression patterns of these genes and not on differences within the proteins (Gallego-Bartolomé et al. 2010). Here we show that the 21 novel DELLA interactors do not display an identical binding affinity for RGA and RGL2, which suggests that these two DELLA proteins differ in their regulatory activity. This discrepancy may obey to the fact that in the previous report it was only tested interaction with

four bHLH of the same subfamily, while here we analyzed TFs belonging to different families. Thus, we show that results obtained for bHLHs cannot be extrapolated for other families. Out of the 21 factors analyzed, 12 interacted both with M5RGA and M5RGL2, but 7 were found to bind only one of these proteins (Figure 7). Also, preference for either of Arabidopsis DELLAs depended on the TF, as seen in Figure 8.

DELLAs interact with PIF3 and PIF4, and other members of the bHLH family through the LHRI domain (de Lucas et al. 2008). By mapping the DELLA domain involved in the interaction with these TFs, we observed that 13 of them bind the LHRI domain, but only in 4 cases this domain is sufficient for the interaction. For the other 9, LHRI is essential but not sufficient, and an additional motif at the C-terminus of the DELLAs is also required for the interaction. WOX9 seemed to interact with different regions of the DELLAs, since all analyzed deletions displayed some binding affinity (Figure 8). These results are highly remarkable, because they support that different DELLAs domains mediate growth inhibition and promotion of stress tolerance, suggesting that these two responses may be uncoupled.

We also studied whether WUSCHEL and the other WOX family members interacted with the DELLA proteins in the same way as WOX9 did, which would indicate that DELLAs have a general function in regulating homeodomain factors activity. In these studies we observed clear differences among members of the WOX family (Figure 9). Indeed, none of the ancient clade members, WUS or its closest homologs, WOX5 and WOX7, showed any interaction. Members of the intermediate and modern clades differed in their binding preferences, with only WOX9 found to interact with all Arabidopsis DELLAs. Besides, the strongest binding affinity was observed for WOX9 and its closest homologue WOX8, although WOX8 does not interact either with RGA or GAI. This would indicate that DELLAs interaction is a recent trait acquired during the evolution of this gene family, and that other family members are unlikely to have redundant functions in salt stress tolerance. In fact, Dolzblasz et al. (2016) reported that only members of the modern clade are able to replace WUS function, which suggests that stress-related function might be restricted to members of the intermediate clade. Interaction with the DELLAs probably plays a relevant role in modulating the activity of these factors under stress conditions.

WOX9 is expressed in the shoot and root meristems. In the SAM, it is expressed in cells forming a ring around the meristem, while in roots is specifically expressed in trichoblast cells, in the transition zone between the meristem and differentiated root cells. By GUS staining we observed that *WOX9* expression is reduced in response to salt and ABA, although western blot studies with the *35S::HA-WOX9* line showed that stability of the protein is not affected by salt or ABA (Figure 15). This means that salt and ABA modulate *WOX9* expression at a transcriptional level and because down-regulation of the gene is observed after 5 days of treatment, it might reflect a negative feedback regulation.

Notably, both the SAM and root meristems are smaller in *wox9*/*stip-2* mutants (Figure 16). WOX9 has been reported to regulate WUS, and reduced WUS expression may result in premature SAM termination (Wu et al. 2005). Lines with reduced levels of CKs were also reported to have a smaller SAM (Werner et al. 2003). However, although *35S::HA-WOX9* plants have lower levels of CKs compared to Col-0 (Figure 19), they do not show a smaller SAM. It has been reported that WOX9 plays a role in CK signaling (Skylar et al. 2010), and in fact we observed that *35S::HA-WOX9* is hypersensitive to these hormones, thus supporting a function of WOX9 downstream of CK signaling. Therefore, we cannot rule out a role of this factor in negative feed-back regulation of CK biosynthesis, with enhanced response of *WOX9* over-expressors compensating for reduced CK levels. Besides, our results show that WOX9 also plays an important role in root meristem maintenance. CKs have opposite roles in the SAM and RAM, with these hormones found to promote in roots cell differentiation instead of cell proliferation. In the RAM, an essential role in promoting cell division is exerted by auxins (Muraro et al. 2016), but IAA levels were not found to be elevated in *35S::HA-WOX9* compared to wild-type plants (Figure 19), consistent with previous studies showing a normal distribution of auxins in the *stip* mutant (Wu et al. 2007). Function of WOX9 in CK signaling might be different in root and shoot tissues, and studies in which downstream regulated expression is analyzed separately in shoots and roots would be required to further confirm this hypothesis.

Concerning WOX9 mechanism of action, we showed that this factor interacts with RGA (Figure 12), but this interaction differs from PIF4-RGA interaction in two main aspects: it requires at least two different RGA protein regions (in contrast to LHRI) and it does not involve the DNA-binding domain of WOX9, but the conserved WUS-box and an EAR-like motif. This would mean that interaction with RGA does not inactivate WOX9 transcriptional activity but likely modulates its function. Moreover, given that the domain of interaction in the DELLAs is different from PIF4, it should be feasible to identify an allelic version of RGA that does not interact with PIFs but still binds WOX9, and in this way uncoupling RGA function in growth restraint and stress responses activation.

EAR motifs are recognized by the co-repressor TOPLESS and we showed that RGA competes with TPL for WOX9 interaction. Therefore, we propose that WOX9 acts as a transcriptional repressor by binding the TPL co-repressor, and that interaction with the DELLAs switches WOX9 activity from a repressor to an activator. Ikeda et al. (2009) reported that WUS can act both as a repressor and activator and that the WUS box is essential for both of these functions. These authors could not explain how this switch occurs at the molecular level, but here we provide evidence that in the case of WOX9 it can be mediated by the interaction with the DELLAs. To this respect, there are two reports showing an equivalent mechanism for members of the zinc finger IDD family (Fukazawa et al. 2014; Yoshida et al. 2014). These factors function as transcriptional repressors by binding TPR or SCL3, whereas interaction with the DELLAs leads

to the activation of their target genes. Hence, our finding that RGA competes for WOX9-TPL interaction is in support of a regulatory model whereby DELLAs contribute to switch WOX9 repressor activity into a transcriptional activation function (Figure 29).

Remarkably, our findings show that *35S::HA-WOX9* line accumulates lower levels of cytokinins (Figure 19), but these plants show a hypersensitive response to these hormones (Figure 21), which supports a role of WOX9 in CK signaling. Mutants with lower levels of CKs (mutants in the biosynthetic genes or over-expressing cytokinin oxidases) were reported to be more tolerant to drought stress (Nishiyama et al. 2011) and display a hypersensitive response to ABA, although they accumulate lower ABA levels. Regarding CK insensitive plants, due to CK receptor loss-of-function, these mutants behave different according to the gene that is mutated. *ahk1* is insensitive to ABA and its over-expression leads to an increased tolerance to salt, while *ahk2*, *ahk3* and *ahk4* mutants are hypersensitive to ABA and accumulate wt levels of ABA (Tran et al. 2007), but their hypersensitive response is not correlated with an increased tolerance to abiotic stresses (Kumar & Verslues 2015). This indicates that although there is a cross-talk between CKs and ABA signaling, this interaction is quite complex and not fully understood. Moreover, AHK3 exhibits a higher sensitivity to tZ than iP (Stolz et al. 2011), and whereas DHZ is resistant to cytokinin oxidases, iP and tZ are inactivated by these enzymes. We observed that iP and tZ leves are both reduced in *35S::HA-WOX9*, but this reduction is much stronger in the case of tZ. The main site of tZ synthesis is the root, from where it is transported via the xylem to the shoot, and likely sensed by AHK3 (Kieber & Schaller 2014). Since we only used whole rosettes to measure these hormones and detected significant differences in tZ levels, it is possible that expression of *CYP735A* genes, involved in conversion of iP to tZ, is down-regulated in *35S::HA-WOX9* lines or that root to shoot transport is impaired in these plants. As it occurs with CKs mutants, *35S::HA-WOX9* plants accumulate normal levels of ABA but show a hypersensitive response to this hormone. ABA is widely accepted as the most important hormone for activation of osmotic stress responses and it accumulates upon stress. This hormone activates a signaling cascade that promotes stress tolerance at the same time that inhibits growth (Fujita et al. 2011). So, it seems reasonable that an enhanced response of ABA leads to the increased salt tolerance phenotype of *35S::HA-WOX9*, even though basal ABA levels were not increased. Last, *35S::HA-WOX9* plants have also lower levels of GAs and display an insensitive response to these hormones, while *stip-2* mutants were hypersensitive to GAs. In fact, GAs suppress abiotic stress responses (Colebrook et al. 2014), which explains the increased tolerance to salt of *35S::HA-WOX9* lines, both in the absence and presence of GAs. Given that GA mutants are more tolerant to stress and this response has been directly associated to DELLAs accumulation (Achard et al. 2006), we expected DELLAs to be stabilized in *35S::HA-WOX9*. However, RGA levels in these plants were similar to the wild-type, while they were notably elevated in the *wox9*/*stip-2* mutants (Figure 20). This means that when *WOX9* is lacking, DELLAs accumulation is not able itself to confer increased salt tolerance,

which demonstrates that WOX9 activity is essential for this response. It also indicates that basal DELLA levels are sufficient for the increased tolerance of *35S::HA-WOX9* lines. *WOX9* over-expression may favor interaction with the DELLA repressors, although we only analyzed RGA levels, so we cannot exclude that levels of other DELLAs change.

In addition to a smaller root meristem, *stip-2* mutant also has much shorter roots, while those of *35S::HA-WOX9* and the activation tagging *stip-D* mutant were slightly shorter than in the wt. As the RAM of these two over-expressors is normal or slightly larger than in the wt, we would have expected roots to be similar to Col-0, and not to be shorter as in the case of *stip-2*. It is possible that this phenotype is indeed caused by reduced cell elongation, as a result of their reduced GA levels. Number of lateral roots was also reduced in *stip-2*, *stip-D* and *35S::HA-WOX9*, although this phenotype was stronger in *stip-2* seedlings, which do not develop LRs. In a recent report, WOX7 was shown to inhibit LR formation in a sugar dependent manner, by controlling cell cycle gene expression (Kong et al. 2016), and a similar regulation was reported for WOX9 in SAM (Skylar et al. 2011). These two reports would link WOX function with sugar and auxin signaling. However, *WOX9* is expressed in root trichoblasts, and not in the pericycle, from where LRs are initiated. Moreover, auxins seem to be essential for LR formation, and distribution of these hormones is not affected either in *wox7* or *stip* mutants (Kong et al., 2016; Wu et al., 2007). Therefore, further experiments need to be addressed to understand how WOX9 regulates LR formation.

Regarding root growth, ABA has a similar inhibitory effect on *WOX9* lines as in the wild-type. However, *stip-D* and *35S::HA-WOX9* seedlings are less affected by salt. In response to NaCl, primary root length and especially formation of new LRs is inhibited. Moreover, already emerged LRs enter in a temporal quiescent stage, partially due to an arrest in cell cycle (Duan et al. 2013). WOX9 up-regulates the expression of *CYCB1;1* in SAM (Skylar et al. 2011) and this cyclin is down-regulated by osmotic stress in leaves (Claeys et al. 2012). *CYCB1;1* expression is also up-regulated by WOX7 during new LRs formation (Kong et al. 2016), and is suppressed after salt treatment, which leads to an arrest of LRs growth (Duan et al. 2013), and primary root growth inhibition (West et al. 2004). Effects of salt on primary and LRs are less severe in the over-expression lines. In fact, although over-expressor lines grown on salt have the same number of LRs as Col-0, these are much longer. Because DELLAs accumulate after osmotic stress, we propose a model in which WOX9 activates cell cycle, possibly through the repression of an intermediate, as occurs in the SAM, and that in response to salt, DELLAs interact with WOX9 and switch its repression activity into an activation function. Root growth effects of osmotic stress are mediated by ABA (Duan et al. 2013). However, despite the ABA-hypersensitivity of *35S::HA-WOX9* seeds in germination assays, we did not detect such hypersensitivity regarding LRs inhibition in response to ABA, indicating that WOX9 function during salt stress is also regulated independently of ABA signaling.

Abiotic stresses also affect formation of root hairs. In response to salt, the number of atrichoblasts decrease and although the number of trichoblasts is the same, they are reprogrammed to an atrichoblast fate, so less number of root hairs is produced. These effects are higher in *sos* mutants, which also have less root hairs in mock conditions, thus pointing to an important role of the SOS pathway in root hairs development (Wang et al. 2008). Notably, lines with a decreased number in root hairs are more sensitive to osmotic and salt stress (Tanaka et al. 2014), which suggests that root hairs are critical to sense these stresses and trigger an adaptive response. The biggest differences in root hair formation were observed in *stip-2* (Figure 23). This mutant has shorter root hairs in mock conditions, and is devoid of root hairs when grown on salt media, which is indicative of an increased sensitivity to NaCl. Growth of root hairs is inhibited in response to ABA (Schnall & Quatrano 1992), and this response is exacerbated in the *stip-2* root differentiation zone, indicating that WOX9 suppresses ABA effects on root hair elongation. However, *stip-2* mutant shows a totally opposite response at the root tip, where in response to ABA it is observed a massive overproduction of root hairs, that is not seen in response to any other treatment, or the rest of genotypes (Figure 23). This indicates that WOX9 has a different function in the meristem and differentiation zones, consistent with its specific expression in the root transition zone. Remarkably, *stip-2* has a shorter RAM and in response to ABA almost lacks any root meristem. On ABA, epidermal cells close to the tip differentiate into root hairs, which indicates a premature differentiation of the meristem. Besides, these cells do not elongate as occurs for cells that left the meristematic zone in the wild-type, but acquire a hexagonal shape. This morphology indicates that even these cells stopped dividing, they are not able to elongate, but do differentiate into root hairs, meaning that these processes are somehow exclusive to each other.

As seen in the transcriptomic analysis, most of the WOX9 regulated genes are repressed (Figure 25), indicating that WOX9 is a transcriptional repressor. In the case of WUS, the WUS box was shown to be essential for repression activity (Ikeda et al. 2009) and several members of this gene family have been described as interactors of the co-repressor TOPLESS: WUS (Kieffer et al. 2006), WOX5 (Pi et al. 2015), WOX2 and WOX4 (Causier et al. 2012). Actually, we proved that WOX9 interacts with TPL, which also underscores that this protein acts as a repressor. Remarkably, in seedlings treated with PAC, these target genes are de-repressed, which implies that DELLAs accumulation switches WOX9 activity to an activation function, as discussed above. Clustering of the differentially regulated genes, identified two clusters (cluster 1 and 5) of WOX9 activated genes. Number of genes in these clusters is smaller than for clusters 2-4 (repressed genes) and therefore we cannot rule out that they correspond to indirect target genes, activated due to WOX9-mediated repression of a direct transcriptional repressor of these genes. In line with this hypothesis, these genes are no longer activated upon application of PAC.

Notably, cluster 1 is enriched in genes related to biotic stresses, while cluster 5 does not seem to be enriched in genes related to any biological function (Figure 26). Regarding WOX9 repressed genes, cluster 2 is enriched in genes involved in water transport, nutrient assimilation and ROS, which are processes found to be associated with root hairs development (Grierson et al. 2014). Clusters 3 and 4 are enriched in genes with a similar biological function, which includes translation, response to abiotic stresses, and response to bacteria. Moreover, cluster 3 is enriched in genes involved in actin polymerization and depolymerization, and cluster 4 in trichoblasts differentiation and stomatal closure. The actin cytoskeleton has an essential role in rapid root hair growth (Grierson et al. 2014) , while stomatal closure is one of the first responses upon osmotic stress and is mediated by ABA (Sah et al. 2016). Interestingly, in RNA-seq studies of root hair and non-hair cell, Lan et al. (2013) reported that root hair specific genes are enriched in largely identical categories as the ones in clusters 3 and 4, such as translation, response to cadmium stress ion, ribosome biogenesis, response to salt stress, response to cold, protein folding, and defense response to bacterium. Because of this significant overlap and specific expression of *WOX9* in trichoblasts, we can affirm that WOX9 regulates root hair specific gene expression.

Apart from the work of Lan et al. (2013), WOX9 regulated genes show also a significant overlap with other root hair specific datasets (Brady et al. 2007; Bruex et al. 2012; Deal & Henikoff et al. 2010), in particular genes in clusters 3, 4 and to minor extent cluster 2, enriched in genes related to stress and trichoblasts differentiation. Overlap with all these datasets supports a role of WOX9 in modulating trichoblast differentiation.

Given that WOX9 physically interacts with the DELLAs, we also investigated if WOX9 regulated genes overlapped with reported DELLA-regulated genes. Overlap was less than for root hair datasets, but certainly there was a significant overlap. DELLA datasets showed an overlap with genes in clusters 1 and 5, but again clusters 3 and 4 were found to be overrepresented. PAC treatment de-represses expression of these genes (Figure 25), indicating that DELLAs contribute to their activation. Interestingly, in RGA ChIP-seq studies it was found that RGA associates to promoter regions enriched in WUS-recognition sites (Marín de la Rosa et al. 2015). As DELLAs do not bind DNA, RGA must bind these promoter regions via complex formation with members of the WOX family intermediate/modern clades. Our results demonstrate that complex formation with WOX9 plays a relevant role in the control of root hair formation and in preventing precocious meristem termination in response to salt. It appears that WOX9 exerts these effects via cross-talk interaction with the CK-, GA- and ABA-signaling pathways. Mining the WOX9-regulated transcriptome for specific regulators in each of these pathways will be instrumental to the identification of its mechanism of action and uncover the exact mechanism underlying increased salt tolerance by this homeodomain factor. This proposed model is illustrated in Figure 29.

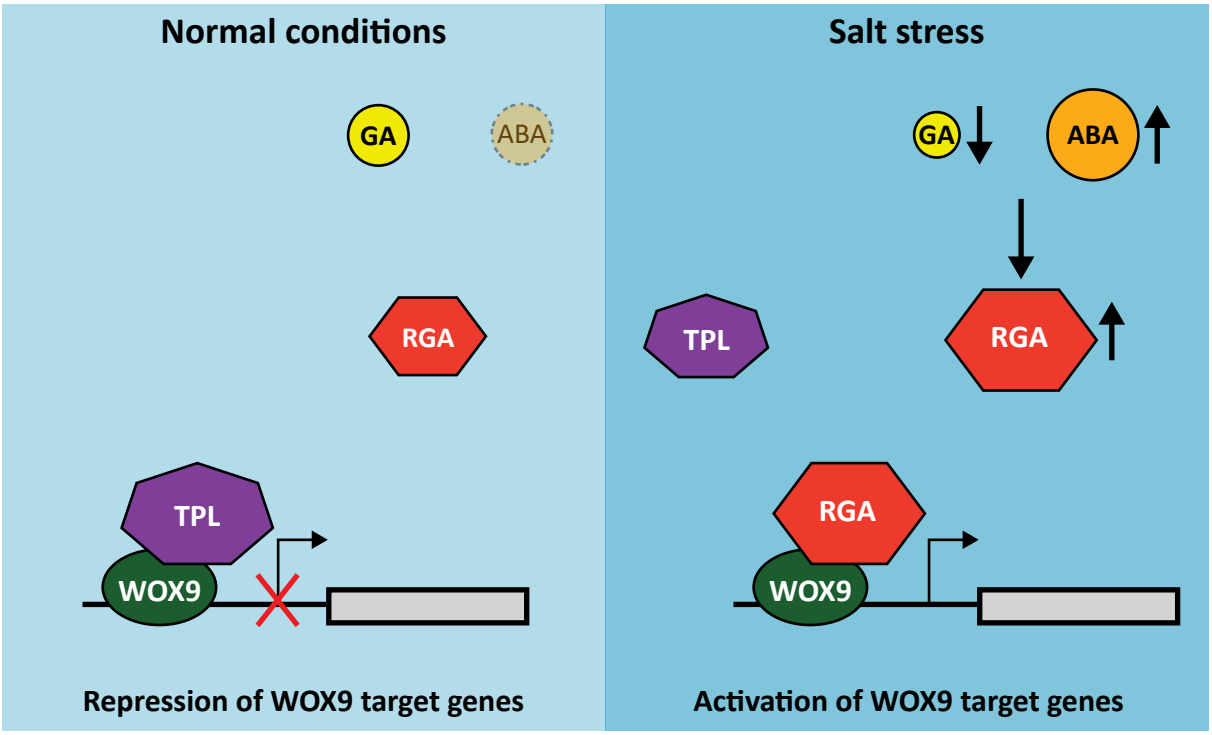

Figure 25. Proposed model for WOX9 mechanism of action. In non-estressed conditions, WOX9 interacts with TOPLESS (TPL) to repress WOX9-target genes. In salt stress conditions, abscisic acid (ABA) synthesis is induced, while gibberellin (GA) levels decrease, leading to an increase in ABA/GA balance. This triggers the stabilization of DELLAs, which replace TPL in the interaction with WOX9, thus modulating its function from a repressor to an activator of transcription.

Conclusions

1. Yeast Two Hybrid studies showed that 21 of the salt-stress related transcription factors identified in the screening directly interact with the DELLA proteins. This indicates that by including gibberellins in the selection media, we strongly enriched the candidates in DELLA partners.

2. In most cases, the interaction domain for these factors is different from the LHRI domain involved in PIF4 interaction, which should facilitate in a future the uncoupling of the function of DELLAs in growth suppression and increase of tolerance to abiotic stresses.

3. Over-expression of the *WOX9* homeobox factor confers a strong salt tolerance phenotype, even in the presence of gibberellins.

4. WOX9 binds the C-terminal domain of the DELLAs, and the conserved WUS-box and EAR1 motif in the WOX9 protein are sufficient for DELLAs interaction.

5. TOPLESS and DELLAs compete for interaction to the WOX9 EAR1 motif, and the complex formation with the TPL co-repressor or the DELLA proteins switches WOX9 transcriptional activity from a target gene repression into an activation function.

6. *WOX9* over-expressor lines accumulate reduced levels of the cytokinins isopentenyladenine and *trans*-zeatin, and display lower bioactive gibberellin levels, hence pointing to a role of this factor in the regulation of cytokinin and gibberellin homeostasis.

7. WOX9 lines show in addition an altered response to gibberellins, abscisic acid and cytokinins, which suggests a role of this homeodomain factor in the crosstalk interaction among these hormonal pathways.

8. The *WOX9* factor is specifically expressed in the root epidermis trichoblasts and gene expression studies using the β-estradiol inducible lines showed a significant overlap with root hair specific transcripts.

9. The reduced root meristem size and root hair phenotype of *wox9*/*stip-2* mutant suggest a role of WOX9 in salt stress tolerance, by preventing premature differentiation of root meristem cells.

Conclusiones

1. Estudios de dos híbridos de levadura mostraron que 21 de los factores de transcripción relacionados con estrés salino que se identificaron en el escrutinio, interaccionan de forma directa con las proteínas DELLA. Esto indica que al incluir giberelinas en el medio de selección enriquecimos los candidatos en interactores de las DELLAs.

2. En la mayoría de los casos el dominio de interacción de estos factores es diferente del dominio LHRI implicado en la interacción con PIF4, lo que debería facilitar en un futuro desacoplar la función de las DELLAs en la supresión del crecimiento y el aumento de la tolerancia a estreses abióticos.

3. La sobre-expresión del factor homeobox *WOX9* confiere un fenotipo de gran tolerancia a sal, incluso en la presencia de giberelinas.

4. WOX9 se une al dominio C-terminal de las DELLAs, y los motivos conservados caja-WUS y EAR1 en la proteína de WOX9 son suficientes para la interacción con las DELLAs.

5. TOPLESS y las DELLAs compiten por la interacción con el motivo EAR1 de WOX9, y la formación del complejo con el co-represor TPL o las proteínas DELLAs cambia la actividad transcripcional de WOX9 de la represión de sus genes diana a una función activadora.

6. Líneas sobre-expresoras de *WOX9* acumulan niveles reducidos de las citokininas isopenteniladenina y trans-zeatina, y muestran menores niveles de giberelinas bioactivas, lo que apunta, pues, al papel de este factor en la regulación de la homeostasis de citokininas y giberelinas.

7. Las líneas de WOX9 muestran además una respuesta alterada a giberelinas, ácido abscísico y citokininas, lo que sugiere un papel de este factor homeobox en la interacción cruzada entre estas vías hormonales.

8. El factor *WOX9* se expresa específicamente en los tricoblastos de la epidermis de raíz, y estudios de expresión génica utilizando la línea inducible por β-estradiol mostraron un solapamiento significativo con tránscritos específicos de pelos radiculares.

9. El reducido tamaño de meristemo de raíz y el fenotipo de pelos radiculares del mutante *wox9*/*stip-2* sugiere un papel de WOX9 en la tolerancia a estrés salino, al prevenir la diferenciación temprana de las células meristemáticas de raíz.

Bibliography

Achard, P. et al., 2009. Gibberellin signaling controls cell proliferation rate in *Arabidopsis*. *Current Biology*, 19(14), pp.1188–93.

Achard, P. et al., 2006. Integration of plant responses to environmentally activated phytohormonal signals. *Science*, 311(5757), pp.91–4.

Achard, P., Renou, J.P., et al., 2008. Plant DELLAs restrain growth and promote survival of adversity by reducing the levels of reactive oxygen species. *Current Biology*, 18(9), pp.656–60.

Achard, P., Gong, F., et al., 2008. The cold-inducible CBF1 factor-dependent signaling pathway modulates the accumulation of the growth-repressing DELLA proteins via its effect on gibberellin metabolism. *The Plant Cell*, 20(8), pp.2117–29.

Achard, P. et al., 2007. The plant stress hormone ethylene controls floral transition via DELLA-dependent regulation of floral meristem-identity genes. *Proceedings of the National Academy of Sciences of the United States of America*, 104, pp.6484–9.

An, F. et al., 2012. Coordinated regulation of apical hook development by gibberellins and ethylene in etiolated *Arabidopsis* seedlings. *Cell Research*, 22(5), pp.915–27.

Arabidopsis Interactiome Mapping Consortium, 2011. Evidence for Network Evolution in an *Arabidopsis* Interactome Map. *Science*, 333(6042), 601-7

Ariizumi, T. et al., 2008. Proteolysis-independent downregulation of DELLA repression in *Arabidopsis* by the gibberellin receptor GIBBERELLIN INSENSITIVE DWARF1. *The Plant Cell*, 20(9), pp.2447–59.

Ariizumi, T. & Steber, C.M., 2011. Mutations in the F-box gene *SNEEZY* result in decreased Arabidopsis GA signaling. P*lant Signaling & Behavior*, 6(6), pp.831–3.

Arnaud, N. et al., 2010. Gibberellins control fruit patterning in *Arabidopsis thaliana*. Genes and *Development*, 24(19), pp.2127–32.

Bai, M.-Y. et al., 2012. Brassinosteroid, gibberellin and phytochrome impinge on a common transcription module in *Arabidopsis*. *Nature Cell Biology*, 14(8), pp.810–7.

Balcerowicz, D., Schoenaers, S. & Vissenberg, K., 2015. Cell fate determination and the switch from diffuse growth to planar polarity in *Arabidopsis* root epidermal cells. *Frontiers in Plant Science*, 6, p.1163

Barton, M.K., 2010. Twenty years on: the inner workings of the shoot apical meristem, a developmental dynamo. *Developmental Biology*, 341(1), pp.95–113.

Belda-Palazón, B. et al., 2012. Aminopropyltransferases involved in polyamine biosynthesis localize preferentially in the nucleus of plant cells. *PLos One*, 7(10), p.e46907

Belkhadir, Y. & Jaillais, Y., 2015. The molecular circuity of brassinosteroid signaling. *New Phytologist*, 206(2), pp.522–40.

Benjamini, Y. & Hochberg, Y., 1995. Controlling the false discovery rate: a practical and powerful approach to multiple testing. *Journal of the Royal Statistical Society*, 57(1), pp.289–300.

Bernard, P. & Couturier, M., 1992. Cell killing by the F plasmid CcdB protein involves poisoning of DNA-topoisomerase II complexes. *Journal of Molecular Biology*, 226(3), pp.735–45.

Bernardo-García, S. et al., 2014. BR-dependent phosphorylation modulates PIF4 transcriptional activity and shapes diurnal hypocotyl growth. *Genes and Development*, 28(15), pp.1681–94.

Blein, T., Pautot, V. & Laufs, P., 2013. Combinations of Mutations Sufficient to Alter *Arabidopsis* Leaf Dissection. *Plants*, 2(2), pp.230–47.

Brady, S.M. et al., 2007. A high-resolution root spatiotemporal map reveals dominant expression patterns. *Science*, 318(5851), pp.801–6.

Breuninger, H. et al., 2008. Differential expression of *WOX* genes mediates apical-basal axis formation in the *Arabidopsis* embryo. *Developmental Cell*, 14(6), pp.867–76.

Bruex, A. et al., 2012. A gene regulatory network for root epidermis cell differentiation in Arabidopsis. *PLoS Genetics*, 8(1), p.e1002446.

Burssens, S. et al., 2000. Expression of cell cycle regulatory genes and morphological alterations in response to salt stress in *Arabidopsis thaliana*. *Planta*, 211(5), pp.632–40.

Busso, D., Delagoutte-Busso, B. & Moras, D., 2005. Construction of a set Gateway-based destination vectors for high-throughput cloning and expression screening in *Escherichia coli*. *Analytical biochemistry*, 343(2), pp.313–21.

Cao, D. et al., 2006. Gibberellin mobilizes distinct DELLA-dependent transcriptomes to regulate seed germination and floral development in Arabidopsis. *Plant Physiology*, 142(2), pp.509–25.

Carmona-Saez, P. et al., 2007. GENECODIS: a web-based tool for finding significant concurrent annotations in gene lists. *Genome Biology*, 8(1), p.R3.

Causier, B. et al., 2012. The TOPLESS Interactome: A Framework for Gene Repression in Arabidopsis. *Plant Physiology*, 158(1), pp.423–38.

Chapman, E.J. et al., 2012. Hypocotyl transcriptome reveals auxin regulation of growth-promoting genes through GA-dependent and -independent pathways. *PLoS One*, 7(5), p.e36210.

Chen, M. & Chory, J., 2011. Phytochrome signaling mechanisms and the control of plant development. *Trends in Cell Biology*, 21(11), pp.664–71.

Chevalier, F. et al., 2014. Plastic Embedding of Arabidopsis Stem Sections. *Bio-Protocol*, 4(20), p.e1261

Cheng, H. et al., 2004. Gibberellin regulates *Arabidopsis* floral development via suppression of DELLA protein function. *Development*, 131(5), pp.1055–64.

Chiang, H.H., Hwang, I. & Goodman, H.M., 1995. Isolation of the Arabidopsis *GA4* locus. *The Plant Cell*, 7(2), pp.195–201.

Chini, A. et al., 2007. The JAZ family of repressors is the missing link in jasmonate signalling. *Nature*, 448(7154), pp.666–71.

Claeys, H. et al., 2012. DELLA signaling mediates stress-induced cell differentiation in Arabidopsis leaves through modulation of anaphase-promoting complex/cyclosome activity. *Plant Physiology*, 159(2), pp.739–47.

Clough, S.J. & Bent, A.F., 1998. Floral dip : a simplified method for *Agrobacterium*-mediated transformation of *Arabidopsis thaliana*. *The Plant Journal*, 16(6), pp.735–43.

Coego, A. et al., 2014. The TRANSPLANTA collection of Arabidopsis lines: A resource for functional analysis of transcription factors based on their conditional overexpression. *The Plant Journal*, 77(6), pp.944–53.

Colebrook, E.H. et al., 2014. The role of gibberellin signalling in plant responses to abiotic stress. *Journal of experimental biology*, 217, pp.67–75.

Conti, L. et al., 2014. Small Ubiquitin-like Modifier protein SUMO enables plants to control growth independently of the phytohormone gibberellin. *Developmental Cell*, 28(1), pp.102–10.

Costanzo, E., Trehin, C. & Vandenbussche, M., 2014. The role of *WOX* genes in flower development. *Annals of Botany*, 114(7), pp.1545-53.

Crocco, C.D. et al., 2015. The transcriptional regulator BBX24 impairs DELLA activity to promote shade avoidance in *Arabidopsis thaliana*. *Nature Communications*, 6, p.6202.

Cui, H. et al., 2007. An evolutionarily conserved mechanism delimiting SHR movement defines a single layer of endodermis in plants. *Science*, 316(5823), pp.421–5.

Curtis, M.D. & Grossniklaus, U., 2003. A Gateway cloning vector set for high-throughput functional analysis of genes in planta. *Plant Physiology*, 133(2), pp.462–9.

Davière, J.M. et al., 2014. Class I TCP-DELLA interactions in inflorescence shoot apex determine plant height. *Current Biology*, 24(16), pp.1923–8.

Davière, J.M. & Achard, P., 2016. A pivotal role of DELLAs in regulating multiple hormone signals. *Molecular Plant*, 9(1), pp.10–20.

de Lucas, M. et al., 2008. A molecular framework for light and gibberellin control of cell elongation. *Nature*, 451(7177), pp.480-4.

De Grauwe, L., Dugardeyn, J. & Van Der Straeten, D., 2008. Novel mechanisms of ethylene-gibberellin crosstalk revealed by the *gai eto2-1* double mutant. *Plant signaling & behavior*, 3(12), pp.1113–5.

Deal, R.B. & Henikoff, S., 2010. A simple method for gene expression and chromatin profiling of individual cell types within a tissue. *Developmental Cell*, 18(6), pp.1030–40.

Dill, A. & Sun, T.P., 2001. Synergistic derepression of gibberellin signaling by removing RGA and GAI function in *Arabidopsis thaliana*. *Genetics*, 159(2), pp.777–85.

Dolzblasz, A. et al., 2016. Stem cell regulation by *Arabidopsis WOX* genes. *Molecular Plant*, 9(7), pp.1028-39

Duan, L. et al., 2013. Endodermal ABA signaling promotes lateral root quiescence during salt stress in *Arabidopsis* seedlings. *The Plant Cell*, 25(1), pp.324–41.

Dubois, M. et al., 2013. Ethylene Response Factor 6 acts as central regulator of leaf growth under water limiting conditions in Arabidopsis. *Plant Physiology*, 162(1), pp.319-32

Dugardeyn, J., Vandenbussche, F. & Van Der Straeten, D., 2008. To grow or not to grow: What can we learn on ethylene-gibberellin cross-talk by *in silico* gene expression analysis? *Journal of Experimental Botany*, 59(1), pp. 1–16.

Eriksson, S. et al., 2006. GA_4 Is the Active Gibberellin in the Regulation of *LEAFY* Transcription and *Arabidopsis* Floral Initiation. *The Plant Cell*, 18(9), pp.2172–81.

Etchells, J.P. et al., 2013. *WOX4* and *WOX14* act downstream of the PXY receptor kinase to regulate plant vascular proliferation independently of any role in vascular organisation. *Development*, 140(10), pp.2224–34.

Feng, S. et al., 2008. Coordinated regulation of *Arabidopsis thaliana* development by light and gibberellins. *Nature*, 451(7177), pp.475–79.

Foo, E. et al., 2006. PhyA and cry1 act redundantly to regulate gibberellin levels during de-etiolation in blue light. *Physiologia Plantarum*, 127(1), pp.149–56.

Franco-Zorrilla, J.M. et al., 2005. Interaction between phosphate-starvation, sugar, and cytokinin signaling in Arabidopsis and the roles of cytokinin receptors CRE1/AHK4 and AHK3. *Plant Physiology*, 138(2), pp.847–57.

Franco-Zorrilla, J.M. et al., 2002. Mutations at *CRE1* impair cytokinin-induced repression of phosphate starvation responses in *Arabidopsis*. *Plant Journal*, 32(3), pp.353–60.

Frigerio, M. et al., 2006. Transcriptional regulation of gibberellin metabolism genes by auxin signaling in Arabidopsis. *Plant Physiology*, 142(2), pp.553–63.

Fu, X. & Harberd, N.P., 2003. Auxin promotes *Arabidopsis* root growth by modulating gibberellin response. *Nature*, 421(6924), pp.740–43.

Fujita, Y. et al., 2011. ABA-mediated transcriptional regulation in response to osmotic stress in plants. *Journal of Plant Research*, 124(4), pp.509–25.

Fukazawa, J. et al., 2014. DELLAs Function as Coactivators of GAI-ASSOCIATED FACTOR1 in Regulation of Gibberellin Homeostasis and Signaling in *Arabidopsis*. *The Plant Cell*, 26(7), pp.2920-38

Gallego-Bartolomé, J. et al., 2012. Molecular mechanism for the interaction between gibberellin and brassinosteroid signaling pathways in *Arabidopsis*. *Proceedings of the National Academy of Sciences of the United States of America*, 109(33), pp.13446–51.

Gallego-Bartolomé, J. et al., 2010. Transcriptional diversification and functional conservation between DELLA proteins in Arabidopsis. *Molecular Biology and Evolution*, 27(6), pp.1247–56.

Galvan-Ampudia, C.S. et al., 2013. Halotropism is a response of plant roots to avoid a saline environment. *Current Biology*, 23(20), pp.2044–50.

González-García, M.-P. et al., 2011. Brassinosteroids control meristem size by promoting cell cycle progression in *Arabidopsis* roots. *Development*, 138(5), pp.849–59.

Grierson, C. et al., 2014. Root hairs. *The Arabidopsis Book*, 12, p.e0172.

Griffiths, J. et al., 2006. Genetic characterization and functional analysis of the GID1 gibberellin receptors in *Arabidopsis*. *The Plant Cell*, 18(12), pp.3399–414.

Haecker, A. et al., 2004. Expression dynamics of *WOX* genes mark cell fate decisions during early embryonic patterning in *Arabidopsis thaliana*. *Development*, 131(3), pp.657–68.

Hajihashemi, S. et al., 2007. Exogenously applied paclobutrazol modulates growth in salt-stressed wheat plants. *Plant Growth Regulation*, 53(2), pp.117–28.

He, J.-X. et al., 2002. The GSK3-like kinase BIN2 phosphorylates and destabilizes BZR1, a positive regulator of the brassinosteroid signaling pathway in *Arabidopsis*. *Proceedings of the National Academy of Sciences of the United States of America*, 99(15), pp.10185–90.

Hedden, P, 2016. Gibberellin biosynthesis in higher plants. *Annual Plant Reviews*, 49, pp.37-72.

Hirakawa, Y., Kondo, Y. & Fukuda, H., 2010. TDIF peptide signaling regulates vascular stem cell proliferation via the *WOX4* homeobox gene in *Arabidopsis*. *The Plant Cell*, 22(8), pp.2618–29.

Hirano, K. et al., 2012. The suppressive function of the rice DELLA protein SLR1 is dependent on its transcriptional activation activity. *The Plant Journal*, 71(3), pp.443–53.

Holsters, M. et al., 1980. The functional organization of the nopaline *A. tumefaciens* plasmid pTiC58. Plasmid, 3(2), pp.212–30.

Hong, G.-J. et al., 2012. *Arabidopsis* MYC2 interacts with DELLA proteins in regulating sesquiterpene synthase gene expression. *The Plant Cell*, 24(6), pp.2635–48.

Hornitschek, P. et al., 2012. Phytochrome interacting factors 4 and 5 control seedling growth in changing light conditions by directly controlling auxin signaling. *The Plant Journal*, 71(5), pp.699–711.

Hou, X. et al., 2010. DELLAs modulate jasmonate signaling via competitive binding to JAZs. *Developmental Cell*, 19(6), pp.884–94.

Hou, X., Ding, L. & Yu, H., 2013. Crosstalk between GA and JA signaling mediates plant growth and defense. *Plant Cell Reports*, 32(7), pp.1067–74.

Hu, J. et al., 2008. Potential sites of bioactive gibberellin production during reproductive growth in *Arabidopsis*. *The Plant Cell*, 20(2), pp.320–36.

Ikeda, M., Mitsuda, N. & Ohme-Takagi, M., 2009. *Arabidopsis* WUSCHEL is a bifunctional transcription factor that acts as a repressor in stem cell regulation and as an activator in floral patterning. *The Plant Cell*, 21(11), pp.3493–505.

Iuchi, S. et al., 2007. Multiple loss-of-function of Arabidopsis gibberellin receptor AtGID1s completely shuts down a gibberellin signal. *The Plant Journal*, 50(6), pp.958–66.

Jasinski, S. et al., 2005. KNOX action in *Arabidopsis* is mediated by coordinate regulation of cytokinin and gibberellin activities. *Current Biology*, 15(17), pp.1560–5.

Jefferson, R.A., Kavanagh, T.A. & Bevan, M.W., 1987. GUS fusions: beta-glucuronidase as a sensitive and versatile gene fusion marker in higher plants. *The EMBO Journal*, 6(13), pp.3901–7.

Josse, E.-M. et al., 2011. A DELLA in disguise: SPATULA restrains the growth of the developing *Arabidopsis* seedling. *The Plant Cell*, 23(4), pp.1337–51.

Julkowska, M.M. & Testerink, C., 2015. Tuning plant signaling and growth to survive salt. *Trends in Plant Science*, 20(9), pp.586–94.

Kaneko, M. et al., 2003. Where do gibberellin biosynthesis and gibberellin signaling occur in rice plants? *The Plant Journal*, 35(1), pp.104–15.

Kendall, S.L. et al., 2011. Induction of dormancy in *Arabidopsis* summer annuals requires parallel regulation of *DOG1* and hormone metabolism by low temperature and CBF transcription factors. *The Plant Cell*, 23(7), pp.2568–80.

Kieber, J.J. & Schaller, G.E., 2014. Cytokinins. *The Arabidopsis Book*, 12, p.e0168.

Kieffer, M. et al., 2006. Analysis of the transcription factor WUSCHEL and its functional homologue in *Antirrhinum* reveals a potential mechanism for their roles in meristem maintenance. *The Plant Cell*, 18(3), pp.560–73.

Kim, T.-W. et al., 2009. Brassinosteroid signal transduction from cell-surface receptor kinases to nuclear transcription factors. *Nature Cell Biology*, 11(10), pp.1254–60.

King, K.E., Moritz, T. & Harberd, N.P., 2001. Gibberellins are not required for normal stem growth in *Arabidopsis thaliana* in the absence of GAI and RGA. *Genetics*, 159(2), pp.767–76.

Ko, J.H., Yang, S.H. & Han, K.H., 2006. Upregulation of an Arabidopsis RING-H2 gene, *XERICO*, confers drought tolerance through increased abscisic acid biosynthesis. *The Plant Journal*, 47(3), pp.343–55.

Kong, D., Hao, Y. & Cui, H., 2016. The WUSCHEL Related Homeobox protein WOX7 regulates the sugar response of lateral root development in *Arabidopsis thaliana*. *Molecular Plant*, 9(2), pp.261–70.

Koornneef, M. & van der Veen, J.H., 1980. Induction and analysis of gibberellin sensitive mutants in *Arabidopsis thaliana* (L.) heynh. *Theoretical and Applied Genetics*, 58(6), pp.257–63.

Kumar, M.N. & Verslues, P.E., 2015. Stress physiology functions of the Arabidopsis histidine kinase cytokinin receptors. *Physiologia Plantarum*, 154(3), pp.369–80.

Kumpf, R.P. & Nowack, M.K., 2015. The root cap: a short story of life and death. *Journal of Experimental Botany*, 66(19), pp.5651–62.

Lan, P. et al., 2013. Mapping gene activity of *Arabidopsis* root hairs. *Genome Biology*, 14(6), p.R67.

Laux, T. et al., 1996. The *WUSCHEL* gene is required for shoot and floral meristem integrity in Arabidopsis. *Development*, 122(1), pp.87–96.

Lee, S. et al., 2002. Gibberellin regulates *Arabidopsis* seed germination via *RGL2*, a *GAI/RGA-like* gene whose expression is up-regulated following imbibition. *Genes and Development*, 16(5), pp.646–58.

Li, K. et al., 2016. DELLA-mediated PIF degradation contributes to coordination of light and gibberellin signalling in *Arabidopsis*. *Nature Communications*, 7, p.11868.

Li, M. et al., 2016. DELLA proteins interact with FLC to repress flowering transition. *Journal of Integrative Plant Biology*, 58(7), pp.642-55.

Li, Q.-F. et al., 2012. An Interaction Between BZR1 and DELLAs Mediates Direct Signaling Crosstalk Between Brassinosteroids and Gibberellins in *Arabidopsis*. *Science Signaling*, 5(244), p.ra72.

Lie, C., Kelsom, C. & Wu, X., 2012. *WOX2* and *STIMPY-LIKE*/*WOX8* promote cotyledon boundary formation in Arabidopsis. *The Plant Journal*, 72(4), pp.674–82.

Lim, S. et al., 2013. ABA-insensitive3, ABA-insensitive5, and DELLAs Interact to Activate the Expression of *SOMNUS* and Other High-Temperature-Inducible Genes in Imbibed Seeds in *Arabidopsis*. *The Plant Cell*, 25(12), pp.4863–78.

Liu, J. et al., 2014. *WOX11* and *12* are involved in the first-step cell fate transition during de novo root organogenesis in Arabidopsis. *The Plant Cell*, 26(3), pp.1081-93.

Liu, W. et al., 2015. Salt stress reduces root meristem size by nitric oxide-mediated modulation of auxin accumulation and signaling in Arabidopsis. *Plant Physiology*, 168(1), pp.343-56.

Lohmann, J.U. et al., 2001. A molecular link between stem cell regulation and floral patterning in *Arabidopsis*. *Cell*, 105(6), pp.793–803.

Magome, H. et al., 2008. The DDF1 transcriptional activator upregulates expression of a gibberellin-deactivating gene, *GA2ox7*, under high-salinity stress in Arabidopsis. *The Plant Journal*, 56(4), pp.613–26.

Marín-de la Rosa, N. et al., 2015. Genome Wide Binding Site Analysis Reveals Transcriptional Coactivation of Cytokinin-Responsive Genes by DELLA Proteins. *PLoS Genetics*, 11(7), p.e1005337.

Marín-de la Rosa, N. et al., 2014. Large-scale identification of gibberellin-related transcription factors defines group VII ETHYLENE RESPONSE FACTORS as functional DELLA partners. *Plant Physiology*, 166(2), pp.1022–32.

Mayer, K.F.X. et al., 1998. Role of *WUSCHEL* in regulating stem cell fate in the *Arabidopsis* shoot meristem. *Cell*, 95(6), pp.805–15.

McGinnis, K.M. et al., 2003. The Arabidopsis *SLEEPY1* gene encodes a putative F-box subunit of an SCF E3 ubiquitin ligase. *The Plant Cell*, 15(5), pp.1120–30.

Mendrinna, A. & Persson, S., 2015. Root hair growth: it's a one way street. *F1000Prime Reports*, 7, p.23.

Mitchum, M.G. et al., 2006. Distinct and overlapping roles of two gibberellin 3-oxidases in Arabidopsis development. *The Plant Journal*, 45(5), pp.804–18.

Mukherjee, K., Brocchieri, L. & Bürglin, T.R., 2009. A comprehensive classification and evolutionary analysis of plant homeobox genes. *Molecular Biology and Evolution*, 26(12), pp.2775–94.

Muraro, D. et al., 2016. A multi-scale model of the interplay between cell signalling and hormone transport in specifying the root meristem of *Arabidopsis thaliana*. J*ournal of Theoretical Biology*, 404, pp.182–205.

Murase, K. et al., 2008. Gibberellin-induced DELLA recognition by the gibberellin receptor GID1. *Nature*, 456, pp.459–63.

Mutasa-Göttgens, E. & Hedden, P., 2009. Gibberellin as a factor in floral regulatory networks. *Journal of Experimental Botany*, 60(7), pp.1979–89.

Nakagawa, T. et al., 2007. Development of series of gateway binary vectors, pGWBs, for realizing efficient construction of fusion genes for plant transformation. *Journal of Bioscience and Bioengineering*, 104(1), pp.34–41.

Nakajima, M. et al., 2006. Identification and characterization of Arabidopsis gibberellin receptors. *The Plant Journal*, 46(5), pp.880–9.

Nakata, M. et al., 2012. Roles of the middle domain-specific *WUSCHEL-RELATED HOMEOBOX* genes in early development of leaves in *Arabidopsis*. *The Plant Cell*, 24(2), pp.519–35.

Nishiyama, R. et al., 2011. Analysis of cytokinin mutants and regulation of cytokinin metabolic genes reveals important regulatory roles of cytokinins in drought, salt and abscisic acid responses, and abscisic acid biosynthesis. *The Plant Cell*, 23(6), pp.2169–83.

Nogales-Cadenas, R. et al., 2009. GeneCodis: Interpreting gene lists through enrichment analysis and integration of diverse biological information. *Nucleic Acids Research*, 37(Web Server Issue), pp.W317-22.

Nomura, T. et al., 2013. Functional analysis of *Arabidopsis* CYP714A1 and CYP714A2 reveals that they are distinct gibberellin modification enzymes. *Plant and Cell Physiology*, 54(11), pp.1837–51.

Ogawa, M. et al., 2003. Gibberellin biosynthesis and response during Arabidopsis seed germination. *The Plant Cell*, 15(7), pp.1591–604.

Ogawa, M. et al., 2000. Rice gibberellin-insensitive gene homolog, *OsGAI*, encodes a nuclear-localized protein capable of gene activation at transcriptional level. *Gene*, 245(1), pp.21–9.

Oh, E. et al., 2007. PIL5, a phytochrome-interacting bHLH protein, regulates gibberellin responsiveness by binding directly to the *GAI* and *RGA* promoters in *Arabidopsis* seeds. *The Plant Cell*, 19(4), pp.1192–208.

Oh, E., Zhu, J.-Y. & Wang, Z.-Y., 2012. Interaction between BZR1 and PIF4 integrates brassinosteroid and environmental responses. *Nature Cell Biology*, 14(8), pp.802–9.

Oliveros, J.C., 2007-2015. Venny An interactive tool for comparing lists with Venn´s diagrams. http://bioinfogp.cnnb.csic.es/tools/venny/index.html

Park, J. et al., 2013. DELLA Proteins and Their Interacting RING Finger Proteins Repress Gibberellin Responses by Binding to the Promoters of a Subset of Gibberellin-Responsive Genes in *Arabidopsis*. *The Plant Cell*, 25(3), pp.927–43.

Park, S.O. et al., 2005. The *Pretty Few Seeds 2* gene encodes an *Arabidopsis* homeodomain protein that regulates ovule development. *Development*, 132(4), pp.841–9.

Peng, J. et al., 1997. The *Arabidopsis GAI* gene defines a signaling pathway that negatively regulates gibberellin responses . *Genes and Development*, 11(23), pp.3194–205.

Pfaffl, M.W., 2001. A new mathematical model for relative quantification in real-time RT-PCR. *Nucleic Acids Research*, 29(9), p.e45.

Pfeiffer, A. et al., 2014. Combinatorial complexity in a transcriptionally centered signaling hub in *Arabidopsis*. *Molecular Plant*, 7(11), pp.1598–618.

Phillips, a L. et al., 1995. Isolation and expression of three gibberellin 20-oxidase cDNA clones from Arabidopsis. *Plant Physiology*, 108(3), pp.1049–57.

Pi, L. et al., 2015. Organizer-derived WOX5 signal maintains root columella stem cells through chromatin-mediated repression of *CDF4* expression. *Developmental Cell*, 33(5), pp.576–88.

Piskurewicz, U. & Lopez-Molina, L., 2009. The GA-signaling repressor RGL3 represses testa rupture in response to changes in GA and ABA levels. *Plant Signaling & Behavior*, 4(1), pp.63–5.

Qi, T. et al., 2014. *Arabidopsis* DELLA and JAZ proteins bind the WD-repeat/bHLH/MYB complex to modulate gibberellin and jasmonate signaling synergy. *The Plant Cell*, 26(3), pp.1118–33.

Regnault, T. et al., 2014. The gibberellin biosynthetic genes *AtKAO1* and *AtKAO2* have overlapping roles throughout *Arabidopsis* development. *The Plant Journal*, 80(3), pp.462–74.

Regnault, T. et al., 2015. The gibberellin precursor GA_{12} acts as a long-distance growth signal in *Arabidopsis*. *Nature Plants*, 1, p.15073.

Regnault, T., Davière, J.-M. & Achard, P., 2016. Long-distance transport of endogenous gibberellins in *Arabidopsis*. *Plant Signaling and Behavior*, 11(1), p.e1110661.

Resentini, F. et al., 2015. TCP14 and TCP15 mediate the promotion of seed germination by gibberellins in *Arabidopsis thaliana*. *Molecular Plant*, 8(3), pp.482–5.

Rieu, I., Eriksson, S., et al., 2008a. Genetic analysis reveals that C_{19}-GA 2-oxidation is a major gibberellin inactivation pathway in *Arabidopsis*. *The Plant Cell*, 20(9), pp.2420–36.

Rieu, I., Ruiz-Rivero, O., et al., 2008b. The gibberellin biosynthetic genes *AtGA20ox1* and *AtGA20ox2* act, partially redundantly, to promote growth and development throughout the Arabidopsis life cycle. *The Plant Journal*, 53(3), pp.488–504.

Rombolá-Caldentey, B. et al., 2014. *Arabidopsis* DELLA and two HD-ZIP transcription factors regulate GA signaling in the epidermis through the L1 box *cis*-element. *The Plant Cell*, 26(7), pp.2905-19.

Romera-Branchat, M. et al., 2013. The *WOX13* homeobox gene promotes replum formation in the *Arabidopsis thaliana* fruit. *The Plant Journal*, 73(1), pp.37–49.

Saeed, A.I. et al., 2003. TM4: A free, open-source system for microarray data management and analysis. *BioTechniques*, 34(2), pp.374–8.

Sah, S.K., Reddy, K.R. & Li, J., 2016. Abscisic acid and abiotic stress tolerance in crop plants. *Frontiers in Plant Science*, 7, p.571.

Sankar, B. et al., 2007. Effect of paclobutrazol on water stress amelioration through antioxidants and free radical scavenging enzymes in *Arachis hypogaea* L. *Colloids and Surfaces B: Biointerfaces*, 60(2), pp.229–35.

Sarkar, A.K. et al., 2007. Conserved factors regulate signalling in *Arabidopsis thaliana* shoot and root stem cell organizers. *Nature*, 446(7137), pp.811–4.

Sarnowska, E.A. et al., 2013. DELLA-interacting SWI3C core subunit of Switch/Sucrose Nonfermenting Chromatin Remodeling Complex modulates gibberellin responses and hormonal cross talk in Arabidopsis. *Plant Physiology*, 163(1), pp.305–17.

Schaller, G.E., Bishopp, A. & Kieber, J.J., 2015. The yin-yang of hormones: cytokinin and auxin interactions in plant development. *The Plant Cell*, 27(1), pp.44–63.

Scheres, B., Benfey, P. & Dolan, L., 2002. Root development. *The Arabidopsis Book*, 1, p.e0101.

Schindelin, J. et al., 2012. Fiji: an open-source platform for biological-image analysis. *Nature Methods*, 9(7), pp.676–82.

Schnall, J. a & Quatrano, R.S., 1992. Abscisic acid elicits the water-stress response in root hairs of *Arabidopsis thaliana*. *Plant Physiology*, 100(1), pp.216–8.

Schneider, G. & Schliemann, W., 1994. Gibberellin conjugates: an overview. *Plant Growth Regulation*, 15(3), pp.247–60.

Schwechheimer, C., 2012. Gibberellin Signaling in Plants – The Extended Version. *Frontiers in Plant Science*, 2, p.107.

Seo, M. et al., 2011. Profiling of hormones and related metabolites in seed dormancy and germination studies. *Methods in Molecular Biology*, 773, pp. 99-111.

Seo, M. et al., 2006. Regulation of hormone metabolism in Arabidopsis seeds: phytochrome regulation of abscisic acid metabolism and abscisic acid regulation of gibberellin metabolism. *The Plant Journal*, 48(3), pp.354–66.

Shani, E. et al., 2013. Gibberellins accumulate in the elongating endodermal cells of *Arabidopsis* root. *Proceedings of the National Academy of Sciences of the United States of America*, 110(12), pp.4834-9

Shrivastava, P. and Kumar, R., 2015. Soil salinity: A serious environmental issue and plant growth promoting bacteria as one of the tools for its alleviation. *Saudi Journal of Biological Sciences*, 22(2), pp.123-31.

Sievers, F. et al., 2011. Fast, scalable generation of high-quality protein multiple sequence alignments using Clustal Omega. *Molecular Systems Biology*, 7, p.539.

Silverstone, a L., Ciampaglio, C.N. & Sun, T., 1998. The Arabidopsis *RGA* gene encodes a transcriptional regulator repressing the gibberellin signal transduction pathway. *The Plant Cell*, 10(2), pp.155–69.

Silverstone, A.L. et al., 1997. The new *RGA* locus encodes a negative regulator of gibberellin response in *Arabidopsis thaliana*. *Genetics*, 146(3), pp.1087–99.

Skylar, A. et al., 2011. Metabolic sugar signal promotes *Arabidopsis* meristematic proliferation via G2. *Developmental Biology*, 351(1), pp.82–9.

Skylar, A. et al., 2010. *STIMPY* mediates cytokinin signaling during shoot meristem establishment in *Arabidopsis* seedlings. *Development*, 137(4), pp.541–9.

Skylar, A. & Wu, X., 2010. STIMPY mutants have increased cytokinin sensitivity during dark germination. *Plant Signaling & Behavior*, 5(11), pp.1437–9.

Smyth, G.K., 2004. Linear models and empirical bayes methods for assessing differential expression in microarray experiments. *Statistical applications in genetics and molecular biology*, 3, p.Article3.

Stavang, J.A. et al., 2005. Thermoperiodic stem elongation involves transcriptional regulation of gibberellin deactivation in pea. *Plant Physiology*, 138(4), pp.2344–53.

Stolz, A. et al., 2011. The specificity of cytokinin signalling in *Arabidopsis thaliana* is mediated by differing ligand affinities and expression profiles of the receptors. *The Plant Journal*, 67(1), pp.157–68.

Strader, L.C. et al., 2004. Recessive-interfering mutations in the gibberellin signaling gene *SLEEPY1* are rescued by overexpression of its homologue, *SNEEZY*. *Proceedings of the National Academy of Sciences of the United States of America*, 101(34), pp.12771–6.

Suer, S. et al., 2011. *WOX4* imparts auxin responsiveness to cambium cells in *Arabidopsis*. *The Plant Cell*, 23(9), pp.3247–59.

Suzuki, H. et al., 2009. Differential expression and affinities of Arabidopsis gibberellin receptors can explain variation in phenotypes of multiple knock-out mutants. *The Plant Journal*, 60(1), pp.48–55.

Symons, G.M. et al., 2008. The hormonal regulation of de-etiolation. *Planta*, 227(5), pp.1115–25.

Szemenyei, H., Hannon, M. & Long, J.A., 2008. TOPLESS mediates auxin-dependent transcriptional repression during *Arabidopsis* embryogenesis. *Science*, 319(5868), pp.1384–6.

Tabas-Madrid, D., Nogales-Cadenas, R. & Pascual-Montano, A., 2012. GeneCodis3: A non-redundant and modular enrichment analysis tool for functional genomics. *Nucleic Acids Research*, 40(Web Server Issue), pp. 478-83.

Takatsuka, H. & Umeda, M., 2015. Epigenetic control of cell division and cell differentiation in the root apex. *Frontiers in Plant Science*, 6, p.1178.

Tamura, K. et al., 2013. MEGA6: Molecular evolutionary genetics analysis version 6.0. *Molecular Biology and Evolution*, 30(12), pp.2725–9.

Tanaka, N. et al., 2014. Characteristics of a root hair-less line of *Arabidopsis thaliana* under physiological stresses. *Journal of Experimental Botany*, 65(6), pp.1497–512.

Thomas, S.G., Phillips, a L. & Hedden, P., 1999. Molecular cloning and functional expression of gibberellin 2- oxidases, multifunctional enzymes involved in gibberellin deactivation. *Proceedings of the National Academy of Sciences of the United States of America*, 96(8), pp.4698–703.

Tong, H. et al., 2014. Brassinosteroid regulates cell elongation by modulating gibberellin metabolism in rice. *The Plant Cell*, 26(11), pp.4376-93.

Tran, L.-S.P. et al., 2007. Functional analysis of AHK1/ATHK1 and cytokinin receptor histidine kinases in response to abscisic acid, drought, and salt stress in *Arabidopsis*. *Proceedings of the National Academy of Sciences of the United States of America*, 104(51), pp.20623–8.

Tyler, L. et al., 2004. DELLA proteins and gibberellin-regulated seed germination and floral development in Arabidopsis. *Plant Physiology*, 135(2), pp.1008–19.

Ubeda-Tomás, S. et al., 2008. Root growth in *Arabidopsis* requires gibberellin/DELLA signalling in the endodermis. *Nature Cell Biology*, 10(5), pp.625–8.

Umezawa, T. et al., 2010. Molecular basis of the core regulatory network in ABA responses: sensing, signaling and transport. *Plant & Cell Physiology*, 51(11), pp.1821–39.

Valenzuela, C.E. et al., 2016. Salt stress response triggers activation of the jasmonate signaling pathway leading to inhibition of cell elongation in Arabidopsis primary root. *Journal of Experimental Botany*, 67(14), pp.4209-20.

van der Graaff, E., Laux, T. & Rensing, S.A., 2009. Protein family review The WUS homeobox-containing (WOX) protein family. *Genome Biology*, 10(12), p.248.

Vandenbussche, F. et al., 2007. Ethylene-induced *Arabidopsis* hypocotyl elongation is dependent on but not mediated by gibberellins. *Journal of Experimental Botany*, 58(15-16), pp.4269–81.

Varbanova, M. et al., 2007. Methylation of gibberellins by *Arabidopsis* GAMT1 and GAMT2. *The Plant Cell*, 19(1), pp.32–45.

Veit, B., 2009. Hormone mediated regulation of the shoot apical meristem. *Plant Molecular Biology*, 69(4), pp.397–408.

Vermeer, J.E.M. & Geldner, N., 2015. Lateral root initiation in *Arabidopsis thaliana*: a force awakens. *F1000prime Reports*, 7, p.32.

Vilches-Barro, A. & Maizel, A., 2014. Talking through walls: Mechanisms of lateral root emergence in *Arabidopsis thaliana*. *Current Opinion in Plant Biology*, 23, pp.31–8.

Vranová, E., Coman, D. & Gruissem, W., 2013. Network analysis of the MVA and MEP pathways for isoprenoid synthesis. *Annu. Rev. Plant Biol.*, 64, pp.665–700.

Wang, Y. et al., 2008. Salt-induced plasticity of root hair development is caused by ion disequilibrium in *Arabidopsis thaliana*. Journal of Plant Research, 121(1), pp.87–96.

Wang, Y. & Li, X., 2008. Salt stress-induced cell reprogramming, cell fate switch and adaptive plasticity during root hair development in Arabidopsis. *Plant signaling and behavior*, 3(7), pp.436–8.

Wen, C.-K. & Chang, C., 2002. Arabidopsis *RGL1* encodes a negative regulator of gibberellin responses. *The Plant Cell*, 14(1), pp.87–100.

Werner, T. et al., 2003. Cytokinin-Deficient Transgenic Arabidopsis Plants Show Functions of Cytokinins in the regulation of shoot and root meristem activity. *The Plant Cell*, 15(11), pp.2532–50.

West, G. et al., 2004. Cell cycle modulation in the response of the primary root of Arabidopsis to salt stress. *Plant Physiology*, 135(2), pp.1050–8.

Wild, M. et al., 2012. The Arabidopsis DELLA *RGA-LIKE3* is a direct target of MYC2 and modulates jasmonate signaling responses. *The Plant Cell*, 24(8), pp.3307–19.

Willige, B.C. et al., 2007. The DELLA domain of GA INSENSITIVE mediates the interaction with the GA INSENSITIVE DWARF1A gibberellin receptor of *Arabidopsis*. *The Plant Cell*, 19(4), pp.1209–20.

Woodcock, D.M. et al., 1989. Quantitative evaluation of *Escherichia coli* host strains for tolerance to cytosine methylation in plasmid and phage recombinants. *Nucleic Acids Research*, 17(9), pp.3469–78.

Wu, X., Chory, J. & Weigel, D., 2007. Combinations of *WOX* activities regulate tissue proliferation during *Arabidopsis* embryonic development. *Developmental Biology*, 309(2), pp.306–16.

Wu, X., Dabi, T. & Weigel, D., 2005. Requirement of homeobox gene *STIMPY*/*WOX9* for *Arabidopsis* meristem growth and maintenance. *Current Biology*, 15(5), pp.436–40.

Xing, S. et al., 2007. *GAMT2* encodes a methyltransferase of gibberellic acid that is involved in seed maturation and germination in *Arabidopsis*. *Journal of Integrative Plant Biology*, 49(3), pp.368–81.

Yadav, R.K. et al., 2011. WUSCHEL protein movement mediates stem cell homeostasis in the *Arabidopsis* shoot apex. *Genes and Development*, 25(19), pp.2025–30.

Yamaguchi, N. et al., 2014. Gibberellin Acts Positively Then Negatively to Control Onset of Flower Formation in *Arabidopsis*. *Science*, 344(6184), pp.638–41.

Yamauchi, Y. et al., 2004. Activation of gibberellin biosynthesis and response pathways by low temperature during imbibition of *Arabidopsis thaliana* seeds. *The Plant Cell*, 16(2), pp.367–78.

Yamauchi, Y. et al., 2007. Contribution of gibberellin deactivation by AtGA2ox2 to the suppression of germination of dark-imbibed *Arabidopsis thaliana* seeds. *Plant and Cell Physiology*, 48(3), pp.555–61.

Yin, Y. et al., 2002. BES1 accumulates in the nucleus in response to brassinosteroids to regulate gene expression and promote stem elongation. *Cell*, 109(2), pp.181–91.

Yoshida, H. et al., 2014. DELLA protein functions as a transcriptional activator through the DNA binding of the INDETERMINATE DOMAIN family proteins. *Proceedings of the National Academy of Sciences of the United States of America*, 111(21), pp.7861–6.

Yu, S. et al., 2012. Gibberellin regulates the *Arabidopsis* floral transition through miR156-targeted SQUAMOSA promoter binding-like transcription factors. *The Plant Cell*, 24(8), pp.3320–32.

Zentella, R. et al., 2007. Global analysis of della direct targets in early gibberellin signaling in *Arabidopsis*. *The Plant Cell*, 19(10), pp.3037–57.

Zhang, D. et al., 2014. The Chromatin-Remodeling Factor PICKLE Integrates Brassinosteroid and Gibberellin Signaling during Skotomorphogenic Growth in *Arabidopsis*. *The Plant Cell*, 26(6), pp.2472–85.

Zhang, Y. et al., 2013. A quartet of PIF bHLH factors provides a transcriptionally centered signaling hub that regulates seedling morphogenesis through differential expression-patterning of shared target Genes in *Arabidopsis*. *PLoS Genetics*, 9(1), p.e1003244.

Zhang, Y. et al., 2011. Over-expression of *WOX1* leads to defects in meristem development and polyamine homeostasis in *Arabidopsis*. *Journal of Integrative Plant Biology*, 53(6), pp.493–506.

Zhang, Y. et al., 2011. Two Arabidopsis cytochrome P450 monooxygenases, CYP714A1 and CYP714A2, function redundantly in plant development through gibberellin deactivation. *The Plant Journal*, 67(2), pp.342–53.

Zhang, Z.-L. et al., 2011. Scarecrow-like 3 promotes gibberellin signaling by antagonizing master growth repressor DELLA in Arabidopsis. *Proceedings of the National Academy of Sciences of the United States of America*, 108(5), pp.2160–5.

Zhao, X. et al., 2007. A study of gibberellin homeostasis and cryptochrome-mediated blue light inhibition of hypocotyl elongation. *Plant Physiology*, 145(1), pp.106–18.

Annex 1: Supplemental Data

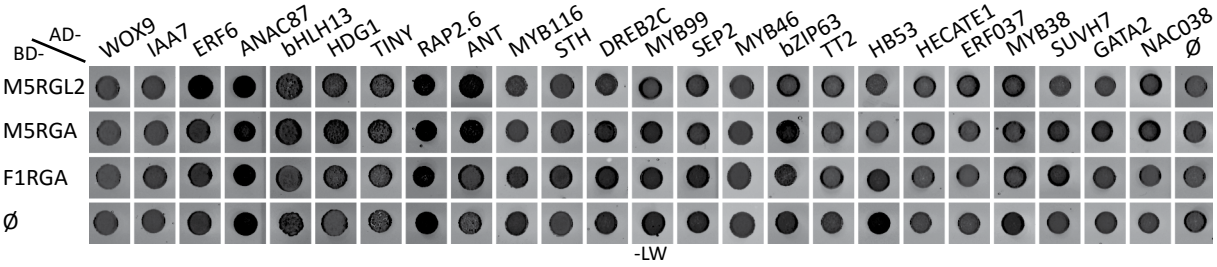

Figure S1. Yeast-Two-Hybrid screening. Interaction of the DELLA constructs (M5RGL2, M5RGA, F1RGA) and the different candidate proteins identified in the salt tolerance screening (WOX9, IAA7, ERF6, ANAC87, bHLH13, HDG1, TINY, RAP2.6, ANT, MYB116, STH, DREB2C, MYB99, SEP2, MYB46, bZIP63, TT2, HB53, HECATE1, ERF037, MYB38, SUVH7, GATA2, NAC038). The AH109 and Y187 yeast strains were respectively transformed with pGBKT7 (BD) and pGADT7 (AD) fusion constructs and mating was performed with the different construct combinations as specified. Control of growth was performed plating yeasts ond minimal medium lacking leucine (L) and tryptophan (W).

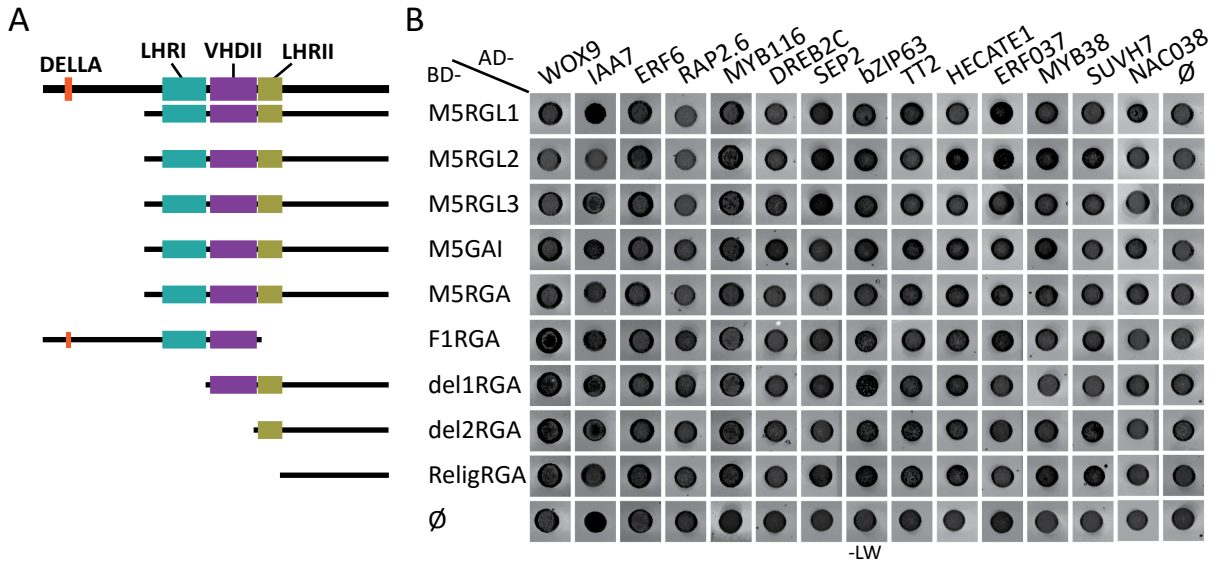

Figure S2. Yeast-Two-Hybrid mapping of the interaction domain of the best interactors (A) Scheme of the five Arabidopsis DELLAs M5 constructs (RGL1, RGL2, RGL3, GAI, RGA) and RGA deletions (F1, del1, del2, Relig) used for localization of the interaction domain. The DELLA (DELLA), first leucine heptad repeat (LHRI), VHDII and second leucine heptad repeat (LHRII) motifs are highlighted. (B) Interaction of the DELLA constructs and the different candidate genes. AH109 and Y187 yeast strains were transformed with pGBKT7 (BD) and pGADT7 (AD) fusion constructs of the DELLAs and candidate genes, respectively, and mating was performed with the different indicated combinations. Control of growth was performed plating yeasts ond minimal medium lacking leucine (L) and tryptophan (W).

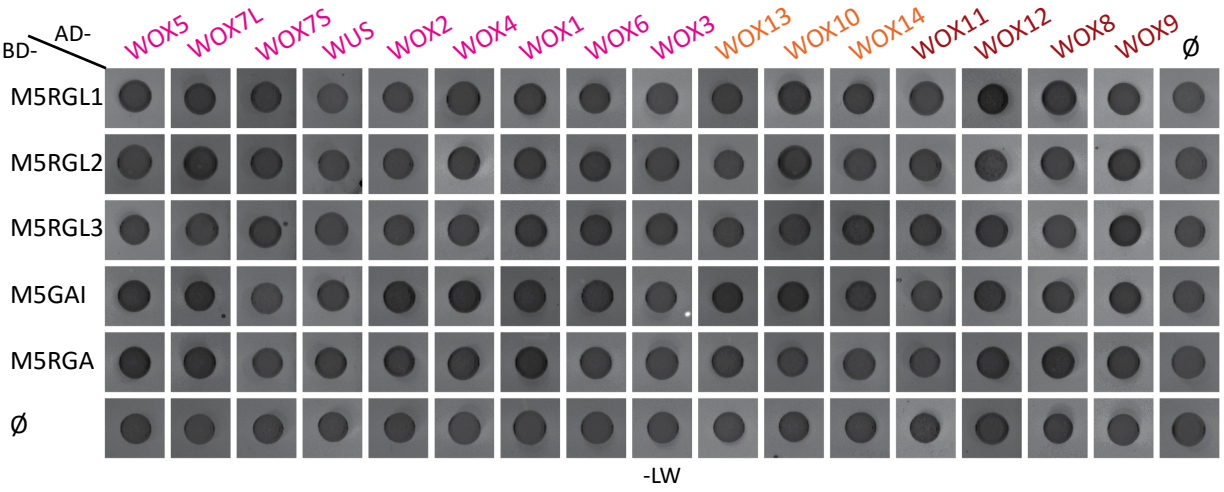

Figure S3. Yeast-Two-Hybrid interaction studies of DELLAs and the WOX family members. Interactions of the M5 DELLAs constructs (RGL1, RGL2, RGL3, GAI, RGA) and WOX family members (WOX1-WOX14, WUS). AH109 and Y187 yeast strains were transformed with the DELLA pGBKT7 (BD) and WOX pGADT7 (AD) constructs and mating was performed with the different construct combinations as indicated.. Control of growth was performed plating yeasts on minimal medium lacking leucine (L) and tryptophan (W). WOX7 has two versions, one short, lacking the WUS box and EAR domain (WOX7) and one long (WOX7L).

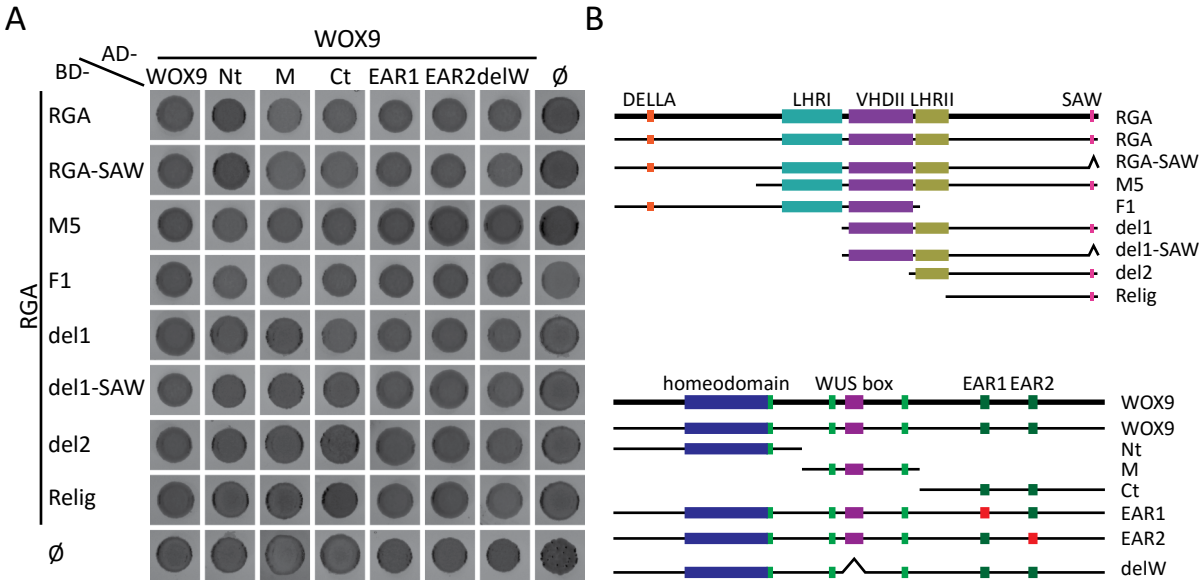

Figure S4. Yeast-Two-Hybrid assay among WOX9 and RGA deletions (A) Yeast-Two-Hybrid (Y2H) assay with the truncated WOX9 (Nt, M, Ct, EAR1, EAR2, delW) and RGA proteins (RGA-SAW, M5, F1, del1, del1-SAW, del2, Relig) to map their interaction domains. AH109 and Y187 strains were transformed with the pGBKT7 (BD) and the pGADT7 (AD) constructs and mating was performed with the indicated combinations. Control of growth was checked on minimal medium lacking leucine (L) and tryptophan (W). (B) Schematic representation of the RGA and WOX9 deletions used in Y2H. Light green boxes represent the leucine repeats (L-X-L). EAR1 (IMLHI) is mutated to IMAHA in the so-called EAR1 deletion and EAR2 (IRVFI) to ARAFA (orange boxes) in the EAR2 deletion.

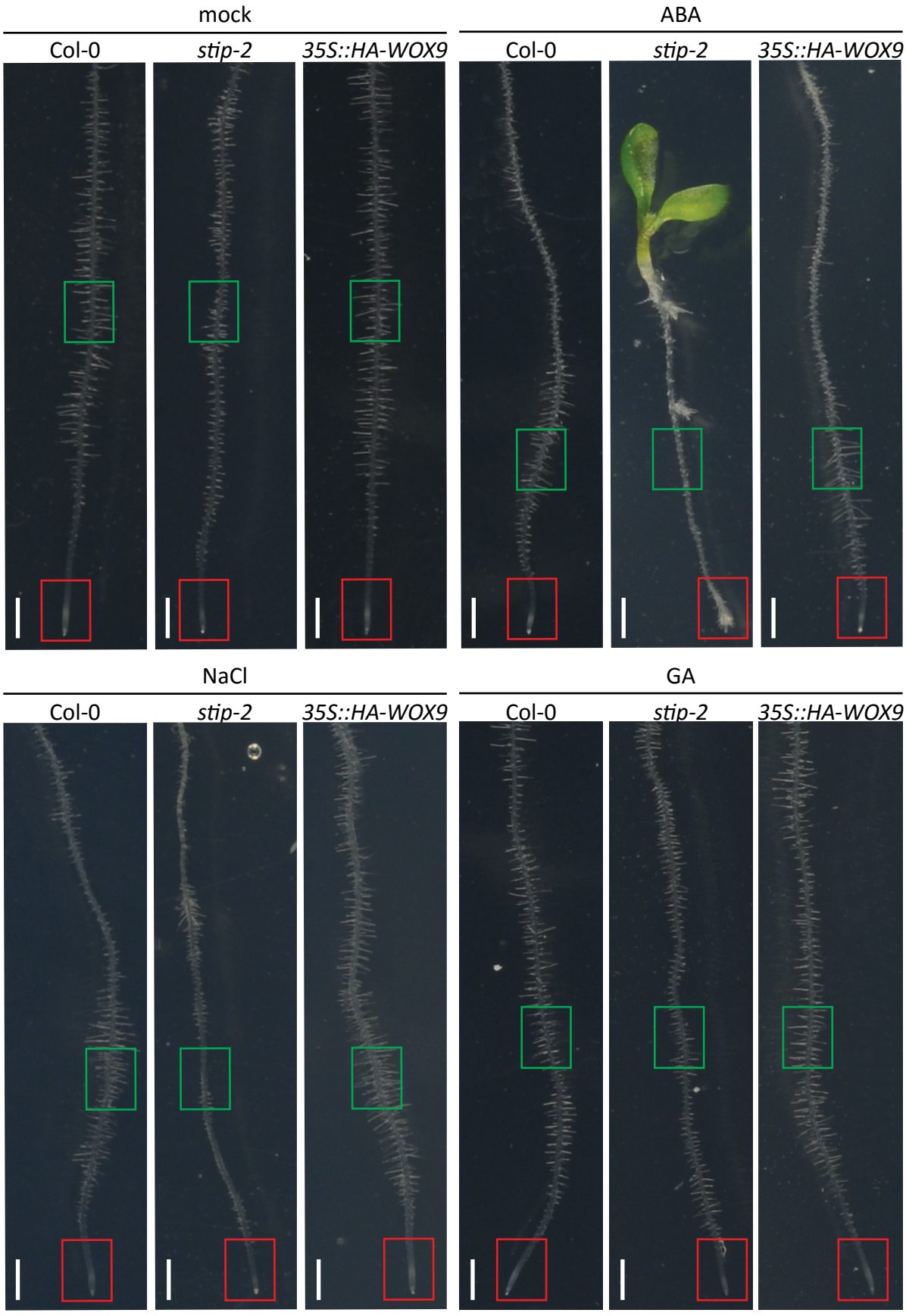

Figure S5. WOX9 lines show a root hair phenotype. 3-day-old seedlings were transferred to vertical GM plates (mock) or GM supplemented with 10µM ABA (ABA), 100mM NaCl (NaCl) or 25µM GA3 (GA), and pictures of the roots were taken after 3 days of treatment.

Table S1. Microarray data: Cluster 1 genes

		Root Hair specific*				DELLAs regulated*		
AGI	**DESCRIPTION**	**Dea**	**Lan**	**Bra**	**Bru**	**Ach**	**Zen**	**Mar**
AT1G01470	LATE EMBRYOGENESIS ABUNDANT 14 (LEA14)					UP	UP	
AT1G02930	GLUTATHIONE S-TRANSFERASE 6 (GSTF6)		x					
AT1G05520	Sec23/Sec24 protein transport family protein							
AT1G08410	P-loop containing nucleoside triphosphate hydrolases superfamily protein							
AT1G08630	THREONINE ALDOLASE 1 (THA1)							
AT1G09240	NICOTIANAMINE SYNTHASE 3 (NAS3)						DO	
AT1G09415	NIM1-INTERACTING 3 (NIMIN-3)							
AT1G11320	unknown protein							
AT1G11530	C-TERMINAL CYSTEINE RESIDUE IS CHANGED TO A SERINE 1 (CXXS1)							
AT1G11910	ASPARTIC PROTEINASE A1 (APA1)							
AT1G13320	PROTEIN PHOSPHATASE 2A SUBUNIT A3 (PP2AA3)							
AT1G13340	Regulator of Vps4 activity in the MVB pathway protein							
AT1G14120	2-oxoglutarate (2OG) and Fe(II)-dependent oxygenase superfamily protein							
AT1G14310	Haloacid dehalogenase-like hydrolase (HAD) superfamily protein				x			
AT1G14510	ALFIN-LIKE 7 (AL7)							
AT1G14560	Mitochondrial substrate carrier family protein							
AT1G15010	unknown protein		x					
AT1G15420	CONTAINS InterPro DOMAIN/s: Small-subunit processome, Utp12							
AT1G15470	Transducin/WD40 repeat-like superfamily protein							
AT1G17020	SENESCENCE-RELATED GENE 1 (SRG1)				x			
AT1G17830	Rhodanese/Cell cycle control phosphatase superfamily protein							
AT1G19250	FLAVIN-DEPENDENT MONOOXYGENASE 1 (FMO1)				x			
AT1G19610	PDF1.4, Predicted to encode a PR (pathogenesis-related) protein							
AT1G19740	ATP-dependent protease La (LON) domain protein							
AT1G20140	SKP1-LIKE 4 (SK4)							
AT1G20350	TRANSLOCASE INNER MEMBRANE SUBUNIT 17-1 (TIM17-1)							
AT1G21250	CELL WALL-ASSOCIATED KINASE (WAK1)							
AT1G21525	pseudogene of unknown protein							
AT1G22270	Encodes SMO2 (Small Organ 2). Modulates progression of cell division during organ growth							
AT1G22940	THIAMINE REQUIRING 1 (TH1)							
AT1G24145	unknown protein							

* Dea: Deal & Henikoff (2010); Lan: Lan et al. (2013); Bra: Brady et al. (2007); Bruex et al. (2012); Ach: Achard et al. (2007); Zen: Zentella et al. (2007); Mar: Marín de la Rosa et al. (2015); UP: up-regulated; DO: down-regulated

Table S1. Microarray data: Cluster 1 genes (cont.)

AGI	DESCRIPTION	Dea	Lan	Bra	Bru	Ach	Zen	Mar
AT1G24147	unknown protein							
AT1G25570	Di-glucose binding protein with Leucine-rich repeat domain							
AT1G27200	unknown protein	x						
AT1G27390	TRANSLOCASE OUTER MEMBRANE 20-2 (TOM20-2)		x					
AT1G30880	unknown protein		x					
AT1G33960	AVRRPT2-INDUCED GENE 1 (AIG1)					UP		
AT1G35710	Protein kinase family protein with leucine-rich repeat domain	x						
AT1G36370	SERINE HYDROXYMETHYLTRANSFERASE 7 (SHM7)							
AT1G45050	ATUBC2-1, member of ubiquitin-conjugating E2-proteins							
AT1G45332	Translation elongation factor EFG/EF2 protein							
AT1G50110	D-aminoacid aminotransferase-like PLP-dependent enzymes superfamily protein							
AT1G51620	Protein kinase superfamily protein							
AT1G51720	Amino acid dehydrogenase family protein							
AT1G51850	Leucine-rich repeat protein kinase family protein			x				
AT1G52370	Ribosomal protein L22p/L17e family protein							
AT1G52780	unknown protein							
AT1G53035	unknown protein	x						
AT1G56440	TETRATRICOPEPTIDE REPEAT 5 (TPR5)							
AT1G58470	RNA-BINDING PROTEIN 1 (RBP1)							
AT1G60230	Radical SAM superfamily protein							
AT1G61255	glycine-rich protein							
AT1G63055	unknown protein							
AT1G64160	DIRIGENT PROTEIN 5 (DIR5)biosynthetic process							
AT1G65040	HOMOLOG OF YEAST HRD1 (Hrd1B)							
AT1G65410	ATP-BINDING CASSETTE I13 (ABCI13)							
AT1G65500	unknown protein							
AT1G65690	Late embryogenesis abundant (LEA) hydroxyproline-rich glycoprotein family							
AT1G66070	Translation initiation factor eIF3 subunit							
AT1G66160	CYS, MET, PRO, AND GLY PROTEIN 1 (CMPG1)		x					
AT1G68290	ENDONUCLEASE 2 (ENDO2)							
AT1G68370	ALTERED RESPONSE TO GRAVITY 1 (ARG1)							
AT1G74010	Calcium-dependent phosphotriesterase superfamily protein		x				UP	
AT1G74790	FUNCTIONS IN: catalytic activity							x
AT1G78630	EMBRYO DEFECTIVE 1473 (emb1473)							
AT1G80130	Tetratricopeptide repeat (TPR)-like superfamily protein							

* Dea: Deal & Henikoff (2010); Lan: Lan et al. (2013); Bra: Brady et al. (2007); Bruex et al. (2012); Ach: Achard et al. (2007); Zen: Zentella et al. (2007); Mar: Marín de la Rosa et al. (2015); UP: up-regulated; DO: down-regulated

Table S1. Microarray data: Cluster 1 genes (cont.)

AGI	DESCRIPTION	Dea	Lan	Bra	Bru	Ach	Zen	Mar
AT2G03390	uvrB/uvrC motif-containing protein							
AT2G04390	Ribosomal S17 family protein	x	x					
AT2G09990	Ribosomal protein S5 domain 2-like superfamily protein	x	x					
AT2G17670	Tetratricopeptide repeat (TPR)-like superfamily protein							
AT2G18690	unknown protein		x		x			
AT2G19190	FLG22-INDUCED RECEPTOR-LIKE KINASE 1 (FRK1)							
AT2G19740	Ribosomal protein L31e family protein		x					
AT2G20142	Toll-Interleukin-Resistance (TIR) domain family protein							
AT2G24600	Ankyrin repeat family protein		x			UP		
AT2G25870	haloacid dehalogenase-like hydrolase family protein							
AT2G28310	unknown protein		x					
AT2G28330	unknown protein							
AT2G28500	LOB DOMAIN-CONTAINING PROTEIN 11 (LBD11)							
AT2G32600	hydroxyproline-rich glycoprotein family protein							
AT2G34750	RNA polymerase I specific transcription initiation factor RRN3 protein					UP		
AT2G35430	Zinc finger C-x8-C-x5-C-x3-H type family protein							
AT2G38240	2-oxoglutarate (2OG) and Fe(II)-dependent oxygenase superfamily protein							
AT2G39050	EUONYMUS LECTIN S3 (EULS3)				x			
AT2G39210	Major facilitator superfamily protein							
AT2G39725	LYR family of Fe/S cluster biogenesis protein						UP	
AT2G41160	Ubiquitin-associated (UBA) protein							
AT2G42070	NUDIX HYDROLASE HOMOLOG 23 (NUDX23)							
AT2G43620	Chitinase family protein					UP		
AT2G44180	METHIONINE AMINOPEPTIDASE 2A (MAP2A)		x					
AT2G44410	RING/U-box superfamily protein							
AT2G45760	BON ASSOCIATION PROTEIN 2 (BAP2)							
AT3G03560	unknown protein							
AT3G05700	Drought-responsive family protein							
AT3G10480	NAC DOMAIN CONTAINING PROTEIN 50 (NAC050)							
AT3G13050	NICOTINATE TRANSPORTER (NiaP)			x				
AT3G18250	Putative membrane lipoprotein							
AT3G20660	ORGANIC CATION/CARNITINE TRANSPORTER4 (OCT4)							
AT3G23250	MYB DOMAIN PROTEIN 15 (MYB15)							x
AT3G23490	CYANASE (CYN)							
AT3G25290	Auxin-responsive family protein							
AT3G44150	unknown protein							

* Dea: Deal & Henikoff (2010); Lan: Lan et al. (2013); Bra: Brady et al. (2007); Bruex et al. (2012); Ach: Achard et al. (2007); Zen: Zentella et al. (2007); Mar: Marín de la Rosa et al. (2015); UP: up-regulated; DO: down-regulated

Table S1. Microarray data: Cluster 1 genes (cont.)

AGI	DESCRIPTION	Dea	Lan	Bra	Bru	Ach	Zen	Mar
AT3G44260	CCR4- ASSOCIATED FACTOR 1A (CAF1a)							
AT3G47480	Calcium-binding EF-hand family protein				x			
AT3G48520	CYTOCHROME P450, FAMILY 94, SUBFAMILY B, POLYPEPTIDE 3 (CYP94B3)	x	x			UP	UP	
AT3G48640	unknown protein							
AT3G50770	CALMODULIN-LIKE 41 (CML41)							
AT3G52710	unknown protein							
AT3G55760	unknown protein							
AT3G55970	JASMONATE-REGULATED GENE 21 (JRG21)							
AT3G56400	WRKY DNA-BINDING PROTEIN 70 (WRKY70)							
AT3G59220	PIRIN (PRN), encodes a cupin-domain containing protein. Mutant has defects in germination			x				
AT3G59880	unknown protein							
At3TU073130	unknown protein							
AT4G01600	GRAM domain family protein							
AT4G02330	ATPMEPCRB, Encodes a pectin methylesterase that is sensitive to chilling stress and brassinosteroid regulation.			x				
AT4G02360	unknown protein							
AT4G06599	ubiquitin family protein							
AT4G09560	Protease-associated (PA) RING/U-box zinc finger family protein							
AT4G09830	Uncharacterised conserved protein UCP009193							
AT4G10450	Ribosomal protein L6 family		x					
AT4G11890	ABA- AND OSMOTIC-STRESS-INDUCIBLE RECEPTOR-LIKE CYTOSOLIC KINASE1 (ARCK1)							
AT4G12490	Bifunctional inhibitor/lipid-transfer protein/seed storage 2S albumin superfamily protein							
AT4G12500	Bifunctional inhibitor/lipid-transfer protein/seed storage 2S albumin superfamily protein							
AT4G14020	Rapid alkalinization factor (RALF) family protein							
AT4G14365	XB3 ORTHOLOG 4 IN ARABIDOPSIS THALIANA (XBAT34)							
AT4G14400	ACCELERATED CELL DEATH 6 (ACD6)						UP	
AT4G15210	BETA-AMYLASE 5 (BAM5)							
AT4G15880	EARLY IN SHORT DAYS 4 (ESD4)							
AT4G15975	RING/U-box superfamily protein							
AT4G20970	basic helix-loop-helix (bHLH) DNA-binding superfamily protein							
AT4G21380	RECEPTOR KINASE 3 (RK3)							
AT4G21910	MATE efflux family protein							
AT4G22470	protease inhibitor/seed storage/lipid transfer protein (LTP) family protein					UP		
AT4G24930	thylakoid lumenal 17.9 kDa protein, chloroplast							

* Dea: Deal & Henikoff (2010); Lan: Lan et al. (2013); Bra: Brady et al. (2007); Bruex et al. (2012); Ach: Achard et al. (2007); Zen: Zentella et al. (2007); Mar: Marín de la Rosa et al. (2015); UP: up-regulated; DO: down-regulated

Table S1. Microarray data: Cluster 1 genes (cont.)

AGI	DESCRIPTION	Dea	Lan	Bra	Bru	Ach	Zen	Mar
AT4G25580	CAP160 protein						UP	
AT4G26080	ABA INSENSITIVE 1 (ABI1)		x					
AT4G29700	Alkaline-phosphatase-like family protein							
AT4G30270	XYLOGLUCAN ENDOTRANSGLUCOSYLASE/ HYDROLASE 24 (XTH24)					DO		x
AT4G37990	ELICITOR-ACTIVATED GENE 3-2 (ELI3-2)						UP	
AT4G38560	Arabidopsis phospholipase-like protein (PEARLI 4) family							
AT4G38930	Ubiquitin fusion degradation UFD1 family protein							
AT5G01810	CBL-INTERACTING PROTEIN KINASE 15 (CIPK15)						UP	
AT5G02630	CANDIDATE G-PROTEIN COUPLED RECEPTOR 6 (CAND6)				x			
AT5G03850	Nucleic acid-binding, OB-fold-like protein	x	x					
AT5G04440	unknown protein							
AT5G05340	PEROXIDASE 52 (PRX52)							
AT5G05600	2-oxoglutarate (2OG) and Fe(II)-dependent oxygenase superfamily protein							
AT5G05930	GUANYLYL CYCLASE 1 (GC1), guanylyl cyclase 1 (GC1)							
AT5G07910	Leucine-rich repeat (LRR) family protein							
AT5G08550	INCREASED LEVEL OF POLYPLOIDY1-1D (ILP1)							
AT5G10380	RING1, Encodes a RING finger domain protein with E3 ligase activity that is localized to the lipid rafts of the plasma membrane							
AT5G13320	AVRPPHB SUSCEPTIBLE 3 (PBS3)							
AT5G14180	MYZUS PERSICAE-INDUCED LIPASE 1 (MPL1)		x					
AT5G19240	Glycoprotein membrane precursor GPI-anchored				x			
AT5G19320	RAN GTPASE ACTIVATING PROTEIN 2 (RANGAP2)							
AT5G21280	hydroxyproline-rich glycoprotein family protein		x					
AT5G22250	CCR4- ASSOCIATED FACTOR 1B (CAF1b)							
AT5G24140	SQUALENE MONOOXYGENASE 2 (SQP2)	x	x	x	x			
AT5G24200	alpha/beta-Hydrolases superfamily protein							
AT5G25260	SPFH/Band 7/PHB domain-containing membrane-associated protein family							
AT5G26270	unknown protein	x		x				
AT5G26690	Heavy metal transport/detoxification superfamily protein							
AT5G27430	Signal peptidase subunit							
AT5G27520	PEROXISOMAL ADENINE NUCLEOTIDE CARRIER 2 (PNC2)							
AT5G28510	BETA GLUCOSIDASE 24 (BGLU24)							
AT5G36220	CYTOCHROME P450, FAMILY 81, SUBFAMILY D, POLYPEPTIDE 1 (CYP81D1)							

* Dea: Deal & Henikoff (2010); Lan: Lan et al. (2013); Bra: Brady et al. (2007); Bruex et al. (2012); Ach: Achard et al. (2007); Zen: Zentella et al. (2007); Mar: Marín de la Rosa et al. (2015); UP: up-regulated; DO: down-regulated

Table S1. Microarray data: Cluster 1 genes (cont.)

AGI	DESCRIPTION	Dea	Lan	Bra	Bru	Ach	Zen	Mar
AT5G40670	PQ-loop repeat family protein / transmembrane family protein							
AT5G41220	GLUTATHIONE S-TRANSFERASE THETA 3 (GSTT3)							x
AT5G43290	WRKY DNA-BINDING PROTEIN 49 (WRKY49)							
AT5G44390	FAD-binding Berberine family protein							
AT5G44570	unknown protein					UP		
AT5G44575	unknown protein							
AT5G47590	Heat shock protein HSP20/alpha crystallin family							
AT5G52750	Heavy metal transport/detoxification superfamily protein							
AT5G53890	PHYTOSYLFOKINE-ALPHA RECEPTOR 2 (PSKR2)							
AT5G54610	ANKYRIN (ANK)							
AT5G55450	Bifunctional inhibitor/lipid-transfer protein/seed storage 2S albumin superfamily protein							
AT5G57630	CBL-INTERACTING PROTEIN KINASE 21 (CIPK21)						DO	
AT5G61890	encodes a member of the ERF (ethylene response factor) subfamily B-4 of ERF/AP2 transcription factor family							
AT5G65870	PHYTOSULFOKINE 5 PRECURSOR (PSK5)			x				
AT5G65900	DEA(D/H)-box RNA helicase family							
AT5G66120	3-dehydroquinate synthase, putative							
AT5G67290	FAD-dependent oxidoreductase family				x			
AT5G67500	VOLTAGE DEPENDENT ANION CHANNEL 2 (VDAC2)							

Table S2. Microarray data: Cluster 2 genes

AGI	DESCRIPTION	Dea	Lan	Bra	Bru	Ach	Zen	Mar
AT1G09460	Carbohydrate-binding X8 domain superfamily protein							
AT1G11080	SERINE CARBOXYPEPTIDASE-LIKE 31 (scpl31)							
AT1G11580	METHYLESTERASE PCR A (PMEPCRA)	x	x		x	UP		
AT1G11600	CYTOCHROME P450, FAMILY 77, SUBFAMILY B, POLYPEPTIDE 1 (CYP77B1)							
AT1G11684	unknown protein	x						
AT1G12560	EXPANSIN A7 (EXPA7)	x	x	x	x			
AT1G13650	BEST Arabidopsis thaliana protein match is: 18S pre-ribosomal assembly protein gar2-related							
AT1G19530	unknown protein					UP		
AT1G19640	JASMONIC ACID CARBOXYL METHYLTRANSFERASE (JMT)							
AT1G20070	unknown protein							
AT1G21202	MICRORNA781A (MIR781A)							

* Dea: Deal & Henikoff (2010); Lan: Lan et al. (2013); Bra: Brady et al. (2007); Bruex et al. (2012); Ach: Achard et al. (2007); Zen: Zentella et al. (2007); Mar: Marín de la Rosa et al. (2015); UP: up-regulated; DO: down-regulated

Table S2. Microarray data: Cluster 2 genes (cont.)

AGI	DESCRIPTION	Dea	Lan	Bra	Bru	Ach	Zen	Mar
AT1G22880	CELLULASE 5 (CEL5)							
AT1G24068	other RNA							
AT1G24440	RING/U-box superfamily protein							
AT1G25240	ENTH/VHS/GAT family protein	x			x			
AT1G25440	B-box type zinc finger protein with CCT domain							
AT1G26480	GENERAL REGULATORY FACTOR 12 (GRF12)							
AT1G26796	Plant self-incompatibility protein S1 family;							
AT1G28140	unknown protein							
AT1G29020	Calcium-binding EF-hand family protein		x	x				
AT1G30520	ACYL-ACTIVATING ENZYME 14 (AAE14)							
AT1G32450	NITRATE TRANSPORTER 1.5 (NRT1.5)							
AT1G34510	Peroxidase superfamily protein	x			x			
AT1G35461	unknown protein							
AT1G35480	transposable element gene							
AT1G37020	Cysteine proteinases superfamily protein							
AT1G44575	NONPHOTOCHEMICAL QUENCHING 4 (NPQ4), Encoding PSII-S (CP22)							
AT1G50060	CAP (Cysteine-rich secretory proteins, Antigen 5, and Pathogenesis-related 1 protein)		x					
AT1G51480	Disease resistance protein (CC-NBS-LRR class) family							
AT1G54040	EPITHIOSPECIFIER PROTEIN (ESP), Epithiospecifier protein, interacts with WRKY53. Involved in pathogen resistance and leaf senescence.					DO		
AT1G54970	PROLINE-RICH PROTEIN 1 (PRP1)	x	x	x	x			
AT1G56430	NICOTIANAMINE SYNTHASE 4 (NAS4)							
AT1G57750	CYTOCHROME P450, FAMILY 96, SUBFAMILY A, POLYPEPTIDE 15 (CYP96A15)							
AT1G61795	PAK-box/P21-Rho-binding family protein							
AT1G64770	PHOTOSYNTHETIC NDH SUBCOMPLEX B 2 (PnsB2)							
AT1G66200	GLUTAMINE SYNTHASE CLONE F11 (GSR2)							
AT1G69350	Tetratricopeptide repeat (TPR)-like superfamily protein							
AT1G71200	basic helix-loop-helix (bHLH) DNA-binding superfamily protein							
AT1G73580	Calcium-dependent lipid-binding (CaLB domain) family protein		x					
AT1G80240	DUF642 L-GALL RESPONSIVE GENE 1 (DGR1)							
At1TU038660	chr1:10776989-10777449, strand 1							
At1TU107240	chr1:28748800-28749177, strand -1							
AT2G04039	unknown protein							
AT2G05070	PHOTOSYSTEM II LIGHT HARVESTING COMPLEX GENE 2.2 (LHCB2.2)							
AT2G13100	GLYCEROL-3-PHOSPHATE PERMEASE 5 (G3Pp5)							

* Dea: Deal & Henikoff (2010); Lan: Lan et al. (2013); Bra: Brady et al. (2007); Bruex et al. (2012); Ach: Achard et al. (2007); Zen: Zentella et al. (2007); Mar: Marín de la Rosa et al. (2015); UP: up-regulated; DO: down-regulated

Table S2. Microarray data: Cluster 2 genes (cont.)

AGI	DESCRIPTION	Dea	Lan	Bra	Bru	Ach	Zen	Mar
AT2G18370	Predicted to encode a PR (pathogenesis-related) protein.							
AT2G20515	unknown protein							
AT2G20520	FASCICLIN-LIKE ARABINOGALACTAN 6 (FLA6), fasciclin-like arabinogalactan-protein 6 (Fla6)	x			x			
AT2G20720	Pentatricopeptide repeat (PPR) superfamily protein				x			
AT2G23630	SKU5 SIMILAR 16 (sks16)		x					
AT2G29000	Leucine-rich repeat protein kinase family protein							
AT2G29140	PUMILIO 3 (PUM3)							
AT2G33790	ARABINOGALACTAN PROTEIN 30 (AGP30)		x			DO		
AT2G34620	Mitochondrial transcription termination factor family protein							
AT2G36255	Encodes a defensin-like (DEFL) family protein.							
AT2G36750	UDP-GLUCOSYL TRANSFERASE 73C1 (UGT73C1)					UP	UP	
AT2G36790	UDP-GLUCOSYL TRANSFERASE 73C6 (UGT73C6)							
AT2G36830	GAMMA TONOPLAST INTRINSIC PROTEIN (GAMMA-TIP)	x	x			DO		
AT2G43880	Pectin lyase-like superfamily protein		x					
AT2G47050	Plant invertase/pectin methylesterase inhibitor superfamily protein							
At2TU032280	chr2:7330258-7330747, strand -1							
At2TU043780	chr2:10386964-10387329, strand 1							
At2TU044420	chr2:10550391-10550647, strand -1							
At2TU055250	chr2:13406606-13406995, strand -1							
At2TU060200	chr2:14731203-14731534, strand -1							
AT3G01080	WRKY DNA-BINDING PROTEIN 58 (WRKY58)							
AT3G01260	Galactose mutarotase-like superfamily protein							
AT3G02020	ASPARTATE KINASE 3 (AK3)					DO		
AT3G03190	GLUTATHIONE S-TRANSFERASE F11 (GSTF11)					DO		
AT3G03350	NAD(P)-binding Rossmann-fold superfamily protein							
AT3G04903	Encodes a defensin-like (DEFL) family protein.							
AT3G05560	Ribosomal L22e protein family		x					
AT3G05930	GERMIN-LIKE PROTEIN 8 (GLP8)							
AT3G06000	RNI-like superfamily protein							
AT3G08510	PHOSPHOLIPASE C 2 (PLC2)							
AT3G09040	Pentatricopeptide repeat (PPR) superfamily protein							
AT3G13580	Ribosomal protein L30/L7 family protein		x					
AT3G14040	Pectin lyase-like superfamily protein							
AT3G14530	Terpenoid synthases superfamily protein							
AT3G14940	PHOSPHOENOLPYRUVATE CARBOXYLASE 3 (PPC3)							
AT3G17150	Plant invertase/pectin methylesterase inhibitor superfamily protein							

* Dea: Deal & Henikoff (2010); Lan: Lan et al. (2013); Bra: Brady et al. (2007); Bruex et al. (2012); Ach: Achard et al. (2007); Zen: Zentella et al. (2007); Mar: Marín de la Rosa et al. (2015); UP: up-regulated; DO: down-regulated

Table S2. Microarray data: Cluster 2 genes (cont.)

AGI	DESCRIPTION	Dea	Lan	Bra	Bru	Ach	Zen	Mar
AT3G18200	nodulin MtN21-like transporter family protein							
AT3G20380	TRAF-like family protein							
AT3G20940	CYTOCHROME P450, FAMILY 705, SUBFAMILY A, POLYPEPTIDE 30 (CYP705A30)		x					
AT3G21940	Receptor protein kinase-related							
AT3G22231	PATHOGEN AND CIRCADIAN CONTROLLED 1 (PCC1)							
AT3G23125	MICRORNA173 (MIR173)							
AT3G28674	unknown protein							
AT3G30120	pseudogene, similar to CTV.22							
AT3G32040	Terpenoid synthases superfamily protein							
AT3G42798	transposable element gene; pseudogene.							
AT3G47470	LIGHT-HARVESTING CHLOROPHYLL-PROTEIN COMPLEX I SUBUNIT A4 (LHCA4)					DO		
AT3G47740	ATP-BINDING CASSETTE A3 (ABCA3)	x			x			
AT3G48340	CYSTEINE ENDOPEPTIDASE 2 (CEP2)	x						
AT3G49190	O-acyltransferase (WSD1-like) family protein		x					
AT3G49832	pseudogene of kelch repeat-containing F-box family							
AT3G50640	unknown protein							
AT3G51950	Zinc finger (CCCH-type) family protein / RNA recognition motif (RRM)-containing protein							
AT3G52720	ALPHA CARBONIC ANHYDRASE 1 (ACA1)							
AT3G53420	PLASMA MEMBRANE INTRINSIC PROTEIN 2A (PIP2A)		x					
AT3G53750	ACTIN 3 (ACT3)							
AT3G54720	ALTERED MERISTEM PROGRAM 1 (AMP1)							
AT3G55930	Pre-mRNA-splicing factor 3							
AT3G56140	Protein of unknown function (DUF399 and DUF3411)							
AT3G57100	Protein of unknown function (DUF677)							
AT3G61430	PLASMA MEMBRANE INTRINSIC PROTEIN 1A (PIP1A)							
AT3G61670	Protein of unknown function (DUF3133)							
AT3G62040	Haloacid dehalogenase-like hydrolase (HAD) superfamily protein							
AT3G62670	RESPONSE REGULATOR 20 (RR20)							
At3TU032350	chr3:8897873-8898190, strand 1							
At3TU089330	chr3:22343568-22343809, strand -1							
AT4G00140	EMBRYO SAC DEVELOPMENT ARREST 34 (EDA34)							
AT4G00680	ACTIN DEPOLYMERIZING FACTOR 8 (ADF8)	x	x	x	x			
AT4G03330	SYNTAXIN OF PLANTS 123 (SYP123)			x	x			
AT4G03710	transposable element gene							
AT4G05553	zinc knuckle (CCHC-type) family protein							
AT4G06477	transposable element gene							

* Dea: Deal & Henikoff (2010); Lan: Lan et al. (2013); Bra: Brady et al. (2007); Bruex et al. (2012); Ach: Achard et al. (2007); Zen: Zentella et al. (2007); Mar: Marín de la Rosa et al. (2015); UP: up-regulated; DO: down-regulated

Table S2. Microarray data: Cluster 2 genes (cont.)

AGI	DESCRIPTION	Dea	Lan	Bra	Bru	Ach	Zen	Mar
AT4G07706	transposable element gene							
AT4G08073	This gene encodes a small protein and has either evidence of transcription or purifying selection.							
AT4G11911	unknown protein							
AT4G12030	BILE ACID TRANSPORTER 5 (BAT5)				x	DO		
AT4G13390	EXTENSIN 12 (EXT12)	x	x		x			
AT4G16350	CALCINEURIN B-LIKE PROTEIN 6 (CBL6)		x	x	x			
AT4G16370	OLIGOPEPTIDE TRANSPORTER (OPT3)							
AT4G18340	Glycosyl hydrolase superfamily protein							
AT4G19030	NOD26-LIKE MAJOR INTRINSIC PROTEIN 1 (NLM1)		x					
AT4G20160	BEST Arabidopsis thaliana protein match is: RING/U-box superfamily protein	x						
AT4G25910	NFU DOMAIN PROTEIN 3 (NFU3)							
AT4G26010	Peroxidase superfamily protein	x	x		x			
AT4G26050	PLANT INTRACELLULAR RAS GROUP-RELATED LRR 8 (PIRL8)							
AT4G27030	FATTY ACID DESATURASE A (FADA)							
AT4G27140	SEED STORAGE ALBUMIN 1 (SESA1)							
AT4G27440	PROTOCHLOROPHYLLIDE OXIDOREDUCTASE B (PORB)							
AT4G28170	unknown protein				x			
AT4G28760	TON1 RECRUITING MOTIF 20 (TRM20)							
AT4G28780	GDSL-like Lipase/Acylhydrolase superfamily protein					DO		
AT4G28850	XYLOGLUCAN ENDOTRANSGLUCOSYLASE/ HYDROLASE 26 (XTH26)	x	x		x			
AT4G33730	CAP (Cysteine-rich secretory proteins, Antigen 5, and Pathogenesis-related 1 protein)	x			x			
AT4G34700	B22 SUBUNIT OF EUKARYOTIC MITOCHONDRIAL COMPLEX I (CIB22)							
AT4G37925	NADH DEHYDROGENASE-LIKE COMPLEX M (NdhM)							
At4TU055910	chr4:13652421-13652966, strand -1							
At4TU061490	chr4:15211391-15212026, strand -1							
At4TU062080	chr4:15357228-15357496, strand -1							
AT5G01015	unknown protein							
AT5G01480	Cysteine/Histidine-rich C1 domain family protein	x						
AT5G05250	unknown protein							
AT5G05890	UDP-Glycosyltransferase superfamily protein							
AT5G08450	CONTAINS InterPro DOMAIN/s: Histone deacetylation protein Rxt3							
AT5G10130	Pollen Ole e 1 allergen and extensin family protein		x				UP	
AT5G10250	DEFECTIVELY ORGANIZED TRIBUTARIES 3 (DOT3)							
AT5G13030	unknown protein							
AT5G15180	Peroxidase superfamily protein		x		x			

* Dea: Deal & Henikoff (2010); Lan: Lan et al. (2013); Bra: Brady et al. (2007); Bruex et al. (2012); Ach: Achard et al. (2007); Zen: Zentella et al. (2007); Mar: Marín de la Rosa et al. (2015); UP: up-regulated; DO: down-regulated

Table S2. Microarray data: Cluster 2 genes (cont.)

AGI	DESCRIPITION	Dea	Lan	Bra	Bru	Ach	Zen	Mar
AT5G15230	GAST1 PROTEIN HOMOLOG 4 (GASA4)		x					
AT5G15510	TPX2 (targeting protein for Xklp2) protein family							
AT5G19040	ISOPENTENYLTRANSFERASE 5 (IPT5)							
AT5G20290	Ribosomal protein S8e family protein	x	x					
AT5G22880	HISTONE B2 (HTB2)	x	x			DO		
AT5G23020	2-ISOPROPYLMALATE SYNTHASE 2 (IMS2)					DO		
AT5G24880	BEST Arabidopsis thaliana protein match is: calmodulin-binding protein-related	x		x	x			
AT5G25380	CYCLIN A2;1 (CYCA2;1)							
AT5G25420	Xanthine/uracil/vitamin C permease							
AT5G25990	unknown protein							
AT5G27580	AGAMOUS-LIKE 89 (AGL89)							
AT5G32513	transposable element gene							
AT5G33390	glycine-rich protein							
AT5G35480	unknown protein							
AT5G36722	unknown protein							
AT5G40880	WD-40 repeat family protein / zfwd3 protein (ZFWD3)							
AT5G42120	Concanavalin A-like lectin protein kinase family protein							
AT5G44300	Dormancy/auxin associated family protein							
AT5G46900	Bifunctional inhibitor/lipid-transfer protein/seed storage 2S albumin superfamily protein		x					
AT5G47450	TONOPLAST INTRINSIC PROTEIN 2;3 (TIP2;3)	x	x					
AT5G51470	Auxin-responsive GH3 family protein							
AT5G56850	unknown protein							
AT5G60010	ferric reductase-like transmembrane component family protein							
AT5G60530	late embryogenesis abundant protein-related / LEA protein-related		x					
AT5G62340	Plant invertase/pectin methylesterase inhibitor superfamily protein		x					
AT5G66580	unknown protein		x					
AT5G67370	Protein of unknown function (DUF1230)				x			
At5TU037540	chr5:10071485-10071888, strand 1							
At5TU103260	chr5:26811049-26811258, strand -1							
ATMG01190	ATP SYNTHASE SUBUNIT 1 (ATP1)							
miR3434	miR3434							

* Dea: Deal & Henikoff (2010); Lan: Lan et al. (2013); Bra: Brady et al. (2007); Bruex et al. (2012); Ach: Achard et al. (2007); Zen: Zentella et al. (2007); Mar: Marín de la Rosa et al. (2015); UP: up-regulated; DO: down-regulated

Table S3. Microarray data: Cluster 3 genes

AGI	DESCRIPTION	Dea	Lan	Bra	Bru	Ach	Zen	ar
AT1G01080	RNA-binding (RRM/RBD/RNP motifs) family protein							
AT1G02110	Protein of unknown function (DUF630 and DUF632)							
AT1G02130	RAS 5 (RA-5), Belongs to the Rab1 GTPase subfamily							
AT1G02500	S-ADENOSYLMETHIONINE SYNTHETASE 1 (SAM1)							
AT1G02780	EMBRYO DEFECTIVE 2386 (emb2386)		x					
AT1G02860	NITROGEN LIMITATION ADAPTATION (NLA)	x						
AT1G03160	FZO-LIKE (FZL)							
AT1G03630	PROTOCHLOROPHYLLIDE OXIDOREDUCTASE C (POR C)							
AT1G04800	glycine-rich protein							
AT1G05070	unknown protein							
AT1G05710	basic helix-loop-helix (bHLH) DNA-binding superfamily protein				x			
AT1G05870	unknown protein							
AT1G06400	ARA-2, small GTP-binding protein (ara-2)							
AT1G06410	TREHALOSE-PHOSPHATASE/SYNTHASE 7 (TPS7)							
AT1G06680	PHOTOSYSTEM II SUBUNIT P-1 (PSBP-1)							
AT1G06850	BASIC LEUCINE-ZIPPER 52 (bZIP52)							
AT1G07360	MOS4-ASSOCIATED COMPLEX SUBUNIT 5A (MAC5A)							
AT1G07960	PDI-LIKE 5-1 (PDIL5-1)				x			
AT1G08090	NITRATE TRANSPORTER 2:1 (NRT2:1)		x					
AT1G08540	RNAPOLYMERASE SIGMA SUBUNIT 2 (SIG2)							
AT1G08880	H2AXA, Encodes HTA5, a histone H2A protein				x			
AT1G09200	Histone superfamily protein		x					
AT1G09340	CHLOROPLAST RNA BINDING (CRB)							
AT1G10030	HOMOLOG OF YEAST ERGOSTEROL28 (ERG28)							
AT1G10760	STARCH EXCESS 1 (SEX1)							
AT1G10970	ZINC TRANSPORTER 4 PRECURSOR (ZIP4)							
AT1G11000	MILDEW RESISTANCE LOCUS O 4 (MLO4)		x					
AT1G11820	O-Glycosyl hydrolases family 17 protein							
AT1G11840	GLYOXALASE I HOMOLOG (GLX1)							
AT1G12650	unknown protein							
AT1G12900	GLYCERALDEHYDE 3-PHOSPHATE DEHYDROGENASE A SUBUNIT 2 (GAPA-2)							
AT1G14410	WHIRLY 1 (WHY1)							
AT1G14610	TWIN 2 (TWN2)							
AT1G14860	NUDIX HYDROLASE HOMOLOG 18 (NUDT18)		x			UP		
AT1G15350	unknown protein							
AT1G15670	Galactose oxidase/kelch repeat superfamily protein		x					
AT1G15930	Ribosomal protein L7Ae/L30e/S12e/Gadd45 family protein	x	x					
AT1G16220	Protein phosphatase 2C family protein							

* Dea: Deal & Henikoff (2010); Lan: Lan et al. (2013); Bra: Brady et al. (2007); Bruex et al. (2012); Ach: Achard et al. (2007); Zen: Zentella et al. (2007); Mar: Marín de la Rosa et al. (2015); UP: up-regulated; DO: down-regulated

Table S3. Microarray data: Cluster 3 genes (cont.)

AGI	DESCRIPTION	Dea	Lan	Bra	Bru	Ach	Zen	Mar
AT1G16445	S-adenosyl-L-methionine-dependent methyltransferases superfamily protein	x						
AT1G17120	CATIONIC AMINO ACID TRANSPORTER 8 (CAT8)							
AT1G17280	UBIQUITIN-CONJUGATING ENZYME 34 (UBC34)							
AT1G18460	alpha/beta-Hydrolases superfamily protein							
AT1G18700	DNAJ heat shock N-terminal domain-containing protein							x
AT1G18880	Pentatricopeptide repeat (PPR) superfamily protein	x						
AT1G19660	Wound-responsive family protein							
AT1G19850	MONOPTEROS (MP)	x	x					
AT1G20020	FERREDOXIN-NADP(+)-OXIDOREDUCTASE 2 (FNR2)							
AT1G20220	Alba DNA/RNA-binding protein		x					
AT1G20830	MULTIPLE CHLOROPLAST DIVISION SITE 1 (MCD1)							
AT1G21440	Phosphoenolpyruvate carboxylase family protein							
AT1G21810	Plant protein of unknown function (DUF869)							
AT1G23400	CAF2, Promotes the splicing of chloroplast group II introns.							
AT1G25472	CONSERVED PEPTIDE UPSTREAM OPEN READING FRAME 54 (CPuORF54)							
AT1G25490	ROOTS CURL IN NPA (RCN1)							
AT1G26740	Ribosomal L32p protein family							
AT1G27070	5'-AMP-activated protein kinase-related							
AT1G27130	GLUTATHIONE S-TRANSFERASE TAU 13 (GSTU13)							
AT1G29340	PLANT U-BOX 17 (PUB17)							
AT1G29400	MEI2-LIKE PROTEIN 5 (ML5)							
AT1G30680	toprim domain-containing protein							
AT1G31850	S-adenosyl-L-methionine-dependent methyltransferases superfamily protein		x					
AT1G31920	Tetratricopeptide repeat (TPR)-like superfamily protein							
AT1G32070	NUCLEAR SHUTTLE INTERACTING (NSI)							
AT1G33110	MATE efflux family protein							
AT1G33750	Terpenoid cyclases/Protein prenyltransferases superfamily protein		x					
AT1G45145	THIOREDOXIN H-TYPE 5 (TRX5)	x	x					
AT1G45688	unknown protein							
AT1G49340	ATPI4K ALPHA							
AT1G49860	GLUTATHIONE S-TRANSFERASE (CLASS PHI) 14 (GSTF14)							
AT1G50460	HEXOKINASE-LIKE 1 (HKL1)				x			
AT1G50900	GRANA DEFICIENT CHLOROPLAST 1 (GDC1)				x			
AT1G51830	Leucine-rich repeat protein kinase family protein				x			
AT1G52630	O-fucosyltransferase family protein							

* Dea: Deal & Henikoff (2010); Lan: Lan et al. (2013); Bra: Brady et al. (2007); Bruex et al. (2012); Ach: Achard et al. (2007); Zen: Zentella et al. (2007); Mar: Marín de la Rosa et al. (2015); UP: up-regulated; DO: down-regulated

Table S3. Microarray data: Cluster 3 genes (cont.)

AGI	DESCRIPTION	Dea	Lan	Bra	Bru	Ach	Zen	Mar
AT1G53320	TUBBY LIKE PROTEIN 7 (TLP7)							
AT1G55100	transposable element gene; pseudogene, putative ATP synthase beta subunit							x
AT1G58250	SABRE (SAB), SABRE, putative gene of unknown function							
AT1G58602	LRR and NB-ARC domains-containing disease resistance protein							
AT1G60810	ATP-CITRATE LYASE A-2 (ACLA-2)	x						
AT1G60900	U2 snRNP auxilliary factor, large subunit, splicing factor							
AT1G61000	unknown protein							
AT1G61900	unknown protein		x					
AT1G63180	UDP-D-GLUCOSE/UDP-D-GALACTOSE 4-EPIMERASE 3 (UGE3)							
AT1G63680	MURE, Encodes AtMurE							
AT1G64370	unknown protein							
AT1G64720	CP5, membrane related protein CP5					UP		
AT1G67090	RIBULOSE BISPHOSPHATE CARBOXYLASE SMALL CHAIN 1A (RBCS1A)							
AT1G67230	LITTLE NUCLEI1 (LINC1)							
AT1G67400	ELMO/CED-12 family protein							
AT1G67590	Remorin family protein							
AT1G67750	Pectate lyase family protein				x		UP	
AT1G68790	LITTLE NUCLEI3 (LINC3)							
AT1G69800	Cystathionine beta-synthase (CBS) protein							
AT1G70350	unknown protein							
AT1G70570	anthranilate phosphoribosyltransferase							
AT1G70850	MLP-LIKE PROTEIN 34 (MLP34)		x			DO		
AT1G71730	unknown protein							
AT1G73110	P-loop containing nucleoside triphosphate hydrolases superfamily protein					DO		
AT1G73680	ALPHA DIOXYGENASE (ALPHA DOX2)	x			x			
AT1G73990	SIGNAL PEPTIDE PEPTIDASE (SPPA)					DO		
AT1G74030	ENOLASE 1 (ENO1)							
AT1G74050	Ribosomal protein L6 family protein	x	x					
AT1G74510	Galactose oxidase/kelch repeat superfamily protein							
AT1G74560	NAP1-RELATED PROTEIN 1 (NRP1)		x			DO		
AT1G74880	NADH DEHYDROGENASE-LIKE COMPLEX (NdhO)							
AT1G74970	RIBOSOMAL PROTEIN S9 (RPS9)							
AT1G75310	AUXILIN-LIKE 1 (AUL1)							
AT1G75350	EMBRYO DEFECTIVE 2184 (emb2184)	x						
AT1G76310	CYCLIN B2;4 (CYCB2;4)							
AT1G76680	12-OXOPHYTODIENOATE REDUCTASE 1 (OPR1)		x					

* Dea: Deal & Henikoff (2010); Lan: Lan et al. (2013); Bra: Brady et al. (2007); Bruex et al. (2012); Ach: Achard et al. (2007); Zen: Zentella et al. (2007); Mar: Marín de la Rosa et al. (2015); UP: up-regulated; DO: down-regulated

Table S3. Microarray data: Cluster 3 genes (cont.)

AGI	DESCRIPTION	Dea	Lan	Bra	Bru	Ach	Zen	Mar
AT1G77510	PDI-LIKE 1-2 (PDIL1-2)		x					
AT1G78040	Pollen Ole e 1 allergen and extensin family protein							
AT1G78150	unknown protein		x					
AT1G78260	RNA-binding (RRM/RBD/RNP motifs) family protein							
AT1G78850	curculin-like (mannose-binding) lectin family protein							
AT1G79040	PHOTOSYSTEM II SUBUNIT R (PSBR)							
AT1G79280	NUCLEAR PORE ANCHOR (NUA)							
AT1G79430	ALTERED PHLOEM DEVELOPMENT (APL)							
AT1G79510	Uncharacterized conserved protein (DUF2358)							
AT1G79750	NADP-MALIC ENZYME 4 (NADP-ME4)							
AT1G80910	Protein of unknown function (DUF1712)			x	x			
AT2G01020	rRNA; 5SrRNA							
AT2G02400	NAD(P)-binding Rossmann-fold superfamily protein							
AT2G02500	ISPD, Encodes a protein with 4-Diphosphocytidyl-2C-methyl-D-erythritol synthase activity							
AT2G03420	unknown protein							x
AT2G03760	SULPHOTRANSFERASE 12 (SOT12)				x	UP		
AT2G04170	TRAF-like family protein		x					x
AT2G04530	CPZ, Encodes a protein with RNAse Z activity suggesting a role in tRNA processing							
AT2G05380	GLYCINE-RICH PROTEIN 3 SHORT ISOFORM (GRP3S)					UP		
AT2G06010	OBP3-RESPONSIVE GENE 4 (ORG4)							
AT2G07050	CYCLOARTENOL SYNTHASE 1 (CAS1)							
AT2G13820	XYLOGEN PROTEIN 2 (XYP2)							
AT2G15490	UDP-GLYCOSYLTRANSFERASE 73B4 (UGT73B4)		x					
AT2G15860	unknown protein							
AT2G16500	ARGININE DECARBOXYLASE 1 (ADC1)					UP		
AT2G16790	P-loop containing nucleoside triphosphate hydrolases superfamily protein							
AT2G17070	Arabidopsis protein of unknown function (DUF241)							
AT2G17780	MID1-COMPLEMENTING ACTIVITY 2 (MCA2)							
AT2G17790	VPS35 HOMOLOG A (VPS35A)				x			
AT2G18020	EMBRYO DEFECTIVE 2296 (EMB2296)	x	x					
AT2G18700	TREHALOSE PHOSPHATASE/SYNTHASE 11 (TPS11)	x						
AT2G19150	Pectin lyase-like superfamily protein							
AT2G19760	PROFILIN 1 (PRF1)		x					
AT2G20280	Zinc finger C-x8-C-x5-C-x3-H type family protein							
AT2G20450	Ribosomal protein L14		x					
AT2G21045	Rhodanese/Cell cycle control phosphatase superfamily protein				x			
AT2G21160	Translocon-associated protein (TRAP), alpha subunit							

* Dea: Deal & Henikoff (2010); Lan: Lan et al. (2013); Bra: Brady et al. (2007); Bruex et al. (2012); Ach: Achard et al. (2007); Zen: Zentella et al. (2007); Mar: Marín de la Rosa et al. (2015); UP: up-regulated; DO: down-regulated

Table S3. Microarray data: Cluster 3 genes (cont.)

AGI	DESCRIPTION	Dea	Lan	Bra	Bru	Ach	Zen	Mar
AT2G21385	unknown protein							
AT2G21870	MALE GAMETOPHYTE DEFECTIVE 1 (MGP1)							
AT2G22410	SLOW GROWTH 1 (SLO1)							
AT2G23040	unknown protein							
AT2G23600	ACETONE-CYANOHYDRIN LYASE (ACL)							
AT2G23672	Potential natural antisense gene							
AT2G23820	Metal-dependent phosphohydrolase							
AT2G24490	REPLICON PROTEIN A2 (RPA2)							
AT2G24762	GLUTAMINE DUMPER 4 (GDU4)							
AT2G24790	CONSTANS-LIKE 3 (COL3)							
AT2G25560	DNAJ heat shock N-terminal domain-containing protein							
AT2G25950	CONTAINS InterPro DOMAIN/s							
AT2G26460	SUPPRESSORS OF MEC-8 AND UNC-52 2 (SMU2)							
AT2G26600	Glycosyl hydrolase superfamily protein							
AT2G27430	ARM repeat superfamily protein		x					
AT2G27710	60S acidic ribosomal protein family		x					
AT2G27860	UDP-D-APIOSE/UDP-D-XYLOSE SYNTHASE 1 (AXS1)							
AT2G30540	Thioredoxin superfamily protein							
AT2G31390	pfkB-like carbohydrate kinase family protein		x					
AT2G33150	PEROXISOMAL 3-KETOACYL-COA THIOLASE 3 (PKT3)							
AT2G33255	Haloacid dehalogenase-like hydrolase (HAD) superfamily protein				x			
AT2G33610	SWITCH SUBUNIT 3 (SWI3B)							
AT2G34260	HUMAN WDR55 (WD40 REPEAT) HOMOLOG (WDR55)							
AT2G34570	MATERNAL EFFECT EMBRYO ARREST 21 (MEE21)							
AT2G34590	Transketolase family protein		x					
AT2G34660	ATP-BINDING CASSETTE C2 (ABCC2)				x			
AT2G36620	RIBOSOMAL PROTEIN L24 (RPL24A)	x	x					
AT2G36835	unknown protein							
AT2G37190	Ribosomal protein L11 family protein	x	x					
AT2G37270	RIBOSOMAL PROTEIN 5B (RPS5B)		x					
AT2G37660	NAD(P)-binding Rossmann-fold superfamily protein							
AT2G38320	TRICHOME BIREFRINGENCE-LIKE 34 (TBL34)				x			
AT2G38370	Plant protein of unknown function (DUF827)							
AT2G39730	RUBISCO ACTIVASE (RCA)					UP		
AT2G39990	EUKARYOTIC TRANSLATION INITIATION FACTOR 2 (EIF2)		x					
AT2G40660	Nucleic acid-binding, OB-fold-like protein							
AT2G41680	NADPH-DEPENDENT THIOREDOXIN REDUCTASE C (NTRC)							

* Dea: Deal & Henikoff (2010); Lan: Lan et al. (2013); Bra: Brady et al. (2007); Bruex et al. (2012); Ach: Achard et al. (2007); Zen: Zentella et al. (2007); Mar: Marín de la Rosa et al. (2015); UP: up-regulated; DO: down-regulated

Table S3. Microarray data: Cluster 3 genes (cont.)

AGI	DESCRIPTION	Dea	Lan	Bra	Bru	Ach	Zen	Mar
AT2G42330	GC-rich sequence DNA-binding factor-like protein with Tuftelin interacting domain							
AT2G42840	PROTODERMAL FACTOR 1 (PDF1)							
AT2G43150	Proline-rich extensin-like family protein							
AT2G43920	HARMLESS TO OZONE LAYER 2 (HOL2)							
AT2G44420	protein N-terminal asparagine amidohydrolase family protein				x			
AT2G44620	MITOCHONDRIAL ACYL CARRIER PROTEIN 1 (MTACP-1)							x
AT2G44860	Ribosomal protein L24e family protein		x					
AT2G45170	AUTOPHAGY 8E (ATG8E)							x
AT2G46030	UBIQUITIN-CONJUGATING ENZYME 6 (UBC6)		x		x			
AT2G46800	ZINC TRANSPORTER OF ARABIDOPSIS THALIANA (ZAT)							
AT2G46930	Pectinacetylesterase family protein							
AT2G47450	CHAOS (CAO), A component of the chloroplast signal recognition particle pathway that is involved in LHCP targeting							
AT2G47700	RED AND FAR-RED INSENSITIVE 2 (RFI2)							
AT2G48010	RECEPTOR-LIKE KINASE IN IN FLOWERS 3 (RKF3)							
At2TU000020	chr2:5607-6129, strand 1							
AT3G01516	unknown protein							
AT3G01800	Ribosome recycling factor							
AT3G02080	Ribosomal protein S19e family protein		x					
AT3G02230	REVERSIBLY GLYCOSYLATED POLYPEPTIDE 1 (RGP1)							
AT3G02340	RING/U-box superfamily protein							
AT3G02360	6-phosphogluconate dehydrogenase family protein							
AT3G03630	CYSTEINE SYNTHASE 26 (CS26)							
AT3G04240	SECRET AGENT (SEC)							
AT3G04260	PLASTID TRANSCRIPTIONALLY ACTIVE 3 (PTAC3)							
AT3G04340	EMBRYO DEFECTIVE 2458 (emb2458)							
AT3G04450	Homeodomain-like superfamily protein							
AT3G05030	SODIUM HYDROGEN EXCHANGER 2 (NHX2)							
AT3G05280	Integral membrane Yip1 family protein							
AT3G06125	Unknown protein							
AT3G06690	acyl-CoA oxidases;oxidoreductases							
AT3G07060	EMBRYO DEFECTIVE 1974 (emb1974)							
AT3G07200	RING/U-box superfamily protein							
AT3G07950	rhomboid protein-related							
AT3G08030	unknown protein		x					
AT3G09350	FES1A (Fes1A)							
AT3G09500	Ribosomal L29 family protein	x	x					

* Dea: Deal & Henikoff (2010); Lan: Lan et al. (2013); Bra: Brady et al. (2007); Bruex et al. (2012); Ach: Achard et al. (2007); Zen: Zentella et al. (2007); Mar: Marín de la Rosa et al. (2015); UP: up-regulated; DO: down-regulated

Table S3. Microarray data: Cluster 3 genes (cont.)

AGI	DESCRIPTION	Dea	Lan	Bra	Bru	Ach	Zen	Mar
AT3G09630	Ribosomal protein L4/L1 family		x					
AT3G09940	MONODEHYDROASCORBATE REDUCTASE (MDHAR)							
AT3G10060	FKBP-like peptidyl-prolyl cis-trans isomerase family protein							
AT3G11560	LETM1-like protein							
AT3G11940	RIBOSOMAL PROTEIN 5A (RPS5A)	x	x					
AT3G11964	RNA binding;RNA binding							
AT3G12050	Aha1 domain-containing protein							
AT3G12145	FLOR1 (FLR1)							
AT3G12490	CYSTATIN B (CYSB)		x					
AT3G12740	ALA-INTERACTING SUBUNIT 1 (ALIS1)							
AT3G12930	Lojap-related protein							
AT3G13470	CHAPERONIN-60BETA2 (CPN60BETA2)					DO		
AT3G13882	Ribosomal protein L34							
AT3G14172	unknown protein							
AT3G14190	unknown protein							
AT3G14900	EMBRYO DEFECTIVE 3120 (EMB3120)							
AT3G16480	MITOCHONDRIAL PROCESSING PEPTIDASE ALPHA SUBUNIT (MPPalpha)							
AT3G16780	Ribosomal protein L19e family protein		x					
AT3G18420	Protein prenylyltransferase superfamily protein							
AT3G18740	RECEPTOR-LIKE KINASE 902 (RLK902)	x	x					
AT3G20350	unknown protein							
AT3G20920	translocation protein-related							
AT3G22230	Ribosomal L27e protein family		x					
AT3G22237	pseudogene, putative ribulose 1,5-bisphosphate carboxylase							
AT3G23030	INDOLE-3-ACETIC ACID INDUCIBLE 2 (IAA2)							
AT3G23470	Cyclopropane-fatty-acyl-phospholipid synthase							
AT3G23890	TOPOISOMERASE II (TOPII)							
AT3G23940	dehydratase family		x					
AT3G24240	Leucine-rich repeat receptor-like protein kinase family protein							
AT3G24570	Peroxisomal membrane 22 kDa (Mpv17/PMP22) family protein							
AT3G27280	PROHIBITIN 4 (PHB4)							
AT3G28130	nodulin MtN21-like transporter family protein							
AT3G29280	unknown protein							
AT3G29762	pseudogene, RNA polymerase A beta prime subunit (fragment)							
AT3G42150	unknown protein							

* Dea: Deal & Henikoff (2010); Lan: Lan et al. (2013); Bra: Brady et al. (2007); Bruex et al. (2012); Ach: Achard et al. (2007); Zen: Zentella et al. (2007); Mar: Marín de la Rosa et al. (2015); UP: up-regulated; DO: down-regulated

Table S3. Microarray data: Cluster 3 genes (cont.)

AGI	DESCRIPTION	Dea	Lan	Bra	Bru	Ach	Zen	Mar
AT3G44110	J3, homologous to the co-chaperon DNAJ protein from *E.coli*							
AT3G44735	PHYTOSULFOKINE 3 PRECURSOR (PSK3)				x			
AT3G45190	SIT4 phosphatase-associated family protein							
AT3G46970	ALPHA-GLUCAN PHOSPHORYLASE 2 (PHS2)					UP		
AT3G48430	RELATIVE OF EARLY FLOWERING 6 (REF6)							
AT3G48500	PIGMENT DEFECTIVE 312 (PDE312)							
AT3G48560	CHLORSULFURON/IMIDAZOLINONE RESISTANT 1 (CSR1)							
AT3G49010	BREAST BASIC CONSERVED 1 (BBC1)		x					
AT3G50240	KICP-02, Encodes a kinesin-related protein.						UP	
AT3G50820	PHOTOSYSTEM II SUBUNIT O-2 (PSBO2)							
AT3G51780	BCL-2-ASSOCIATED ATHANOGENE 4 (BAG4)							
AT3G53020	SHORT VALVE1 (STV1), RPL24B encodes ribosomal protein L24, homolog of cytosolic RPL24	x	x					
AT3G53380	Concanavalin A-like lectin protein kinase family protein							
AT3G54210	Ribosomal protein L17 family protein							
AT3G54600	DJ1F, Class I glutamine amidotransferase-like superfamily protein							
AT3G54890	PHOTOSYSTEM I LIGHT HARVESTING COMPLEX GENE 1 (LHCA1)							
AT3G54900	CAX INTERACTING PROTEIN 1 (CXIP1)							
AT3G55170	Ribosomal L29 family protein							
AT3G55770	WLIM2B (WLIM2b)							
AT3G56910	PLASTID-SPECIFIC 50S RIBOSOMAL PROTEIN 5 (PSRP5)							
AT3G57170	N-acetylglucosaminyl transferase component family protein / Gpi1 family protein							
AT3G58460	RHOMBOID-LIKE PROTEIN 15 (RBL15)							
AT3G58640	Mitogen activated protein kinase kinase kinase-related							x
AT3G58690	Protein kinase superfamily protein							
AT3G59765	unknown protein							
AT3G60330	H(+)-ATPASE 7 (HA7)	x	x	x	x			
AT3G61260	Remorin family protein	x	x					
AT3G61480	Quinoprotein amine dehydrogenase							
AT3G61860	ARGININE/SERINE-RICH SPLICING FACTOR 31 (RS31)							
AT3G62870	Ribosomal protein L7Ae/L30e/S12e/Gadd45 family protein		x					
AT4G00710	BR-SIGNALING KINASE 3 (BSK3)		x					
AT4G01150	unknown protein							
AT4G01900	GLNB1 HOMOLOG (GLB1)							

* Dea: Deal & Henikoff (2010); Lan: Lan et al. (2013); Bra: Brady et al. (2007); Bruex et al. (2012); Ach: Achard et al. (2007); Zen: Zentella et al. (2007); Mar: Marín de la Rosa et al. (2015); UP: up-regulated; DO: down-regulated

Table S3. Microarray data: Cluster 3 genes (cont.)

AGI	DESCRIPTION	Dea	Lan	Bra	Bru	Ach	Zen	Mar
AT4G02110	transcription coactivator							
AT4G02430	SERINE/ARGININE-RICH PROTEIN SPLICING FACTOR 34B (SR34b)							
AT4G02500	UDP-XYLOSYLTRANSFERASE 2 (XT2)							
AT4G02530	chloroplast thylakoid lumen protein							
AT4G02940	oxidoreductase, 2OG-Fe(II) oxygenase family protein							
AT4G03156	small GTPase-related	x						
AT4G03200	catalytics							
AT4G03550	GLUCAN SYNTHASE-LIKE 5 (GSL05)				x			
AT4G04720	CALCIUM-DEPENDENT PROTEIN KINASE 21 (CPK21)							
AT4G04830	METHIONINE SULFOXIDE REDUCTASE B5 (MSRB5)							
AT4G05320	POLYUBIQUITIN 10 (UBQ10)							
AT4G05420	DAMAGED DNA BINDING PROTEIN 1A (DDB1A)							
AT4G05520	EPS15 HOMOLOGY DOMAIN 2 (EHD2)							
AT4G08520	SNARE-like superfamily protein							
AT4G09250	SPla/RYanodine receptor (SPRY) domain-containing protein							
AT4G09670	Oxidoreductase family protein							
AT4G09730	RH39 (RH39)							
AT4G09990	unknown protein		x		x			
AT4G10060	Beta-glucosidase, GBA2 type family protein							
AT4G11630	Ribosomal protein L19 family protein							
AT4G12050	Predicted AT-hook DNA-binding family protein							
AT4G13170	Ribosomal protein L13 family protein							
AT4G13430	ISOPROPYL MALATE ISOMERASE LARGE SUBUNIT 1 (IIL1)							
AT4G13940	HOMOLOGY-DEPENDENT GENE SILENCING 1 (HOG1)		x					
AT4G14230	unknown protein						UP	
AT4G15420	Ubiquitin fusion degradation UFD1 family protein							
AT4G15510	Photosystem II reaction center PsbP family protein							
AT4G15620	Uncharacterised protein family (UPF049)							
AT4G15910	DROUGHT-INDUCED 21 (DI21)				x			
AT4G15920	SWEET17, Nodulin MtN3 family protein				x			
AT4G16140	proline-rich family protein							
AT4G16190	Papain family cysteine protease				x			
AT4G17050	UREIDOGLYCINE AMINOHYDROLASE (UGLYAH)							
AT4G17270	Mo25 family protein							
AT4G17615	CALCINEURIN B-LIKE PROTEIN 1 (CBL1)						UP	
AT4G18050	ATP-BINDING CASSETTE B9 (ABCB9)							
AT4G18070	unknown protein		x					

* Dea: Deal & Henikoff (2010); Lan: Lan et al. (2013); Bra: Brady et al. (2007); Bruex et al. (2012); Ach: Achard et al. (2007); Zen: Zentella et al. (2007); Mar: Marín de la Rosa et al. (2015); UP: up-regulated; DO: down-regulated

Table S3. Microarray data: Cluster 3 genes (cont.)

AGI	DESCRIPTION	Dea	Lan	Bra	Bru	Ach	Zen	Mar
AT4G18730	RIBOSOMAL PROTEIN L16B (RPL16B)		x					
AT4G19500	nucleoside-triphosphatases				x			
AT4G20380	LESION SIMULATING DISEASE (LSD1)							
AT4G21510	F-BOX STRESS INDUCED 2 (FBS2)							
AT4G21830	METHIONINE SULFOXIDE REDUCTASE B7 (MSRB7)							
AT4G21960	PRXR1	x	x					
AT4G23420	NAD(P)-binding Rossmann-fold superfamily protein							
AT4G23800	3XHIGH MOBILITY GROUP-BOX2 (3xHMG-box2)		x					
AT4G24015	RING/U-box superfamily protein							
AT4G27090	Ribosomal protein L14	x	x					
AT4G27470	RING MEMBRANE-ANCHOR 3 (RMA3)							
AT4G27700	Rhodanese/Cell cycle control phosphatase superfamily protein							
AT4G29070	Phospholipase A2 family protein							
AT4G29350	PROFILIN 2 (PFN2)							
AT4G29520	unknown protein							
AT4G29950	Ypt/Rab-GAP domain of gyp1p superfamily protein							
AT4G30020	PA-domain containing subtilase family protein							
AT4G30140	CUTICLE DESTRUCTING FACTOR 1 (CDEF1)							
AT4G30350	Double Clp-N motif-containing P-loop nucleoside triphosphate hydrolases superfamily protein						UP	
AT4G30460	glycine-rich protein		x		x			
AT4G30480	TETRATRICOPEPTIDE REPEAT 1 (TPR1)							x
AT4G30580	ATS2, Encodes a plastidic lysophosphatidic acid acyltransferase (LPAAT)							
AT4G31700	RIBOSOMAL PROTEIN S6 (RPS6)		x					
AT4G32850	NUCLEAR POLY(A) POLYMERASE (nPAP)							
AT4G33220	PECTIN METHYLESTERASE 44 (PME44)				x			
AT4G33270	CELL DIVISION CYCLE 20.1 (CDC20.1)		x					
AT4G33700	unknown protein							
AT4G34270	TIP41-like family protein							
AT4G34730	ribosome-binding factor A family protein							
AT4G34760	SAUR-like auxin-responsive protein family				x			
AT4G36060	BASIC HELIX-LOOP-HELIX 11 (bHLH11)							
AT4G36515	unknown protein	x						
AT4G37270	HEAVY METAL ATPASE 1 (HMA1)				x			
AT4G37300	MATERNAL EFFECT EMBRYO ARREST 59 (MEE59)				x			
AT4G37560	Acetamidase/Formamidase family protein							
AT4G37590	NAKED PINS IN YUC MUTANTS 5 (NPY5)	x						
AT4G37910	MITOCHONDRIAL HEAT SHOCK PROTEIN 70-1 (mtHsc70-1)					DO		

* Dea: Deal & Henikoff (2010); Lan: Lan et al. (2013); Bra: Brady et al. (2007); Bruex et al. (2012); Ach: Achard et al. (2007); Zen: Zentella et al. (2007); Mar: Marín de la Rosa et al. (2015); UP: up-regulated; DO: down-regulated

Table S3. Microarray data: Cluster 3 genes (cont.)

AGI	DESCRIPTION	Dea	Lan	Bra	Bru	Ach	Zen	Mar
AT4G37930	SERINE TRANSHYDROXYMETHYLTRANSFERASE 1 (SHM1)							
AT4G38800	METHYLTHIOADENOSINE NUCLEOSIDASE 1 (MTN1)							
AT4G38840	SAUR-like auxin-responsive protein family	x				DO	DO	
AT4G39700	Heavy metal transport/detoxification superfamily protein							
AT5G01350	unknown protein	x						
AT5G01670	NAD(P)-linked oxidoreductase superfamily protein							
AT5G02490	Hsp70-2, Heat shock protein 70 (Hsp 70) family protein							
AT5G02950	Tudor/PWWP/MBT superfamily protein							
AT5G03490	UDP-Glycosyltransferase superfamily protein							
AT5G04470	SIAMESE (SIM), containins a cyclin binding motif and a motif found in ICK/KRP cell cycle inhibitor proteins.					UP		
AT5G05010	clathrin adaptor complexes medium subunit family protein							
AT5G05435	Potential natural antisense gene							x
AT5G06410	DNAJ heat shock N-terminal domain-containing protein							
AT5G06970	unknown protein							
AT5G07020	proline-rich family protein							
AT5G07090	Ribosomal protein S4 (RPS4A) family protein		x					
AT5G08180	Ribosomal protein L7Ae/L30e/S12e/Gadd45 family protein		x			DO		
AT5G08540	unknown protein							
AT5G08600	U3 ribonucleoprotein (Utp) family protein							x
AT5G12040	Nitrilase/cyanide hydratase and apolipoprotein N-acyltransferase family protein				x			
AT5G13740	ZINC INDUCED FACILITATOR 1 (ZIF1)					UP	UP	
AT5G13910	LEAFY PETIOLE (LEP), Encodes a member of the ERF (ethylene response factor) subfamily B-1 of ERF/AP2 transcription factor family (LEAFY PETIOLE)							
AT5G14680	Adenine nucleotide alpha hydrolases-like superfamily protein							
AT5G15090	VOLTAGE DEPENDENT ANION CHANNEL 3 (VDAC3)							
AT5G15450	CASEIN LYTIC PROTEINASE B3 (CLPB3)							
AT5G15520	Ribosomal protein S19e family protein		x					
AT5G15550	Transducin/WD40 repeat-like superfamily protein							
AT5G15802	unknown protein							
AT5G16510	REVERSIBLY GLYCOSYLATED POLYPEPTIDE 5 (RGP5)							
AT5G16760	INOSITOL (1,3,4) P3 5/6-KINASE 1 (ITPK1)							
AT5G17160	unknown protein							

* Dea: Deal & Henikoff (2010); Lan: Lan et al. (2013); Bra: Brady et al. (2007); Bruex et al. (2012); Ach: Achard et al. (2007); Zen: Zentella et al. (2007); Mar: Marín de la Rosa et al. (2015); UP: up-regulated; DO: down-regulated

Table S3. Microarray data: Cluster 3 genes (cont.)

AGI	DESCRIPTION	Dea	Lan	Bra	Bru	Ach	Zen	Mar
AT5G17210	unknown protein							
AT5G17920	METHIONINE SYNTHESIS 1 (ATMS1)							
AT5G18030	SAUR-like auxin-responsive protein family							
AT5G18100	COPPER/ZINC SUPEROXIDE DISMUTASE 3 (CSD3)							
AT5G18500	Protein kinase superfamily protein							
AT5G18860	NUCLEOSIDE HYDROLASE 3 (NSH3)		x					
AT5G19010	MITOGEN-ACTIVATED PROTEIN KINASE 16 (MPK16)							
AT5G19750	Peroxisomal membrane 22 kDa (Mpv17/PMP22) family protein							
AT5G19940	Plastid-lipid associated protein PAP / fibrillin family protein							
AT5G20090	unknown protein							
AT5G20570	RING-BOX 1 (RBX1)							
AT5G20740	Plant invertase/pectin methylesterase inhibitor superfamily protein							
AT5G21326	Ca2+regulated serine-threonine protein kinase family protein							
AT5G22950	VPS24.1, BEST Arabidopsis thaliana protein match is: SNF7 family protein							
AT5G23240	DNAJ heat shock N-terminal domain-containing protein					UP		
AT5G23310	FE SUPEROXIDE DISMUTASE 3 (FSD3)							
AT5G23590	DNAJ heat shock N-terminal domain-containing protein							
AT5G24270	SALT OVERLY SENSITIVE 3 (SOS3),	x						
AT5G24570	unknown protein							
AT5G24590	TCV-INTERACTING PROTEIN (TIP)							
AT5G26280	TRAF-like family protein							
AT5G27860	unknown protein							
AT5G35210	PHD TYPE TRANSCRIPTION FACTOR WITH TRANSMEMBRANE DOMAINS (PTM)							
AT5G35980	YEAST YAK1-RELATED GENE 1 (YAK1)					UP		
AT5G37660	PLASMODESMATA-LOCATED PROTEIN 7 (PDLP7)							
AT5G42220	Ubiquitin-like superfamily protein							
AT5G42350	Galactose oxidase/kelch repeat superfamily protein							
AT5G43520	Cysteine/Histidine-rich C1 domain family protein			x				
AT5G43970	TRANSLOCASE OF OUTER MEMBRANE 22-V (TOM22-V)							
AT5G44100	CASEIN KINASE I-LIKE 7 (ckl7)							
AT5G45040	CYTOCHROME C6A (CYTC6A)							
AT5G46070	Guanylate-binding family protein							
AT5G47480	RGPR-related							
AT5G47520	RAB GTPASE HOMOLOG A5A (RABA5a)							

* Dea: Deal & Henikoff (2010); Lan: Lan et al. (2013); Bra: Brady et al. (2007); Bruex et al. (2012); Ach: Achard et al. (2007); Zen: Zentella et al. (2007); Mar: Marín de la Rosa et al. (2015); UP: up-regulated; DO: down-regulated

Table S3. Microarray data: Cluster 3 genes (cont.)

AGI	DESCRIPTION	Dea	Lan	Bra	Bru	Ach	Zen	Mar
AT5G47860	unknown protein							
AT5G48520	AUGMIN 3 (AUG3)							
AT5G49400	zinc knuckle (CCHC-type) family protein							
AT5G49470	PAS domain-containing protein tyrosine kinase family protein							
AT5G49660	XYLEM INTERMIXED WITH PHLOEM 1 (XIP1)							
AT5G50840	unknown protein							
AT5G50850	MACCI-BOU (MAB1)							
AT5G51220	ubiquinol-cytochrome C chaperone family protein							
AT5G51440	HSP20-like chaperones superfamily protein							
AT5G52650	RNA binding Plectin/S10 domain-containing protein		x					
AT5G52780	unknown protein					UP		
AT5G52970	thylakoid lumen 15.0 kDa protein							
AT5G53000	2A PHOSPHATASE ASSOCIATED PROTEIN OF 46 KD (TAP46)							
AT5G54750	Transport protein particle (TRAPP) component							
AT5G55100	SWAP (Suppressor-of-White-APricot)/surp domain-containing protein				x			
AT5G55280	HOMOLOG OF BACTERIAL CYTOKINESIS Z-RING PROTEIN FTSZ 1-1 (FTSZ1-1)							
AT5G55310	DNA TOPOISOMERASE 1 BETA (TOP1BETA)							
AT5G55730	FASCICLIN-LIKE ARABINOGALACTAN 1 (FLA1)							
AT5G56550	OXIDATIVE STRESS 3 (OXS3)							
AT5G56950	NUCLEOSOME ASSEMBLY PROTEIN 1;3 (NAP1;3)				x			
AT5G57030	LUTEIN DEFICIENT 2 (LUT2)							
AT5G57180	CHLOROPLAST IMPORT APPARATUS 2 (CIA2)							
AT5G57655	xylose isomerase family protein					UP		
AT5G58110	chaperone binding; ATPase activators		x					
AT5G58787	RING/U-box superfamily protein							
AT5G59430	TELOMERIC REPEAT BINDING PROTEIN 1 (TRP1)							
AT5G60410	SIZ1, Encodes a plant small ubiquitin-like modifier (SUMO) E3 ligase that is a focal controller of Pi starvation-dependent responses							
AT5G60520	Late embryogenesis abundant (LEA) protein-related		x					
AT5G60670	Ribosomal protein L11 family protein		x					
AT5G60950	COBRA-LIKE PROTEIN 5 PRECURSOR (COBL5)			x				
AT5G61240	Leucine-rich repeat (LRR) family protein							
AT5G62140	unknown protein							
AT5G62190	PRH75, DEAD/DEAH box RNA helicase PRH75		x					
AT5G62580	ARM repeat superfamily protein							
AT5G62700	TUBULIN BETA CHAIN 3 (TUB3)		x					

* Dea: Deal & Henikoff (2010); Lan: Lan et al. (2013); Bra: Brady et al. (2007); Bruex et al. (2012); Ach: Achard et al. (2007); Zen: Zentella et al. (2007); Mar: Marín de la Rosa et al. (2015); UP: up-regulated; DO: down-regulated

Table S3. Microarray data: Cluster 3 genes (cont.)

AGI	DESCRIPTION	Dea	Lan	Bra	Bru	Ach	Zen	Mar
AT5G62760	P-loop containing nucleoside triphosphate hydrolases superfamily protein							
AT5G63530	FARNESYLATED PROTEIN 3 (FP3), Farnesylated protein that binds metals.							
AT5G63940	Protein kinase protein with adenine nucleotide alpha hydrolases-like domain							
AT5G64100	Peroxidase superfamily protein		x					
AT5G64560	MAGNESIUM TRANSPORTER 9 (MGT9)							
AT5G65220	Ribosomal L29 family protein							
AT5G66190	FERREDOXIN-NADP(+)-OXIDOREDUCTASE 1 (FNR1)							
AT5G66690	UGT72E2, UGT72E2 is an UDPG:coniferyl alcohol glucosyltransferase which glucosylates sinapyl- and coniferyl aldehydes as well as sinapyl- and coniferyl alcohol							
AT5G66920	SKU5 SIMILAR 17 (sks17), FUNCTIONS IN: oxidoreductase activity, copper ion binding		x		x			
AT5G67250	SKP1/ASK1-INTERACTING PROTEIN 2 (SKIP2)							
ATCG00020	PHOTOSYSTEM II REACTION CENTER PROTEIN A (PSBA)							
ATCG00040	MATURASE K (MATK), Encodes a maturase located in the trnK intron in the chloroplast genome.							
ATCG00160	RIBOSOMAL PROTEIN S2 (RPS2), Chloroplast ribosomal protein S2							
ATCG00540	PHOTOSYNTHETIC ELECTRON TRANSFER A (PETA), Encodes cytochrome f apoprotein							
ATCG00760	RIBOSOMAL PROTEIN L36 (RPL36)							
ATCG01070	NDHE, NADH dehydrogenase ND4L							
ATCG01200	TRNI.3, tRNA-Ile							
ATMG00020	RIBOSOMAL RNA26S (RRN26)		x					
ATMG00090	RESISTANCE TO PSEUDOMONAS SYRINGAE 3 (RPS3), ribosomal protein S3							
ATMG00500	ORF141, hypothetical protein							
ATMG00690	ORF240A, hypothetical protein							

Table S4. Microarray data: Cluster 4 genes

AGI	DESCRIPTION	Dea	Lan	Bra	Bru	Ach	Zen	Mar
AT1G01020	ARV1							
AT1G01350	Zinc finger (CCCH-type/C3HC4-type RING finger) family protein							
AT1G01560	MAP KINASE 11 (MPK11)							
AT1G01750	ACTIN DEPOLYMERIZING FACTOR 11 (ADF11)	x	x	x	x			
AT1G01970	Tetratricopeptide repeat (TPR)-like superfamily protein							

* Dea: Deal & Henikoff (2010); Lan: Lan et al. (2013); Bra: Brady et al. (2007); Bruex et al. (2012); Ach: Achard et al. (2007); Zen: Zentella et al. (2007); Mar: Marín de la Rosa et al. (2015); UP: up-regulated; DO: down-regulated

Table S4. Microarray data: Cluster 4 genes (cont.)

AGI	DESCRIPTION	Dea	Lan	Bra	Bru	Ach	Zen	Mar
AT1G02570	unknown protein							
AT1G02870	unknown protein							
AT1G03040	basic helix-loop-helix (bHLH) DNA-binding superfamily protein							
AT1G03740	Protein kinase superfamily protein							
AT1G04830	Ypt/Rab-GAP domain of gyp1p superfamily protein							
AT1G06310	ACYL-COA OXIDASE 6 (ACX6)							
AT1G06470	Nucleotide/sugar transporter family protein							
AT1G06560	NOL1/NOP2/sun family protein							
AT1G07170	Similar to human splicing factor 3b, 14 kda subunit, SF3b14b.							
AT1G07260	UDP-GLUCOSYL TRANSFERASE 71C3 (UGT71C3)							
AT1G07350	SERINE/ARGININE RICH-LIKE PROTEIN 45A (SR45a)						UP	
AT1G08315	ARM repeat superfamily protein							
AT1G08360	Ribosomal protein L1p/L10e family		x					
AT1G08550	NON-PHOTOCHEMICAL QUENCHING 1 (NPQ1)						UP	
AT1G08800	unknown protein				x			
AT1G08970	NUCLEAR FACTOR Y, SUBUNIT C9 (NF-YC9)							
AT1G09090	RESPIRATORY BURST OXIDASE HOMOLOG B (RBOHB)				x			
AT1G09590	Translation protein SH3-like family protein	x	x					
AT1G09630	RAB GTPASE 11C (RAB11c)						UP	
AT1G09640	Translation elongation factor EF1B, gamma chain							
AT1G09690	Translation protein SH3-like family protein	x	x					
AT1G10522	PLASTID REDOX INSENSITIVE 2 (PRIN2)					DO		
AT1G11300	protein serine/threonine kinases							
AT1G12040	LEUCINE-RICH REPEAT/EXTENSIN 1 (LRX1)	x	x		x			
AT1G12230	Aldolase superfamily protein							
AT1G12710	PHLOEM PROTEIN 2-A12 (PP2-A12)							
AT1G12920	EUKARYOTIC RELEASE FACTOR 1-2 (ERF1-2)		x					
AT1G12950	ROOT HAIR SPECIFIC 2 (RSH2)	x	x		x			
AT1G13440	GLYCERALDEHYDE-3-PHOSPHATE DEHYDROGENASE C2 (GAPC2)		x					
AT1G13690	ATPASE E1 (ATE1), AtE1 - stimulates the ATPase activity of DnaK/DnaJ							
AT1G13990	unknown protein		x					
AT1G14130	2-oxoglutarate (2OG) and Fe(II)-dependent oxygenase superfamily protein							
AT1G15170	MATE efflux family protein							
AT1G15500	ATNTT2							
AT1G16540	ABA DEFICIENT 3 (ABA3)							
AT1G16916	unknown protein							

* Dea: Dea l& Henikoff (2010); Lan: Lan et al. (2013); Bra: Brady et al. (2007); Bruex et al. (2012); Ach: Achard et al. (2007); Zen: Zentella et al. (2007); Mar: Marín de la Rosa et al. (2015); UP: up-regulated; DO: down-regulated

Table S4. Microarray data: Cluster 4 genes (cont.)

AGI	DESCRIPTION	Dea	Lan	Bra	Bru	Ach	Zen	Mar
AT1G17410	Nucleoside diphosphate kinase family protein							
AT1G18090	5'-3' exonuclease family protein							
AT1G18200	RAB GTPASE HOMOLOG A6B (RABA6b)							
AT1G18340	alpha/beta-Hydrolases superfamily protein							
AT1G19690	NAD(P)-binding Rossmann-fold superfamily protein							
AT1G19980	cytomatrix protein-related							
AT1G20010	TUBULIN BETA-5 CHAIN (TUB5), beta tubulin		x					
AT1G20380	Prolyl oligopeptidase family protein							
AT1G20440	COLD-REGULATED 47 (COR47), Belongs to the dehydrin protein family		x			UP		
AT1G20620	CATALASE 3 (CAT3)	x				UP		
AT1G21880	LYSM DOMAIN GPI-ANCHORED PROTEIN 1 PRECURSOR (LYM1)							
AT1G26930	Galactose oxidase/kelch repeat superfamily protein		x					
AT1G29320	Transducin/WD40 repeat-like superfamily protein							
AT1G29880	glycyl-tRNA synthetase / glycine--tRNA ligase		x					
AT1G30230	EUKARYOTIC ELONGATION FACTOR 1B BETA 1 (EEF-1BB1)		x					
AT1G30990	Polyketide cyclase/dehydrase and lipid transport superfamily protein		x		x			
AT1G32470	Single hybrid motif superfamily protein							
AT1G32500	ATP-BINDING CASSETTE I7 (ABCI7)							
AT1G34020	Nucleotide-sugar transporter family protein							
AT1G35580	CYTOSOLIC INVERTASE 1 (CINV1)							
AT1G37130	NITRATE REDUCTASE 2 (NIA2)					UP		
AT1G41880	Ribosomal protein L35Ae family protein		x					
AT1G43170	RIBOSOMAL PROTEIN 1 (RP1)	x	x					
AT1G43560	THIOREDOXIN Y2 (ty2)							
AT1G43860	sequence-specific DNA binding transcription factors							
AT1G44920	unknown protein							
AT1G47580	Pentatricopeptide repeat (PPR) superfamily protein							
AT1G48920	NUCLEOLIN LIKE 1 (NUC-L1)		x					
AT1G49360	F-box family protein							x
AT1G50200	ALANYL-TRNA SYNTHETASE (ALATS)		x					
AT1G51510	Y14, This gene is predicted to encode a protein involved in the exon junction complex							
AT1G51745	Tudor/PWWP/MBT superfamily protein							
AT1G52347	unknown protein							
AT1G53130	GRIM REAPER (GRI), involved in the regulation of cell death induced by extracellular ROS							
AT1G53645	hydroxyproline-rich glycoprotein family protein							
AT1G54350	ATP-BINDING CASSETTE D2 (ABCD2)							

* Dea: Deal & Henikoff (2010); Lan: Lan et al. (2013); Bra: Brady et al. (2007); Bruex et al. (2012); Ach: Achard et al. (2007); Zen: Zentella et al. (2007); Mar: Marín de la Rosa et al. (2015); UP: up-regulated; DO: down-regulated

Table S4. Microarray data: Cluster 4 genes (cont.)

AGI	DESCRIPTION	Dea	Lan	Bra	Bru	Ach	Zen	Mar
AT1G54610	Protein kinase superfamily protein		x					
AT1G54770	Fcf2 pre-rRNA processing protein							
AT1G55480	PROTEIN CONTAINING PDZ DOMAIN, A K-BOX DOMAIN							
AT1G55490	CHAPERONIN 60 BETA (CPN60B)		x					
AT1G55710	unknown protein							
AT1G58590	unknown protein							
AT1G59750	AUXIN RESPONSE FACTOR 1 (ARF1)							
AT1G59900	PYRUVATE DEHYDROGENASE COMPLEX E1 ALPHA SUBUNIT (E1 ALPHA)							
AT1G62600	Flavin-binding monooxygenase family protein							
AT1G62810	COPPER AMINE OXIDASE1 (CUAO1)							
AT1G63940	MONODEHYDROASCORBATE REDUCTASE 6 (MDAR6)			x				
AT1G64060	RESPIRATORY BURST OXIDASE PROTEIN F (RBOH F)							
AT1G65800	RECEPTOR KINASE 2 (RK2)							
AT1G66040	VARIANT IN METHYLATION 4 (VIM4)							
AT1G67840	CHLOROPLAST SENSOR KINASE (CSK)							
AT1G68690	PROLINE-RICH EXTENSIN-LIKE RECEPTOR KINASE 9 (PERK9)							
AT1G69200	FRUCTOKINASE-LIKE 2 (FLN2)							
AT1G69380	RETARDED ROOT GROWTH (RRG)							
AT1G69740	HEMB1, Encodes a putative 5-aminolevulinate dehydratase involved in chlorophyll biosynthesis.				x			
AT1G70190	Ribosomal protein L7/L12, oligomerisation							
AT1G71720	PIGMENT DEFECTIVE 338 (PDE338)							
AT1G74390	Polynucleotidyl transferase, ribonuclease H-like superfamily protein							
AT1G75670	DNA-directed RNA polymerases							
AT1G76405	unknown protein							
AT1G78010	tRNA modification GTPase, putative							
AT1G78900	VACUOLAR ATP SYNTHASE SUBUNIT A (VHA-A)				x			
AT1G79050	HOMOLOG OF BACTERIAL RECA (RECA1)							
AT1G79690	NUDIX HYDROLASE HOMOLOG 3 (NUDT3)							
AT1G79990	structural molecules		x					
AT1G80750	Ribosomal protein L30/L7 family protein		x					
AT2G01010	rRNA; 18SrRNA							
AT2G01830	WOODEN LEG (WOL)							
AT2G03720	MORPHOGENESIS OF ROOT HAIR 6 (MRH6), Involved in root hair development	x	x		x			
AT2G05140	phosphoribosylaminoimidazole carboxylase family protein / AIR carboxylase family protein							
AT2G06210	EARLY FLOWERING 8 (ELF8)							

* Dea: Deal & Henikoff (2010); Lan: Lan et al. (2013); Bra: Brady et al. (2007); Bruex et al. (2012); Ach: Achard et al. (2007); Zen: Zentella et al. (2007); Mar: Marín de la Rosa et al. (2015); UP: up-regulated; DO: down-regulated

Table S4. Microarray data: Cluster 4 genes (cont.)

AGI	DESCRIPTION	Dea	Lan	Bra	Bru	Ach	Zen	Mar
AT2G07600	pseudogene					DO		
AT2G07708	unknown protein	x						
AT2G07719	Putative membrane lipoprotein							
AT2G14120	DYNAMIN RELATED PROTEIN (DRP3B)							
AT2G16400	BEL1-LIKE HOMEODOMAIN 7 (BLH7)							
AT2G17240	unknown protein							
AT2G19180	unknown protein							
AT2G19730	Ribosomal L28e protein family	x	x					
AT2G20420	ATP citrate lyase (ACL) family protein							
AT2G20830	transferases;folic acid binding							
AT2G21010	C2 domain-containing protein							
AT2G21210	Putative auxin-regulated protein whose expression is downregulated in response to chitin oligomers.							
AT2G21620	RD2, Encodes gene that is induced in response to dessication	x						
AT2G21660	GLYCINE-RICH RNA-BINDING PROTEIN 7 (GRP7)		x					
AT2G23430	ICK1, Encodes a cyclin-dependent kinase inhibitor							
AT2G26060	EMBRYO DEFECTIVE 1345 (emb1345)							
AT2G28000	CHAPERONIN-60ALPHA (CPN60A)		x					
AT2G28290	SPLAYED (SYD), Encodes a SWI2/SNF2-like protein in the SNF2 subclass							
AT2G28890	POLTERGEIST LIKE 4 (PLL4), Encodes a protein phosphatase 2C like gene, similar to POL							
AT2G29180	unknown protein							
AT2G29480	GLUTATHIONE S-TRANSFERASE TAU 2 (GSTU2)		x					
AT2G29660	zinc finger (C2H2 type) family protein							
AT2G29750	UDP-GLUCOSYL TRANSFERASE 71C1 (UGT71C1)		x					
AT2G29970	Double Clp-N motif-containing P-loop nucleoside triphosphate hydrolases superfamily protein							
AT2G30260	U2 SMALL NUCLEAR RIBONUCLEOPROTEIN B (U2B'')							
AT2G31400	GENOMES UNCOUPLED 1 (GUN1)				x			
AT2G31660	SUPER SENSITIVE TO ABA AND DROUGHT2 (SAD2)					UP		
AT2G32400	GLUTAMATE RECEPTOR 5 (GLR5), Glr5							
AT2G32560	F-box family protein							
AT2G33770	PHOSPHATE 2 (PHO2), Encodes a ubiquitin-conjugating E2 enzyme							
AT2G35155	Trypsin family protein							
AT2G35410	RNA-binding (RRM/RBD/RNP motifs) family protein							
AT2G35480	unknown protein							
AT2G35720	ORIENTATION UNDER VERY LOW FLUENCES OF LIGHT 1 (OWL1)							
AT2G37390	SODIUM POTASSIUM ROOT DEFECTIVE 2 (NAKR2)				x			
AT2G38025	Cysteine proteinases superfamily protein							

* Dea: Deal & Henikoff (2010); Lan: Lan et al. (2013); Bra: Brady et al. (2007); Bruex et al. (2012); Ach: Achard et al. (2007); Zen: Zentella et al. (2007); Mar: Marín de la Rosa et al. (2015); UP: up-regulated; DO: down-regulated

Table S4. Microarray data: Cluster 4 genes (cont.)

AGI	DESCRIPTION	Dea	Lan	Bra	Bru	Ach	Zen	Mar
AT2G38695	unknown protein							
AT2G40700	P-loop containing nucleoside triphosphate hydrolases superfamily protein							
AT2G40840	DISPROPORTIONATING ENZYME 2 (DPE2)		x					
AT2G41900	OXIDATIVE STRESS 2 (OXS2), CCCH-type zinc finger protein with ARM repeat domain							
AT2G42190	unknown protein				x			
AT2G42740	RIBOSOMAL PROTEIN LARGE SUBUNIT 16A (RPL16A)							
AT2G43235	unknown protein							
AT2G43630	unknown protein							
AT2G43790	MAP KINASE 6 (MPK6)							
AT2G43970	RNA-binding protein							
AT2G44790	UCLACYANIN 2 (UCC2)		x			UP		
AT2G45000	EMBRYO DEFECTIVE 2766 (EMB2766)							
AT2G45360	unknown protein							
AT2G46860	PYROPHOSPHORYLASE 3 (PPa3)		x		x			
AT2G47440	Tetratricopeptide repeat (TPR)-like superfamily protein							
AT3G01360	Family of unknown function (DUF716)							
AT3G02320	N2,N2-dimethylguanosine tRNA methyltransferase							x
AT3G02780	ISOPENTENYL PYROPHOSPHATE:DIMETHYLALLYL PYROPHOSPHATE ISOMERASE 2 (IPP2)							
AT3G03150	unknown protein							
AT3G04840	Ribosomal protein S3Ae		x					
AT3G07440	unknown protein							
AT3G07490	ARF-GAP DOMAIN 11 (AGD11)				x			
AT3G07790	DGCR14-related							
AT3G09680	Ribosomal protein S12/S23 family protein							
AT3G09820	ADENOSINE KINASE 1 (ADK1), Involved in the salvage synthesis of adenylates and methyl recycling		x					
AT3G11830	TCP-1/cpn60 chaperonin family protein		x					
AT3G12600	NUDIX HYDROLASE HOMOLOG 16 (NUDT16)							
AT3G12700	Eukaryotic aspartyl protease family protein	x	x					
AT3G12770	MITOCHONDRIAL EDITING FACTOR 22 (MEF22)							
AT3G13160	Tetratricopeptide repeat (TPR)-like superfamily protein							
AT3G13570	SC35-LIKE SPLICING FACTOR 30A (SCL30A)							
AT3G14060	unknown protein							
AT3G14920	Peptide-N4-(N-acetyl-beta-glucosaminyl)asparagine amidase A protein							

* Dea: Deal & Henikoff (2010); Lan: Lan et al. (2013); Bra: Brady et al. (2007); Bruex et al. (2012); Ach: Achard et al. (2007); Zen: Zentella et al. (2007); Mar: Marín de la Rosa et al. (2015); UP: up-regulated; DO: down-regulated

Table S4. Microarray data: Cluster 4 genes (cont.)

AGI	DESCRIPTION	Dea	Lan	Bra	Bru	Ach	Zen	Mar
AT3G15840	POST-ILLUMINATION CHLOROPHYLL FLUORESCENCE INCREASE (PIFI)							
AT3G16420	PYK10-BINDING PROTEIN 1 (PBP1)							
AT3G18010	WUSCHEL RELATED HOMEOBOX 1 (WOX1)							
AT3G18040	MAP KINASE 9 (MPK9)				x			
AT3G18130	RECEPTOR FOR ACTIVATED C KINASE 1C (RACK1C_ AT)		x					
AT3G18190	TCP-1/cpn60 chaperonin family protein		x					
AT3G18410	Complex I subunit NDUFS6							
AT3G19460	Reticulon family protein							
AT3G19710	BRANCHED-CHAIN AMINOTRANSFERASE4 (BCAT4)					DO		
AT3G19720	ACCUMULATION AND REPLICATION OF CHLOROPLAST 5 (ARC5)							
AT3G19820	DWARF 1 (DWF1)		x					
AT3G20470	GLYCINE-RICH PROTEIN 5 (GRP5)					DO		
AT3G20540	POLYMERASE GAMMA 1 (POLGAMMA1)							
AT3G20557	unknown protein							
AT3G20970	NFU DOMAIN PROTEIN 4 (NFU4)							
AT3G21760	HYPOSTATIN RESISTANCE 1 (HYR1), Encodes HYR1, a UDP glycosyltransferase (UGT)							
AT3G22232	pseudogene, putative ribulose 1,5-bisphosphate carboxylase							
AT3G22410	Sec14p-like phosphatidylinositol transfer family protein							
AT3G23400	FIBRILLIN 4 (FIB4), Encodes FIBRILLIN 4 (FIB4)							
AT3G23530	Cyclopropane-fatty-acyl-phospholipid synthase							
AT3G23620	Ribosomal RNA processing Brix domain protein		x					
AT3G23800	SELENIUM-BINDING PROTEIN 3 (SBP3)				x			
AT3G24760	Galactose oxidase/kelch repeat superfamily protein				x			
AT3G24830	Ribosomal protein L13 family protein		x					
AT3G25480	Rhodanese/Cell cycle control phosphatase superfamily protein							
AT3G27560	ATN1, encodes a protein with kinase domains					UP		
AT3G28070	nodulin MtN21-like transporter family protein							
AT3G28480	Oxoglutarate/iron-dependent oxygenase							
AT3G29240	Protein of unknown function (DUF179)					UP		
AT3G30380	alpha/beta-Hydrolases superfamily protein							
AT3G33000	pseudogene, ATP synthase A subunit					DO		
AT3G41768	rRNA; 18SrRNA							
AT3G45770	Polyketide synthase, enoylreductase family protein							
AT3G47780	ATP-BINDING CASSETTE A7 (ABCA7), member of ATH subfamily							

* Dea: Deal & Henikoff (2010); Lan: Lan et al. (2013); Bra: Brady et al. (2007); Bruex et al. (2012); Ach: Achard et al. (2007); Zen: Zentella et al. (2007); Mar: Marín de la Rosa et al. (2015); UP: up-regulated; DO: down-regulated

Table S4. Microarray data: Cluster 4 genes (cont.)

AGI	DESCRIPTION	Dea	Lan	Bra	Bru	Ach	Zen	Mar
AT3G48980	CONTAINS InterPro DOMAIN/s: Lipopolysaccharide-modifying protein							
AT3G49120	PEROXIDASE CB (PRXCB)			x				
AT3G49960	Its expression is enriched in root hair cells (compared to non-root hair cells)	x	x	x	x			
AT3G50670	U1 SMALL NUCLEAR RIBONUCLEOPROTEIN-70K (U1-70K), Encodes U1 snRNP 70K							
AT3G51090	unknown protein	x						
AT3G51820	G4, Encodes a protein with chlorophyll synthase activity							
AT3G52580	Ribosomal protein S11 family protein		x					
AT3G52940	FACKEL (FK), Encodes a sterol C-14 reductase required for cell division and expansion							
AT3G53000	PHLOEM PROTEIN 2-A15 (PP2-A15)							
AT3G54110	PLANT UNCOUPLING MITOCHONDRIAL PROTEIN 1 (PUMP1)				x	UP		
AT3G54130	Josephin family protein							
AT3G54640	TRYPTOPHAN SYNTHASE ALPHA CHAIN (TSA1)					UP		
AT3G54710	HOMOLOG OF YEAST CDT1 B HOMOLOG OF YEAST CDT1 B (CDT1B)							
AT3G55520	FKBP-like peptidyl-prolyl cis-trans isomerase family protein							
AT3G56070	ROTAMASE CYCLOPHILIN 2 (ROC2)		x					
AT3G56090	FERRITIN 3 (FER3)		x					
AT3G56230	BTB/POZ domain-containing protein							
AT3G57320	unknown protein							
AT3G59490	unknown protein							
AT3G59640	glycine-rich protein							
AT3G60770	Ribosomal protein S13/S15		x					
AT3G61400	1-aminocyclopropane-1-carboxylate oxidase-like protein							
AT3G62400	unknown protein							
AT3G62680	PROLINE-RICH PROTEIN 3 (PRP3), Proline-rich protein	x	x		x			
AT3G63460	transducin family protein / WD-40 repeat family protein							
AT4G00231	MATERNAL EFFECT EMBRYO ARREST 50 (MEE50)							
AT4G00700	C2 calcium/lipid-binding plant phosphoribosyltransferase family protein				x			
AT4G01037	WHAT'S THIS FACTOR? (WTF1)							
AT4G01290	unknown protein							
AT4G02100	Heat shock protein DnaJ with tetratricopeptide repeat							

* Dea: Deal & Henikoff (2010); Lan: Lan et al. (2013); Bra: Brady et al. (2007); Bruex et al. (2012); Ach: Achard et al. (2007); Zen: Zentella et al. (2007); Mar: Marín de la Rosa et al. (2015); UP: up-regulated; DO: down-regulated

Table S4. Microarray data: Cluster 4 genes (cont.)

AGI	DESCRIPTION	Dea	Lan	Bra	Bru	Ach	Zen	Mar
AT4G03610	Metallo-hydrolase/oxidoreductase superfamily protein							
AT4G04020	FIBRILLIN (FIB)							
AT4G05050	UBIQUITIN 11 (UBQ11)							
AT4G05160	Encodes a peroxisomal protein involved in the activation of fatty acids through esterification with CoA							
AT4G05400	copper ion binding							
AT4G07950	DNA-directed RNA polymerase, subunit M							
AT4G08620	SULPHATE TRANSPORTER 1;1 (SULTR1;1)		x		x			
AT4G11290	Peroxidase superfamily protein		x					
AT4G12970	STOMAGEN (STOMAGEN)							
AT4G13670	PLASTID TRANSCRIPTIONALLY ACTIVE 5 (PTAC5)				x			
AT4G13770	CYTOCHROME P450, FAMILY 83, SUBFAMILY A, POLYPEPTIDE 1 (CYP83A1)					DO		
AT4G13980	AT-HSFA5, member of Heat Stress Transcription Factor (Hsf) family							
AT4G14030	SELENIUM-BINDING PROTEIN 1 (SBP1)		x					
AT4G14040	SELENIUM-BINDING PROTEIN 2 (SBP2)							
AT4G14770	TESMIN/TSO1-LIKE CXC 2 (TCX2)							
AT4G15390	HXXXD-type acyl-transferase family protein				x			
AT4G16260	Glycosyl hydrolase superfamily protein		x			UP		
AT4G16270	Peroxidase superfamily protein							
AT4G16830	Hyaluronan / mRNA binding family							
AT4G18100	Ribosomal protein L32e		x					
AT4G18440	L-Aspartase-like family protein		x					
AT4G18910	NOD26-LIKE INTRINSIC PROTEIN 1;2 (NIP1;2),							
AT4G19003	VPS25, VPS25							
AT4G19680	IRON REGULATED TRANSPORTER 2 (IRT2)		x	x	x			
AT4G20020	MULTIPLE ORGANELLAR RNA EDITING FACTOR 1 (MORF1)							
AT4G20260	PLASMA-MEMBRANE ASSOCIATED CATION-BINDING PROTEIN 1 (PCAP1)							
AT4G20340	Transcription factor TFIIE, alpha subunit							
AT4G21270	KINESIN 1 (ATK1)							
AT4G21470	RIBOFLAVIN KINASE/FMN HYDROLASE (FMN/FHY)							
AT4G21520	Transducin/WD40 repeat-like superfamily protein							
AT4G21710	NRPB2, Encodes the unique second-largest subunit of DNA-dependent RNA polymerase II							
AT4G21850	METHIONINE SULFOXIDE REDUCTASE B9 (MSRB9)				x			
AT4G22000	unknown protein							
AT4G23790	TRICHOME BIREFRINGENCE-LIKE 24 (TBL24)							

* Dea: Deal & Henikoff (2010); Lan: Lan et al. (2013); Bra: Brady et al. (2007); Bruex et al. (2012); Ach: Achard et al. (2007); Zen: Zentella et al. (2007); Mar: Marín de la Rosa et al. (2015); UP: up-regulated; DO: down-regulated

Table S4. Microarray data: Cluster 4 genes (cont.)

AGI	DESCRIPTION	Dea	Lan	Bra	Bru	Ach	Zen	Mar
AT4G24510	ECERIFERUM 2 (CER2), Involved in C28 to C30 fatty acid elongation.							
AT4G24550	Clathrin adaptor complexes medium subunit family protein							
AT4G24620	PHOSPHOGLUCOSE ISOMERASE 1 (PGI1)							
AT4G25190	QWRF DOMAIN CONTAINING 7 (QWRF7)	x						
AT4G25790	CAP (Cysteine-rich secretory proteins, Antigen 5, and Pathogenesis-related 1 protein) superfamily protein	x	x		x			
AT4G26600	S-adenosyl-L-methionine-dependent methyltransferases superfamily protein							
AT4G30060	Core-2/I-branching beta-1,6-N-acetylglucosaminyltransferase family protein							
AT4G30320	CAP (Cysteine-rich secretory proteins, Antigen 5, and Pathogenesis-related 1 protein) superfamily protein		x		x			
AT4G30440	UDP-D-GLUCURONATE 4-EPIMERASE 1 (GAE1), UDP-D-glucuronate 4-epimerase							
AT4G30530	GAMMA-GLUTAMYL PEPTIDASE 1 (GGP1)				x			
AT4G31430	unknown protein							
AT4G31500	CYTOCHROME P450, FAMILY 83, SUBFAMILY B, POLYPEPTIDE 1 (CYP83B1)				x			
AT4G32010	HSI2-LIKE 1 (HSL1), HSI2-like 1 (HSL1)							
AT4G32920	glycine-rich protein				x			
AT4G33690	unknown protein							
AT4G34190	STRESS ENHANCED PROTEIN 1 (SEP1)							
AT4G34220	Leucine-rich repeat protein kinase family protein					UP		
AT4G34230	CINNAMYL ALCOHOL DEHYDROGENASE 5 (CAD5)							
AT4G34950	Major facilitator superfamily protein					DO		
AT4G35450	ANKYRIN REPEAT-CONTAINING PROTEIN 2 (AKR2)							
AT4G35550	WUSCHEL RELATED HOMEOBOX 13 (WOX13)							
AT4G36400	D-2-HYDROXYGLUTARATE DEHYDROGENASE (D2HGDH)							
AT4G36440	unknown protein							
AT4G37070	PLP1, Patatin-related phospholipase A		x					
AT4G37380	Tetratricopeptide repeat (TPR)-like superfamily protein							
AT4G37540	LOB DOMAIN-CONTAINING PROTEIN 39 (LBD39)							
AT4G38160	PIGMENT DEFECTIVE 191 (pde191)							
AT4G38360	LAZARUS 1 (LAZ1), Protein of unknown function							
AT4G39235	unknown protein							
AT4G39660	ALANINE:GLYOXYLATE AMINOTRANSFERASE 2 (AGT2)							
AT4G39960	Molecular chaperone Hsp40/DnaJ family protein							

* Dea: Deal & Henikoff (2010); Lan: Lan et al. (2013); Bra: Brady et al. (2007); Bruex et al. (2012); Ach: Achard et al. (2007); Zen: Zentella et al. (2007); Mar: Marín de la Rosa et al. (2015); UP: up-regulated; DO: down-regulated

Table S4. Microarray data: Cluster 4 genes (cont.)

AGI	DESCRIPTION	Dea	Lan	Bra	Bru	Ach	Zen	Mar
AT4G40060	HOMEOBOX PROTEIN 16 (HB16)				x			
AT5G02050	Mitochondrial glycoprotein family protein		x					
AT5G02480	HSP20-like chaperones superfamily protein					UP	DO	
AT5G02500	HEAT SHOCK COGNATE PROTEIN 70-1 (HSC70-1)					UP		
AT5G03690	FRUCTOSE-BISPHOSPHATE ALDOLASE 4 (FBA4)							
AT5G04910	unknown protein							
AT5G04950	NICOTIANAMINE SYNTHASE 1 (NAS1)							
AT5G04960	Plant invertase/pectin methylesterase inhibitor superfamily	x	x	x	x			
AT5G05310	TLC ATP/ADP transporter							
AT5G05670	signal recognition particle binding							
AT5G05780	RP NON-ATPASE SUBUNIT 8A (RPN8A), Encodes a putative 26S proteasome subunit RPN8a.							
AT5G05790	Duplicated homeodomain-like superfamily protein							
AT5G05960	Bifunctional inhibitor/lipid-transfer protein/seed storage 2S albumin superfamily protein							
AT5G05987	PRENYLATED RAB ACCEPTOR 1.A2 (PRA1.A2)							
AT5G07920	DIACYLGLYCEROL KINASE1 (DGK1), diacylglycerol kinase							
AT5G07990	TRANSPARENT TESTA 7 (TT7), Required for flavonoid 3’ hydroxylase activity				x	UP		
AT5G08390	Transducin/WD40 repeat-like superfamily protein							
AT5G08470	PEROXISOME 1 (PEX1), an AAA-ATPase							
AT5G09650	PYROPHOSPHORYLASE 6 (PPa6), Encodes a protein with inorganic pyrophosphatase activity		x					
AT5G09870	CELLULOSE SYNTHASE 5 (CESA5)				x			
AT5G10780	unknown protein							
AT5G11840	Protein of unknown function (DUF1230)							
AT5G11900	Translation initiation factor SUI1 family protein							
AT5G12910	Histone superfamily protein							
AT5G13680	ABA-OVERLY SENSITIVE 1 (ABO1)							
AT5G14550	Core-2/I-branching beta-1,6-N-acetylglucosaminyltransferase family protein							
AT5G15610	Proteasome component (PCI) domain protein							
AT5G16880	Target of Myb protein 1							
AT5G18650	CHY-type/CTCHY-type/RING-type Zinc finger protein							
AT5G20160	Ribosomal protein L7Ae/L30e/S12e/Gadd45 family protein		x					
AT5G20900	JASMONATE-ZIM-DOMAIN PROTEIN 12 (JAZ12)							
AT5G20960	ALDEHYDE OXIDASE 1 (AO1)							
AT5G21222	protein kinase family protein							
AT5G22410	ROOT HAIR SPECIFIC 18 (RHS18)	x	x	x	x			
AT5G22440	Ribosomal protein L1p/L10e family		x					

* Dea: Deal & Henikoff (2010); Lan: Lan et al. (2013); Bra: Brady et al. (2007); Bruex et al. (2012); Ach: Achard et al. (2007); Zen: Zentella et al. (2007); Mar: Marín de la Rosa et al. (2015); UP: up-regulated; DO: down-regulated

Table S4. Microarray data: Cluster 4 genes (cont.)

AGI	DESCRIPTION	Dea	Lan	Bra	Bru	Ach	Zen	Mar
AT5G22580	Stress responsive A/B Barrel Domain							
AT5G23290	PREFOLDIN 5 (PFD5)							
AT5G23420	HIGH-MOBILITY GROUP BOX 6 (HMGB6)							
AT5G24060	Pentatricopeptide repeat (PPR) superfamily protein							
AT5G24500	unknown protein							
AT5G27770	Ribosomal L22e protein family	x	x			DO		
AT5G27850	Ribosomal protein L18e/L15 superfamily protein		x					
AT5G28770	BZO2H3							
AT5G35940	Mannose-binding lectin superfamily protein		x					
AT5G37070	unknown protein							
AT5G38220	alpha/beta-Hydrolases superfamily protein							
AT5G38410	RUBISCO SMALL SUBUNIT 3B (RBCS3B)					DO		
AT5G40480	EMBRYO DEFECTIVE 3012 (EMB3012)							
AT5G41520	RNA binding Plectin/S10 domain-containing protein		x					
AT5G41770	crooked neck protein, putative / cell cycle protein							
AT5G42130	MITOFERRINLIKE1 (Mfl1)							
AT5G42510	Disease resistance-responsive (dirigent-like protein) family protein	x	x					
AT5G42700	AP2/B3-like transcriptional factor family protein							
AT5G43720	Protein of unknown function (DUF2361)							
AT5G44340	TUBULIN BETA CHAIN 4 (TUB4)							
AT5G44460	CALMODULIN LIKE 43 (CML43)							
AT5G45370	nodulin MtN21-like transporter family protein			x	x			
AT5G46110	ACCLIMATION OF PHOTOSYNTHESIS TO ENVIRONMENT 2 (APE2)							
AT5G46250	RNA-binding protein				x			
AT5G46620	unknown protein							
AT5G47370	HAT2, homeobox-leucine zipper genes induced by auxin, but not by other phytohormones							
AT5G47630	MITOCHONDRIAL ACYL CARRIER PROTEIN 3 (mtACP3)							
AT5G48120	ARM repeat superfamily protein							
AT5G48580	FK506- AND RAPAMYCIN-BINDING PROTEIN 15 KD-2 (FKBP15-2)							
AT5G48760	Ribosomal protein L13 family protein	x	x					
AT5G49270	SHAVEN 2 (SHV2), Involved in successfully establishing tip growth in root hairs.	x		x	x			
AT5G49650	XYLULOSE KINASE-2 (XK-2)							
AT5G49720	GLYCOSYL HYDROLASE 9A1 (GH9A1), involved in cellulose biosynthesis					UP		
AT5G50410	unknown protein							
AT5G52310	LOW-TEMPERATURE-INDUCED 78 (LTI78)	x				UP		
AT5G53310	myosin heavy chain-related							

* Dea: Deal & Henikoff (2010); Lan: Lan et al. (2013); Bra: Brady et al. (2007); Bruex et al. (2012); Ach: Achard et al. (2007); Zen: Zentella et al. (2007); Mar: Marín de la Rosa et al. (2015); UP: up-regulated; DO: down-regulated

Table S4. Microarray data: Cluster 4 genes (cont.)

AGI	DESCRIPTION	Dea	Lan	Bra	Bru	Ach	Zen	Mar
AT5G54280	MYOSIN 2 (ATM2), Type VII myosin gene	x						
AT5G54780	Ypt/Rab-GAP domain of gyp1p superfamily protein			x	x			
AT5G54810	TRYPTOPHAN SYNTHASE BETA-SUBUNIT 1 (TSB1)							
AT5G55120	VITAMIN C DEFECTIVE 5 (VTC5), Encodes a GDP-L-galactose phosphorylase							x
AT5G55190	RAN GTPASE 3 (RAN3)		x					
AT5G55920	OLIGOCELLULA 2 (OLI2)							
AT5G56000	HEAT SHOCK PROTEIN 81.4 (Hsp81.4)							
AT5G56030	HEAT SHOCK PROTEIN 81-2 (HSP81-2)							
AT5G57090	ETHYLENE INSENSITIVE ROOT 1 (EIR1)		x					
AT5G57290	60S acidic ribosomal protein family	x						
AT5G57440	GS1, a member of haloacid dehalogenase-like hydrolase family							
AT5G57530	XYLOGLUCAN ENDOTRANSGLUCOSYLASE/ HYDROLASE 12 (XTH12)	x	x		x			
AT5G57540	XYLOGLUCAN ENDOTRANSGLUCOSYLASE/ HYDROLASE 13 (XTH13)	x	x	x	x			
AT5G57890	Glutamine amidotransferase type 1 family protein							
AT5G58750	NAD(P)-binding Rossmann-fold superfamily protein	x						
AT5G59613	unknown protein							
AT5G59750	DHBP synthase RibB-like alpha/beta domain;GTP cyclohydrolase II							
AT5G59910	HTB4	x						
AT5G59970	Histone superfamily protein		x					
AT5G60030	unknown protein							
AT5G61820	unknown protein		x					
AT5G63320	NUCLEAR PROTEIN X1 (NPX1), a nuclear factor regulating abscisic acid responses.							
AT5G64130	cAMP-regulated phosphoprotein 19-related protein							
AT5G65685	UDP-Glycosyltransferase superfamily protein							
AT5G65860	ankyrin repeat family protein							
AT5G65880	unknown protein							
ATCG00180	RPOC1, RNA polymerase beta' subunit-1							
ATCG00200	TRNC, a chloroplast-encoded tRNA for cysteine							
ATCG00360	YCF3, Encodes a protein required for photosystem I assembly and stability.							
ATCG00490	RBCL, large subunit of RUBISCO							
ATCG00600	PETG, Cytochrome b6-f complex, subunit V							
ATCG00700	PHOTOSYSTEM II REACTION CENTER PROTEIN N (PSBN), PSII low MW protein							
ATCG00720	PHOTOSYNTHETIC ELECTRON TRANSFER B (PETB)							
ATCG00770	RIBOSOMAL PROTEIN S8 (RPS8), chloroplast 30S ribosomal protein S8							

* Dea: Deal & Henikoff (2010); Lan: Lan et al. (2013); Bra: Brady et al. (2007); Bruex et al. (2012); Ach: Achard et al. (2007); Zen: Zentella et al. (2007); Mar: Marín de la Rosa et al. (2015); UP: up-regulated; DO: down-regulated

Table S4. Microarray data: Cluster 4 genes (cont.)

AGI	DESCRIPTION	Dea	Lan	Bra	Bru	Ach	Zen	Mar
ATCG00780	RIBOSOMAL PROTEIN L14 (RPL14)							
ATCG01100	NDHA, NADH dehydrogenase ND1							
ATCG01110	NAD(P)H DEHYDROGENASE SUBUNIT H (NDHH)							
ATCG01300	RIBOSOMAL PROTEIN L23 (RPL23.2)							

Table S5. Microarray data: Cluster 5 genes

AGI	DESCRIPTION	Dea	Lan	Bra	Bru	Ach	Zen	Mar
AT1G01140	CBL-INTERACTING PROTEIN KINASE 9 (CIPK9)		x					
AT1G01190	CYTOCHROME P450, FAMILY 78, SUBFAMILY A, POLYPEPTIDE 8 (CYP78A8)							
AT1G01420	UDP-GLUCOSYL TRANSFERASE 72B3 (UGT72B3)							
AT1G02335	GERMIN-LIKE PROTEIN SUBFAMILY 2 MEMBER 2 PRECURSOR (GL22)							
AT1G02405	proline-rich family protein							
AT1G03340	unknown protein							
AT1G03700	Uncharacterised protein family (UPF0497)							
AT1G05090	dentin sialophosphoprotein-related							
AT1G05760	RESTRICTED TEV MOVEMENT 1 (RTM1)							
AT1G05770	Mannose-binding lectin superfamily protein							
AT1G06010	unknown protein				x			
AT1G06650	encodes a protein whose sequence is similar to 2-oxoglutarate-dependent dioxygenase							
AT1G08050	Zinc finger (C3HC4-type RING finger) family protein	x						
AT1G08480	SUCCINATE DEHYDROGENASE 6 (SDH6)							
AT1G10480	ZINC FINGER PROTEIN 5 (ZFP5)							
AT1G10630	ADP-RIBOSYLATION FACTOR A1F (ARFA1F)							
AT1G10870	ARF-GAP DOMAIN 4 (AGD4)							
AT1G10900	Phosphatidylinositol-4-phosphate 5-kinase family protein				x			
AT1G11200	unknown protein							
AT1G11880	transferases, transferring hexosyl groups							
AT1G13000	unknown protein							
AT1G13520	unknown protein							
AT1G14180	RING/U-box superfamily protein							
AT1G14880	PLANT CADMIUM RESISTANCE 1 (PCR1)					UP		
AT1G16370	ORGANIC CATION/CARNITINE TRANSPORTER 6 (OCT6)							x
AT1G16930	F-box/RNI-like/FBD-like domains-containing protein							
AT1G17420	LIPOXYGENASE 3 (LOX3)							
AT1G17790	Putative integral membrane protein conserved region							

* Dea: Deal & Henikoff (2010); Lan: Lan et al. (2013); Bra: Brady et al. (2007); Bruex et al. (2012); Ach: Achard et al. (2007); Zen: Zentella et al. (2007); Mar: Marín de la Rosa et al. (2015); UP: up-regulated; DO: down-regulated

Table S5. Microarray data: Cluster 5 genes (cont.)

AGI	DESCRIPTION	Dea	Lan	Bra	Bru	Ach	Zen	Mar
AT1G17940	Endosomal targeting BRO1-like domain-containing protein							
AT1G19020	transposable element gene		x				UP	
AT1G19350	BRI1-EMS-SUPPRESSOR 1 (BES1)							
AT1G19960	BEST Arabidopsis thaliana protein match is: transmembrane receptors (TAIR:AT2G32140.1)							
AT1G20630	CATALASE 1 (CAT1)							
AT1G21065	unknown protein							
AT1G21240	WALL ASSOCIATED KINASE 3 (WAK3)							
AT1G22065	unknown protein							
AT1G22520	unknown protein							
AT1G23200	Plant invertase/pectin methylesterase inhibitor superfamily							
AT1G23730	BETA CARBONIC ANHYDRASE 3 (BCA3)							
AT1G24260	SEPALLATA3 (SEP3), Member of the MADs box transcription factor family					DO	DO	
AT1G25320	Leucine-rich repeat protein kinase family protein				x			
AT1G25425	CLAVATA3/ESR-RELATED 43 (CLE43)							
AT1G26390	FAD-binding Berberine family protein							
AT1G26420	FAD-binding Berberine family protein							
AT1G28380	NECROTIC SPOTTED LESIONS 1 (NSL1)							
AT1G28660	GDSL-like Lipase/Acylhydrolase superfamily protein							
AT1G29390	COLD REGULATED 314 THYLAKOID MEMBRANE 2 (COR314-TM2)							
AT1G30700	FAD-binding Berberine family protein						UP	
AT1G31460	unknown protein							
AT1G32350	ALTERNATIVE OXIDASE 1D (AOX1D)							
AT1G32760	Glutaredoxin family protein							
AT1G34200	Glyceraldehyde-3-phosphate dehydrogenase-like family protein							
AT1G34418	unknown protein							
AT1G35140	PHOSPHATE-INDUCED 1 (PHI-1)							
AT1G47480	alpha/beta-Hydrolases superfamily protein							
AT1G47720	ORGANELLAR SINGLE-STRANDED (OSB1)							
AT1G48000	MYB DOMAIN PROTEIN 112 (MYB112)							
AT1G52040	MYROSINASE-BINDING PROTEIN 1 (MBP1)							
AT1G52540	Protein kinase superfamily protein							
AT1G52855	unknown protein							
AT1G53210	sodium/calcium exchanger family protein							
AT1G55190	PRA7,INVOLVED IN: vesicle-mediated transport							
AT1G55915	zinc ion binding	x						
AT1G59590	ZCF37							

* Dea: Deal & Henikoff (2010); Lan: Lan et al. (2013); Bra: Brady et al. (2007); Bruex et al. (2012); Ach: Achard et al. (2007); Zen: Zentella et al. (2007); Mar: Marín de la Rosa et al. (2015); UP: up-regulated; DO: down-regulated

Table S5. Microarray data: Cluster 5 genes (cont.)

AGI	DESCRIPTION	Dea	Lan	Bra	Bru	Ach	Zen	Mar
AT1G61120	TERPENE SYNTHASE 04 (TPS04)							
AT1G61380	S-DOMAIN-1 29 (SD1-29)							
AT1G62045	BEST *Arabidopsis thaliana* protein match is: ankyrin repeat family protein							
AT1G65230	Uncharacterized conserved protein (DUF2358)							
AT1G65486	unknown protein							
AT1G65730	YELLOW STRIPE LIKE 7 (YSL7)		x					
AT1G65820	microsomal glutathione s-transferase, putative		x					
AT1G67530	ARM repeat superfamily protein							
AT1G68150	WRKY DNA-BINDING PROTEIN 9 (WRKY9)			x				
AT1G68360	C2H2 and C2HC zinc fingers superfamily protein							
AT1G71270	POKY POLLEN TUBE (POK), Encodes a homolog of the yeast Vps52p/SAC2							
AT1G71960	ATP-BINDING CASETTE G25 (ABCG25)							
AT1G71970	unknown protein							
AT1G72060	serine-type endopeptidase inhibitors							
AT1G72550	tRNA synthetase beta subunit family protein							
AT1G72855	Potential natural antisense gene, locus overlaps with AT1G72860							
AT1G74240	Mitochondrial substrate carrier family protein							
AT1G74330	Protein kinase superfamily protein							
AT1G74520	HVA22 HOMOLOGUE A (HVA22A). Protein expression is ABA- and stress-inducible.							
AT1G75880	SGNH hydrolase-type esterase superfamily protein							
AT1G76030	V-ATPASE B SUBUNIT 1 (VAB1)							
AT1G76960	unknown protein							
AT1G78560	Sodium Bile acid symporter family		x					
AT1G78870	UBIQUITIN-CONJUGATING ENZYME 35 (UBC35)							
AT1G79340	METACASPASE 4 (MC4)		x		x			
AT1G79570	Protein kinase superfamily protein with octicosapeptide/Phox/Bem1p domain							
AT1G79700	Integrase-type DNA-binding superfamily protein							
AT1G80610	unknown protein							
AT2G01190	PIGMENT DEFECTIVE 331 (PDE331), Octicosapeptide/Phox/Bem1p family protein							
AT2G01210	Leucine-rich repeat protein kinase family protein							
AT2G01980	SALT OVERLY SENSITIVE 1 (SOS1)							
AT2G02610	Cysteine/Histidine-rich C1 domain family protein							
AT2G02960	RING/FYVE/PHD zinc finger superfamily protein		x					
AT2G02970	GDA1/CD39 nucleoside phosphatase family protein							
AT2G04230	FBD, F-box and Leucine Rich Repeat domains containing protein							
AT2G10950	BSD domain-containing protein							

* Dea: Deal & Henikoff (2010); Lan: Lan et al. (2013); Bra: Brady et al. (2007); Bruex et al. (2012); Ach: Achard et al. (2007); Zen: Zentella et al. (2007); Mar: Marín de la Rosa et al. (2015); UP: up-regulated; DO: down-regulated

Table S5. Microarray data: Cluster 5 genes (cont.)

AGI	DESCRIPTION	Dea	Lan	Bra	Bru	Ach	Zen	Mar
AT2G13560	NAD-DEPENDENT MALIC ENZYME 1 (NAD-ME1)		x					
AT2G13690	PRLI-interacting factor, putative							
AT2G13810	AGD2-LIKE DEFENSE RESPONSE PROTEIN 1 (ALD1)							
AT2G14560	LATE UPREGULATED IN RESPONSE TO HYALOPERONOSPORA PARASITICA (LURP1)							
AT2G14610	PATHOGENESIS-RELATED GENE 1 (PR1)							
AT2G15580	RING/U-box superfamily protein							
AT2G16380	Sec14p-like phosphatidylinositol transfer family protein						DO	
AT2G17040	NAC DOMAIN CONTAINING PROTEIN 36 (NAC036)							
AT2G17120	LYSM DOMAIN GPI-ANCHORED PROTEIN 2 PRECURSOR (LYM2)							
AT2G17290	CALCIUM DEPENDENT PROTEIN KINASE 6 (CPK6)							
AT2G17980	ATSLY1, member of SLY1 Gene Family							
AT2G18260	SYNTAXIN OF PLANTS 112 (SYP112)							
AT2G19350	unknown protein							
AT2G19460	unknown protein							
AT2G19710	Regulator of Vps4 activity in the MVB pathway protein							
AT2G20760	Clathrin light chain protein							
AT2G20900	DIACYLGLYCEROL KINASE 5 (DGK5)							
AT2G21170	TRIOSEPHOSPHATE ISOMERASE (TIM)							
AT2G22880	VQ motif-containing protein							
AT2G23690	unknown protein							
AT2G24240	BTB/POZ domain with WD40/YVTN repeat-like protein							
AT2G24610	CYCLIC NUCLEOTIDE-GATED CHANNEL 14 (CNGC14)							
AT2G24850	TYROSINE AMINOTRANSFERASE 3 (TAT3)					UP		
AT2G25510	unknown protein							
AT2G25670	BEST Arabidopsis thaliana protein match is: copper ion binding							
AT2G26695	Ran BP2/NZF zinc finger-like superfamily protein							
AT2G27690	CYTOCHROME P450, FAMILY 94, SUBFAMILY C, POLYPEPTIDE 1 (CYP94C1)						DO	
AT2G28130	unknown protein							
AT2G28320	Pleckstrin homology (PH) and lipid-binding START domains-containing protein							
AT2G29350	SENESCENCE-ASSOCIATED GENE 13 (SAG13)							
AT2G30000	PHF5-like protein							
AT2G30250	WRKY DNA-BINDING PROTEIN 25 (WRKY25)							
AT2G30770	CYTOCHROME P450, FAMILY 71, SUBFAMILY A, POLYPEPTIDE 13 (CYP71A13)							
AT2G31260	AUTOPHAGY 9 (APG9)	x						

* Dea: Deal & Henikoff (2010); Lan: Lan et al. (2013); Bra: Brady et al. (2007); Bruex et al. (2012); Ach: Achard et al. (2007); Zen: Zentella et al. (2007); Mar: Marín de la Rosa et al. (2015); UP: up-regulated; DO: down-regulated

Table S5. Microarray data: Cluster 5 genes (cont.)

AGI	DESCRIPTION	Dea	Lan	Bra	Bru	Ach	Zen	Mar
AT2G31450	ATNTH1							
AT2G32070	Polynucleotidyl transferase							
AT2G33130	RALF-LIKE 18 (RALFL18)							
AT2G34600	JASMONATE-ZIM-DOMAIN PROTEIN 7 (JAZ7)							
AT2G35110	GNARLED (GRL)						UP	
AT2G35290	unknown protein							
AT2G35330	RING/U-box superfamily protein							
AT2G35658	unknown protein							
AT2G35760	Uncharacterised protein family (UPF0497)							
AT2G35820	ureidoglycolate hydrolases							
AT2G35960	NDR1/HIN1-LIKE 12 (NHL12)							
AT2G35980	YELLOW-LEAF-SPECIFIC GENE 9 (YLS9)							
AT2G36300	Integral membrane Yip1 family protein							
AT2G36730	Pentatricopeptide repeat (PPR) superfamily protein							
AT2G36770	UDP-Glycosyltransferase superfamily protein							
AT2G37170	PLASMA MEMBRANE INTRINSIC PROTEIN 2 (PIP2B)							
AT2G39270	P-loop containing nucleoside triphosphate hydrolases superfamily protein							
AT2G39450	MTP11, Encodes a Golgi-localized manganese transporter that is involved in Mn tolerance			x				
AT2G40630	unknown protein							
AT2G40880	CYSTATIN A (CYSA)							
AT2G41420	WINDHOSE 2 (WIH2), proline-rich family protein		x					
AT2G41540	GPDHC1, Encodes a protein with NAD-dependent glycerol-3-phosphate (G3P) dehydrogenase							
AT2G41830	unknown protein							
AT2G42485	unknown protein							
AT2G45060	unknown protein							
AT2G45690	SHRUNKEN SEED 1 (SSE1)							
AT2G46220	unknown protein						UP	
AT2G46430	CYCLIC NUCLEOTIDE GATED CHANNEL 3 (CNGC3)							
AT2G46440	CYCLIC NUCLEOTIDE-GATED CHANNELS (CNGC11),							
AT2G46870	NGATHA1 (NGA1); Transcriptional factor B3							
AT2G47770	TSPO(OUTER MEMBRANE TRYPTOPHAN-RICH SENSORY PROTEIN)-RELATED					UP		
AT2G47950	unknown protein							
AT3G01300	Protein kinase superfamily protein							
AT3G01640	GLUCURONOKINASE G (GLCAK)						UP	
AT3G01760	Transmembrane amino acid transporter family protein							
AT3G02610	Plant stearoyl-acyl-carrier-protein desaturase family protein							

* Dea: Deal & Henikoff (2010); Lan: Lan et al. (2013); Bra: Brady et al. (2007); Bruex et al. (2012); Ach: Achard et al. (2007); Zen: Zentella et al. (2007); Mar: Marín de la Rosa et al. (2015); UP: up-regulated; DO: down-regulated

Table S5. Microarray data: Cluster 5 genes (cont.)

AGI	DESCRIPTION	Dea	Lan	Bra	Bru	Ach	Zen	Mar
AT3G02880	Leucine-rich repeat protein kinase family protein		x					
AT3G03360	F-box/RNI-like superfamily protein							
AT3G04930	DNA-binding storekeeper protein-related transcriptional regulator							
AT3G05510	Phospholipid/glycerol acyltransferase family protein							
AT3G07780	OBERON1 (OBE1)							
AT3G11773	Thioredoxin superfamily protein							
AT3G12010	unknown protein							
AT3G12210	DNA binding							
AT3G12940	2-oxoglutarate (2OG) and Fe(II)-dependent oxygenase superfamily protein							
AT3G13222	GBF-INTERACTING PROTEIN 1 (GIP1)							
AT3G13226	regulatory protein RecX family protein							
AT3G13672	TRAF-like superfamily protein							
AT3G13950	unknown protein							
AT3G14440	NINE-CIS-EPOXYCAROTENOID DIOXYGENASE 3 (NCED3)							
AT3G15070	RING/U-box superfamily protein							
AT3G15500	NAC DOMAIN CONTAINING PROTEIN 3 (NAC3)							
AT3G16470	JASMONATE RESPONSIVE 1 (JR1)							
AT3G18215	unknown protein			x				
AT3G19010	2-oxoglutarate (2OG) and Fe(II)-dependent oxygenase superfamily protein							
AT3G19660	unknown protein							
AT3G21500	1-DEOXY-D-XYLULOSE 5-PHOSPHATE SYNTHASE 1 (DXPS1)							
AT3G22060	unknown protein		x					
AT3G22235	BEST Arabidopsis thaliana protein match is: pathogen and circadian controlled 1							
AT3G22240	unknown protein							
AT3G24030	hydroxyethylthiazole kinase family protein							
AT3G24090	L-GLUTAMINE D-FRUCTOSE-6-PHOSPHATE AMIDOTRANSFERASE (GFAT)							
AT3G24900	RECEPTOR LIKE PROTEIN 39 (RLP39)							
AT3G24982	RECEPTOR LIKE PROTEIN 40 (RLP40)							
AT3G25010	RECEPTOR LIKE PROTEIN 41 (RLP41)							
AT3G25020	RECEPTOR LIKE PROTEIN 42 (RLP42)							
AT3G25140	QUASIMODO 1 (QUA1), encodes a glycosyltransferase							
AT3G25180	CYTOCHROME P450, FAMILY 82, SUBFAMILY G, POLYPEPTIDE 1 (CYP82G1)							
AT3G25840	Protein kinase superfamily protein							
AT3G26820	Esterase/lipase/thioesterase family protein							

* Dea: Deal & Henikoff (2010); Lan: Lan et al. (2013); Bra: Brady et al. (2007); Bruex et al. (2012); Ach: Achard et al. (2007); Zen: Zentella et al. (2007); Mar: Marín de la Rosa et al. (2015); UP: up-regulated; DO: down-regulated

Table S5. Microarray data: Cluster 5 genes (cont.)

AGI	DESCRIPTION	Dea	Lan	Bra	Bru	Ach	Zen	Mar
AT3G27400	Pectin lyase-like superfamily protein							
AT3G27809	unknown protein							
AT3G28510	P-loop containing nucleoside triphosphate hydrolases superfamily protein							
AT3G28540	P-loop containing nucleoside triphosphate hydrolases superfamily protein							
AT3G29400	EXOCYST SUBUNIT EXO70 FAMILY PROTEIN E1 (EXO70E1)			x	x			
AT3G43440	JASMONATE-ZIM-DOMAIN PROTEIN 11 (JAZ11)							
AT3G44530	HOMOLOG OF HISTONE CHAPERONE HIRA (HIRA)							
AT3G44860	FARNESOIC ACID CARBOXYL-O-METHYLTRANSFERASE (FAMT)							
AT3G44870	S-adenosyl-L-methionine-dependent methyltransferases superfamily protein							
AT3G46000	ACTIN DEPOLYMERIZING FACTOR 2 (ADF2)							
AT3G47940	DNAJ heat shock family protein							
AT3G49340	Cysteine proteinases superfamily protein							
AT3G49720	unknown protein		x					
AT3G50310	MITOGEN-ACTIVATED PROTEIN KINASE KINASE KINASE 20 (MAPKKK20)							
AT3G50900	unknown protein						DO	
AT3G50910	unknown protein							
AT3G51600	LIPID TRANSFER PROTEIN 5 (LTP5), Predicted to encode a PR (pathogenesis-related) protein							
AT3G51770	ETHYLENE OVERPRODUCER 1 (ETO1)							
AT3G51850	CALCIUM-DEPENDENT PROTEIN KINASE 13 (CPK13)							
AT3G52748	unknown protein							
AT3G53920	RNAPOLYMERASE SIGMA-SUBUNIT C (SIGC)							
AT3G54930	Protein phosphatase 2A regulatory B subunit family protein							
AT3G55230	Disease resistance-responsive (dirigent-like protein) family protein							
AT3G57260	BETA-1,3-GLUCANASE 2 (BGL2)							
AT3G57740	Protein kinase superfamily protein							x
AT3G58550	Bifunctional inhibitor/lipid-transfer protein/seed storage 2S albumin superfamily protein							
AT3G60200	unknown protein							
AT3G60270	Cupredoxin superfamily protein							
AT3G63080	GLUTATHIONE PEROXIDASE 5 (GPX5)							x
AT4G00290	Mechanosensitive ion channel protein							
AT4G01250	WRKY22. It is involved in regulation of dark induced leaf senescence.							

* Dea: Deal & Henikoff (2010); Lan: Lan et al. (2013); Bra: Brady et al. (2007); Bruex et al. (2012); Ach: Achard et al. (2007); Zen: Zentella et al. (2007); Mar: Marín de la Rosa et al. (2015); UP: up-regulated; DO: down-regulated

Table S5. Microarray data: Cluster 5 genes (cont.)

AGI	DESCRIPTION	Dea	Lan	Bra	Bru	Ach	Zen	Mar
AT4G01370	MAP KINASE 4 (MPK4)							
AT4G01430	nodulin MtN21-like transporter family protein							
AT4G02140	unknown protein							
AT4G02740	F-box/RNI-like superfamily protein							
AT4G03020	transducin family protein / WD-40 repeat family protein							
AT4G04220	RECEPTOR LIKE PROTEIN 46 (RLP46)							
AT4G04850	K+ EFFLUX ANTIPORTER 3 (KEA3)							
AT4G09340	SPla/RYanodine receptor (SPRY) domain-containing protein							
AT4G10500	2-oxoglutarate (2OG) and Fe(II)-dependent oxygenase superfamily protein							
AT4G13370	unknown protein							
AT4G16515	ROOT MERISTEM GROWTH FACTOR 6 (RGF6)	x						
AT4G17360	encodes one of the two putative formyltetrahydrofolate deformylase							
AT4G17570	GATA TRANSCRIPTION FACTOR 26 (GATA26)			x	x			
AT4G18760	RECEPTOR LIKE PROTEIN 51 (RLP51)							
AT4G19530	Encodes a TIR-NB-LRR resistance protein						DO	
AT4G20030	RNA-binding (RRM/RBD/RNP motifs) family protein							
AT4G20280	TBP-ASSOCIATED FACTOR 11 (TAF11)							
AT4G23215	pseudogene of cysteine-rich receptor-like protein kinase family protein							
AT4G23220	CYSTEINE-RICH RLK (RECEPTOR-LIKE PROTEIN KINASE) 14 (CRK14)							
AT4G23810	WRKY53							
AT4G24340	Phosphorylase superfamily protein		x					
AT4G24805	S-adenosyl-L-methionine-dependent methyltransferases superfamily protein							
AT4G24940	SUMO-ACTIVATING ENZYME 1A (SAE1A)							
AT4G26580	RING/U-box superfamily protein							
AT4G27780	ACYL-COA BINDING PROTEIN 2 (ACBP2)			x	x			
AT4G27820	BETA GLUCOSIDASE 9 (BGLU9)							
AT4G28220	NAD(P)H DEHYDROGENASE B1 (NDB1)							
AT4G28600	NO POLLEN GERMINATION RELATED 2 (NPGR2)							
AT4G28770	Tetraspanin family protein							
AT4G29440	Regulator of Vps4 activity in the MVB pathway protein							
AT4G31910	HXXXD-type acyl-transferase family protein							
AT4G32450	Pentatricopeptide repeat (PPR) superfamily protein	x						
AT4G33920	Protein phosphatase 2C family protein		x					
AT4G33960	unknown protein							
AT4G34310	alpha/beta-Hydrolases superfamily protein							

* Dea: Deal & Henikoff (2010); Lan: Lan et al. (2013); Bra: Brady et al. (2007); Bruex et al. (2012); Ach: Achard et al. (2007); Zen: Zentella et al. (2007); Mar: Marín de la Rosa et al. (2015); UP: up-regulated; DO: down-regulated

Table S5. Microarray data: Cluster 5 genes (cont.)

AGI	DESCRIPTION	Dea	Lan	Bra	Bru	Ach	Zen	Mar
AT4G34370	ARIADNE 1 (ARI1); FUNCTIONS IN: zinc ion binding							
AT4G34390	EXTRA-LARGE GTP-BINDING PROTEIN 2 (XLG2)							
AT4G34650	SQUALENE SYNTHASE 2 (SQS2)							x
AT4G34840	METHYLTHIOADENOSINE NUCLEOSIDASE 2 (MTN2)							x
AT4G35110	Arabidopsis phospholipase-like protein (PEARLI 4) family							
AT4G35770	SENESCENCE 1 (SEN1)			x		UP		
AT4G35780	SERINE/THREONINE/TYROSINE KINASE 17 (STY17), ACT-like protein tyrosine kinase family protein							
AT4G36110	SMALL AUXIN UPREGULATED RNA 9 (SAUR9)							
AT4G36430	Peroxidase superfamily protein				x			
AT4G36650	PLANT-SPECIFIC TFIIB-RELATED PROTEIN (PBRP)							
AT4G36810	GERANYLGERANYL PYROPHOSPHATE SYNTHASE 1 (GGPS1)							
AT4G37220	Cold acclimation protein WCOR413 family							
AT4G38040	Exostosin family protein							
AT4G38495	unknown protein	x						
AT4G39404	other RNA							
AT5G01550	LECTIN RECEPTOR KINASE A4.1 (LECRKA4.2)							
AT5G02090	unknown protein							
AT5G02400	POL-LIKE 2 (PLL2)							
AT5G02670	BEST Arabidopsis thaliana protein match is: poly(A) polymerase 3							
AT5G04990	SAD1/UNC-84 DOMAIN PROTEIN 1 (SUN1)							
AT5G05390	LACCASE 12 (LAC12)							
AT5G06220	LETM1-like protein							
AT5G06760	LATE EMBRYOGENESIS ABUNDANT 4-5 (LEA4-5)	x	x					
AT5G07590	Transducin/WD40 repeat-like superfamily protein							
AT5G08150	SUPPRESSOR OF PHYTOCHROME B 5 (SOB5)							
AT5G08630	DDT domain-containing protein							
AT5G09450	Tetratricopeptide repeat (TPR)-like superfamily protein						UP	
AT5G10625	BEST Arabidopsis thaliana protein match is: flowering promoting factor 1							
AT5G10650	RING/U-box superfamily protein				x			
AT5G10770	Eukaryotic aspartyl protease family protein							
AT5G13160	AVRPPHB SUSCEPTIBLE 1 (PBS1)							
AT5G13720	unknown protein							
AT5G14360	Ubiquitin-like superfamily protein							
AT5G14930	SENESCENCE-ASSOCIATED GENE 101 (SAG101)							
AT5G15400	U-box domain-containing protein							
AT5G16110	unknown protein							

* Dea: Deal & Henikoff (2010); Lan: Lan et al. (2013); Bra: Brady et al. (2007); Bruex et al. (2012); Ach: Achard et al. (2007); Zen: Zentella et al. (2007); Mar: Marín de la Rosa et al. (2015); UP: up-regulated; DO: down-regulated

Table S5. Microarray data: Cluster 5 genes (cont.)

AGI	DESCRIPTION	Dea	Lan	Bra	Bru	Ach	Zen	Mar
AT5G16300	Vps51/Vps67 family (components of vesicular transport) protein							
AT5G17190	unknown protein							
AT5G17280	CONTAINS InterPro DOMAIN/s: Oxidoreductase-like							
AT5G17350	unknown protein							
AT5G17450	HEAVY METAL ASSOCIATED ISOPRENYLATED PLANT PROTEIN 21 (HIPP21)							
AT5G17460	unknown protein		x					
AT5G19930	Protein of unknown function DUF92							
AT5G20480	EF-TU RECEPTOR (EFR), Encodes a predicted leucine-rich repeat receptor kinase (LRR-RLK)							
AT5G23150	ENHANCER OF AG-4 2 (HUA2), Putative transcription factor							
AT5G24170	Got1/Sft2-like vescicle transport protein family		x					
AT5G26740	unknown protein		x					
AT5G27670	HISTONE H2A 7 (HTA7)		x		x	UP		
AT5G35520	MINICHROMOSOME INSTABILITY 12 (MIS12)-LIKE (MIS12)							
AT5G35680	Nucleic acid-binding, OB-fold-like protein;	x						
AT5G36920	unknown protein							
AT5G38900	Thioredoxin superfamily protein		x					
AT5G39020	Malectin/receptor-like protein kinase family protein							
AT5G39590	TLD-domain containing nucleolar protein							
AT5G40200	DEGP PROTEASE 9 (DegP9), Encodes a putative DegP protease.							
AT5G40720	unknown protein							
AT5G40890	CHLORIDE CHANNEL A (CLC-A)		x					
AT5G43190	Galactose oxidase/kelch repeat superfamily protein							
AT5G44130	FASCICLIN-LIKE ARABINOGALACTAN PROTEIN 13 PRECURSOR (FLA13)						DO	
AT5G45310	unknown protein							
AT5G45820	CBL-INTERACTING PROTEIN KINASE 20 (CIPK20)							
AT5G45830	DELAY OF GERMINATION 1 (DOG1)							
AT5G46840	RNA-binding (RRM/RBD/RNP motifs) family protein							
AT5G47090	unknown protein							
AT5G47445	transposable element gene							
AT5G48657	defense protein-related							
AT5G49555	FAD/NAD(P)-binding oxidoreductase family protein							
AT5G52390	PAR1 protein; unknown function							
AT5G52560	UDP-SUGAR PYROPHOSPHORYLASE (USP)							
AT5G53370	PECTIN METHYLESTERASE PCR FRAGMENT F (PMEPCRF)							

* Dea: Deal & Henikoff (2010); Lan: Lan et al. (2013); Bra: Brady et al. (2007); Bruex et al. (2012); Ach: Achard et al. (2007); Zen: Zentella et al. (2007); Mar: Marín de la Rosa et al. (2015); UP: up-regulated; DO: down-regulated

Table S5. Microarray data: Cluster 5 genes (cont.)

AGI	DESCRIPTION	Dea	Lan	Bra	Bru	Ach	Zen	Mar
AT5G53900	Serine/threonine-protein kinase WNK (With No Lysine)-related							
AT5G54400	S-adenosyl-L-methionine-dependent methyltransferases superfamily protein							
AT5G54840	SGP1, Monomeric G protein				x			
AT5G56150	UBIQUITIN-CONJUGATING ENZYME 30 (UBC30)		x					
AT5G56270	WRKY DNA-BINDING PROTEIN 2 (WRKY2)							
AT5G56680	SYNC1, Encodes a putative cytosolic asparaginyl-tRNA synthetase.		x					
AT5G57060	unknown protein							
AT5G57800	ECERIFERUM 3 (CER3)		x			DO	DO	
AT5G58003	C-TERMINAL DOMAIN PHOSPHATASE-LIKE 4 (CPL4)							
AT5G59370	ACTIN 4 (ACT4)							
AT5G59520	ZRT/IRT-LIKE PROTEIN 2 (ZIP2), encodes a metal ion transporter whose expression is regulated by copper.			x				
AT5G61560	U-box domain-containing protein kinase family protein						UP	
AT5G61810	ATP/PHOSPHATE CARRIER 1 (APC1)							
AT5G61930	ACCUMULATION OF PHOTOSYSTEM ONE 3 (APO3),							
AT5G62460	RING/FYVE/PHD zinc finger superfamily protein	x						
AT5G62620	Galactosyltransferase family protein							
AT5G63260	Zinc finger C-x8-C-x5-C-x3-H type family protein				x			
AT5G63905	unknown protein							
AT5G64050	GLUTAMATE TRNA SYNTHETASE (ERS), Glutamate-tRNA ligase							
AT5G64500	Major facilitator superfamily protein							
AT5G67488	Potential natural antisense gene, locus overlaps with AT5G67490							
AT5G67590	FROSTBITE1 (FRO1)							
At5TU018960	chr5:5209400-5209716, strand -1							
At5TU102420	chr5:26633011-26633512, strand -1							
miR5657	miR5657							

* Dea: Deal & Henikoff (2010); Lan: Lan et al. (2013); Bra: Brady et al. (2007); Bruex et al. (2012); Ach: Achard et al. (2007); Zen: Zentella et al. (2007); Mar: Marín de la Rosa et al. (2015); UP: up-regulated; DO: down-regulated